MEASUREMENT OF FAST NEUTRON LEAKAGE FROM COPPER BLOCK WITH ^{252}Cf(s.f.) SOURCE IN CENTER

Evaluators

Michal Košťál
Martin Schulc
Tomáš Czakoj
Vojtěch Rypar
Evžen Novák
Research Centre Řež

Filip Mravec
Zdeněk Matěj
Masaryk University, Brno

František Cvachovec
University of Defence, Brno

Internal Reviewer

Evžen Losa
Research Centre Řež

Independent Reviewers

Thomas Miller
Oak Ridge National Laboratory

Jason Haverkamp
Naval Nuclear Laboratory

Dennis Mennerdahl
Contractor

ALARM-CF-CU-SHIELD-001

Acknowledgment

Revision: 1

Date: March 3, 2022

MEASUREMENT OF FAST NEUTRON LEAKAGE FROM COPPER BLOCK WITH ^{252}CF SOURCE IN CENTER

IDENTIFICATION NUMBER: RCR ALARM-CF-CU-SHIELD-001

KEY WORDS: neutron leakage flux, copper block, ^{252}Cf neutron source, scintillation spectrometer, recoil protons

1.0   DETAILED DESCRIPTION

The measured neutron leakage flux from a copper block is evaluated. The targeted neutron energy range is between 1.0 MeV and 11.0 MeV, divided into 0.1 MeV groups. The current experiment is covering transport of ^{252}Cf spontaneous fission neutrons from the center of the copper block to the detector. Prior to reaching the detector, neutrons are passing through an at least 22.7 cm layer of copper (in a straight direction to the detector). Copper has various applications in the nuclear energy industry. It is used in equipment of fusion facilities as divertors, magnets, microwave waveguides, and mirrors. In fission facilities, it is often used as an important structural component of spent fuel disposal cask.

The results of integral experiments of the simple geometries (sphere or slab) can be compared with calculations using different nuclear data libraries, making them very effective tools to test the validity of the neutron cross-section data. The reason is in fact, that an integral quantity, such as a neutron flux, can usually be measured much more accurately than differential nuclear data, so it is tempting to use such data to refine the nuclide cross-section evaluations[a].

In the past, number of measurements of the neutron flux originating from a neutron source and passing through the layers of different materials and geometries have been carried out in Research Centre Řež[b]. Some of them were focused on the measurement of the fast neutron leakage when filtered by iron spheres with different diameters and with a neutron source in its center.

1.1.   Overview of the Experiment

The benchmark describes the measurement, which was carried out at the Research Centre Řež (RCR, Centrum výzkumu Řež), of fast neutron leakage fluxes from a copper block 49.5 cm × 49.5 cm × 48 cm with a ^{252}Cf(s.f.) (spontaneous fission) neutron source placed in the center. The block is composed of 48 Cu plates, each with dimensions 49.5 cm × 49.5 cm and thickness of 1 cm. The plates are screwed into separate assemblies (see Figures 1 and 2) together forming a copper block 48 cm in width (due to air gaps between single assemblies the measured width is 48.2 cm). The block consists of a total 7 assemblies with different thickness; 2 assemblies with 8 cm, 2 with 4 cm, one with 7 cm. Central copper assembly is 8 cm thick and has a cylindrical hole with a diameter (ø) of 2.6 cm and a height of 27.75 cm for placement of the ^{252}Cf(s.f.) neutron source and one edge assembly is 9 cm thick and has a square cavity 7 cm × 7 cm (see Figure 2) used for measurements[c]. The central hole is optimized for positioning of the neutron source. During the measurement, ^{252}Cf(s.f.) neutron source is in the transport capsule at the bottom of the end tube of the flexo-rabbit transport system, which is at a position of 27.75 cm below the top of the block and thus the bottom end of tube is 3 cm below the axis. This ensures the position of the source ^{252}Cf (s.f.) in the middle of the Cu block.

[a] V. Radulovic, A. Trkov, Integral Data in Nuclear Data Evaluation, INDC(NDS)-0746, IAEA, 2018.

[b] M. Schulc, M. Košťál, E. Novák, V. Rypar, Measuring neutron leakage spectra using spherical benchmarks with 252Cf source in its centers, Nuclear Instruments and Methods in Physics Research Section A: Accelerators, Spectrometers, Detectors and Associated Equipment, Vol. 914, (2019), pp. 53-56

[c] M. Schulc, M. Košťál, E. Novák, J. Šimon, Copper neutron transport libraries validation by means of a ^{252}Cf standard neutron source, Nuclear Engineering and Technology, https://doi.org/10.1016/j.net.2021.04.029

In each assembly, there is a protruding part, 2 cm thick, and 5 cm long with drilled holes (Figure C.3. in Appendix C) for assembly manipulation. Holders are made of copper with the same properties as the Cu block benchmark assembly. The copper assemblies are joined together only in the upper protruding parts, which means that they are not connected to each other at the bottom. To minimize the gaps between the assemblies at the bottom, the copper block is not suspended on a crane but is placed on a special aluminum support (see Figures 1 and 3).

A fast neutron leakage flux measurement in the RCR uses a proton recoil method with a digital spectrometer and a stilbene scintillation detector in the energy interval 1 MeV to 11 MeV. The methodology and techniques of fast neutron flux measurement in spherical benchmark arrangements are presented in [1].

Based on the analysis of the data and uncertainties (in tables 1 sigma uncertainty is listed) of the measurements, the data are found to be acceptable for use as benchmark measurements.

1.2.   **Description of the Experimental Configuration**

The experiment was carried out in the Neutron Source Laboratory (NSL) on a Cu block 49.5 cm $\times$ 49.5 cm $\times$ 48 cm. The room effect in this case has low magnitude because of the large dimensions of the lab. The ^{252}Cf(s.f.) source is transported in a special transport capsule from the storage container located in a neighboring lab to the irradiating position in the center of the copper block by the pneumatic flexo-rabbit transport system. The components of the flexo-rabbit are made from aluminum alloys, the source is ^{252}Cf oxide in palladium matrix and stored in a hermetically sealed double-coat stainless steel box.. Felt is used as shock absorber.

Four experiments were carried out when the first experiment lasting 5.233E+05 seconds started on 30.5.2020, second lasting 3.257E+05 seconds on 5.6.2020, third lasting 5.957E+05 seconds on 9.6.2020, and fourth with the cone lasting 1.640E+06 seconds on 16.6.2020.

The NSL room dimensions are 7.24 m $\times$ 6.5 m with a height of 7.2 m. The center of the copper block, where the neutron source is located, is in a horizontal plane in the center of the lab, in a vertical plane 2 m above the floor. Photos of the copper block and the LNS laboratory are shown in Figure 1, the scheme of the block is shown in Figure 2. The geometry with a shielding cone can be seen in Figure 3. The block axis, which is identical to the stilbene axis, passes horizontally through the plates and is oriented parallel to the longer lab wall. Towards the stilbene measuring position, the block is full, on the opposite side, there is a 7 cm $\times$ 7 cm $\times$ 49.5 cm rectangular cavity. The center of the cavity is in the central plane of the block, 19.5 cm from its axis (See Figure 2). This cavity is primarily intended for in-block measurements (by stilbene or activation).

Although the NSL laboratory room is large, it has still a limited size, then the neutron leakage is affected by scattering from the floor, walls, and structural components present in the room. Accurate measurement, evaluation and description of the scattered neutron share are therefore very important for the evaluation of leakage from the copper block with a ^{252}Cf neutron source in its center. The experimental procedure consists of measurements with and without the shielding cone. The signal plus the background (scattered neutrons from the walls, ceiling, and floor of the laboratory room) is determined by measurement without the shielding cone. When the leakage flux is measured using the shielding cone, only the background contribution is determined. Finally, both primary proton fluxes are subtracted to determine the final "pure" recoil proton flux. The pure neutron flux is evaluated by deconvolution of the pure proton recoil flux.

A digital spectrometer and a small stilbene scintillation detector (1x1 cm) were used in measurements. The center of a crystal was placed at the distance of 100 cm from the center of the benchmark assembly where the ^{252}Cf(s.f) neutron source was positioned (i.e. 76 cm from the surface of the block). The detector-source plane is parallel with and 200 cm above the floor. As the center of the copper block is in the center of the room, the detector center is 500 cm and 300 cm from the walls and approximately 500 cm below the ceiling.

Figure 1: Photo of Copper Block in LNS Laboratory.
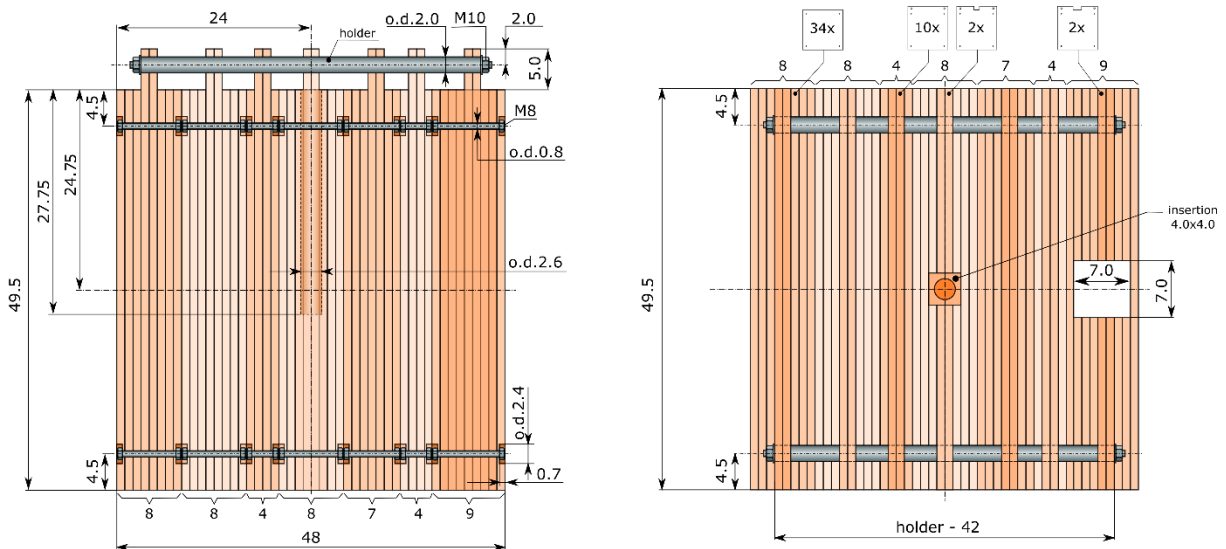
Figure 2a: Scheme of Copper Block used in Experiments in horizontal and vertical cuts.
In the vertical plane it is square 49.5 cm × 49.5 cm. Dimensions are in cm.
In the vertical plane it is square 49.5 cm × 49.5 cm. Different colors indicate single assemblies or details for each assembly.
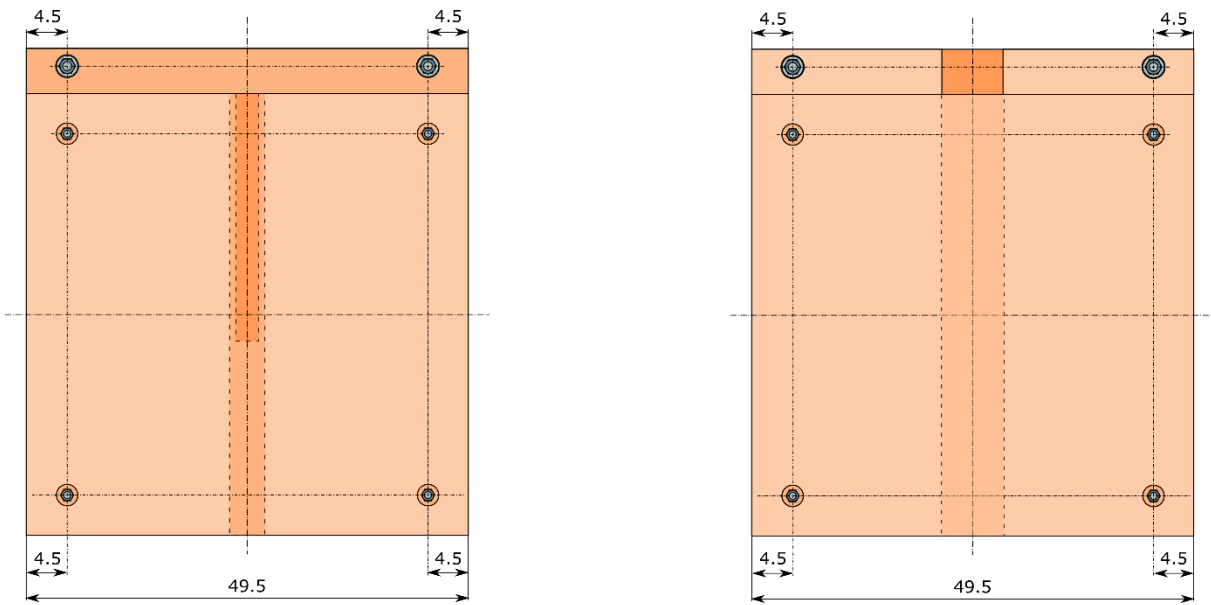
Figure 2b: Scheme of Copper Block used in Experiments in frontal cuts. Dimensions are in cm.
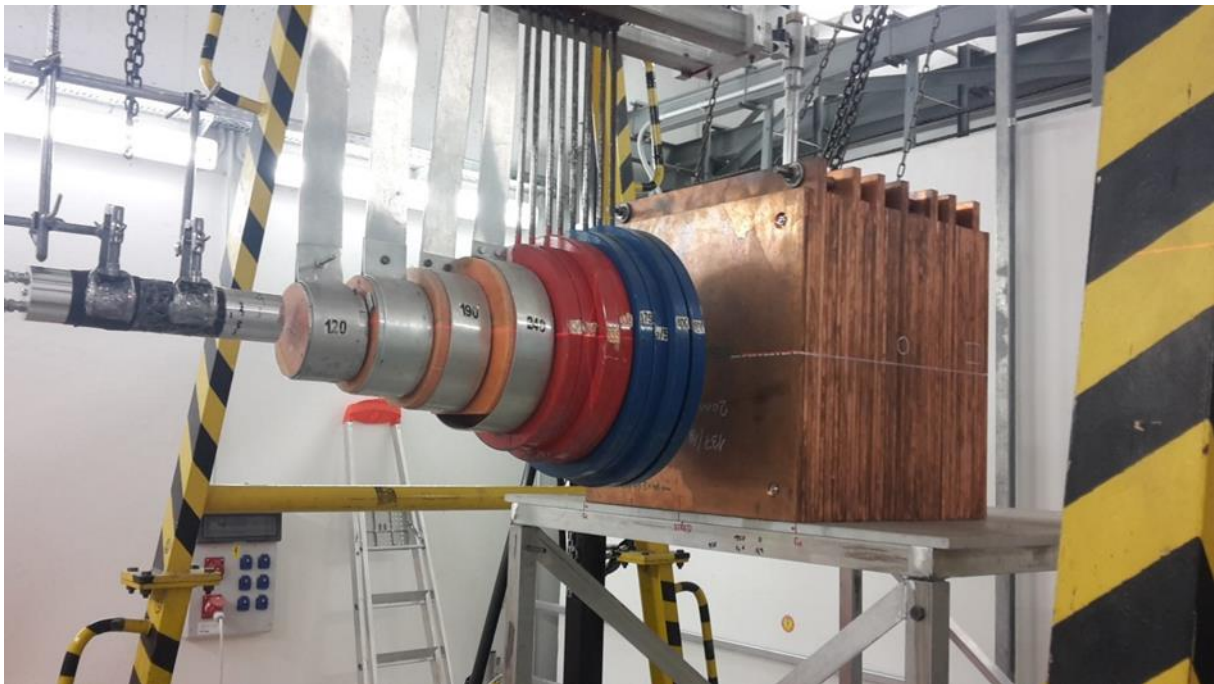
Figure 3: Photo of Copper Block with Shielding Cone.
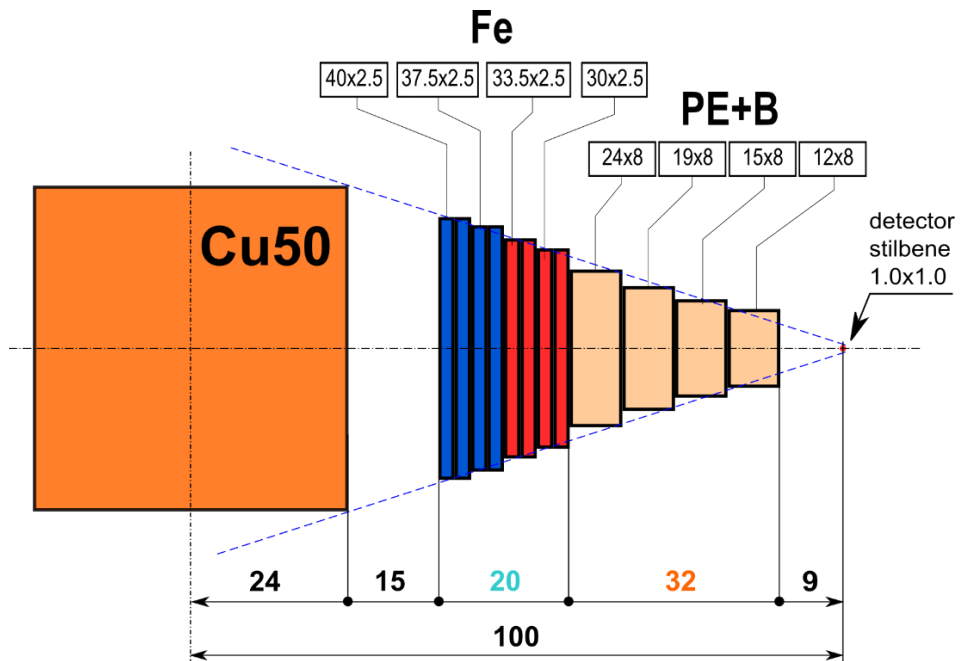
Figure 4: Copper Block with a Shielding Cone (Iron and Borated Polyethylene Cylinders). Dimensions in cm.

The geometry of the shielding cone used for measurement with copper block is illustrated in Figure 4, where radial distances are in cm and the dimensions of the shielding cone are given in cm and in the notation diameter × thickness. The sources contributing to the room effect can be seen in Figure 5.
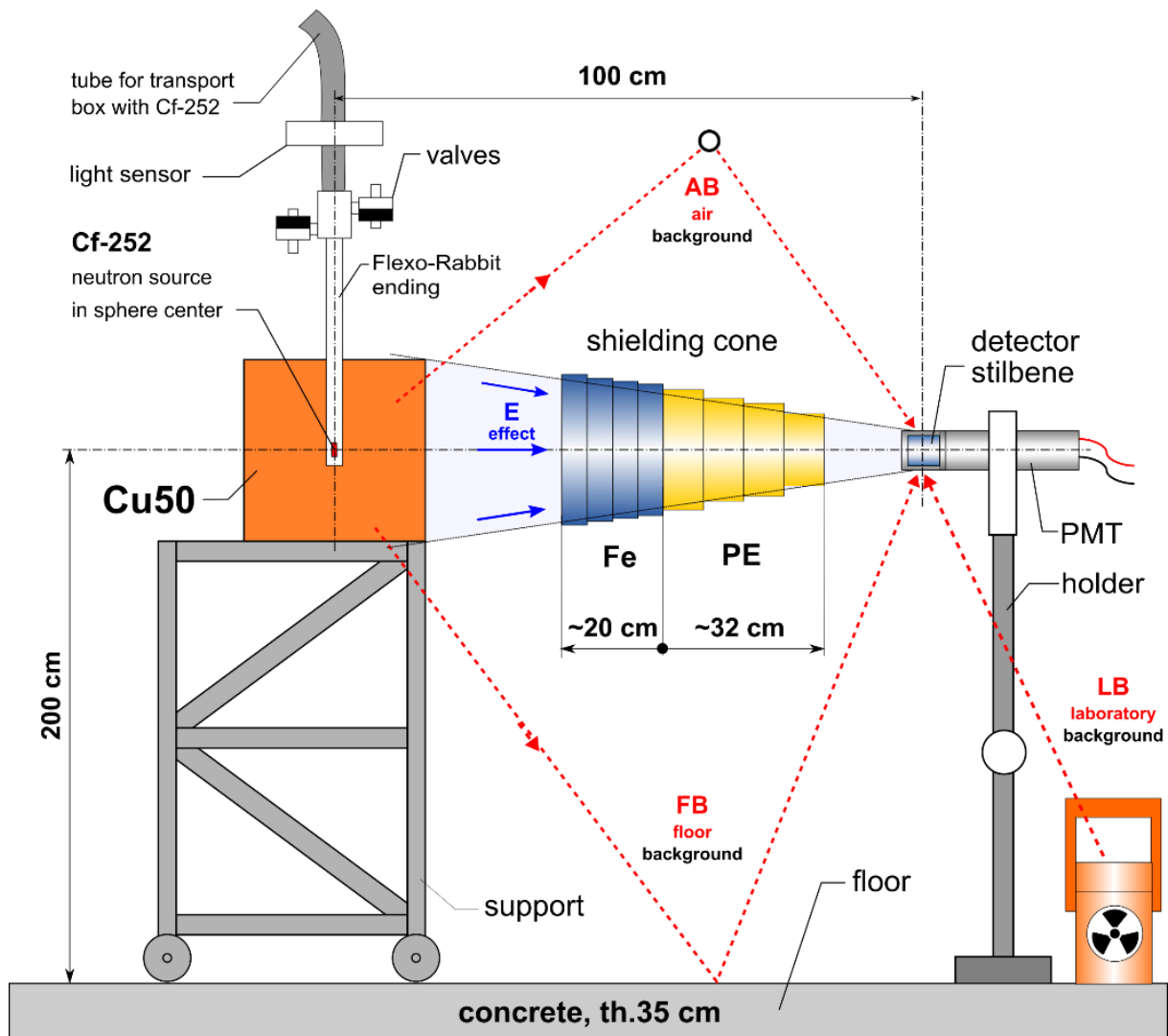
Figure 5: Background Measurement with Copper Block and Shielding Cone.
Dimensions in cm.

1.3. Description of Material Data

The material description for the neutron source flexo-rabbit system was analyzed in the central analytical laboratory of the Nuclear Research Institute Rez (NRI Rez, UJV Rez) and is given in Tables 1.1 and 1.2, the density of flexo-rabbit ending tube was measured to be 2.7 g/cm³ and for transport capsule 2.63 g/cm³. The properties defined by producer are given in Table 1.8. The data in these tables differ slightly because data in Tables 1.1 and 1.2 were obtained experimentally, while the data in Table 1.8 are tabulated data for material used in the production of components. For copper, the composition was obtained from the material data sheet (Table 1.3) with declared density 8.9 g/cm³ ± 0.09 g/cm³. XRF (X-ray fluorescence) analysis, which is shown in table 1.4, was used to verify the producer data. Further, the material description for the copper experiment uses the resulting composition determined by XRF analysis (see Table 1.4, and more details in APPENDIX F) and the experimentally measured density (using He pycnometry see APPENDIX G) of 8.8635 g/cm³ ± 0.0088 g/cm³. It is worth noting both data are in good agreement. The experimental data are burdened by smaller uncertainties than those tabulated by copper plates producer. The felt parameters, density, 0.185 g/cm³, and composition were taken from radiation shielding compendium[a] and are listed in Table 1.5.

---

[a] R.G. Williams III, C.J. Gesh, R.T. Pagh, Compendium of Material Composition Data for Radiation Transport Modeling, PNNL-15870, 2006

Table 1.1. Ending tube of flexo-rabbit mass fraction.

Element	Mass fraction
Al	0.966
Mg	0.032
Mn	0.002

Table 1.2. Transport capsule mass fraction.

Element	Mass fraction
Al	0.946
Mg	0.05
Mn	0.004

Table 1.3. Copper mass fraction, Cu plates producer data sheet[a]

Element	Mass fraction
Cu	> 0.999
Pb	0.00005
O	0.0004
Bi	0.000005
Ag	0.00015

Table 1.4. Copper mass fraction , XRF analysis.

Element	Mass fraction	Unc.
Cu	0.99856	0.00041
Cl	0.00077	0.00008
Ni	0.00012	0.00004
Ca	0.00022	0.00016
K	0.00023	0.00016
Fe	0.00008	0.00002
Ag	0.00002	0.00001

Table 1.5. Felt mass fraction, data from compendium[b]

Element	Mass fraction
H	0.0442
C	0.4346
N	0.1765
O	0.3447

1.4. Description of the Source

Neutron source ^{252}Cf was manufactured by the Frontier Technology Corp. (USA, FTC) [c]. The source is encapsulated in a Frontier model 100SNS capsule loaded within the piping of the flexo-rabbit post into a measurement position (Figures 2, 5). FTC documentation describes neutron source as a double-encapsulated ^{252}Cf source, where the Cf needle (little stick "bundle") is sealed in an FTC model 10S

[a] EN 1652: 1998 Copper and copper alloys. Plate, sheet, strip and circles for general purposes
[b] R.G. Williams III, C.J. Gesh, R.T. Pagh, Compendium of Material Composition Data for Radiation Transport Modeling, PNNL-15870, 2006
[c] https://www.frontier-cf252.com/neutron-sources/

inner case and outer 100SNS case, both welded by TIG method (tungsten-inert gas welding). The FTC10 and FTC 100S capsules are made of stainless steel of type 304L with the dimension given below in Table 1.6.

The ^{252}Cf neutron source had an emission rate of $(9.53 \pm 0.055) \times 10^8$ s^{-1} on August 13th, 2015 (Certificate of calibration involving manganese sulphate bath performed in National Physical Laboratory, UK). The absolute calibration uses a pure ^{252}Cf neutron source.

The illustration of the transport aluminum box and FTC-CF-5209 neutron source ending is shown in Figure 6. The geometry of the aluminum transport box for flexo-rabbit (pneumatic transport system) is shown in Figure 7. The FTC neutron source stainless steel cases of 100SNS and 10S type are shown in Figure 8. The geometry and schematic drawing of FTC-Cf-5209 assembly with double coated neutron source ^{252}Cf in transport box for flexo-rabbit are shown in Figure 9. The materials of the transport capsule, including the detail of the Cf needle position in the transport capsule, are shown in Figure 9, where the ^{252}Cf "needle" is in red, the aluminum transport capsule is in blue, the felt liner (it absorbs the shock of the source falling to the bottom of the flexo-rabbit ending and back to the storage container) is in yellow, and the 304L stainless steel capsule is in green. The geometry of the Pneumatic flexo-rabbit End Cap (Al) with the Cf source position within a measurement is shown in Figure 10.
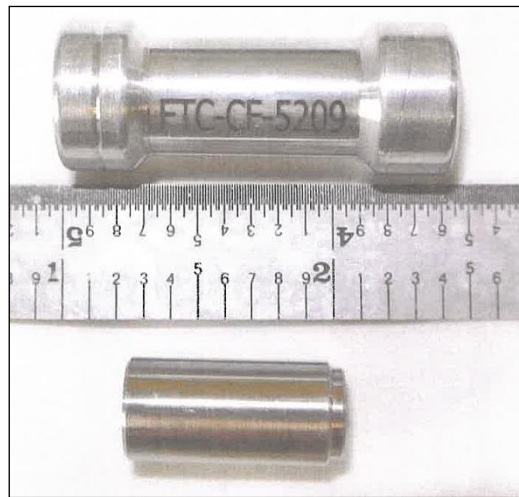
Figure 6: FTC-CF-5209 Neutron Source.
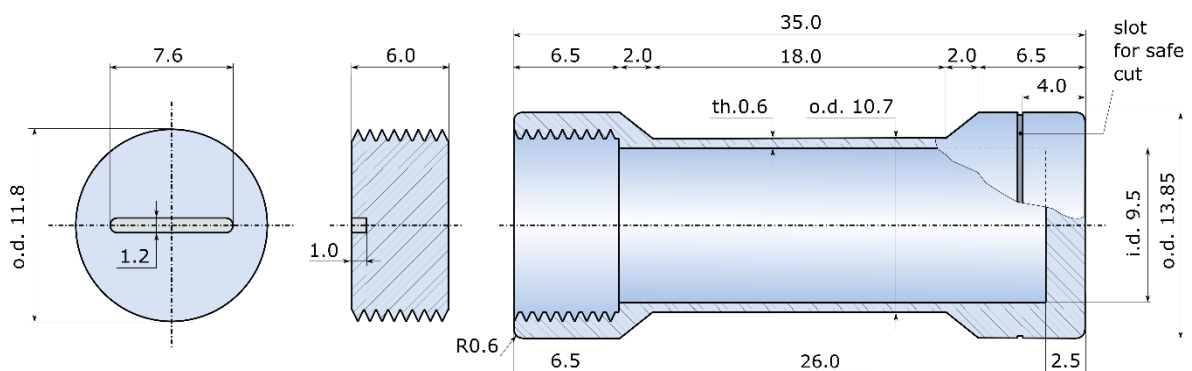
Figure 7: RCR Aluminum Transport Box for Flexo-Rabbit (pneumatic transport system). Dimensions in mm.

100SNS

10S
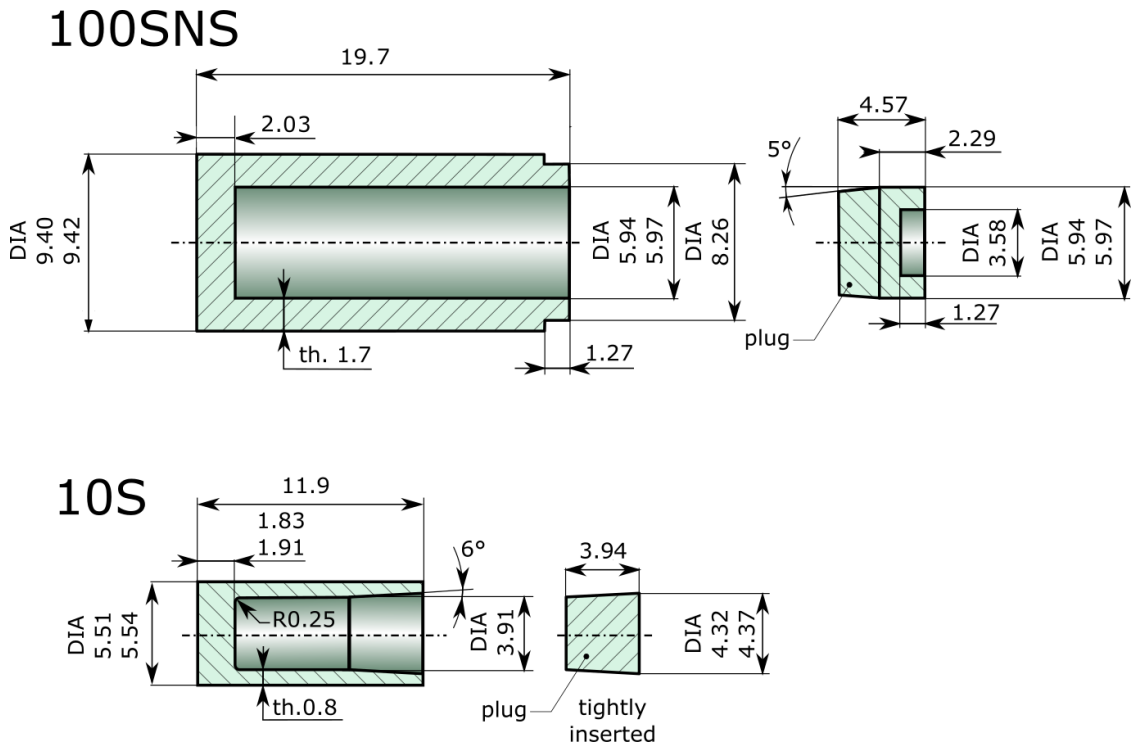
Figure 8: FTC Neutron Source Cases of 100SNS and 10S type – Stainless steel 304L. The dimensions (in mm) are taken from technical drawing in APPENDIX D "^{252}Cf Frontier Technology Corporation information" and recalculated from inches to mm (1 inch = 2.54 cm). The two values for the source capsule diameter correspond to the lower and upper limits taking into account the manufacturing tolerance (see Table 1.6).
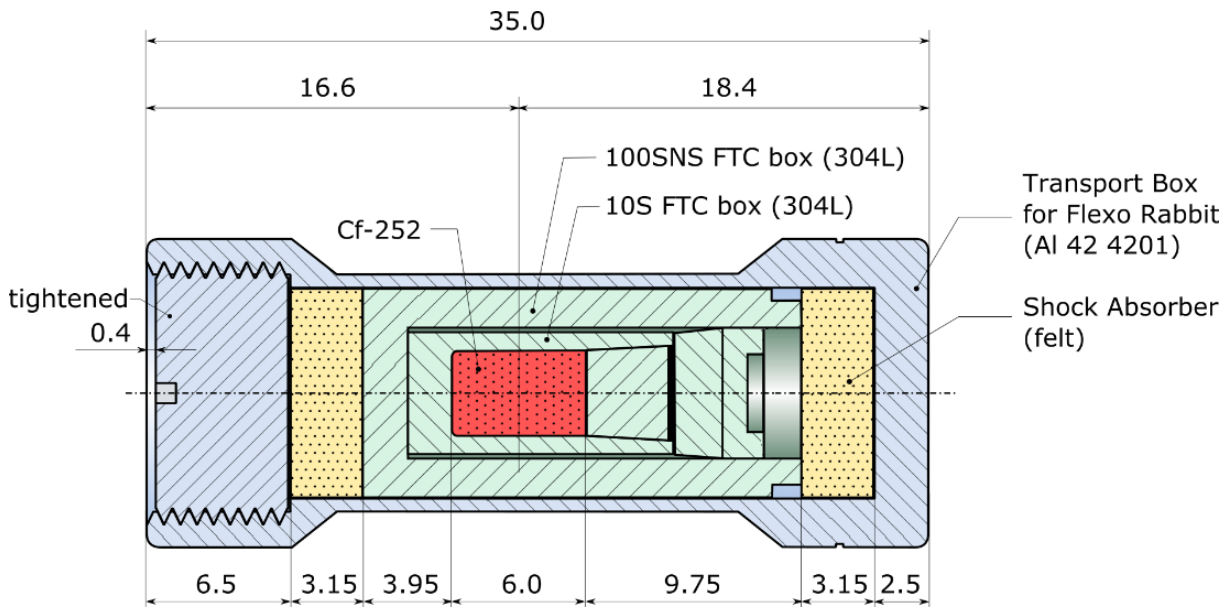
Figure 9: FTC-Cf-5209 Assembly with Double coated Neutron Source ^{252}Cf(s.f.) in transport box for Flexo-Rabbit. Dimensions in mm.

Table 1.6. Model FTC 100S and FTC 10S Source Capsules Geometry – Main Dimensions [inch].

Parameter	Dimension FTC 100SNS	Dimension FTC 10S
Outside diameter	0.370 to 0.371	0.217 to 0.218
Outside length	0.775	0.470
Inside diameter	0.234 to 0.235	0.154
Inside length/ Bottom thickness (10S)	0.695 0.08	NA (0.072 to 0.075)
Plug diameter	0.234 to 0.235	0.170 to 0.172
Plug length	0.180	0.155
Plug "gap" diameter	0.141	X
Plug "gap" length	min. 0.05	max. 0.005
Cavity length	max. 0.475	min. 0.235

Table 1.7. Source capsule composition (Stainless steel 304L).

Element	Mass fraction
Mn	0.02 max.
C	0.0003 max.
Si	0.0075 max.
Cr	0.18 – 0.20
P	0.00045 max
S	0.0003 max
Ni	0.08 – 0.12
N	0.001 max
Fe	Balance

Table 1.8. Composition of source transport capsule and transport tube materials (flexo rabbit producer's data).

Material	Element	Mass fraction	Corresponding standard or reference
Aluminum transport capsule density: 2.79 g/cm^3	Al	0.946	ČSN 42 4201
	Mg	0.05	
	Mn	0.004	
Aluminum flexo-rabbit tubes density: 2.68 g/cm^3	Al	0.966	ČSN 42 4413
	Mg	0.032	
	Mn	0.002	

The geometry of FTC 10 and FTC 100S source capsules are given in Table 1.6, where the data were recalculated from the source manufacturer's data (Frontier Technology Corporation.) given in inches. The composition of the source capsule is in Table 1.7, the density of used material is defined density 8.0 g/cm^3. and is given by the producer with a density of 8.0 g/cm^3. The composition of the flexo-rabbit end cap is in Table 1.8 and is specified by the flexo-rabbit producer, the densities are listed in the same table.
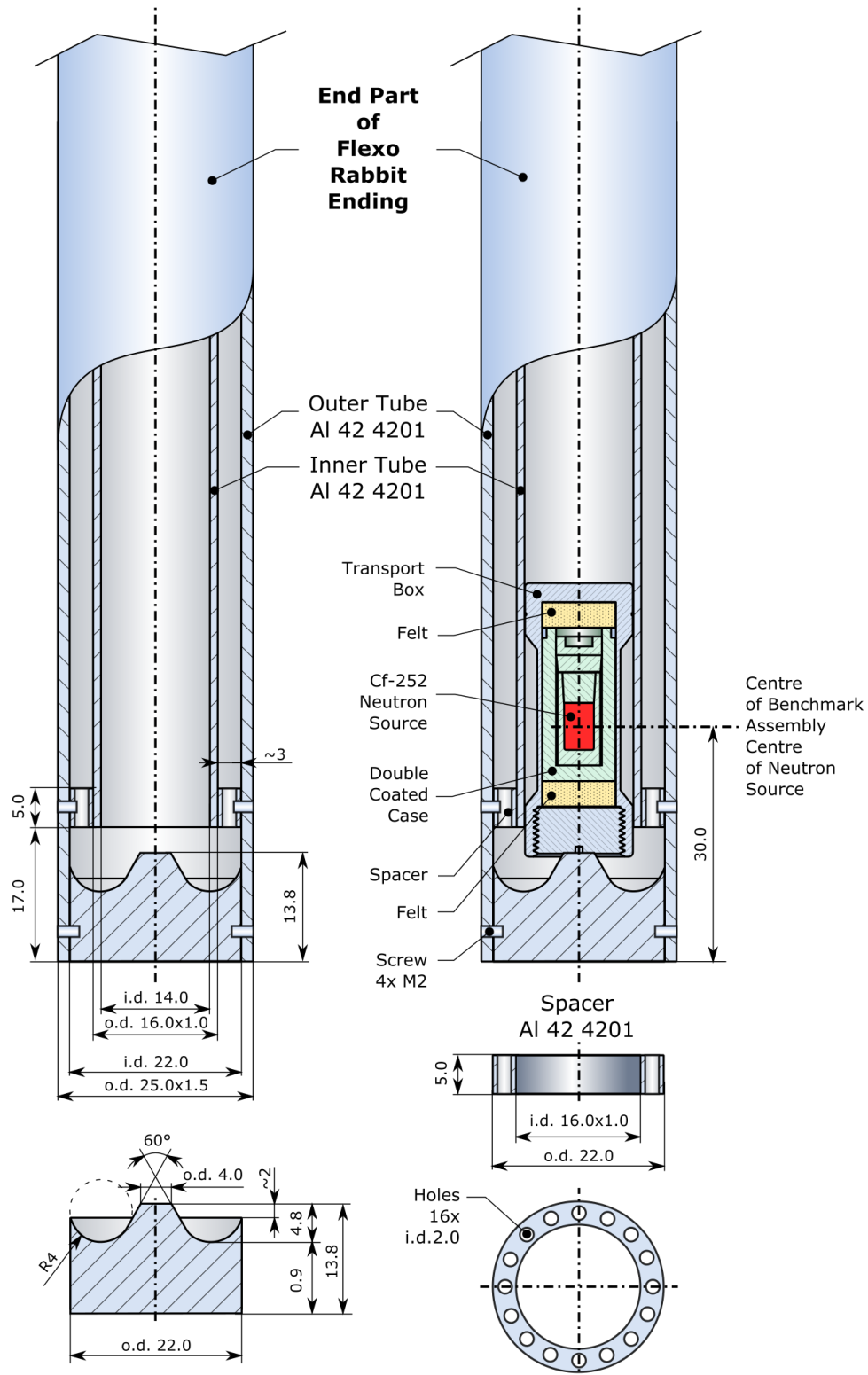
Figure 10: Pneumatic Flexo-Rabbit End Cap (Al) with the Cf Source in Measurement Position. Dimensions in mm.

1.5. Description of the Detector

The cylindrical ø 10 mm × 10 mm scintillation stilbene detector was used for measuring neutron leakage fluxes in the energy range of 1.0 MeV to 11 MeV in 100 keV groups.

The stilbene detector uses the proton recoil method with neutron and gamma pulse shape discrimination by digital processing of the detector signal. More about this two-parametric spectrometric system can be found in a separate publication[a]. The ø 10 mm × 10 mm stilbene detector crystal (diameter × height) is shown in Figure 11. This figure also shows the ø 45 mm × 45 mm detector for comparison; but it should be noted that this detector is used mostly for gamma measurements. In case of neutrons it can be used for measurements in environments with low gamma share in N/G field (Am-Be sources, DT sources, accelerator sources).

Figure 11: Stilbene Crystals ø 45 mm × 45 mm and ø 10 mm × 10 mm.

1.6. Measurement Techniques

The method of recoil proton measurement inferred from the elastic scattering of neutrons on hydrogen nuclei, (n, n) reaction, was utilized to determine fast neutron leakage fluxes. The fast neutron fluxes in the energy range 1 MeV to 11 MeV were determined from the measured signal of a two-parameter multichannel analyzer and detection system with stilbene cylindrical scintillators. A block diagram of the Stilbene spectrometric system is shown in Figure 12. This two-parameter system allows simultaneous measurement of recoil proton (from neutron) and Compton electron (resulting from gamma rays' interactions) fluxes with a stilbene scintillator. Measured pulse height fluxes due to recoil protons and electrons are separated with the pulse shape discrimination method described in a separate publication[b]. An illustration of a measured neutron and gamma caused pulse of similar height is plotted in Figure 13. The detector response functions of the neutrons and photons[c] were calculated with the in-house-made Monte Carlo type code NEU6. The response functions were later validated in PTB (Physikalisch-Technische Bundesanstalt, Braunschweig) on 5 monoenergetic lines and in the whole energy spectrum with a pure ^{252}Cf source.

The verification was performed with a silicon-filtered beam, a radial beam coming from a VR-1 research reactor, and also a ^{241}AmBe radioisotope field. (This part can be found in Aappendix B.)

---

[a] J. Bureš, F. Cvachovec, P. Cvachovec, P. Čeleda, B. Ošmera: Multiparameter multichannel analyser system for characterisation of mixed neutron-gamma field in the experimental reactor LR-0, Reactor Dosimetry in the 21st Century: Proceedings of the 11th International Symposium on Reactor Dosimetry Brussels, 2002, 194-201

[b] M. Veškrna, Z. Matěj, F. Mravec, V. Přenosil, F. Cvachovec, M. Košťál, Digitalized two parametric system for gamma/neutron spectrometry, 18th Topical Meeting of the Radiation Protection & Shielding Division of ANS, Knoxville, TN USA, 2014

[c] F. Cvachovec, P. Tajovsky, J. Cvachovec, Neutron Response Function for Stilbene Detector in Energy Range 0.5 to 20 MeV, International Workshop on Neutron Field Spectrometry in Science, Technology and Radiation Protection, Pisa, Italy, 2000
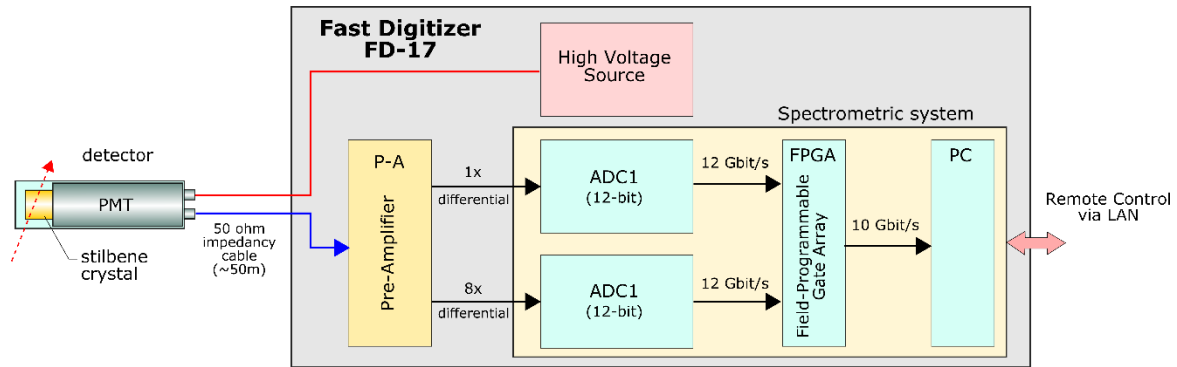
Figure 12: Spectrometric System with Stilbene Detector - Basic Scheme.

Neutron fluxes measured by stilbene were evaluated in a wide energy group format (0.1 MeV) corresponding to the spectrometer energy resolution. Scintillations in organic scintillation detectors are caused not only by neutron interactions, but also by gamma ray interactions. Separation of the recoiled proton signal from the signal caused by Compton electrons produced from interactions of gamma rays in the crystal and in its cover is based on the different shapes of the scintillation pulses. These result from different stopping powers of protons and electrons. In organic materials, the Compton scattering effect dominates, therefore during interactions with gamma rays the electrons in the atomic envelope may be recoiled. The light pulses from gamma interactions are slightly different than those from neutrons. In case of fast electron interactions, a larger fraction of their scintillation light output is generated in a prompt component, compared to proton interactions. This manifests itself in a longer decay time of scintillations caused by neutrons (see Figure 13) and enables separation of photon pulses from neutron pulses by means of pulse shape discrimination (PSD). This feature, i.e. PSD, shows that the organic scintillation detector is suitable for detection of particles in a mixed neutron/gamma field. The main advantage is that neutron data are measured simultaneously with photon data. The evaluated response where each particle has an assigned discrimination factor, see Eq. (2), is plotted in Figure 13.

Energy-dependent recoil proton responses $S(E_p)$ can be deconvoluted to fast neutron fluxes using Eq. (1), where $K(E_N,E_P)$ is the response function of a spectrometer and $\phi(E_N)$ is the energy-dependent neutron flux in the detector.

$$S\left(E_p\right) = \int K(E_N, E_P)\phi(E_N)dE_N \qquad (1)$$

Measurements require collecting (integrating) responses and fluxes in energy groups (bins). The proton recoil response $S_{pg} = \int_{pg} S(E_p)$ where the integral is over the specific proton energy group pg. The neutron flux $\Phi_{ng} = \int_{ng}\Phi(E_n)$ where the integral is over the specific neutron energy group ng. Deconvolution of measured, time-integrated, energy-binned proton responses $\int_t S_{pg}$ into time-integrated, energy-binned neutron fluxes $\int_t \Phi_{ng}$ was performed using Maximum Likelihood Estimation[a] (see Appendix B).

The primary data for determining the fast neutron leakage flux, the recoiled proton response, is measured in two steps. In the first step, the proton recoil response is measured with the room effect, then a shielding cone is employed to shield the primary leakage neutrons and allowing to determine the effect of the background. Finally, the responses are subtracted from each other.

The background due to scattered neutrons from walls, floor and ceiling is measured with the experiment arrangement shown in Figure 5, where the marking of individual components is as follows: E - pure leakage neutrons, FB - neutrons scattered from laboratory walls and floor, AB - neutrons reflected from air, and LB - laboratory background neutrons. If we denote S and C neutron leakage fluxes measured with and without shielding cone, then S = E + FB + AB + LB, C = FB + AB + LB and pure spectrum E = S - C.

---

[a] J. Cvachovec, F. Cvachovec, Maximum Likelihood Estimation of a Neutron Spectrum and Associated Uncertainties, Advances in Military Technology, Vol.1, No. 2 January 2007, pp. 5 – 28

1.6.1. Neutron and photon spectrometry with stilbene detector

Fluxes in the energy range above 0.6 MeV for neutrons and above 0.2 MeV for photons are measured with a two-parameter multichannel analyzer, nuclear electronics for detector signal processing (preamplifier, high voltage supply, analyzer) and stilbene scintillator of cylindrical geometry with dimensions ø 10 mm × 10 mm and photomultiplier RCA 8575.

The two-parameter spectrometric system is fully digitized and is able to process up to 500 000 cps (impulses per second) in the energy range from 0.6 MeV to 15 MeV. A tapered active voltage divider was used for the photomultiplier tube. This type of divider has better output linearity than previously used passive resistance, where the problem with non-linearity could exist even at relatively low rates about 10^4 impulses per second. Solving the non-linearity problem with an active voltage divider based on MOSFETs also solves the problem of non-linearity depending on the amplitude of the signal.

The input analog signal from the photomultiplier is divided in the amplifier into two branches. Each branch is differently amplified in the ratio of 1:8 and digitized by separate analog to digital converters with 12 bits resolution. This different amplification increases the dynamic range of particle energy. The spectrometer is capable of processing and increase the signal to noise ratio. Two fast analog to digital converters (ADC12D1000), working with the sampling frequency 500 MHz, are used and the digital signal processing is implemented in a field-programmable gate array (FPGA Xilinx Virtex-6). Therefore, it is able to process all data flow from both analog to digital converters without any dead time.

The type of the detected particle is the first parameter determined by the spectrometric system. The separation between neutron and gamma pulses is realized by means of the shape discrimination [OBJ] of the measured response. Pulse Shape Discrimination parameter (D) is derived by an integration algorithm which principle lies in comparison of area limited by part of a trailing edge of the measured response (Q1) with area limited by the whole response (Q2). Q1 and Q2 areas, as integrals over time, are expressed in Eq. (2) and their illustration is shown in Figure 13.

$$Q_1 = \int_{t_2}^{t_3} i(t)dt, \quad Q_2 = \int_{t_0}^{t_3} i(t)dt, \quad D = \frac{Q_1}{Q_2} \tag{2}$$

The time offset t_2, at the maximum neutron amplitude, for calculating the area of the integral depends on the time constant of the apparatus and the use of a scintillator from the maximum gamma amplitude at time t_1. It is usually in the range of 5 ns to 16 ns for the stilbene detector and 50 Ω working resistor on the anode of the photomultiplier.

The time offset t_2 is set for the optimal discrimination properties (namely as the biggest as possible difference in the discrimination parameter for neutrons and gammas) to about 1/10 to 1/3 of the trailing edge. It varies for each scintillation material (stilbene, p-terfenyl). In this way, it is possible to eliminate the classification mistakes caused by the dependency of the response shape on its amplitude.

Charge Q_1 is determined by an area limited by the course of response within a time interval (t_2, t_3). The charge Q_2 is determined by an area that is limited by the course of response within firmly defined times t_0 and t_3. Times t_0 and t_3 are parameters dependent on parameters of the measuring apparatus. Time t_3 is defined as the end of the response.

The implemented integration method has linear computational complexity and therefore it is suitable for online measurement with a high number of impulses per second.

In environments with very high gamma background, the separation between neutrons and gammas might be complicated, which effect manifests itself in higher thresholds of neutron detection. Above-mentioned fact plays a significant role, especially in the case of environments with large amounts of

hydrogen. In the case of a large copper block, both neutron and gamma signals are well-evaluated at low energies (see Figure 14). The energy of the detected particle is the second parameter determined by the spectrometer. The energy is evaluated from the integral of the whole response to the incident particle.
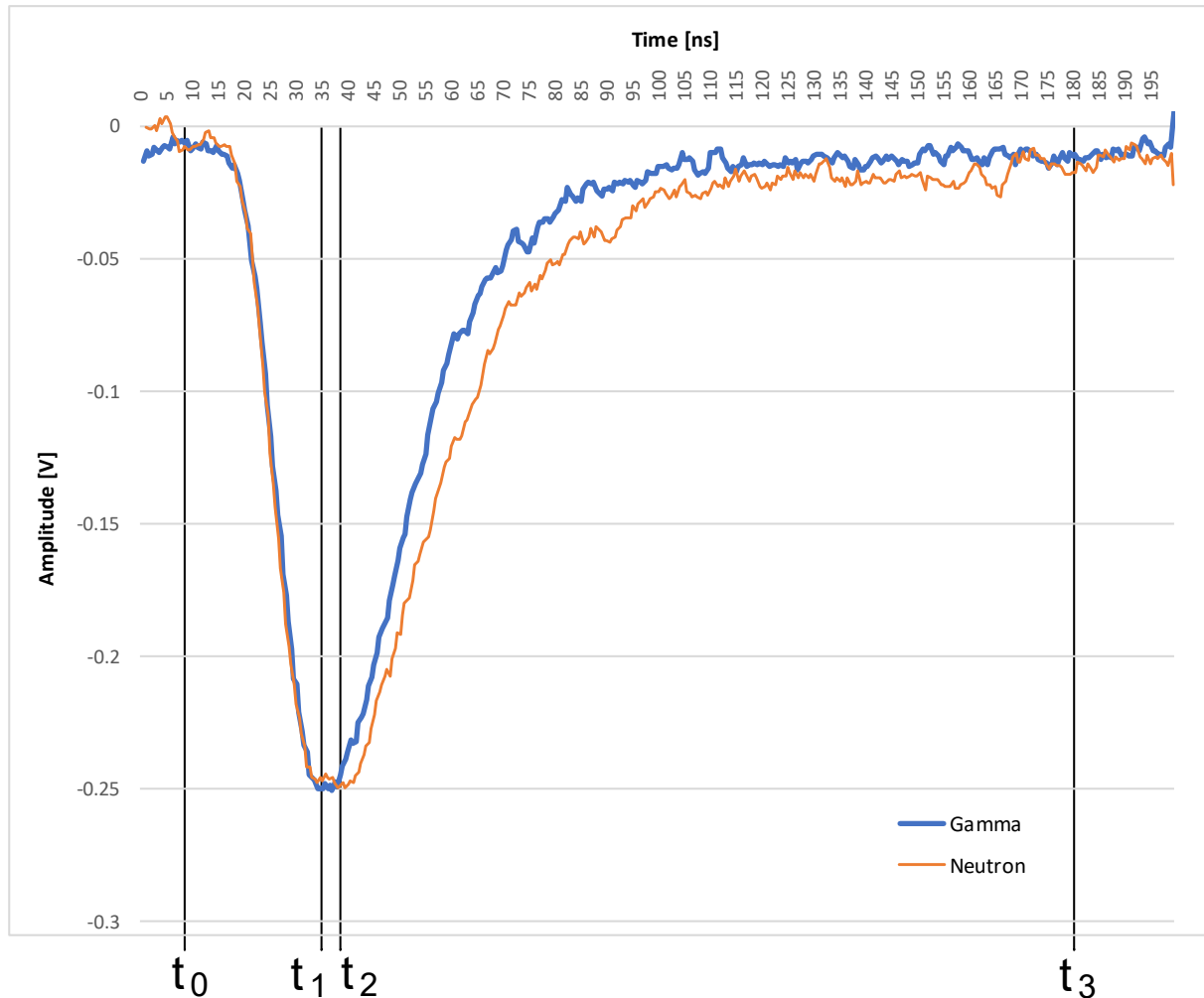
Figure 13: Example of Separation Boundary for Integration Algorithm on Real Data for Normalized Neutron and Gamma Output Pulses from Stilbene Scintillation Detector.

The next step for the neutron leakage flux evaluation is deconvolution of the recoiled proton response, which was performed using Maximum Likelihood Estimation. This method is described in detail in Appendix B.

Similarly, the photon flux is obtained from the deconvolution of recoiled electron responses. It is performed by Maximum Likelihood Estimation as in the case of neutrons. Photon flux is not included in this benchmark, because the gamma flux measured by small stilbene crystal is usable only for calibration purposes.
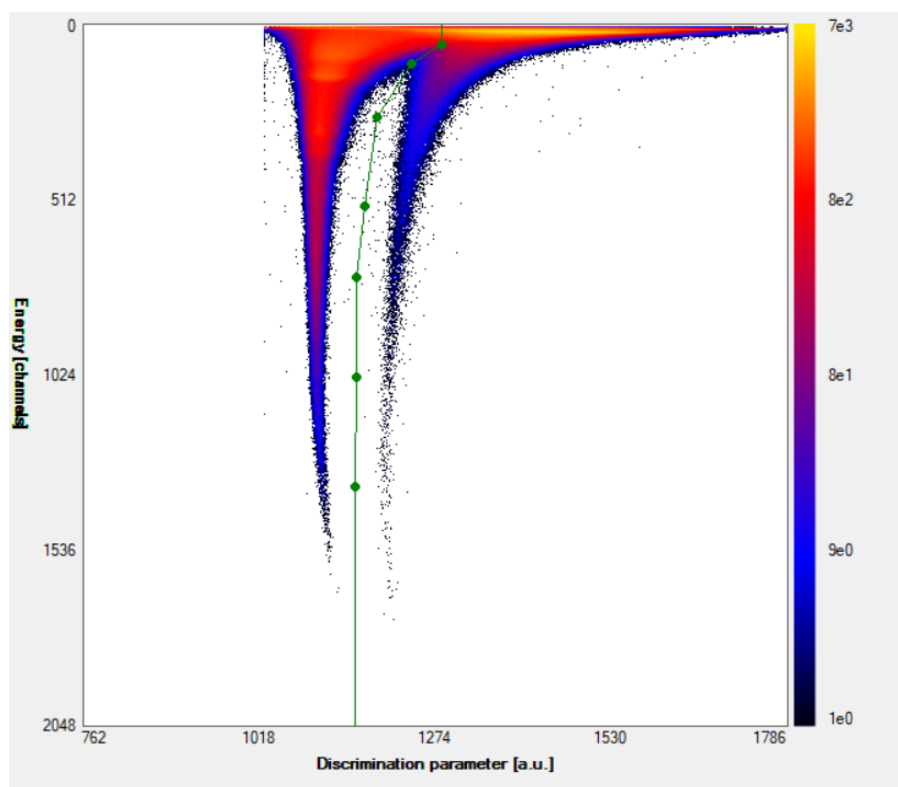
Figure 14: Measured Two Parametric Leakages from Copper Block.
The separation line is green, the gamma part (recoil electrons) is left, the neutron part (recoil protons) is right.

1.6.2. Energy calibration of Stilbene spectrometer

As the light outputs of the scintillator coming from gamma and neutron reactions are different, their precise characteristics are important in the determination of the stilbene response function and calibration. The neutrons and gammas in mixed fields can then be distinguished. The specialists from University of Defence (Brno, Czech Republic) tested the developed stilbene spectrometer in a Physikalisch-Technische Bundesanstalt (PTB, Braunschweig, Germany) reference neutron field. An accelerator, producing mono-energetic neutron fields (1.2 MeV, 2.5 MeV, 5 MeV, 14.6 MeV, and 19 MeV), has been used for absolute sensitivity and detector response function studies. Neutron flux evaluation procedures have also been tested in silicon filtered beams in RCR (see Figure B.4 in Appendix B). A measurement with a pure ^{252}Cf(s.f.) spectrum has been used for estimation of uncertainty in deconvolution (Figures 22 and 23, Section 2.1.1) because the ^{252}Cf(s.f.) is the primary neutron standard, which means the ^{252}Cf(s.f.) neutron spectrum is well known with low uncertainty [a].

The resulting electrons from gamma interactions are standardly used for organic scintillator calibration. This procedure is applicable under the assumption that the detection system including crystal, photomultiplier tube, and associated electronics is linear. The neutron calibration curve is determined using the gamma calibration curve (Figure 15) from the measurement using the gamma standards' Compton edge energy. An example of the calibration for ^{60}Co peaks is depicted in Figure 15, the calibration for ^{1}H(n,γ) peak in Figure 16. The linearity of the system is confirmed when the channels of the peaks and their corresponding energies have a linear dependence. For this measurement, the linearity is plotted in Figure 17.

[a] A. Trkov, P.J. Griffin, S.P. Simakov et. al., IRDFF-II a new neutron metrology library, Nuclear Data Sheets, Vol. 163, pp. 1-108 (2020).

With the known relation of scintillator light output to gammas and to neutrons, see Figure 18[a], the energy-to-channel number dependence, corresponding to gammas and neutrons, can be calculated and compared. Between the neutron and the gamma responses in stilbene, there is a linear dependence on neutron energy above ~0.5 MeV, see Figure 18. Thus, an indirect method for calibration by standard photon sources can be used, based on registration of the mono-energetic gamma source spectrum. A stilbene detector is usually calibrated by the ^{137}Cs peak at 661 keV (Compton edge E = 477 keV), and the ^{60}Co peak at 1332 keV (Compton edge E= 1118 keV) before or after a measurement. Another possibility is online calibration using gammas present in the mixed N/G field. Such gamma is, for example, the [1]H(n,γ) peak at 2223 keV (Compton Edge E=1994 keV) originating in neutron capture in the hydrogen present in the concrete in the floor, walls, and ceiling. This calibration approach was used for the evaluation of the current experiment.
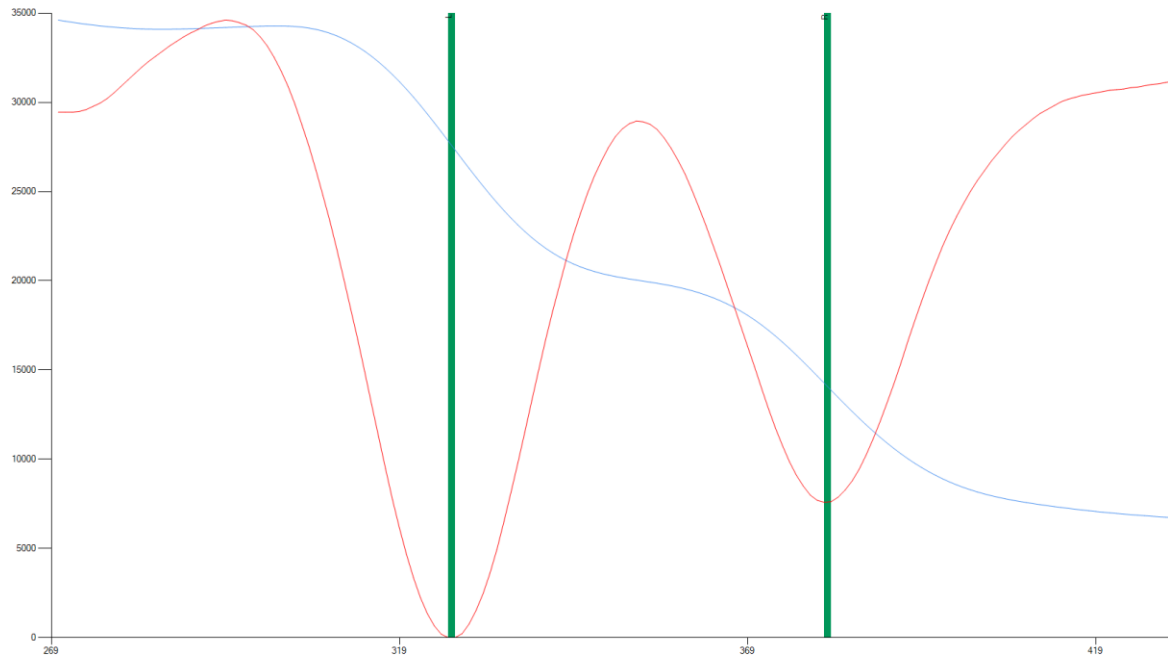
Figure 15: Calibration of the Apparatus Spectrum using [60]Co Peak.
The electron spectrum is the blue line, the differentiation of the spectrum with visible inflections is the red line. Green lines show channel number settings for energy scale calibration.

---

[a] V. I. Kuchtevic,V.I., O. A. Trykov,, L. A. Trykov,.: ODNOKRYSTALLNYJ SCINTILLJACIONNYJ SPEKTROMETR, Moskva, Atomizdat,1973.
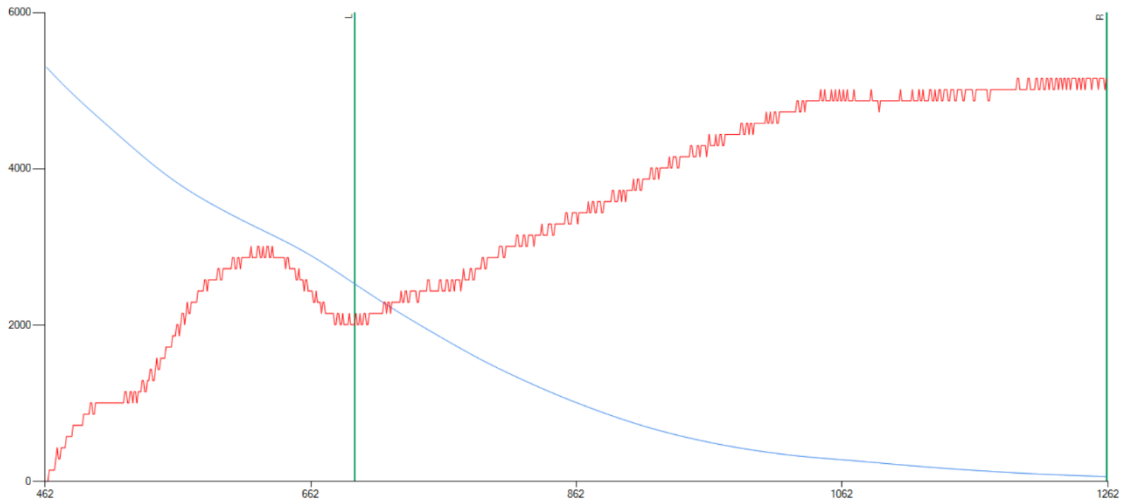
Figure 16: Calibration of Apparatus Spectrum using $^1H(n,\gamma)$ peak 2223 keV.
The electron spectrum is the blue line, the differentiation of the spectrum with visible inflections is the red line. Green lines show channel number settings for energy scale calibration.
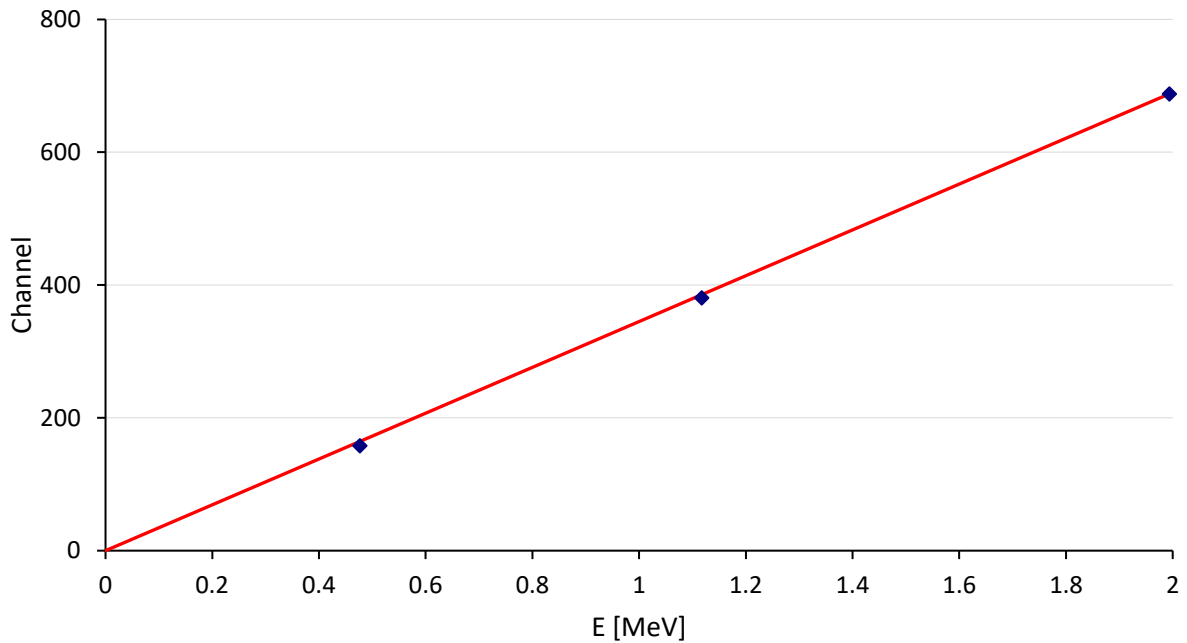
Figure 17: Linearity of Calibration (Cs line, Co line, $^1H(n,\gamma)$) U_{PMT}=1400 V.
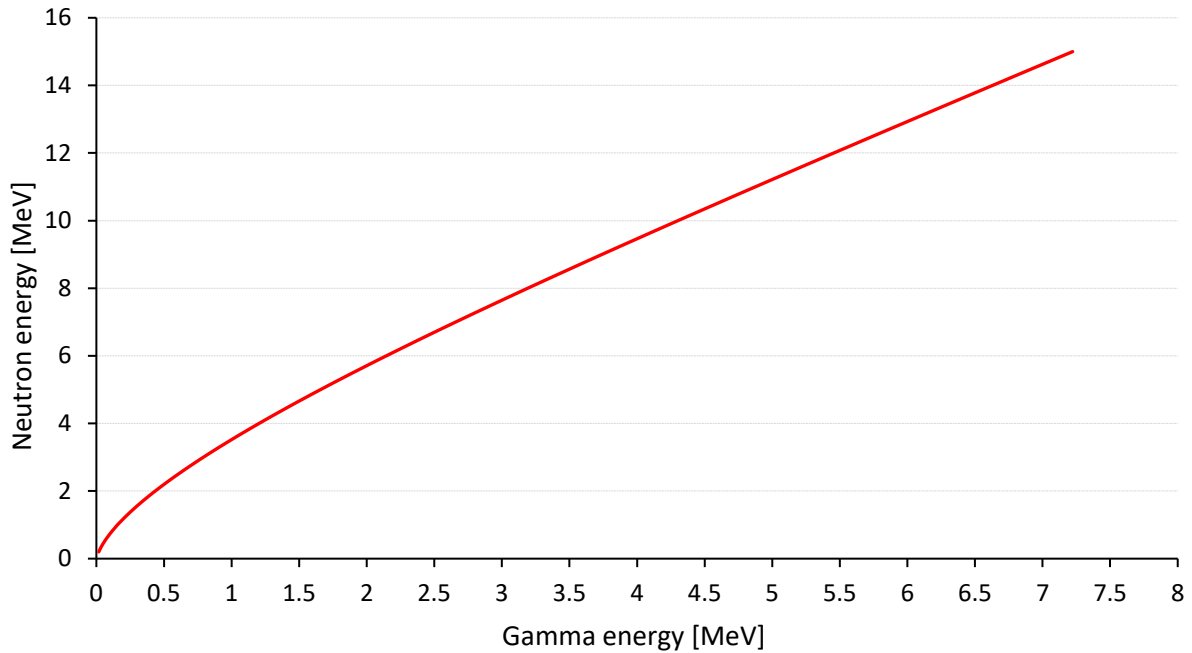
Figure 18: Relation between Neutron and Gamma Energy in Stilbene Detector.

1.6.3. Determination of the background effect

Both computational and experimental evaluations of the effect of backscattered neutrons are essential for the correct evaluation of the escape flux of neutrons from the copper block. In order to exclude scattered radiation background from the experimental data, measurements with a special shielding cone were always performed. An illustration of a shielding cone is shown in Figure 5. The shielding cylinders of different diameters are put together to constitute a cone. The diameter of cylinders is determined for covering of solid angle from the detector to the block.
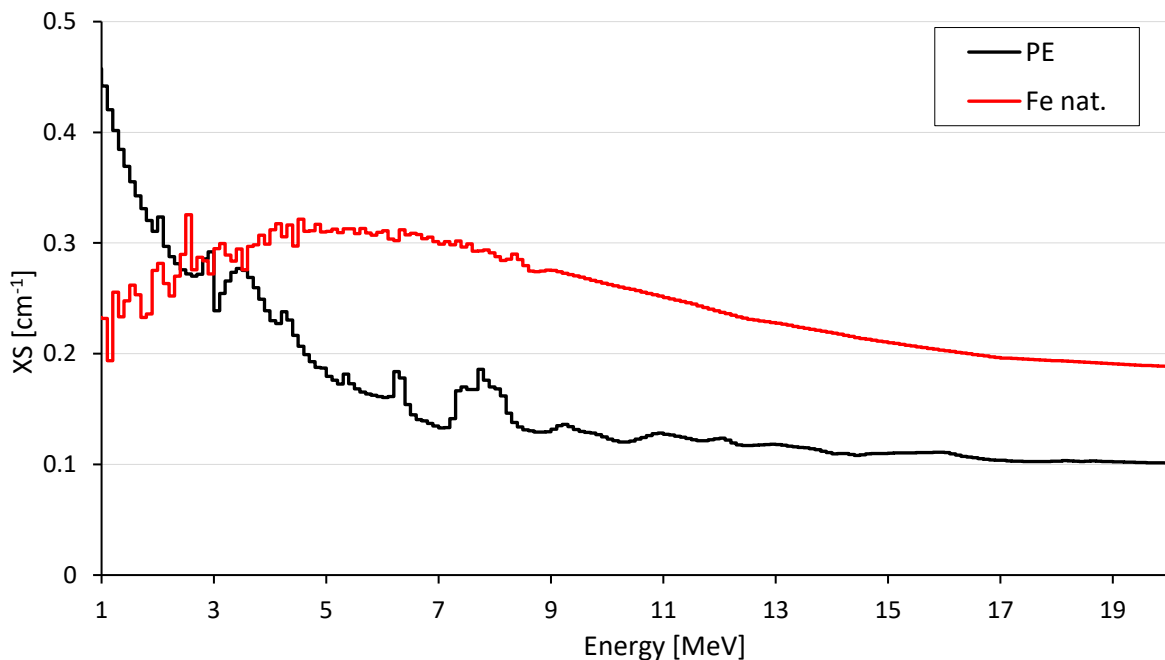
Figure 19: Total Cross Sections of Polyethylene and Natural Iron in ENDF/B-VIII.0.

The cone consists of iron and borated polyethylene, which are optimal to ensure the maximum possible attenuation with respect to the different cross-sections of the materials (see Figure 19). Iron is excellent

for slowing down the higher energy neutrons, while borated polyethylene is used for thermalization and following absorption of low energy neutrons.

Due to the large dimensions of the lab, the room effect in this experiment is relatively low. A comparison of the directly measured proton responses in measured channels with and without the shielding cone is shown in Figure 20, showing the fraction of all relevant proton measurement counts in each energy channel to the total associated neutron source (i.e., normalized to one source neutron).
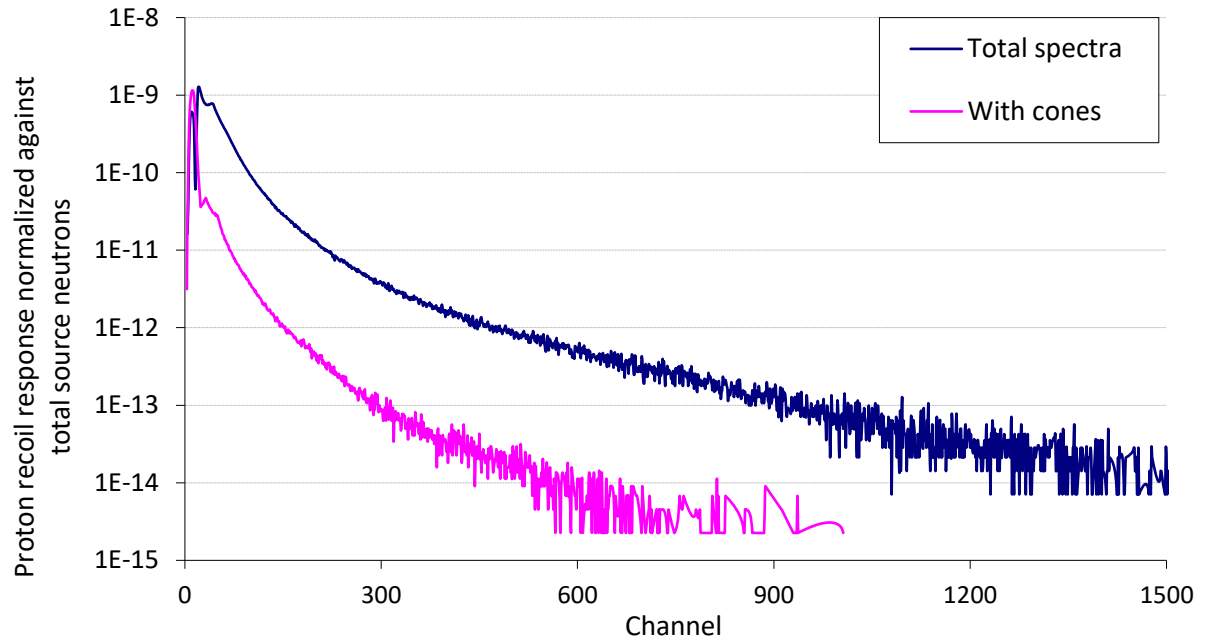
Figure 20: Comparison of Proton Recoil Responses in Standard Geometry and with a Cone. Fractions of all relevant proton counts in each energy channel to the total associated neutron source (i.e. measurements normalized to one source neutron).

1.7. **Measurement Results**

The experiments were performed at a temperature of 18 °C ± 3 °.

The proton recoil method with a digital spectrometer and a ø 10 mm × 10 mm stilbene scintillation detector was used to measure the neutron leakage from the copper block. The target energy range was 1.0 MeV to 11.0 MeV in 100 keV steps. The ^{252}Cf neutron source was placed in the center of the copper block. The center of the stilbene scintillator detector was placed 200 cm above the floor and at the distance of 100 cm from the center of the copper block.

The summarized source neutron emission rates and times of measurement are listed in Table 1.9. Primary experimental data are the measured recoil proton counts, which are given in broad 100 keV energy groups in Table 1.10. The upper energy E_{up} is specified for each group. The primary proton recoil method together with its calibration is described in Appendix B. The primary data evaluated by NGA-01 software, $\int_t \Phi_{ng}$ time-integrated neutron fluxes for each energy group, are listed in Table 1.11, also in broad 100 keV energy groups. The listed uncertainties are statistical uncertainties of measurement.

In this evaluation, the effect of the background was subtracted directly in the proton responses, and the neutron flux evaluation was based on such data.

Table 1.9 Summary of emission rates and measurement times in each measurement.

	^{252}Cf(s.f.) neutron source emission [1/s]	Measurement time [s]
Measurement 1	2.696E+08	5.233E+05
Measurement 2	2.689E+08	3.257E+05
Measurement 3	2.675E+08	5.957E+05
Measurement 4 (cone)	2.639E+08	1.640E+06

Table 1.10 Measured proton-recoil counts in studied experiments.

Energy Group E_{up} [MeV]	Measured counts of proton-recoils			
	Measurement 1	Measurement 2	Measurement 3	Measurement 4
0.6	1.04E+7	9.69E+1	7.03E+3	1.61E+6
0.7	7.88E+6	8.80E+1	1.27E+4	1.91E+5
0.8	4.12E+6	5.60E+4	1.44E+4	1.49E+5
0.9	2.17E+6	1.57E+5	8.59E+4	1.29E+5
1.0	1.13E+6	2.32E+5	6.05E+5	1.10E+5
1.1	6.27E+5	3.07E+5	7.24E+5	7.48E+4
1.2	4.15E+5	2.54E+5	4.72E+5	4.87E+4
1.3	2.90E+5	1.79E+5	3.30E+5	3.46E+4
1.4	2.10E+5	1.31E+5	2.40E+5	2.55E+4
1.5	1.56E+5	9.73E+4	1.79E+5	1.95E+4
1.6	1.18E+5	7.32E+4	1.35E+5	1.46E+4
1.7	9.17E+4	5.77E+4	1.06E+5	1.10E+4
1.8	7.24E+4	4.54E+4	8.35E+4	8.55E+3
1.9	5.70E+4	3.62E+4	6.59E+4	6.72E+3
2.0	4.69E+4	2.97E+4	5.41E+4	5.24E+3
2.1	3.89E+4	2.47E+4	4.47E+4	4.44E+3
2.2	3.23E+4	2.06E+4	3.72E+4	3.58E+3
2.3	2.70E+4	1.68E+4	3.09E+4	3.16E+3
2.4	2.29E+4	1.44E+4	2.60E+4	2.43E+3
2.5	1.89E+4	1.22E+4	2.21E+4	2.07E+3
2.6	1.60E+4	1.03E+4	1.86E+4	1.73E+3
2.7	1.39E+4	8.55E+3	1.60E+4	1.33E+3
2.8	1.19E+4	7.54E+3	1.38E+4	1.07E+3
2.9	1.03E+4	6.49E+3	1.19E+4	8.84E+2
3.0	8.92E+3	5.66E+3	1.03E+4	7.41E+2
3.1	7.79E+3	5.01E+3	8.92E+3	6.52E+2
3.2	6.93E+3	4.47E+3	7.83E+3	5.16E+2
3.3	6.12E+3	3.97E+3	7.25E+3	4.73E+2
3.4	5.39E+3	3.31E+3	6.16E+3	3.97E+2
3.5	4.86E+3	3.13E+3	5.59E+3	3.62E+2
3.6	4.34E+3	2.77E+3	5.10E+3	3.19E+2
3.7	3.93E+3	2.46E+3	4.44E+3	2.61E+2
3.8	3.55E+3	2.31E+3	4.15E+3	2.21E+2
3.9	3.31E+3	2.00E+3	3.87E+3	2.35E+2
4.0	2.96E+3	1.91E+3	3.36E+3	2.30E+2
4.1	2.55E+3	1.72E+3	3.12E+3	1.74E+2
4.2	2.53E+3	1.61E+3	2.80E+3	1.55E+2
4.3	2.19E+3	1.49E+3	2.65E+3	1.51E+2
4.4	2.09E+3	1.37E+3	2.38E+3	1.28E+2
4.5	1.88E+3	1.22E+3	2.19E+3	1.32E+2
4.6	1.77E+3	1.15E+3	2.07E+3	1.28E+2
4.7	1.69E+3	1.04E+3	1.80E+3	8.00E+1
4.8	1.48E+3	9.19E+2	1.69E+3	8.07E+1
4.9	1.40E+3	8.74E+2	1.57E+3	6.31E+1
5.0	1.25E+3	8.22E+2	1.46E+3	6.09E+1

Table 1.10 (cont. 1) Measured proton-recoil counts in studied experiments.

Energy Group E_{up} [MeV]	Measured counts of proton-recoils			
	Measurement 1	Measurement 2	Measurement 3	Measurement 4
5.1	1.23E+3	7.41E+2	1.32E+3	5.30E+1
5.2	1.05E+3	6.94E+2	1.23E+3	5.47E+1
5.3	9.92E+2	5.98E+2	1.20E+3	4.56E+1
5.4	9.81E+2	6.35E+2	1.10E+3	3.89E+1
5.5	8.67E+2	5.57E+2	9.31E+2	3.59E+1
5.6	7.36E+2	5.34E+2	9.05E+2	4.35E+1
5.7	7.17E+2	4.67E+2	8.32E+2	3.38E+1
5.8	7.20E+2	4.31E+2	8.02E+2	2.48E+1
5.9	6.42E+2	4.00E+2	6.54E+2	2.42E+1
6.0	6.42E+2	3.45E+2	6.34E+2	2.00E+1
6.1	5.25E+2	3.48E+2	6.11E+2	1.70E+1
6.2	5.25E+2	2.89E+2	5.90E+2	2.00E+1
6.3	4.65E+2	2.84E+2	5.21E+2	2.25E+1
6.4	4.38E+2	2.64E+2	4.68E+2	9.68E+0
6.5	3.44E+2	2.65E+2	4.86E+2	1.48E+1
6.6	3.61E+2	2.39E+2	4.24E+2	1.97E+1
6.7	3.70E+2	2.15E+2	3.92E+2	1.92E+1
6.8	2.86E+2	1.85E+2	3.72E+2	1.81E+1
6.9	2.83E+2	2.06E+2	3.23E+2	1.50E+1
7.0	2.34E+2	1.70E+2	2.90E+2	6.00E+0
7.1	2.30E+2	1.58E+2	2.89E+2	7.00E+0
7.2	1.86E+2	1.38E+2	2.49E+2	2.00E+0
7.3	1.98E+2	1.38E+2	2.36E+2	1.30E+1
7.4	1.87E+2	1.19E+2	2.01E+2	6.15E+0
7.5	1.84E+2	1.14E+2	1.80E+2	4.90E+0
7.6	1.42E+2	8.70E+1	1.93E+2	5.95E+0
7.7	1.32E+2	6.25E+1	1.59E+2	3.00E+0
7.8	1.05E+2	9.13E+1	1.42E+2	2.00E+0
7.9	1.34E+2	9.31E+1	1.33E+2	3.00E+0
8.0	1.12E+2	7.49E+1	1.36E+2	3.00E+0
8.1	1.10E+2	6.40E+1	1.23E+2	2.00E+0
8.2	9.20E+1	6.74E+1	1.24E+2	3.00E+0
8.3	7.95E+1	5.23E+1	1.03E+2	1.00E+0
8.4	9.77E+1	5.66E+1	9.07E+1	
8.5	8.88E+1	5.38E+1	8.33E+1	
8.6	8.19E+1	5.34E+1	9.28E+1	
8.7	6.18E+1	4.96E+1	8.42E+1	
8.8	7.76E+1	5.36E+1	7.51E+1	
8.9	6.98E+1	3.74E+1	5.85E+1	
9.0	5.70E+1	3.47E+1	7.54E+1	
9.1	5.22E+1	3.86E+1	4.57E+1	
9.2	4.94E+1	3.69E+1	5.24E+1	
9.3	4.40E+1	2.29E+1	5.45E+1	
9.4	4.17E+1	3.07E+1	4.22E+1	
9.5	3.63E+1	2.17E+1	4.17E+1	
9.6	3.10E+1	2.03E+1	4.53E+1	
9.7	2.47E+1	2.70E+1	2.90E+1	
9.8	2.03E+1	1.80E+1	4.00E+1	

Table 1.10 (cont. 2) Measured proton-recoil counts in studied experiments.

Energy Group E_{up} [MeV]	Measured counts of proton-recoils			
	Measurement 1	Measurement 2	Measurement 3	Measurement 4
9.9	1.82E+1	1.20E+1	3.61E+1	
10.0	2.74E+1	1.00E+1	2.22E+1	
10.1	9.69E+0	9.02E+0	1.77E+1	
10.2	1.36E+1	1.20E+1	1.81E+1	
10.3	1.31E+1	6.00E+0	1.59E+1	
10.4	1.40E+1	8.00E+0	1.72E+1	
10.5	2.10E+1	8.00E+0	1.87E+1	
10.6	1.00E+1	6.00E+0	1.38E+1	
10.7	1.00E+1	1.05E+1	9.27E+0	
10.8	5.00E+0	4.46E+0	3.55E+0	
10.9	7.00E+0	2.00E+0	9.04E+0	
11.0	2.00E+0	3.00E+0	6.41E+0	
11.1	4.00E+0	4.00E+0	4.00E+0	
11.2	5.00E+0		3.21E+0	
11.3	4.00E+0		5.79E+0	
11.4	8.41E-1		4.00E+0	
11.5	4.16E+0		5.00E+0	
11.6	3.34E+0		2.00E+0	
11.7	1.66E+0		3.00E+0	

A comparison of the calibrated proton measurements is shown in Figure 21, where the x-axis shows the calibrated energy of the spectrometer and the y-axis shows the measured fraction of proton counts in each energy group to the total neutron source (i.e. normalized to one source neutron).
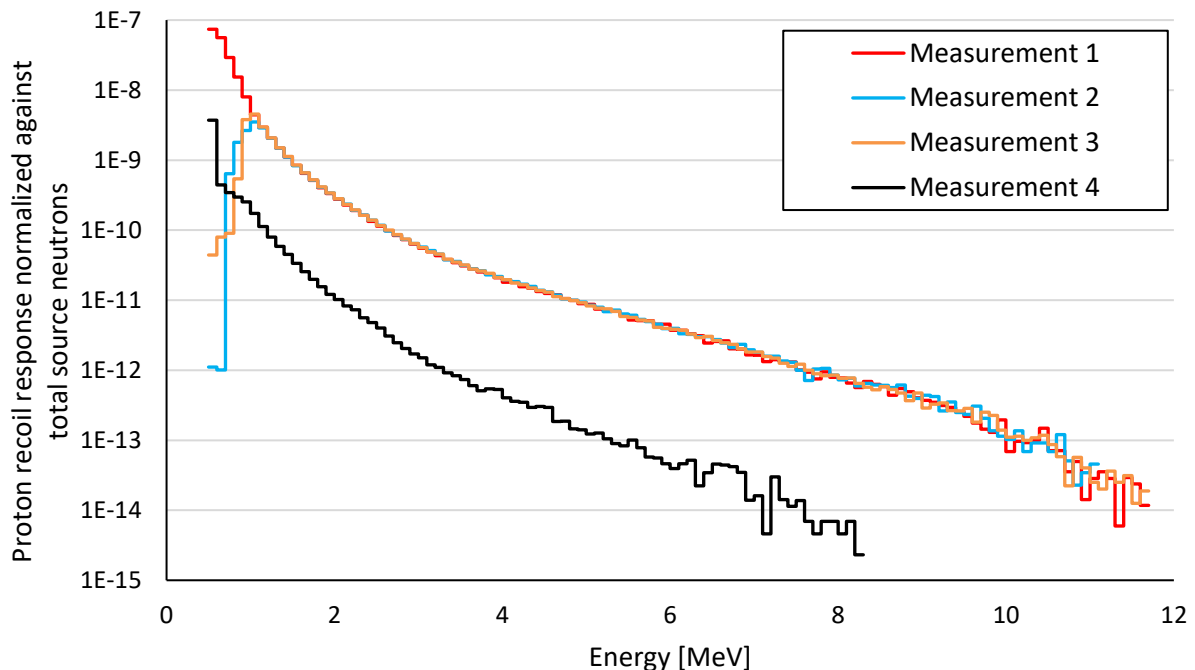
Figure 21: Measured Proton Recoil Fraction of Total Neutron Source,

Data given in Table 1.11 are deconvoluted from calibrated proton recoil counts listed in Table 1.10. The volume of the stilbene is accounted for.

Table 1.11 Measured neutron flux $\int_t \Phi_{ng}$ time-integrated per energy group.

Energy Group E_{up} [MeV]	Measured time-integrated neutron flux $\int_t \Phi_{ng}$ with its relative standard uncertainty u_r							
	Measurement 1		Measurement 2		Measurement 3		Measurement 4 (Experiment with cone)	
	$\int_t \Phi$ [cm^{-2}]	u_r [%]	$\int_t \Phi$ [cm^{-2}]	u_r [%]	$\int_t \Phi$ [cm^{-2}]	u_r [%]	$\int_t \Phi$ [cm^{-2}]	u_r [%]
1.1	9.27E+06	0.1	4.09E+06	0.7	8.31E+06	0.2	3.25E+06	0.5
1.2	6.87E+06	0.3	3.81E+06	0.2	7.60E+06	0.1	2.32E+06	0.6
1.3	5.06E+06	0.2	3.56E+06	0.1	6.96E+06	0.1	1.68E+06	1.0
1.4	3.94E+06	0.3	2.79E+06	0.1	5.27E+06	0.1	1.16E+06	0.4
1.5	3.02E+06	0.3	2.17E+06	0.1	3.98E+06	0.1	8.04E+05	0.5
1.6	2.45E+06	0.3	1.69E+06	0.1	3.03E+06	0.0	5.77E+05	0.4
1.7	1.96E+06	0.2	1.30E+06	0.1	2.29E+06	0.1	4.08E+05	0.6
1.8	1.67E+06	0.2	1.10E+06	0.1	1.94E+06	0.1	3.22E+05	1.0
1.9	1.41E+06	0.3	9.18E+05	0.2	1.63E+06	0.1	2.51E+05	1.5
2.0	1.24E+06	0.4	7.85E+05	0.1	1.40E+06	0.2	2.11E+05	0.6
2.1	1.08E+06	0.5	6.66E+05	0.0	1.19E+06	0.4	1.74E+05	0.4
2.2	9.46E+05	0.7	5.89E+05	0.3	1.06E+06	0.5	1.55E+05	0.2
2.3	8.19E+05	0.5	5.18E+05	0.6	9.36E+05	0.6	1.37E+05	0.7
2.4	7.26E+05	0.3	4.52E+05	0.4	8.25E+05	0.7	1.21E+05	0.2
2.5	6.39E+05	0.4	3.92E+05	0.7	7.22E+05	0.8	1.07E+05	0.3
2.6	5.68E+05	0.4	3.47E+05	0.7	6.41E+05	0.5	9.33E+04	0.4
2.7	5.02E+05	0.4	3.05E+05	1.1	5.66E+05	0.4	8.09E+04	0.9
2.8	4.49E+05	0.7	2.76E+05	0.8	5.07E+05	0.5	6.83E+04	1.1
2.9	3.99E+05	0.9	2.49E+05	0.5	4.51E+05	0.7	5.72E+04	1.3
3.0	3.63E+05	1.2	2.27E+05	0.3	4.13E+05	0.8	4.95E+04	0.7
3.1	3.28E+05	1.1	2.06E+05	0.4	3.76E+05	0.9	4.25E+04	0.7
3.2	2.96E+05	1.1	1.87E+05	0.5	3.41E+05	0.7	3.71E+04	1.2
3.3	2.65E+05	0.9	1.68E+05	0.8	3.07E+05	0.6	3.22E+04	1.8
3.4	2.42E+05	0.8	1.52E+05	0.8	2.78E+05	0.2	2.82E+04	2.4
3.5	2.20E+05	0.9	1.37E+05	0.8	2.50E+05	0.4	2.46E+04	3.1
3.6	2.04E+05	1.2	1.26E+05	0.5	2.31E+05	0.6	2.14E+04	2.3
3.7	1.88E+05	1.2	1.14E+05	0.3	2.13E+05	0.8	1.84E+04	1.9
3.8	1.73E+05	1.2	1.07E+05	0.5	1.99E+05	0.7	1.67E+04	1.2
3.9	1.60E+05	1.2	1.00E+05	0.8	1.85E+05	0.8	1.51E+04	0.8
4.0	1.48E+05	1.2	9.51E+04	0.7	1.74E+05	0.5	1.41E+04	1.7
4.1	1.37E+05	1.3	9.03E+04	0.5	1.64E+05	0.4	1.32E+04	2.8
4.2	1.29E+05	1.6	8.50E+04	0.3	1.54E+05	0.5	1.21E+04	3.0
4.3	1.20E+05	1.4	7.99E+04	0.1	1.44E+05	0.7	1.10E+04	3.1
4.4	1.15E+05	1.3	7.54E+04	0.4	1.35E+05	0.9	1.06E+04	4.9
4.5	1.09E+05	1.1	7.09E+04	0.9	1.27E+05	1.1	1.01E+04	6.8
4.6	1.04E+05	1.2	6.70E+04	1.3	1.20E+05	1.2	9.37E+03	5.8
4.7	9.84E+04	0.8	6.31E+04	1.7	1.13E+05	1.3	8.62E+03	5.2
4.8	9.39E+04	0.6	5.96E+04	1.7	1.07E+05	0.9	7.80E+03	4.4
4.9	8.94E+04	0.9	5.62E+04	1.7	1.00E+05	0.5	7.02E+03	3.7
5.0	8.50E+04	1.3	5.36E+04	1.7	9.71E+04	0.9	6.42E+03	3.4
5.1	8.06E+04	1.5	5.10E+04	1.7	9.41E+04	1.2	5.84E+03	3.5
5.2	7.69E+04	1.8	4.91E+04	2.1	8.88E+04	0.8	5.35E+03	3.4
5.3	7.33E+04	1.4	4.71E+04	2.6	8.36E+04	0.5	4.89E+03	4.8
5.4	6.94E+04	1.0	4.50E+04	2.6	7.98E+04	0.5	4.52E+03	5.5

Table 1.11 (cont. 1) Measured neutron flux, time-integrated per energy group.

Energy Group E_{up} [MeV]	Measured time-integrated neutron flux $\int_t \Phi_{ng}$ with its relative standard uncertainty u_r							
	Measurement 1		Measurement 2		Measurement 3		Measurement 4 (Experiment with cone)	
	$\int_t\Phi$ [cm^{-2}]	u_r [%]	$\int_t\Phi$ [cm^{-2}]	u_r [%]	$\int_t\Phi$ [cm^{-2}]	u_r [%]	$\int_t\Phi$ [cm^{-2}]	u_r [%]
5.5	6.56E+04	0.6	4.29E+04	2.7	7.60E+04	0.8	4.16E+03	6.3
5.6	6.37E+04	0.4	4.09E+04	2.4	7.17E+04	0.8	3.97E+03	6.6
5.7	6.19E+04	1.5	3.88E+04	2.2	6.74E+04	1.1	3.79E+03	7.1
5.8	5.94E+04	2.7	3.68E+04	1.4	6.45E+04	1.1	3.43E+03	7.4
5.9	5.70E+04	2.5	3.48E+04	0.9	6.15E+04	1.1	3.10E+03	7.8
6.0	5.47E+04	2.2	3.27E+04	1.0	5.86E+04	1.2	2.78E+03	7.1
6.1	5.24E+04	2.1	3.07E+04	1.2	5.58E+04	1.5	2.49E+03	6.4
6.2	4.95E+04	2.0	2.96E+04	0.8	5.38E+04	1.2	2.31E+03	5.7
6.3	4.66E+04	1.5	2.85E+04	0.8	5.18E+04	0.9	2.13E+03	5.6
6.4	4.50E+04	1.0	2.73E+04	0.9	5.01E+04	0.4	2.03E+03	4.9
6.5	4.34E+04	1.3	2.61E+04	1.3	4.84E+04	0.2	1.93E+03	4.2
6.6	4.08E+04	1.6	2.51E+04	1.4	4.59E+04	0.6	1.97E+03	6.4
6.7	3.83E+04	1.3	2.41E+04	1.6	4.34E+04	1.1	2.01E+03	8.7
6.8	3.55E+04	0.9	2.29E+04	1.7	4.14E+04	1.3	1.99E+03	5.1
6.9	3.29E+04	1.0	2.17E+04	1.8	3.94E+04	1.7	1.97E+03	4.3
7.0	3.07E+04	1.1	2.06E+04	1.7	3.70E+04	1.6	1.72E+03	4.9
7.1	2.87E+04	1.6	1.95E+04	1.5	3.48E+04	1.6	1.49E+03	5.6
7.2	2.73E+04	2.1	1.84E+04	1.1	3.25E+04	1.6	1.44E+03	7.9
7.3	2.59E+04	1.9	1.72E+04	0.6	3.04E+04	1.5	1.39E+03	11.0
7.4	2.40E+04	1.8	1.57E+04	1.5	2.85E+04	1.1	1.29E+03	9.1
7.5	2.22E+04	1.9	1.43E+04	2.5	2.66E+04	0.7	1.19E+03	8.1
7.6	2.09E+04	2.1	1.38E+04	1.9	2.50E+04	1.0	1.08E+03	5.8
7.7	1.98E+04	2.3	1.33E+04	1.3	2.35E+04	1.5	9.71E+07	5.2
7.8	1.87E+04	2.6	1.25E+04	0.8	2.24E+04	1.7	8.79E+07	5.1
7.9	1.77E+04	2.1	1.18E+04	0.6	2.14E+04	2.0	7.94E+07	5.1
8.0	1.67E+04	1.5	1.12E+04	0.7	2.04E+04	2.2	7.36E+07	10.0
8.1	1.57E+04	1.7	1.05E+04	0.8	1.94E+04	2.5	6.80E+07	17.0
8.2	1.54E+04	1.9	1.01E+04	1.2	1.83E+04	1.7	5.96E+07	27.0
8.3	1.50E+04	1.3	9.66E+03	1.6	1.72E+04	1.0	5.20E+07	37.0
8.4	1.42E+04	0.6	9.43E+03	2.2	1.65E+04	0.7	4.87E+07	52.0
8.5	1.35E+04	0.4	9.19E+03	2.9	1.59E+04	0.9	4.56E+07	70.0
8.6	1.32E+04	1.2	8.77E+03	3.3	1.50E+04	1.3		
8.7	1.28E+04	1.3	8.36E+03	3.8	1.41E+04	2.0		
8.8	1.23E+04	1.3	8.10E+03	4.2	1.32E+04	2.1		
8.9	1.18E+04	1.1	7.83E+03	4.5	1.24E+04	2.1		
9.0	1.14E+04	1.2	7.55E+03	4.4	1.19E+04	2.0		
9.1	1.10E+04	0.8	7.26E+03	4.4	1.15E+04	2.2		
9.2	1.06E+04	0.3	6.96E+03	4.2	1.11E+04	2.8		
9.3	1.01E+04	0.3	6.66E+03	4.7	1.07E+04	3.4		
9.4	9.40E+03	0.5	6.57E+03	4.4	1.02E+04	3.7		
9.5	8.72E+03	0.3	6.48E+03	4.6	9.82E+03	4.0		
9.6	8.19E+03	0.9	6.06E+03	3.7	9.64E+03	3.8		
9.7	7.68E+03	1.1	5.67E+03	3.0	9.46E+03	3.7		
9.8	7.06E+03	1.4	5.30E+03	4.9	8.77E+03	2.9		

Table 1.11 (cont. 2) Measured neutron flux, time-integrated per energy group.

Energy Group E_{up} [MeV]	Measured time-integrated neutron flux $\int_t \Phi_{ng}$ with its relative standard uncertainty u_r							
	Measurement 1		Measurement 2		Measurement 3		Measurement 4 (Experiment with cone)	
	$\int_t \Phi$ [cm^{-2}]	u_r [%]	$\int_t \Phi$ [cm^{-2}]	u_r [%]	$\int_t \Phi$ [cm^{-2}]	u_r [%]	$\int_t \Phi$ [cm^{-2}]	u_r [%]
9.9	6.47E+03	1.9	4.95E+03	6.8	8.12E+03	2.8		
10.0	6.00E+03	2.6	4.61E+03	7.3	7.57E+03	3.4		
10.1	5.56E+03	3.5	4.28E+03	7.8	7.06E+03	3.9		
10.2	5.54E+03	4.5	4.12E+03	8.3	6.84E+03	2.8		
10.3	5.52E+03	4.7	3.95E+03	8.9	6.62E+03	1.9		
10.4	5.16E+03	5.0	4.06E+03	7.8	6.04E+03	1.9		
10.5	4.82E+03	3.7			5.50E+03	2.3		
10.6	4.38E+03	2.3			5.08E+03	3.9		
10.7	3.98E+03	0.3			4.69E+03	5.6		
10.8	3.65E+03	2.9			4.26E+03	4.8		
10.9	3.33E+03	3.4			3.87E+03	4.2		
11.0	3.12E+03	4.0			3.73E+03	5.1		

2.0   EVALUATION OF EXPERIMENTAL DATA

2.1. <u>Evaluation of Fast Neutron Leakage</u>

The evaluation of proton recoil data from the system with a stilbene detector is carried out by deconvolution of the measured proton response. This is performed using Maximum Likelihood Estimation, and the result is the neutron flux. For details of the method as well as of the detailed validation, see Appendix B.

The uncertainties are expressed as relative standard uncertainties (u_r) unless expressed otherwise. Biases and uncertainties lower than 0.1 % are considered negligible.

The emission rate of the ^{252}Cf neutron source in the measurement period is derived from the emission rate given in the source producer certificate and the exponential decay law (^{252}Cf(α,n) $T_{1/2}$= 2.645 y). The neutron source emission rate has been determined in NPL (UK, 2015) with relative standard uncertainty (u_r) 0.55 %. The neutron emission rates during evaluated measurements are in the interval $2.639 \cdot 10^8$ s^{-1} to $2.696 \cdot 10^8$ s^{-1}, depending on the measurement date. Two components of the source emission uncertainty are considered. The change of the neutron emission during the measurement is neglected because the measurement time is very short compared to the half-life of ^{252}Cf. The uncertainty of the emission evaluated by source manufacturer during the production (0.58 %) is included in the flux evaluation

The background (i.e., proton flux measured with cones) was subtracted directly from the total proton flux. The net proton flux with the extracted room effect was then deconvoluted. However, the background effect was evaluated as well for illustration and is presented in Table 2.3 in Section 2.1.2. The fraction of the room effect in the region above 2 MeV is not higher than 5 % due to the relatively big experimental hall.

The evaluation of the effect of material and geometrical bounding of copper cube on the neutron leakage is listed in Table 2.4 in Section 2.1.3. In general, the effect of thickness uncertainty is dominating and ranges between 1.6 % and 2.2 %, depending on the energy. Other uncertainty sources are significantly smaller.

Propagation of material and geometry uncertainties to measured neutron flux uncertainties is presented in Table 2.5 in Section 2.1.4. Sensitivity analysis presented in Table 2.6 confirms the small effects of Al structural components that are associated with the ^{252}Cf(s.f.) source; the associated uncertainties thus have little effect. The evaluated neutron leakage flux measurement results and their uncertainties are presented in Table 2.7 in Section 2.1.5.

2.1.1.   Evaluation of measurement method uncertainty

The source of uncertainties in the measurement method consists of the following components: energy scale calibration, energy resolution of the detectors, counting statistics, uncertainty in the number of iterations used in deconvolution, stability and noise properties of measuring devices, and source neutron emission uncertainty. The uncertainty in position plays only a minor role because the tolerance in the detector position is not higher than 0.5 mm.

The most significant sources of method uncertainty were evaluated, especially uncertainties of energy calibration, and uncertainty in the number of iterations. The one sigma of standard uncertainty in calibration is between 1 % to 1.5 %, and for a bounding rate, 2 % standard uncertainty is used. The iteration number was halved or increased by half.

Table 2.1 shows the values of the time-integrated flows ($\int t\Phi ng$) of measurement 3, evaluated with experimentally determined and perturbed parameters. The magnitude of perturbation is chosen as a relative standard uncertainty in defined parameters. Thus, the relative change between nominal and perturbed values, listed in Table 2.2, evaluated from Table 2.1., represents a relative standard uncertainty

in the time-integrated neutron flux value due to the associated parameter standard uncertainty. From other sources of uncertainty, it is worth noting: the standard uncertainty in deconvolution is ~ 5 % and estimated based on measurement of standard (pure ^{252}Cf(s.f.) spectrum), the crystal absolute calibration standard uncertainty is 2.0 %, and the neutron emission standard uncertainty of the ^{252}Cf(s.f.) source being 0.58 %.

Table 2.1 Perturbed calibration and iteration number for time-integrated neutron fluxes $\int_t \Phi_{ng}$.

Energy Group E_{up} [MeV]	Perturbations of time-integrated neutron fluxes $\int_t \Phi_{ng}$ [cm^{-2}]				
	Unperturbed parameters	Calibration (+2 %)	Calibration (-2 %)	Deconvolution - under iterated	Deconvolution - over iterated
1.1	8.31E+06	7.83E+06	8.70E+06	7.09E+06	9.22E+06
1.2	7.60E+06	7.50E+06	7.62E+06	6.63E+06	8.18E+06
1.3	6.96E+06	7.19E+06	6.69E+06	6.20E+06	7.27E+06
1.4	5.27E+06	5.51E+06	5.03E+06	5.03E+06	5.27E+06
1.5	3.98E+06	4.21E+06	3.76E+06	4.06E+06	3.81E+06
1.6	3.03E+06	3.19E+06	2.89E+06	3.22E+06	2.87E+06
1.7	2.29E+06	2.40E+06	2.20E+06	2.54E+06	2.14E+06
1.8	1.94E+06	2.03E+06	1.86E+06	2.12E+06	1.85E+06
1.9	1.63E+06	1.69E+06	1.57E+06	1.76E+06	1.59E+06
2.0	1.40E+06	1.45E+06	1.35E+06	1.50E+06	1.38E+06
2.1	1.19E+06	1.24E+06	1.15E+06	1.26E+06	1.19E+06
2.2	1.06E+06	1.10E+06	1.02E+06	1.10E+06	1.07E+06
2.3	9.36E+05	9.74E+05	9.02E+05	9.55E+05	9.58E+05
2.4	8.25E+05	8.57E+05	7.95E+05	8.37E+05	8.44E+05
2.5	7.22E+05	7.49E+05	6.96E+05	7.29E+05	7.37E+05
2.6	6.41E+05	6.67E+05	6.15E+05	6.45E+05	6.54E+05
2.7	5.66E+05	5.90E+05	5.40E+05	5.67E+05	5.76E+05
2.8	5.07E+05	5.29E+05	4.87E+05	5.08E+05	5.14E+05
2.9	4.51E+05	4.72E+05	4.36E+05	4.52E+05	4.56E+05
3.0	4.13E+05	4.31E+05	3.97E+05	4.13E+05	4.17E+05
3.1	3.76E+05	3.92E+05	3.60E+05	3.75E+05	3.80E+05
3.2	3.41E+05	3.54E+05	3.26E+05	3.40E+05	3.43E+05
3.3	3.07E+05	3.18E+05	2.94E+05	3.06E+05	3.08E+05
3.4	2.78E+05	2.89E+05	2.67E+05	2.78E+05	2.77E+05
3.5	2.50E+05	2.60E+05	2.41E+05	2.51E+05	2.48E+05
3.6	2.31E+05	2.39E+05	2.22E+05	2.31E+05	2.30E+05
3.7	2.13E+05	2.19E+05	2.05E+05	2.12E+05	2.12E+05
3.8	1.99E+05	2.06E+05	1.92E+05	1.98E+05	1.98E+05
3.9	1.85E+05	1.92E+05	1.80E+05	1.84E+05	1.84E+05
4.0	1.74E+05	1.81E+05	1.69E+05	1.72E+05	1.74E+05
4.1	1.64E+05	1.71E+05	1.59E+05	1.61E+05	1.65E+05
4.2	1.54E+05	1.59E+05	1.49E+05	1.51E+05	1.54E+05
4.3	1.44E+05	1.48E+05	1.39E+05	1.41E+05	1.44E+05
4.4	1.35E+05	1.40E+05	1.31E+05	1.32E+05	1.35E+05
4.5	1.27E+05	1.31E+05	1.22E+05	1.24E+05	1.26E+05
4.6	1.20E+05	1.24E+05	1.16E+05	1.17E+05	1.20E+05
4.7	1.13E+05	1.17E+05	1.09E+05	1.11E+05	1.13E+05
4.8	1.07E+05	1.10E+05	1.04E+05	1.04E+05	1.06E+05
4.9	1.00E+05	1.04E+05	9.80E+04	9.79E+04	9.92E+04
5.0	9.71E+04	9.98E+04	9.44E+04	9.40E+04	9.72E+04
5.1	9.41E+04	9.59E+04	9.08E+04	9.00E+04	9.51E+04
5.2	8.88E+04	9.14E+04	8.56E+04	8.51E+04	8.94E+04
5.3	8.36E+04	8.70E+04	8.05E+04	8.03E+04	8.39E+04
5.4	7.98E+04	8.27E+04	7.67E+04	7.64E+04	8.02E+04
5.5	7.60E+04	7.84E+04	7.30E+04	7.26E+04	7.65E+04

Table 2.1 (cont. 1) Perturbed calibration and iteration number for time-integrated neutron fluxes $\int_t \Phi_{ng}$.

Energy Group E_{up} [MeV]	Perturbations of time-integrated neutron fluxes $\int_t \Phi_{ng}$ [cm^{-2}]				
	Unperturbed parameters	Calibration (+2 %)	Calibration (-2 %)	Deconvolution - under iterated	Deconvolution - over iterated
5.6	7.17E+04	7.46E+04	6.90E+04	6.89E+04	7.17E+04
5.7	6.74E+04	7.08E+04	6.51E+04	6.52E+04	6.70E+04
5.8	6.45E+04	6.70E+04	6.23E+04	6.22E+04	6.41E+04
5.9	6.15E+04	6.33E+04	5.94E+04	5.92E+04	6.13E+04
6.0	5.86E+04	6.07E+04	5.67E+04	5.64E+04	5.85E+04
6.1	5.58E+04	5.81E+04	5.39E+04	5.36E+04	5.57E+04
6.2	5.38E+04	5.58E+04	5.20E+04	5.15E+04	5.39E+04
6.3	5.18E+04	5.34E+04	5.00E+04	4.93E+04	5.22E+04
6.4	5.01E+04	5.18E+04	4.83E+04	4.75E+04	5.07E+04
6.5	4.84E+04	5.01E+04	4.65E+04	4.57E+04	4.92E+04
6.6	4.59E+04	4.79E+04	4.39E+04	4.34E+04	4.66E+04
6.7	4.34E+04	4.58E+04	4.14E+04	4.12E+04	4.41E+04
6.8	4.14E+04	4.35E+04	3.94E+04	3.92E+04	4.21E+04
6.9	3.94E+04	4.12E+04	3.74E+04	3.73E+04	4.02E+04
7.0	3.70E+04	3.91E+04	3.48E+04	3.53E+04	3.77E+04
7.1	3.48E+04	3.70E+04	3.23E+04	3.33E+04	3.52E+04
7.2	3.25E+04	3.47E+04	3.04E+04	3.15E+04	3.27E+04
7.3	3.04E+04	3.24E+04	2.86E+04	2.97E+04	3.03E+04
7.4	2.85E+04	3.05E+04	2.67E+04	2.82E+04	2.82E+04
7.5	2.66E+04	2.86E+04	2.48E+04	2.66E+04	2.62E+04
7.6	2.50E+04	2.69E+04	2.34E+04	2.53E+04	2.45E+04
7.7	2.35E+04	2.52E+04	2.21E+04	2.40E+04	2.28E+04
7.8	2.24E+04	2.39E+04	2.12E+04	2.29E+04	2.19E+04
7.9	2.14E+04	2.26E+04	2.02E+04	2.18E+04	2.10E+04
8.0	2.04E+04	2.18E+04	1.90E+04	2.09E+04	2.00E+04
8.1	1.94E+04	2.09E+04	1.79E+04	2.00E+04	1.90E+04
8.2	1.83E+04	1.96E+04	1.72E+04	1.90E+04	1.78E+04
8.3	1.72E+04	1.83E+04	1.65E+04	1.80E+04	1.67E+04
8.4	1.65E+04	1.75E+04	1.57E+04	1.72E+04	1.62E+04
8.5	1.59E+04	1.67E+04	1.50E+04	1.65E+04	1.58E+04
8.6	1.50E+04	1.59E+04	1.41E+04	1.56E+04	1.49E+04
8.7	1.41E+04	1.51E+04	1.32E+04	1.47E+04	1.40E+04
8.8	1.32E+04	1.43E+04	1.26E+04	1.39E+04	1.30E+04
8.9	1.24E+04	1.34E+04	1.19E+04	1.31E+04	1.21E+04
9.0	1.19E+04	1.28E+04	1.13E+04	1.26E+04	1.18E+04
9.1	1.15E+04	1.23E+04	1.06E+04	1.21E+04	1.14E+04
9.2	1.11E+04	1.16E+04	1.03E+04	1.16E+04	1.11E+04
9.3	1.07E+04	1.10E+04	9.98E+03	1.12E+04	1.07E+04
9.4	1.02E+04	1.07E+04	9.85E+03	1.07E+04	1.03E+04
9.5	9.82E+03	1.03E+04	9.72E+03	1.02E+04	9.95E+03
9.6	9.64E+03	1.01E+04	9.09E+03	9.92E+03	9.95E+03
9.7	9.46E+03	9.82E+03	8.49E+03	9.59E+03	9.95E+03
9.8	8.77E+03	9.53E+03	7.86E+03	9.09E+03	9.05E+03
9.9	8.12E+03	9.25E+03	7.26E+03	8.61E+03	8.22E+03
10.0	7.57E+03	8.44E+03	7.01E+03	8.14E+03	7.61E+03
10.1	7.06E+03	7.69E+03	6.76E+03	7.69E+03	7.02E+03

| 10.2 | 6.84E+03 | 7.27E+03 | 6.26E+03 | 7.38E+03 | 6.92E+03 |

Table 2.1 (cont. 2) Perturbed calibration and iteration number for time-integrated neutron fluxes $\int_t \Phi_{ng}$.

Energy Group E_{up} [MeV]	Perturbations of time-integrated neutron fluxes $\int_t \Phi_{ng}$ [cm^{-2}]				
	Unperturbed parameters	Calibration (+2 %)	Calibration (-2 %)	Deconvolution - under iterated	Deconvolution - over iterated
10.3	6.62E+03	6.86E+03	5.79E+03	7.07E+03	6.81E+03
10.4	6.04E+03	6.60E+03	5.28E+03	6.64E+03	6.08E+03
10.5	5.50E+03	6.34E+03	4.81E+03	6.22E+03	5.41E+03
10.6	5.08E+03	5.80E+03	4.37E+03	5.87E+03	4.92E+03
10.7	4.69E+03	5.29E+03	3.96E+03	5.53E+03	4.47E+03
10.8	4.26E+03	4.88E+03	3.75E+03	5.20E+03	3.95E+03
10.9	3.87E+03	4.49E+03	3.54E+03	4.88E+03	3.48E+03
11.0	3.73E+03	4.10E+03	3.48E+03	4.69E+03	3.39E+03

Table 2.2 Relative perturbations of time-integrated neutron fluxes $\int_t \Phi_{ng}$
(listed in Table 2.1) for the most significant sources of uncertainty.

Energy Group E_{up} [MeV]	Relative perturbation of $\int_t \Phi_{ng}$ [%]			
	Calibration (+2 %)	Calibration (-2 %)	Under-iterated	Over-iterated
1.1	-5.8	4.7	-14.7	10.9
1.2	-1.3	0.3	-12.8	7.6
1.3	3.4	-3.8	-10.8	4.5
1.4	4.5	-4.6	-4.6	0.0
1.5	5.8	-5.4	2.0	-4.3
1.6	5.2	-4.8	6.2	-5.5
1.7	4.7	-4.2	10.5	-6.8
1.8	4.4	-4.0	9.3	-4.7
1.9	4.1	-3.7	8.1	-2.5
2.0	3.9	-3.6	6.9	-1.4
2.1	3.7	-3.5	5.7	-0.3
2.2	3.9	-3.6	3.9	1.0
2.3	4.0	-3.7	2.0	2.3
2.4	3.9	-3.6	1.5	2.2
2.5	3.7	-3.6	1.0	2.1
2.6	4.0	-4.0	0.6	2.0
2.7	4.2	-4.5	0.2	1.8
2.8	4.3	-3.9	0.2	1.4
2.9	4.5	-3.3	0.2	1.0
3.0	4.4	-3.9	-0.1	1.0
3.1	4.3	-4.5	-0.4	1.0
3.2	4.0	-4.4	-0.3	0.7
3.3	3.8	-4.3	-0.2	0.4
3.4	4.0	-4.0	0.2	-0.3
3.5	4.1	-3.6	0.6	-0.9
3.6	3.6	-3.7	0.2	-0.6
3.7	3.1	-3.8	-0.3	-0.4
3.8	3.5	-3.3	-0.5	-0.4
3.9	4.0	-2.8	-0.7	-0.5
4.0	3.9	-3.0	-1.2	-0.1
4.1	3.8	-3.2	-1.8	0.2
4.2	3.6	-3.3	-1.9	0.1
4.3	3.4	-3.4	-2.0	0.0
4.4	3.6	-3.3	-1.9	-0.2
4.5	3.9	-3.2	-1.9	-0.4
4.6	3.7	-3.3	-2.2	-0.3
4.7	3.5	-3.5	-2.5	-0.2
4.8	3.6	-2.8	-2.3	-0.5
4.9	3.6	-2.1	-2.2	-0.9
5.0	2.8	-2.8	-3.3	0.1
5.1	1.9	-3.5	-4.4	1.0
5.2	3.0	-3.6	-4.2	0.7
5.3	4.1	-3.7	-3.9	0.3
5.4	3.6	-3.8	-4.2	0.5
5.5	3.2	-3.9	-4.5	0.7
5.6	4.0	-3.7	-3.9	0.0

Table 2.2 (cont. 1) Relative perturbations of time-integrated neutron fluxes ∫ₜΦₙg
(listed in Table 2.1) for the most significant sources of uncertainty.

Energy Group Eup [MeV]	Relative perturbation of ∫ₜΦₙg [%]			
	Calibration (+2 %)	Calibration (-2 %)	Under-iterated	Over-iterated
5.7	4.9	-3.5	-3.3	-0.7
5.8	3.9	-3.4	-3.5	-0.5
5.9	2.9	-3.4	-3.8	-0.3
6.0	3.6	-3.3	-3.8	-0.3
6.1	4.2	-3.3	-3.9	-0.2
6.2	3.7	-3.3	-4.3	0.3
6.3	3.1	-3.4	-4.8	0.7
6.4	3.4	-3.6	-5.2	1.2
6.5	3.6	-3.9	-5.6	1.7
6.6	4.5	-4.2	-5.4	1.6
6.7	5.5	-4.5	-5.1	1.5
6.8	5.0	-4.9	-5.2	1.7
6.9	4.5	-5.2	-5.3	2.0
7.0	5.4	-6.1	-4.7	1.7
7.1	6.4	-7.0	-4.1	1.3
7.2	6.6	-6.4	-3.1	0.6
7.3	6.8	-5.7	-2.1	-0.1
7.4	7.0	-6.4	-1.0	-0.8
7.5	7.3	-7.0	0.1	-1.5
7.6	7.4	-6.3	1.1	-2.1
7.7	7.6	-5.6	2.1	-2.7
7.8	6.7	-5.6	2.1	-2.3
7.9	5.8	-5.6	2.1	-1.9
8.0	6.8	-6.7	2.5	-2.0
8.1	7.8	-7.8	3.0	-2.0
8.2	7.1	-5.8	3.8	-2.5
8.3	6.4	-3.7	4.7	-3.0
8.4	5.6	-4.9	4.1	-2.0
8.5	4.7	-6.1	3.4	-1.0
8.6	5.9	-6.2	3.7	-1.0
8.7	7.1	-6.4	4.1	-1.0
8.8	7.8	-5.0	5.0	-1.5
8.9	8.4	-3.6	5.9	-2.1
9.0	7.4	-5.6	5.6	-1.5
9.1	6.4	-7.6	5.3	-0.8
9.2	4.9	-7.0	5.0	-0.2
9.3	3.5	-6.4	4.7	0.4
9.4	4.4	-3.8	4.5	0.9
9.5	5.3	-1.0	4.3	1.4
9.6	4.5	-5.7	2.9	3.2
9.7	3.7	-10.3	1.4	5.1
9.8	8.7	-10.4	3.7	3.2
9.9	13.9	-10.6	6.0	1.3
10 0	11.4	-7.5	7.5	0.4
10.1	8.9	-4.2	9.0	-0.5
10.2	6.3	-8.4	7.9	1.2

Table 2.2 (cont. 2) Relative perturbations of time-integrated neutron fluxes $\int_t \Phi_{ng}$
(listed in Table 2.1) for the most significant sources of uncertainty.

Energy Group E_{up} [MeV]	Relative perturbation of $\int_t \Phi_{ng}$ [%]			
	Calibration (+2 %)	Calibration (-2 %)	Under-iterated	Over-iterated
10.3	3.7	-12.5	6.9	2.9
10.4	9.3	-12.6	9.9	0.6
10.5	15.2	-12.6	13.0	-1.7
10.6	14.1	-14.1	15.5	-3.1
10.7	12.9	-15.5	18.0	-4.6
10.8	14.5	-12.0	22.0	-7.3
10.9	16.2	-8.3	26.2	-9.9
11.0	10.0	-6.8	25.9	-9.2

Due to the indirect calibration method, the detector arrangement was tested in parallel-oriented neutron fields. Stilbene has anisotropy in light output, and the selected field orientation is comparable with leakage beam geometry and can be understood as these for which the response matrices were evaluated. The validation of the accuracy of the detector response function and the Maximum Likelihood Estimation method, using separate experimental data of a silicon filtered neutron source. This field with significant peaks in high energy regions seems to be suitable for testing of calibration as well as of deconvolution. Due to its peak character, it is able to reveal possible discrepancies in the methodology[a]. The good agreement between calculated and measured fluxes (see Figure B.4. in Appendix B) indicates the adequate energy calibration used in evaluations.

The reliability of used deconvolution was moreover successfully tested in various fields. It was namely radioisotope [241]AmBe[b], parallel beam in research reactor[c], reference benchmark neutron field[d] and also D-T neutron generator[e].

The uncertainties of methodology were derived based on validation in the standard neutron field. Using IRDFF-II[f] as a guide, a standard neutron field is defined as a permanent and reproducible neutron field that is characterized to state-of-the-art accuracy in terms of neutron fluence rate and energy spectrum, and one where the associated spatial and angular distributions, and other important field quantities, have been verified by interlaboratory measurements.

The [252]Cf spontaneous fission neutron field is defined to be a standard neutron field over the energy range from 0.1 MeV to 20 MeV.

---

[a] M. Košťál, J. Šoltés, L. Viererbl, Z. Matěj, F. Cvachovec, V. Rypar, E. Losa, Measurement of neutron spectra in a silicon filtered neutron beam using stilbene detectors at the LVR-15 research reactor, Applied Radiation and Isotopes, 128, 2017, pp. 41-48

[b] M. Kostal, M. Schulc, E. Novak, T. Czakoj, Z. Matej, F. Cvachovec, F. Mravec, B. Jansky and L. Leal, Validation of heavy water cross section using AmBe neutron source, EPJ Web Conf., 239 (2020) 18008, DOI: 10.1051/epjconf/202023918008

[c] M. Košťál, E. Losa, Z. Matěj, V. Juříček, D. Harutyunyan, O. Huml, M. Štefánik, F. Cvachovec, F. Mravec, M. Schulc, T. Czakoj, V. Rypar, Characterization of mixed N/G beam of the VR-1 reactor, (2018) Annals of Nuclear Energy, 122, pp. 69-78

[d] Košťál, M., Matěj, Z., Cvachovec, F., Rypar, V., Losa, E., Rejchrt, J., Mravec, F., Veškrna, M., Measurement and calculation of fast neutron and gamma spectra in well defined cores in LR-0 reactor, (2017) Applied Radiation and Isotopes, 120, pp. 45-50

[e] Z. Matej, M. Kostal, E. Novak, P. Alexa, R. Uhlar, F. Mravec, A. Jancar, F. Cvachovec, V. Prenosil, P. Jancar, Characterization and comparison of neutron generators of IEC and linear D-T by the spectrometric system NGA-01, (2020) International Conference on Physics of Reactors: Transition to a Scalable Nuclear Future, PHYSOR 2020, 2020-March, pp. 2786-2793

[f] A. Trkov, P.J. Griffin, S.P. Simakov et. al., Nuclear Data Sheets, Vol. 163, pp. 1-108 (2020).

The comparison between measured neutron spectra and IRDFF-II evaluated data is shown in Figure 22, the C/E-1 comparison for a ø 10 mm × 10 mm crystal is shown in Figure 23. It is worth noting that the agreement is satisfactory and meets the requirements on a maximum discrepancy below 5 %. This value is therefore used as a tolerance to limit the uncertainty in the deconvolution. More detailed validation of the deconvolution method is found in Appendix B.
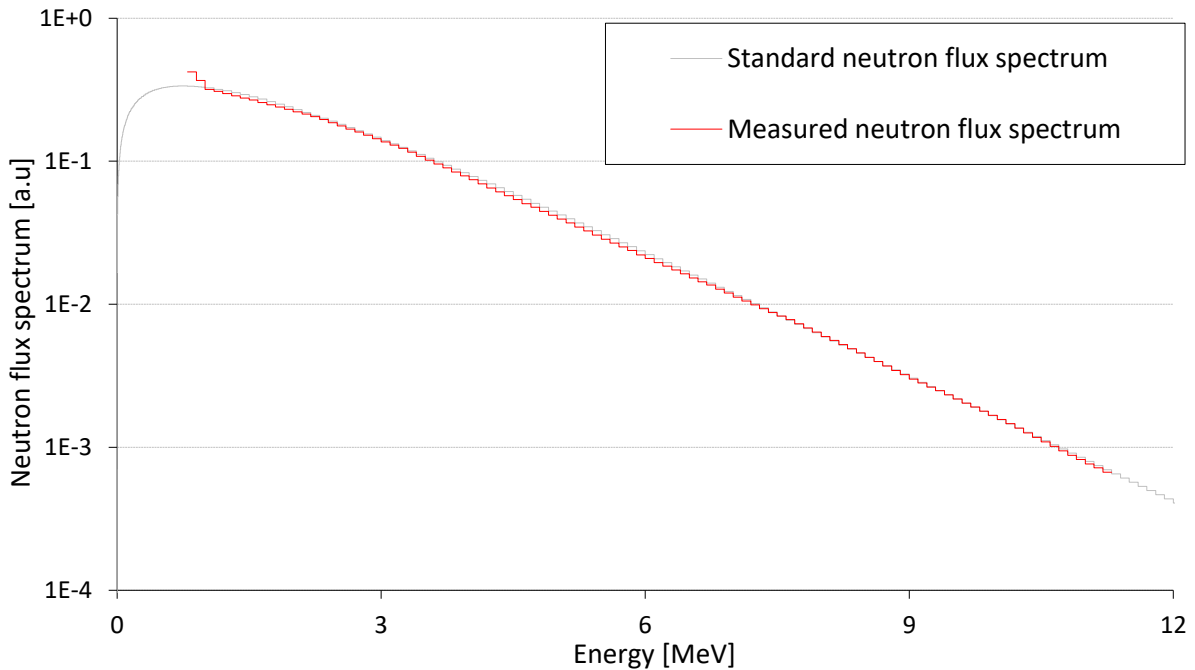
Figure 22: Calculated and Measured Neutron Flux Spectra from ^{252}Cf Source i.
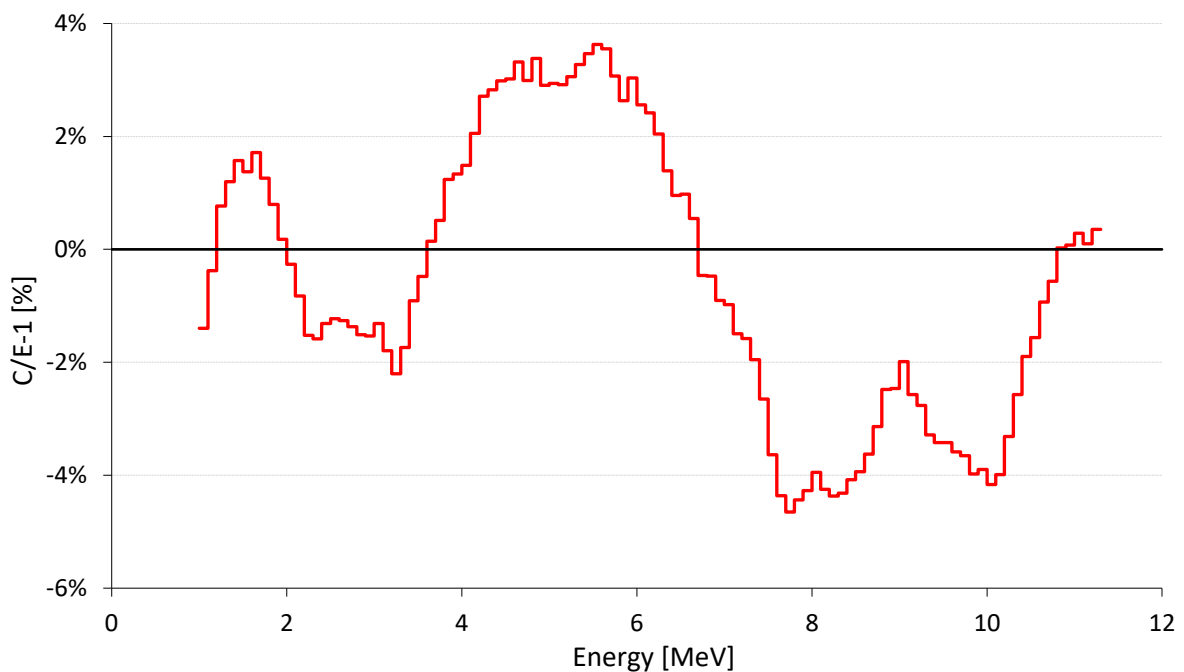
Figure 23: IRDFF-II Eval/E-1 of Cf Flux measured with NGA-01 and ø 10 mm × 10 mm Crystal.

2.1.2. Evaluation of the background effect

For minimization of the uncertainty, the proton recoil flux of the background was subtracted directly from the total proton recoil flux. It implies the fact, that in the evaluation of the leakage, the background

scattered neutrons which orientation is different from leakage does not play role in deconvolution and does not increase uncertainty due to stilbene anisotropy. It also means, that deconvolution of background spectra is not needed. However, for a better understanding of the measurements, its effect was evaluated as well. The same issue was simulated using known dimensions of the laboratory 7.24 m × 6.5 m with a height of 7.2 m and the tabulated composition of the concrete forming walls and ceiling. In the first approach (denoted as direct effect) the effect was determined by subtraction of calculated flux by models with walls and without them. In the second approach (denoted as full-scale calculation) the full geometry with walls and the cone is used for background flux calculation. The results, showing the ratio of background effect to leakage neutron flux, are plotted in Figure 24 and listed in Table 2.3. The results of calculations used for evaluation of background effect are listed in Table A1 in Appendix A.
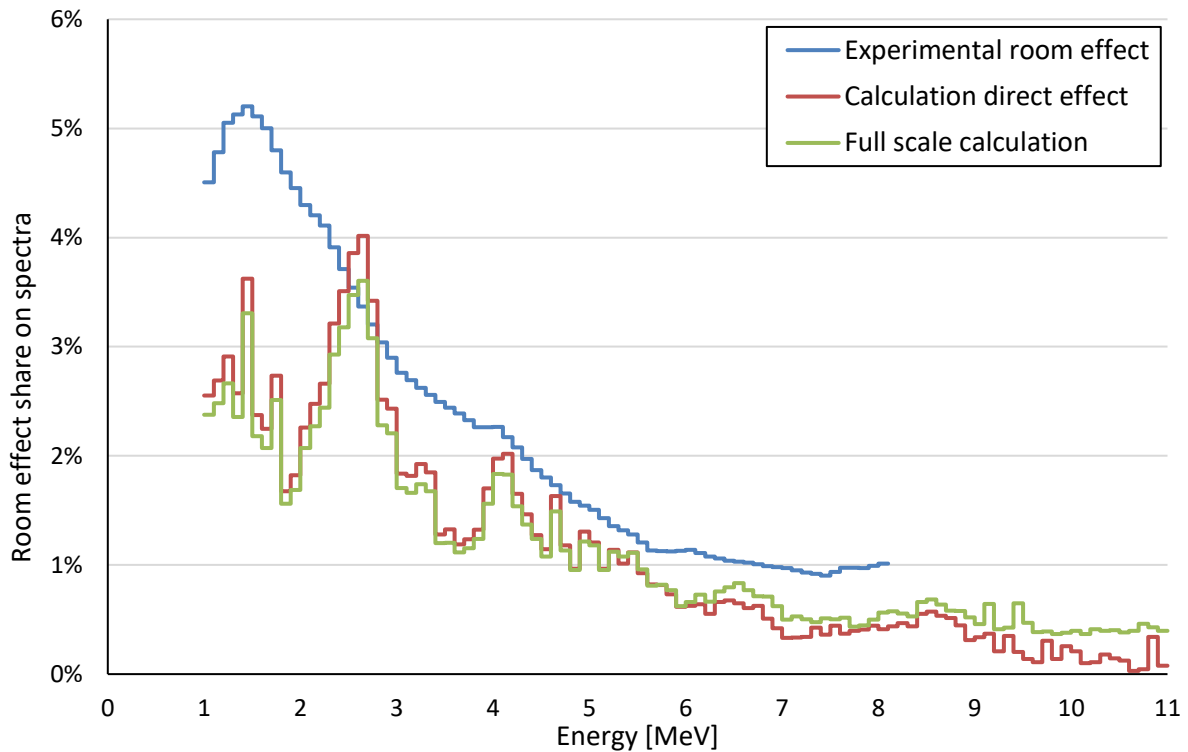
Figure 24: Comparison of the Room Effect Share on Leakage Flux Evaluated from Experiments and Calculation.

The two calculational results of background share are in good agreement. In the experiment, which is reflected in the full-scale approach, the background field is formed also by the neutrons transmitted by the cone. To be sure about the magnitude of this effect, the simulation was performed as well and is shown below in Figure 25. It is worth noting, the transmission effect is below 0.2 % in all energy regions.
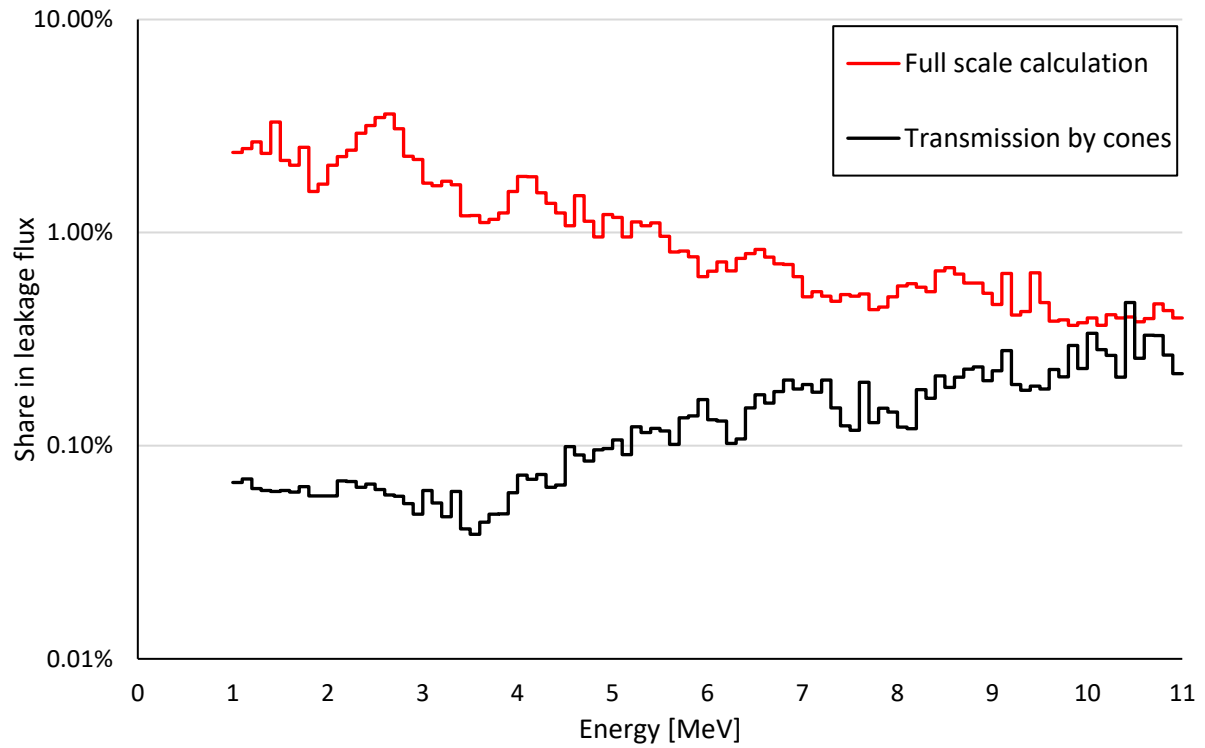
Figure 25: Calculated Ratio of Cone Transmission and Room Effect to Neutron Leakage Flux.

Table 2.3 Evaluation of room effect and transmission by the cone during experimental determination of room effect on pure leakage fluxes.

Energy Group E_{up} [MeV]	Relative effect on $\int_t \Phi_{ng}$ [%]			
	Experimental room effect	Calculation direct effect	Full-scale calculation	Transmission by cone
1.1	4.5	2.6	2.4	0.1
1.2	4.8	2.7	2.5	0.1
1.3	5.1	2.9	2.7	0.1
1.4	5.1	2.6	2.4	0.1
1.5	5.2	3.6	3.3	0.1
1.6	5.1	2.4	2.2	0.1
1.7	5.0	2.2	2.1	0.1
1.8	4.8	2.7	2.5	0.1
1.9	4.6	1.7	1.6	0.1
2.0	4.5	1.8	1.7	0.1
2.1	4.3	2.3	2.1	0.1
2.2	4.2	2.5	2.3	0.1
2.3	4.1	2.7	2.4	0.1
2.4	3.9	3.2	2.9	0.1
2.5	3.7	3.5	3.2	0.1
2.6	3.5	3.9	3.5	0.1
2.7	3.4	4.0	3.6	0.1
2.8	3.2	3.4	3.1	0.1
2.9	3.0	2.5	2.3	0.1
3.0	2.9	2.4	2.2	0.0
3.1	2.8	1.8	1.7	0.1
3.2	2.7	1.8	1.7	0.1
3.3	2.6	1.9	1.7	0.0
3.4	2.6	1.8	1.7	0.1
3.5	2.5	1.3	1.2	0.0
3.6	2.4	1.3	1.2	0.0
3.7	2.4	1.2	1.1	0.0
3.8	2.3	1.2	1.2	0.0
3.9	2.3	1.3	1.2	0.0
4.0	2.3	1.7	1.6	0.1
4.1	2.3	2.0	1.8	0.1
4.2	2.2	2.0	1.8	0.1
4.3	2.1	1.7	1.5	0.1
4.4	2.0	1.5	1.4	0.1
4.5	1.9	1.3	1.2	0.1
4.6	1.8	1.1	1.1	0.1
4.7	1.7	1.6	1.5	0.1
4.8	1.7	1.2	1.1	0.1
4.9	1.6	1.0	1.0	0.1
5.0	1.5	1.3	1.2	0.1
5.1	1.5	1.2	1.2	0.1
5.2	1.4	1.0	1.0	0.1
5.3	1.4	1.1	1.1	0.1
5.4	1.3	1.0	1.1	0.1
5.5	1.3	1.1	1.1	0.1
5.6	1.2	0.9	1.0	0.1

Table 2.3 (cont. 1) Evaluation of room effect and transmission by the cone
during experimental determination of room effect on pure leakage fluxes.

Energy Group E_{up} [MeV]	Relative effect on $\int_t \Phi$ [%]			
	Experimental room effect	Calculation direct effect	Full-scale calculation	Transmission by cone
5.7	1.1	0.8	0.8	0.1
5.8	1.1	0.8	0.8	0.1
5.9	1.1	0.7	0.8	0.1
6.0	1.1	0.6	0.6	0.2
6.1	1.1	0.6	0.7	0.1
6.2	1.1	0.6	0.7	0.1
6.3	1.1	0.6	0.7	0.1
6.4	1.1	0.7	0.8	0.1
6.5	1.0	0.7	0.8	0.2
6.6	1.0	0.6	0.8	0.2
6.7	1.0	0.6	0.8	0.2
6.8	1.0	0.6	0.7	0.2
6.9	1.0	0.5	0.7	0.2
7.0	1.0	0.4	0.6	0.2
7.1	1.0	0.3	0.5	0.2
7.2	1.0	0.3	0.5	0.2
7.3	0.9	0.3	0.5	0.2
7.4	0.9	0.4	0.5	0.2
7.5	0.9	0.4	0.5	0.1
7.6	0.9	0.4	0.5	0.1
7.7	1.0	0.4	0.5	0.2
7.8	1.0	0.4	0.4	0.1
7.9	1.0	0.4	0.4	0.1
8.0	1.0	0.4	0.5	0.1
8.1	1.0	0.4	0.6	0.1
8.2	0.0	0.4	0.6	0.1
8.3	0.0	0.5	0.6	0.2
8.4	0.0	0.4	0.5	0.2
8.5	0.0	0.6	0.7	0.2
8.6	0.0	0.6	0.7	0.2
8.7	0.0	0.5	0.6	0.2
8.8	0.0	0.5	0.6	0.2
8.9	0.0	0.4	0.6	0.2
9.0	0.0	0.3	0.5	0.2
9.1	0.0	0.3	0.5	0.2
9.2	0.0	0.4	0.6	0.3
9.3	0.0	0.2	0.4	0.2
9.4	0.0	0.4	0.4	0.2
9.5	0.0	0.2	0.6	0.2
9.6	0.0	0.1	0.5	0.2
9.7	0.0	0.1	0.4	0.2
9.8	0.0	0.3	0.4	0.2
9.9	0.0	0.1	0.4	0.3
10.0	0.0	0.3	0.4	0.2
10.1	0.0	0.2	0.4	0.3
10.2	0.0	0.1	0.4	0.3

Table 2.3 (cont. 2) Evaluation of room effect and transmission by the cone
during experimental determination of room effect on pure leakage fluxes.

Energy Group E_{up} [MeV]	Relative effect on $\int_t \Phi$ [%]			
	Experimental room effect	Calculation direct effect	Full-scale calculation	Transmission by cone
10.3	0.0	0.1	0.4	0.3
10.4	0.0	0.2	0.4	0.2
10.5	0.0	0.1	0.4	0.5
10.6	0.0	0.1	0.4	0.3
10.7	0.0	0.0	0.4	0.3
10.8	0.0	0.0	0.5	0.3
10.9	0.0	0.3	0.4	0.3
11.0	0.0	0.1	0.4	0.2

2.1.3. Evaluation of material and geometrical uncertainties

The effect of material and geometrical uncertainties was evaluated as well. The most notable identified sources of standard uncertainties are listed in Table 2.4.a, namely copper density (0.0088 g/cm^3), copper block thickness (1 mm), block height (5 mm), copper block width (5 mm), isotopic composition, detector distance (0.5 mm) and detector misalignment (0.5 mm). Cu isotopes ratio of the samples from various mines is given in Table 2.4.b. The relative sensitivities of the neutron leakage flux to boundary Cu isotopes ratio values is given in Table 2.5a.

The evaluated neutron leakage flux effect of each standard uncertainty is listed in Tables 2.5 and 2.5a. The evaluation is done by means of direct perturbation. The results of calculations with parameters perturbed by 3 standard uncertainties are listed in Tables E.2.a, - E.2.d in Appendix E. As expected, the most significant effect is associated with block thickness perturbations, for which the relative effects on the neutron leakage flux are below 2 %. The relative effects on the neutron leakage flux from perturbation of copper density are in the range of 0.4 %, thus playing a significantly lower role than the effect of the thickness perturbation. The standard uncertainties of 0.5 cm in copper block width and height were evaluated as being low, about order of magnitude smaller than effect of density uncertainty. Similarly low effects have uncertainties in the detector distance, detector misalignment or uncertainty in Cu isotopic composition, which effect is not higher than 0.1 - 0.2 %. The small uncertainty is reflecting well defined source position in flexo-rabbit, which was confirmed by activation experiments[a]. This fact agrees with the assumptions, because the exceeding material does not affect the neutron path between source and detector.

Table 2.4.a Considered major sources of uncertainty.

	1σ uncertainty	unit
Material density	0.0088	g/cm^3
Thickness of block	0.1	cm
Block width	0.5	cm
Block height	0.5	cm
Isotopic composition	Table 2.4.b	^{63}Cu/^{65}Cu ratio
Detector distance	0.5	mm
Detector misalignment	0.5	mm

---

[a] Schulc, M., Košťál, M., Šimon, J., Novák, E., Juříček, V., Mareček, M.. Measurement of very high threshold reactions using ^{252}Cf source, (2020) Applied Radiation and Isotopes, 166, art. no. 109355

Table 2.4.b Isotopic composition of copper samples from various mines[a]

Mineral	Mine	Country	$^{63}Cu/^{65}Cu$ ratio
Azurite	Chessy mine	France	2.2403
Bornite	Mufulira mine	Zambia	2.2489
Cuprite	Morenci mine	Arizona	2.2494
Atacamite	Atacama mine	Chile	2.2613
Benchmark value			2.2415

[a] N.H. Galea, A.P. Woodheada, Z.A. Stos-Galea, A. Walderb, I. Bowen, Natural variations detected in the isotopic composition of copper: possible applications to archaeology and geochemistry, International Journal of Mass Spectrometry 184 (1999) 1–9

Table 2.5 Relative sensitivities of the neutron leakage flux to notable component uncertainties.

Energy group E_{up} [MeV]	Relative sensitivities of neutron leakage flux to component perturbations [%]							
	Copper density		Block thickness		Block width		Block height	
	-0.009 g/cm³	+0.009 g/cm³	-1 mm	+1 mm	-0.5 cm	+0.5 cm	-0.5 cm	+0.5 cm
1.1	0.3	-0.3	1.4	-1.3	-0.2	0.2	-0.2	0.2
1.2	0.3	-0.3	1.4	-1.3	-0.2	0.2	-0.2	0.2
1.3	0.3	-0.3	1.4	-1.4	-0.2	0.1	-0.2	0.1
1.4	0.3	-0.3	1.5	-1.4	-0.1	0.1	-0.2	0.1
1.5	0.3	-0.3	1.5	-1.4	-0.1	0.1	-0.1	0.1
1.6	0.4	-0.3	1.6	-1.5	-0.1	0.1	-0.1	0.1
1.7	0.4	-0.4	1.6	-1.5	-0.1	0.1	-0.1	0.1
1.8	0.4	-0.4	1.6	-1.6	-0.1	0.1	-0.1	0.1
1.9	0.4	-0.4	1.7	-1.6	-0.1	0.1	-0.1	0.1
2.0	0.4	-0.4	1.7	-1.6	-0.1	0.1	-0.1	0.1
2.1	0.4	-0.4	1.7	-1.6	-0.1	0.1	-0.1	0.1
2.2	0.4	-0.4	1.7	-1.7	-0.1	0.1	-0.1	0.1
2.3	0.4	-0.4	1.8	-1.7	-0.1	0.1	-0.1	0.1
2.4	0.4	-0.4	1.8	-1.7	-0.1	0.0	-0.1	0.1
2.5	0.4	-0.4	1.8	-1.7	-0.1	0.0	-0.1	0.1
2.6	0.4	-0.4	1.8	-1.7	-0.1	0.0	-0.1	0.0
2.7	0.4	-0.4	1.8	-1.7	-0.1	0.0	-0.1	0.0
2.8	0.4	-0.4	1.8	-1.7	0.0	0.0	-0.1	0.0
2.9	0.4	-0.4	1.8	-1.8	0.0	0.0	-0.1	0.0
3.0	0.4	-0.4	1.9	-1.8	0.0	0.0	-0.1	0.0
3.1	0.4	-0.4	1.9	-1.8	0.0	0.0	-0.1	0.0
3.2	0.4	-0.4	1.9	-1.8	0.0	0.0	0.0	0.0
3.3	0.4	-0.4	1.9	-1.8	0.0	0.0	0.0	0.0
3.4	0.4	-0.4	1.9	-1.8	0.0	0.0	0.0	0.0
3.5	0.4	-0.4	1.9	-1.8	0.0	0.0	0.0	0.0
3.6	0.4	-0.4	1.9	-1.8	0.0	0.0	0.0	0.0
3.7	0.4	-0.4	1.9	-1.8	0.0	0.0	0.0	0.0
3.8	0.4	-0.4	1.9	-1.8	0.0	0.0	0.0	0.0
3.9	0.5	-0.4	2.0	-1.9	0.0	0.0	0.0	0.0
4.0	0.4	-0.4	2.0	-1.9	0.0	0.0	0.0	0.0
4.1	0.4	-0.4	2.0	-1.9	0.0	0.0	0.0	0.0
4.2	0.5	-0.4	2.0	-1.9	0.0	0.0	0.0	0.0
4.3	0.4	-0.4	2.0	-1.8	0.0	0.0	0.0	0.0
4.4	0.5	-0.4	2.0	-1.9	0.0	0.0	0.0	0.0
4.5	0.5	-0.4	2.0	-1.9	0.0	0.0	0.0	0.0
4.6	0.5	-0.4	2.0	-1.9	0.0	0.0	0.0	0.0
4.7	0.4	-0.4	2.0	-1.9	0.0	0.0	0.0	0.0
4.8	0.5	-0.4	2.0	-1.8	0.0	0.0	0.0	0.0
4.9	0.5	-0.4	2.0	-1.9	0.0	0.0	0.0	0.0
5.0	0.5	-0.4	2.0	-1.8	0.0	0.0	0.0	0.0
5.1	0.4	-0.4	2.0	-1.8	0.0	0.0	0.0	0.0
5.2	0.4	-0.4	1.9	-1.9	0.0	0.0	0.0	0.0
5.3	0.4	-0.4	1.9	-1.8	0.0	0.0	0.0	0.0
5.4	0.4	-0.4	1.9	-1.9	0.0	0.0	0.0	0.0
5.5	0.4	-0.4	1.9	-1.8	0.0	0.0	0.0	0.0
5.6	0.5	-0.4	2.0	-1.8	0.0	0.0	0.0	0.0

Table 2.5 (cont. 1) Relative sensitivities of neutron leakage flux to notable component uncertainties.

Energy Group E_{up} [MeV]	Relative sensitivities of neutron leakage flux to component perturbations [%]							
	Copper density		Block thickness		Block width		Block height	
	-0.009 g/cm^3	-0.009 g/cm^3	+1 mm	-1 mm	+0.5 cm	-0.5 cm	+ 1 mm	- 1 mm
5.7	0.4	-0.4	1.9	-1.8	0.0	0.0	0.0	0.0
5.8	0.4	-0.4	1.9	-1.8	0.0	0.0	0.0	0.0
5.9	0.4	-0.4	1.9	-1.8	0.0	0.0	0.0	0.0
6.0	0.4	-0.4	1.9	-1.8	0.0	0.0	0.0	0.0
6.1	0.4	-0.4	1.9	-1.8	0.0	0.0	0.0	0.0
6.2	0.4	-0.4	1.9	-1.8	0.0	0.0	0.0	0.0
6.3	0.4	-0.4	1.9	-1.8	0.0	0.0	0.0	0.0
6.4	0.4	-0.4	1.9	-1.8	0.0	0.0	0.0	0.0
6.5	0.4	-0.4	1.8	-1.7	0.0	0.0	0.0	0.0
6.6	0.4	-0.4	1.9	-1.8	0.0	0.0	0.0	0.0
6.7	0.4	-0.4	1.8	-1.7	0.0	0.0	0.0	0.0
6.8	0.4	-0.4	1.8	-1.7	0.0	0.0	0.0	0.0
6.9	0.4	-0.4	1.9	-1.7	0.0	0.0	0.0	0.0
7.0	0.4	-0.4	1.8	-1.7	0.0	0.0	0.0	0.0
7.1	0.4	-0.4	1.8	-1.7	0.0	0.0	0.0	0.0
7.2	0.4	-0.4	1.8	-1.8	0.0	0.0	0.0	0.0
7.3	0.4	-0.4	1.8	-1.7	0.0	0.0	0.0	0.0
7.4	0.4	-0.4	1.8	-1.7	0.0	0.0	0.0	0.0
7.5	0.4	-0.4	1.8	-1.7	0.0	0.0	0.0	0.0
7.6	0.4	-0.4	1.8	-1.6	0.0	0.0	0.0	0.0
7.7	0.4	-0.4	1.8	-1.6	0.0	0.0	0.0	0.0
7.8	0.4	-0.4	1.8	-1.7	0.0	0.0	0.0	0.0
7.9	0.4	-0.4	1.7	-1.7	0.0	0.0	0.0	0.0
8.0	0.4	-0.4	1.8	-1.6	0.0	0.0	0.0	0.0
8.1	0.4	-0.4	1.7	-1.7	0.0	0.0	0.0	0.0
8.2	0.4	-0.4	1.8	-1.6	0.0	0.0	0.0	0.0
8.3	0.4	-0.4	1.8	-1.6	0.0	0.0	0.0	0.0
8.4	0.4	-0.4	1.7	-1.6	0.0	0.0	0.0	0.0
8.5	0.4	-0.4	1.7	-1.6	0.0	0.0	0.0	0.0
8.6	0.4	-0.4	1.8	-1.7	0.0	0.0	0.0	0.0
8.7	0.4	-0.4	1.8	-1.7	0.0	0.0	0.0	0.0
8.8	0.4	-0.4	1.6	-1.6	0.0	0.0	0.0	0.0
8.9	0.4	-0.3	1.7	-1.5	0.0	0.0	0.0	0.0
9.0	0.4	-0.4	1.7	-1.6	0.0	0.0	0.0	0.0
9.1	0.4	-0.4	1.7	-1.7	0.0	0.0	0.0	0.0
9.2	0.5	-0.4	1.7	-1.6	0.0	0.0	0.0	0.0
9.3	0.4	-0.4	1.7	-1.7	0.0	0.0	0.0	0.0
9.4	0.4	-0.4	1.7	-1.6	0.0	0.0	0.0	0.0
9.5	0.4	-0.3	1.7	-1.6	0.0	0.0	0.0	0.0
9.6	0.4	-0.4	1.7	-1.6	0.0	0.0	0.0	0.0
9.7	0.4	-0.4	1.7	-1.6	0.0	0.0	0.0	0.0
9.8	0.3	-0.4	1.7	-1.6	0.0	0.0	0.0	0.0
9.9	0.5	-0.4	1.8	-1.5	0.0	0.0	0.0	0.0
10.0	0.4	-0.4	1.7	-1.6	0.0	0.0	0.0	0.0
10.1	0.4	-0.3	1.7	-1.5	0.0	0.0	0.0	0.0
10.2	0.3	-0.4	1.6	-1.5	0.0	0.0	0.0	0.0

Table 2.5 (cont. 2) Relative sensitivities of neutron leakage flux to notable component uncertainties.

Energy Group E_{up} [MeV]	Relative sensitivities of neutron leakage flux to component perturbations [%]							
	Copper density		Block thickness		Block width		Block height	
	-0.009 g/cm³	-0.009 g/cm³	+1 mm	-1 mm	+0.5 cm	-0.5 cm	+ 1 mm	- 1 mm
10.3	0.4	-0.4	1.6	-1.6	0.0	0.0	0.0	0.0
10.4	0.4	-0.3	1.7	-1.5	0.0	0.0	0.0	0.0
10.5	0.4	-0.4	1.6	-1.6	0.0	0.0	0.0	0.0
10.6	0.4	-0.3	1.7	-1.5	0.0	0.0	0.0	0.0
10.7	0.4	-0.4	1.6	-1.5	0.0	0.0	0.0	0.0
10.8	0.3	-0.3	1.6	-1.4	0.0	0.0	0.0	0.0
10.9	0.3	-0.3	1.7	-1.4	0.0	0.0	0.0	0.0
11.0	0.3	-0.3	1.4	-1.6	0.0	0.0	0.0	0.0

Table 2.5a Relative sensitivities of the neutron leakage flux to notable component uncertainties.

Energy Group Eup [MeV]	Relative sensitivities of neutron leakage flux to component perturbations [%]					
	Isotopic composition		Detector distance		Detector misalignment	
	Chessy mine	Atacama mine	- 0.5 mm	+0.5 mm	-0.5 mm	+0.5 mm
1.1	0.0	-0.1	-0.1	0.1	0.0	0.0
1.2	0.0	-0.1	-0.1	0.1	0.0	0.0
1.3	0.0	-0.1	-0.1	0.1	0.0	0.0
1.4	0.0	-0.1	-0.1	0.1	0.0	0.0
1.5	0.0	-0.1	-0.1	0.1	0.0	0.0
1.6	0.0	-0.1	-0.1	0.1	0.0	0.0
1.7	0.0	-0.1	-0.1	0.1	0.0	0.0
1.8	0.0	-0.1	-0.1	0.1	0.0	0.0
1.9	0.0	-0.1	-0.1	0.1	0.0	0.0
2.0	0.0	-0.1	-0.1	0.1	0.0	0.0
2.1	0.0	-0.1	-0.1	0.1	0.0	0.0
2.2	0.0	-0.1	-0.1	0.1	0.0	0.0
2.3	0.0	0.0	-0.1	0.1	0.0	0.0
2.4	0.0	0.0	-0.1	0.1	0.0	0.0
2.5	0.0	0.0	-0.1	0.1	0.0	0.0
2.6	0.0	0.0	-0.1	0.1	0.0	0.0
2.7	0.0	0.0	-0.1	0.1	0.0	0.0
2.8	0.0	0.0	-0.1	0.1	0.0	0.0
2.9	0.0	0.0	-0.1	0.1	0.0	0.0
3.0	0.0	0.0	-0.1	0.1	0.0	0.0
3.1	0.0	0.0	-0.1	0.1	0.0	0.0
3.2	0.0	0.0	-0.1	0.1	0.0	0.0
3.3	0.0	0.0	-0.1	0.1	0.0	0.0
3.4	0.0	0.0	-0.1	0.1	0.0	0.0
3.5	0.0	0.0	-0.1	0.1	0.0	0.0
3.6	0.0	0.0	-0.1	0.1	0.0	0.0
3.7	0.0	0.0	-0.1	0.1	0.0	0.0
3.8	0.0	0.0	-0.1	0.1	0.0	0.0
3.9	0.0	0.0	-0.1	0.1	0.0	0.0
4.0	0.0	0.0	-0.1	0.1	0.0	0.0
4.1	0.0	0.0	-0.1	0.1	0.0	0.0
4.2	0.0	0.0	-0.1	0.1	0.0	0.0
4.3	0.0	0.0	-0.1	0.1	0.0	0.0
4.4	0.0	0.0	-0.1	0.1	0.0	0.0
4.5	0.0	0.0	-0.1	0.1	0.0	0.0
4.6	0.0	0.0	-0.1	0.1	0.0	0.0
4.7	0.0	0.0	-0.1	0.1	0.0	0.0
4.8	0.0	0.0	-0.1	0.1	0.0	0.0
4.9	0.0	0.0	-0.1	0.1	0.0	0.0
5.0	0.0	0.0	-0.1	0.1	0.0	0.0
5.1	0.0	0.0	-0.1	0.1	0.0	0.0
5.2	0.0	0.0	-0.1	0.1	0.0	0.0
5.3	0.0	0.0	-0.1	0.1	0.0	0.0
5.4	0.0	0.0	-0.1	0.1	0.0	0.0
5.5	0.0	0.0	-0.1	0.1	0.0	0.0
5.6	0.0	0.0	-0.1	0.1	0.0	0.0

Table 2.5a (cont. 1) Relative sensitivities of neutron leakage flux to notable component uncertainties.

| Energy Group Eup [MeV] | Relative sensitivities of neutron leakage flux to component perturbations [%] | | | | | |
| | Isotopic composition | | Detector distance | | Detector misalignment | |
	Chessy mine	Atacama mine	- 0.5 mm	+0.5 mm	-0.5 mm	+0.5 mm
5.7	0.0	0.0	-0.1	0.1	0.0	0.0
5.8	0.0	0.0	-0.1	0.1	0.0	0.0
5.9	0.0	0.0	-0.1	0.1	0.0	0.0
6.0	0.0	0.0	-0.1	0.1	0.0	0.0
6.1	0.0	0.0	-0.1	0.1	0.0	0.0
6.2	0.0	0.0	-0.1	0.1	0.0	0.0
6.3	0.0	0.0	-0.1	0.1	0.0	0.0
6.4	0.0	0.0	-0.1	0.1	0.0	0.0
6.5	0.0	0.0	-0.1	0.1	0.0	0.0
6.6	0.0	0.0	-0.1	0.1	0.0	0.0
6.7	0.0	0.0	-0.1	0.1	0.0	0.0
6.8	0.0	0.0	-0.1	0.1	0.0	0.0
6.9	0.0	0.0	-0.1	0.1	0.0	0.0
7.0	0.0	0.0	-0.1	0.1	0.0	0.0
7.1	0.0	0.0	-0.1	0.1	0.0	0.0
7.2	0.0	0.0	-0.1	0.1	0.0	0.0
7.3	0.0	0.0	-0.1	0.1	0.0	0.0
7.4	0.0	0.0	-0.1	0.1	0.0	0.0
7.5	0.0	0.0	-0.1	0.1	0.0	0.0
7.6	0.0	0.0	-0.1	0.1	0.0	0.0
7.7	0.0	0.0	-0.1	0.1	0.0	0.0
7.8	0.0	0.0	-0.1	0.1	0.0	0.0
7.9	0.0	0.0	-0.1	0.1	0.0	0.0
8.0	0.0	0.0	-0.1	0.1	0.0	0.0
8.1	0.0	0.0	-0.1	0.1	0.0	0.0
8.2	0.0	0.0	-0.1	0.1	0.0	0.0
8.3	0.0	0.0	-0.1	0.1	0.0	0.0
8.4	0.0	0.0	-0.1	0.1	0.0	0.0
8.5	0.0	0.0	-0.1	0.1	0.0	0.0
8.6	0.0	0.0	-0.1	0.1	0.0	0.0
8.7	0.0	0.0	-0.1	0.1	0.0	0.0
8.8	0.0	0.0	-0.1	0.1	0.0	0.0
8.9	0.0	0.0	-0.1	0.1	0.0	0.0
9.0	0.0	0.0	-0.1	0.1	0.0	0.0
9.1	0.0	0.0	-0.1	0.1	0.0	0.0
9.2	0.0	0.0	-0.1	0.1	0.0	0.0
9.3	0.0	0.0	-0.1	0.1	0.0	0.0
9.4	0.0	0.0	-0.1	0.1	0.0	0.0
9.5	0.0	0.0	-0.1	0.1	0.0	0.0
9.6	0.0	0.0	-0.1	0.1	0.0	0.0
9.7	0.0	0.0	-0.1	0.1	0.0	0.0
9.8	0.0	0.0	-0.1	0.1	0.0	0.0
9.9	0.0	0.0	-0.1	0.1	0.0	0.0
10.0	0.0	0.0	-0.1	0.1	0.0	0.0
10.1	0.0	0.0	-0.1	0.1	0.0	0.0
10.2	0.0	0.0	-0.1	0.1	0.0	0.0

Table 2.5a (cont. 2) Relative sensitivities of neutron leakage flux to notable component uncertainties.

Energy Group Eup [MeV]	Relative sensitivities of neutron leakage flux to component perturbations [%]					
	Isotopic composition		Detector distance		Detector misalignment	
	Chessy mine	Atacama mine	- 0.5 mm	+0.5 mm	-0.5 mm	+0.5 mm
10.3	0.0	0.0	-0.1	0.1	0.0	0.0
10.4	0.0	0.0	-0.1	0.1	0.0	0.0
10.5	0.0	0.0	-0.1	0.1	0.0	0.0
10.6	0.0	-0.1	-0.1	0.1	0.0	0.0
10.7	0.0	0.0	-0.1	0.1	0.0	0.0
10.8	0.0	0.0	-0.1	0.1	0.0	0.0
10.9	0.0	0.0	-0.1	0.1	0.0	0.0
11.0	0.0	-0.1	-0.1	0.1	0.0	-0.1

2.1.4. Evaluation of component biases and uncertainties

Sensitivities were determined for various uncertainties which might have affected the measurements. The associated components and other uncertainty sources include Al table under the block, Cu holder of the block, screws holding the copper plates together, possible gaps between Cu assemblies (each assembly is formed from separate 1 cm thick plates which are screwed together), the cavity in the copper block, Cu contamination, and source components, namely aluminum components and steel casing of the source. The estimated results are presented in Table 2.6. They are based on calculations, as specified in Tables E.3a and E.3b in Appendix E.

For ensuring the precise geometry, the block is located on the Al table. The effect of such support structure is one part of the room effect which is simply subtracted by measurement with the cone. However, the question arises as to how precisely this effect is suppressed by the cone, because the Al plate of the support table adjoins the Cu block. To be sure, the effect of the table adjoining to the block was determined as well. The results show that the increase of flux in detector position is negligible, except for the first group, not higher than 0.5 %. It means that effect of the Al table on Cu block leakage flux, i. e., Al scattered neutrons, partly contribute to evaluated flux, but the effect is small.

Similarly, the same issue appears with copper block holders. As the first holder begins 3 cm from the block flat, the possible neutrons scattered in the holder are shielded by the shielding cone. Therefore, the effect of holders is lower than 0.1 – 0.2%, approximately half regarding to the effect of Al table.

Due to the square geometry of the copper block and the cylindrical geometry of the cone slabs, a small portion of the edges of the copper block corners is unshielded by the shielding cone. This could create a direct streaming path from the edges of the block to the detector during the background measurement. When measuring with the shielding cone, a small portion of the neutrons reflected in this part of the block could appear in the detector signal. The magnitude of this effect was determined by simulation, as it covers neutron transmission through the cone, the room effect and also the direct streaming from copper to the detector. The simulation showed that this total effect is in the range of 0.3 %, so that, the effect of unshielded corners is less than 0.3%.

The effect of gaps between copper blocks was determined to be low as well, being about 0.1 % to 0.2 %. The explanation is that the gaps do not modify the number of copper nuclides between source and detector, and the only change is that scattering matter is closer to the detector. The effect of screws holding together the copper assemblies (and even plates) is not higher than 0.1 %, similarly to the effect of contamination, namely the effect of neglecting Cl, Ni, Ca, K, Fe, Ag (mass fractions in total 0.0014 %) doesn't exceed 0.1 %. Similarly, the effect of the block cavity neglection has negligible effect that does not exceed 0.02 %. This means that the uncertainty of the cavity dimensions has practically no effect.

The effects of Al structural components of the source transport cask, the flexo-rabbit, and stainless steel casing of ^{252}Cf(s.f) source were determined from a calculational model, where Al (or steel) was replaced by a void. The effect of aluminum is lower than 2 % to 3 %, while the effect of steel cladding is about 3 % to 5 %.

Based on such magnitudes it can be concluded that sources of uncertainty which change the mass of Al or steel components not more than by 4 % to 5 % would contribute to total uncertainty by no more than 0.2 %.

The stainless steel casing of the neutron source is modeled, although it is already included in the source during the determination of the emission rate of the ^{252}Cf(s.f.) source, as mentioned in section 1.4. Thus, as the effect of cladding absorption is included also in the calculational model, the source emission rate is underestimated in simulations. The rate of such underestimation is negligible, being smaller than 0.01 %) because the majority of the neutrons interacting with stainless steel cladding are scattered (see Figure 26), and only a very small part is absorbed. Namely, the ratio between both effects is expressed by the scatter to capture ratio (Figure 26). It can be seen that in the relevant interval above 84 keV, where more than 99 % neutrons are emitted, the ratio is between 500 and 7000. It means that only 1 neutron per 500 to 7000 interactions is absorbed. The interaction rate in stainless steel cladding is not higher

than 5 % (computationally determined and listed in Table 2.6), thus the bias in the neutron emission rate caused by this approach cannot be higher than 0.01 %. The source spectrum is affected significantly by the stainless steel casing. The ^{252}Cf source spectrum data apply to the un-collided flux, making the presence of the stainless steel important.

The manganese bath (used in calibration of the source, see Section 1.4) is not sensitive to spectral shift caused by steel cladding, because the scatter neutron causes the same response of the manganese bath as the transmitted one. This approach is most reliable because the emission rate on source sealing reflects the real state, and the introduced bias is about 100 times smaller than the uncertainty in emission rate.
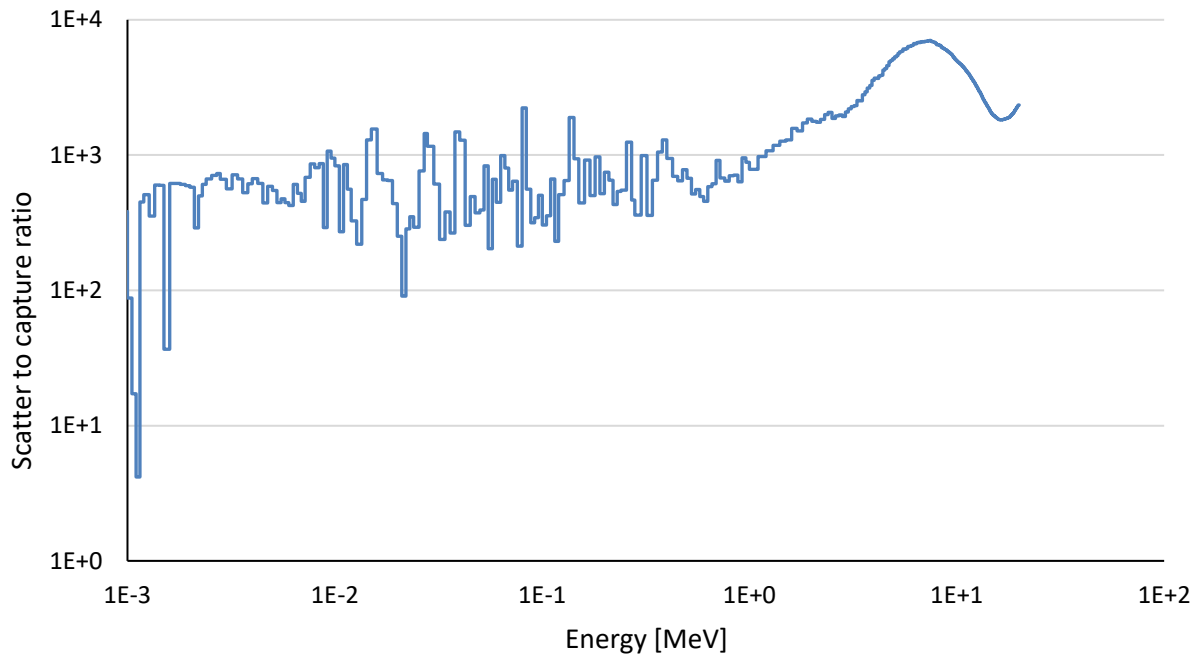
Figure 26: Scatter to Capture Ratio in ENDF/B-VIII.0 for used Steel 304L
.

Table 2.6. Relative sensitivities of neutron leakage flux to selected components

Energy Group	Relative sensitivities of neutron leakage flux to selected component perturbations [%]							
E_{up} [MeV]	Al bottom	Holder of blocks	Screws	Gaps between	Effect of contami-nation	No structural Al	No steel casing	No cavity
1.1	0.2	0.4	0.0	-0.1	0.0	0.5	0.6	0.0
1.2	0.1	0.4	0.0	-0.1	0.0	0.7	0.7	0.0
1.3	0.1	0.3	0.0	-0.1	0.0	0.4	0.9	0.0
1.4	0.1	0.3	0.0	-0.1	0.0	0.5	1.0	0.0
1.5	0.1	0.2	0.0	-0.1	0.0	0.5	1.2	0.0
1.6	0.1	0.2	0.0	0.0	0.0	0.6	1.3	0.0
1.7	0.1	0.2	0.0	0.0	0.0	0.4	1.3	0.0
1.8	0.1	0.2	0.0	0.0	0.0	0.5	1.5	0.0
1.9	0.1	0.2	0.0	0.0	0.1	0.3	1.7	0.0
2.0	0.1	0.2	0.0	0.0	0.1	0.7	1.8	0.0
2.1	0.1	0.2	0.0	0.0	0.1	0.8	1.8	0.0
2.2	0.1	0.1	0.0	0.0	0.1	0.8	1.8	0.0
2.3	0.1	0.1	0.0	0.0	0.1	0.8	1.9	0.0
2.4	0.1	0.1	0.0	0.0	0.1	0.4	1.8	0.0
2.5	0.1	0.1	0.0	0.0	0.1	0.5	2.1	0.0
2.6	0.1	0.1	0.0	0.0	0.1	1.2	2.3	0.0
2.7	0.0	0.1	0.0	0.0	0.1	1.0	2.3	0.0
2.8	0.0	0.1	0.0	0.0	0.1	1.2	2.4	0.0
2.9	0.0	0.1	0.0	0.0	0.1	1.1	2.7	0.0
3.0	0.0	0.1	0.0	-0.1	0.1	1.3	2.7	0.0
3.1	0.0	0.1	0.0	0.0	0.1	1.2	2.9	0.0
3.2	0.0	0.1	0.0	-0.1	0.1	1.2	3.1	0.0
3.3	0.0	0.1	0.0	-0.1	0.1	1.2	2.9	0.0
3.4	0.0	0.1	0.0	0.0	0.1	1.4	3.2	0.0
3.5	0.0	0.1	0.0	-0.1	0.1	1.3	3.3	0.0
3.6	0.0	0.1	0.0	-0.1	0.1	1.7	3.3	0.0
3.7	0.0	0.1	0.0	-0.1	0.1	1.4	3.3	0.0
3.8	0.0	0.1	0.0	-0.1	0.1	1.5	3.5	0.0
3.9	0.0	0.1	0.0	0.0	0.1	1.5	3.6	0.0
4.0	0.0	0.1	0.0	-0.1	0.1	1.6	3.5	0.0
4.1	0.0	0.1	0.0	-0.1	0.1	1.5	3.7	0.0
4.2	0.0	0.1	0.0	-0.1	0.1	1.7	3.9	0.0
4.3	0.0	0.1	0.0	-0.1	0.1	1.5	3.9	0.0
4.4	0.0	0.1	0.0	-0.1	0.1	1.7	3.9	0.0
4.5	0.0	0.1	0.0	0.0	0.1	1.8	4.1	0.0
4.6	0.0	0.1	0.0	0.0	0.1	1.6	4.1	0.0
4.7	0.0	0.1	0.0	0.0	0.1	1.8	4.0	0.0
4.8	0.0	0.1	0.0	-0.1	0.1	1.8	3.8	0.0
4.9	0.0	0.1	0.0	-0.1	0.1	1.7	4.1	0.0
5.0	0.0	0.1	0.0	0.0	0.1	2.3	4.5	0.0
5.1	0.0	0.1	0.0	-0.1	0.1	2.2	4.3	0.0
5.2	0.0	0.1	0.0	0.0	0.1	1.9	4.4	0.0
5.3	0.0	0.1	0.0	-0.1	0.1	2.0	4.3	0.0
5.4	0.0	0.1	0.0	-0.1	0.2	2.3	4.4	0.0
5.5	0.0	0.1	0.0	-0.1	0.1	1.9	4.3	0.0

Table 2.6. (cont. 1) Relative sensitivities of neutron leakage flux to selected components

Energy Group	Relative sensitivities of neutron leakage flux to selected component perturbations [%]							
E_{up} [MeV]	Al bottom	Holder of blocks	Screws	Gaps between	Effect of contami-nation	No structural Al	No steel casing	No cavity
5.6	0.0	0.1	0.0	-0.1	0.1	2.3	4.5	0.0
5.7	0.0	0.1	0.0	-0.1	0.1	1.7	4.0	0.0
5.8	0.0	0.1	0.0	-0.1	0.1	2.3	4.2	0.0
5.9	0.0	0.1	0.0	0.0	0.1	1.9	4.2	0.0
6.0	0.0	0.1	0.0	-0.1	0.1	2.1	4.0	0.0
6.1	0.0	0.1	0.0	-0.1	0.1	2.4	4.6	0.0
6.2	0.0	0.1	0.0	0.0	0.1	2.4	4.3	0.0
6.3	0.0	0.0	0.0	-0.1	0.1	1.7	3.9	0.0
6.4	0.0	0.1	0.0	-0.1	0.1	2.5	4.5	0.0
6.5	0.0	0.0	0.0	-0.1	0.1	1.9	3.9	0.0
6.6	0.0	0.1	0.0	-0.1	0.1	2.1	4.1	0.0
6.7	0.0	0.1	0.0	0.0	0.1	2.0	4.1	0.0
6.8	0.0	0.1	0.0	0.0	0.1	2.1	3.8	0.0
6.9	0.0	0.0	0.0	-0.1	0.1	2.8	4.1	0.0
7.0	0.0	0.1	0.0	0.0	0.1	2.9	4.3	0.0
7.1	0.0	0.1	0.0	-0.1	0.2	2.6	5.0	0.0
7.2	0.0	0.1	0.0	-0.1	0.1	2.2	4.0	0.0
7.3	0.0	0.1	0.0	0.0	0.1	3.2	5.3	0.0
7.4	0.0	0.0	0.0	0.0	0.1	2.2	4.5	0.0
7.5	0.0	0.0	0.0	-0.1	0.1	2.7	5.0	0.0
7.6	0.0	0.0	0.0	0.0	0.1	3.0	4.7	0.0
7.7	0.0	0.1	0.0	0.0	0.1	2.0	4.0	0.0
7.8	0.0	0.0	0.0	-0.1	0.1	2.0	4.4	0.0
7.9	0.0	0.0	0.0	0.0	0.1	2.6	5.0	0.0
8.0	0.0	0.0	0.0	-0.1	0.2	2.3	3.8	0.0
8.1	0.0	0.0	0.0	0.0	0.1	2.5	4.0	0.0
8.2	0.0	0.0	0.0	-0.1	0.1	3.2	5.0	0.0
8.3	0.0	0.0	0.0	-0.1	0.2	3.6	5.2	0.0
8.4	0.0	0.0	0.0	-0.1	0.0	2.1	4.5	0.0
8.5	0.0	0.0	0.0	-0.1	0.2	2.2	5.6	0.0
8.6	0.0	0.0	0.0	-0.1	0.1	2.3	4.8	0.0
8.7	0.0	0.0	0.0	0.0	0.1	2.6	4.9	0.0
8.8	0.0	0.0	0.0	-0.1	0.2	0.7	3.6	0.0
8.9	0.0	0.0	0.0	-0.1	0.2	2.5	4.5	0.0
9.0	0.0	0.0	0.0	0.0	0.1	2.0	2.9	0.0
9.1	0.0	0.0	0.0	-0.1	0.1	2.7	4.9	0.0
9.2	0.0	0.0	0.0	0.0	0.0	1.7	3.7	0.0
9.3	0.0	0.0	0.0	-0.1	0.1	2.1	4.3	0.0
9.4	0.0	0.1	0.0	-0.1	0.1	1.7	3.9	0.0
9.5	0.0	0.1	0.0	-0.1	0.1	2.0	4.6	0.0
9.6	0.0	0.0	0.0	-0.1	0.0	3.1	4.2	0.0
9.7	0.0	0.0	0.0	-0.1	0.1	3.7	4.9	0.0
9.8	0.0	0.0	0.0	-0.1	0.0	0.7	3.6	0.0
9.9	0.0	0.0	0.0	-0.1	0.1	1.0	4.5	0.0
10.0	0.0	0.0	0.0	-0.1	0.2	3.6	3.9	0.0

Table 2.6. (cont. 2) Relative sensitivities of neutron leakage flux to selected components

Energy Group	Relative sensitivities of neutron leakage flux to selected component perturbations [%]							
E_{up} [MeV]	Al bottom	Holder of blocks	Screws	Gaps between	Effect of contami-nation	No structural Al	No steel casing	No cavity
10.1	0.0	0.1	0.0	0.0	0.1	2.5	4.6	0.0
10.2	0.0	0.0	0.0	-0.1	0.1	2.0	3.0	0.0
10.3	0.0	0.0	0.0	-0.1	0.1	2.2	3.7	0.0
10.4	0.0	0.0	0.0	-0.1	0.2	2.2	4.1	0.0
10.5	0.0	0.0	0.0	-0.1	0.1	2.2	4.8	0.0
10.6	0.0	0.0	0.0	-0.1	0.1	4.4	4.8	0.0
10.1	0.0	0.1	0.0	0.0	0.1	2.5	4.6	0.0
10.2	0.0	0.0	0.0	-0.1	0.1	2.0	3.0	0.0
10.3	0.0	0.0	0.0	-0.1	0.1	2.2	3.7	0.0
10.4	0.0	0.0	0.0	-0.1	0.2	2.2	4.1	0.0
10.5	0.0	0.0	0.0	-0.1	0.1	2.2	4.8	0.0
10.6	0.0	0.0	0.0	-0.1	0.1	4.4	4.8	0.0
10.7	0.0	0.0	0.0	0.0	0.2	0.9	3.2	0.0
10.8	0.0	0.0	0.0	-0.1	0.1	2.0	4.9	0.0
10.9	0.0	0.1	0.0	0.0	0.0	1.4	5.1	0.0
11.0	0.0	0.0	0.0	0.0	0.1	0.2	2.5	0.0

2.1.5. Evaluated measurement of neutron leakage fluxes and their uncertainties

Three experimental neutron fluxes (ϕ), normalized to one source neutron per second, in energy groups are listed in Table 2.7 together with related uncertainties. The neutron flux data were evaluated (denoted as Measurement 1, 2, 3), using the proton recoil data in Table 1.10 (or in 4096 groups in Appendix E) and the actual source neutron emission rates and measuring times in Table 1.9.

The primary neutron source emission rate has been determined in the stainless steel clad ^{252}Cf(s.f) source in NPL (UK, 2015). It means that the actual emission rate of the californium in the source is slightly higher than determined by calculation from the primary emission, because some neutrons are absorbed in the cladding. Due to the fact that in the energy region where the neutrons are emitted by the ^{252}Cf(s.f.), source absorption in steel is negligible (scatter to capture ratio is above 5000), this effect of underestimation is also negligible.

The source emission uncertainty is neglected, as is the uncertainty in measurement time is lower than 0.001 %, and uncertainty ^{252}Cf half-life, which effect is lower than 0.1 %.

The overall relative standard uncertainties of the measurements are approximately between 7.0 % and 16 %. The detailed uncertainty evaluation is listed in Table 2.1 and Table 2.2 in Section 2.1.1.

Table 2.7 Evaluated neutron fluxes, normalized to one source neutron per second.

Energy Group E_{up} [MeV]	Normalized neutron fluxes from three separate measurements					
	Measurement 1		Measurement 2		Measurement 3	
	Normalized φ [cm^{-2}·s^{-1}]	u_r [%]	Normalized φ [cm^{-2}·s^{-1}]	u_r [%]	Normalized φ [cm^{-2}·s^{-1}]	u_r [%]
1.1	6.567E-8	16.7	4.669E-8	16.7	5.212E-8	16.7
1.2	4.873E-8	13.9	4.351E-8	13.9	4.767E-8	13.9
1.3	3.587E-8	12.7	4.060E-8	12.7	4.366E-8	12.7
1.4	2.790E-8	8.5	3.180E-8	8.5	3.309E-8	8.5
1.5	2.143E-8	9.0	2.481E-8	9.0	2.497E-8	9.0
1.6	1.734E-8	9.7	1.926E-8	9.7	1.904E-8	9.7
1.7	1.386E-8	12.7	1.483E-8	12.7	1.440E-8	12.7
1.8	1.186E-8	11.6	1.252E-8	11.6	1.218E-8	11.6
1.9	1.003E-8	10.6	1.048E-8	10.6	1.021E-8	10.6
2.0	8.810E-9	9.7	8.960E-9	9.6	8.782E-9	9.6
2.1	7.673E-9	8.8	7.605E-9	8.7	7.497E-9	8.7
2.2	6.705E-9	7.7	6.729E-9	7.7	6.661E-9	7.7
2.3	5.806E-9	7.2	5.909E-9	7.2	5.874E-9	7.2
2.4	5.149E-9	7.0	5.164E-9	7.0	5.177E-9	7.1
2.5	4.530E-9	6.9	4.478E-9	6.9	4.529E-9	7.0
2.6	4.027E-9	7.0	3.965E-9	7.1	4.022E-9	7.1
2.7	3.556E-9	7.3	3.488E-9	7.4	3.550E-9	7.3
2.8	3.180E-9	7.1	3.155E-9	7.1	3.180E-9	7.1
2.9	2.826E-9	7.2	2.838E-9	7.1	2.832E-9	7.1
3.0	2.571E-9	7.1	2.593E-9	7.0	2.593E-9	7.1
3.1	2.327E-9	7.2	2.356E-9	7.1	2.362E-9	7.2
3.2	2.098E-9	7.1	2.132E-9	7.0	2.138E-9	7.0
3.3	1.880E-9	7.0	1.920E-9	7.0	1.924E-9	6.9
3.4	1.717E-9	6.8	1.740E-9	6.8	1.741E-9	6.7
3.5	1.559E-9	6.9	1.569E-9	6.9	1.568E-9	6.9
3.6	1.443E-9	6.7	1.433E-9	6.6	1.450E-9	6.6
3.7	1.329E-9	6.8	1.303E-9	6.7	1.335E-9	6.7
3.8	1.230E-9	6.6	1.222E-9	6.5	1.246E-9	6.5
3.9	1.133E-9	6.9	1.142E-9	6.8	1.159E-9	6.8
4.0	1.051E-9	6.9	1.086E-9	6.8	1.095E-9	6.8
4.1	9.718E-10	7.0	1.031E-9	6.9	1.031E-9	6.9
4.2	9.112E-10	7.0	9.707E-10	6.8	9.651E-10	6.8
4.3	8.517E-10	6.9	9.117E-10	6.7	9.008E-10	6.7
4.4	8.129E-10	6.9	8.605E-10	6.8	8.469E-10	6.9
4.5	7.737E-10	7.0	8.099E-10	7.0	7.938E-10	7.0
4.6	7.357E-10	7.0	7.650E-10	7.1	7.526E-10	7.0
4.7	6.977E-10	7.0	7.206E-10	7.1	7.116E-10	7.1
4.8	6.656E-10	6.9	6.809E-10	7.1	6.694E-10	7.0
4.9	6.334E-10	6.9	6.417E-10	7.1	6.279E-10	6.9
5.0	6.023E-10	7.0	6.118E-10	7.1	6.094E-10	7.0
5.1	5.714E-10	7.9	5.819E-10	8.0	5.904E-10	7.9
5.2	5.453E-10	7.9	5.602E-10	8.0	5.572E-10	7.8
5.3	5.193E-10	8.0	5.382E-10	8.3	5.246E-10	7.9
5.4	4.918E-10	7.9	5.142E-10	8.3	5.006E-10	7.9
5.5	4.646E-10	8.1	4.903E-10	8.5	4.766E-10	8.1
5.6	4.517E-10	7.8	4.667E-10	8.2	4.496E-10	7.9

Table 2.7 (cont. 1) Evaluated neutron fluxes, normalized to one source neutron per second.

Energy Group E_{up} [MeV]	Normalized neutron fluxes from three separate measurements					
	Measurement 1		Measurement 2		Measurement 3	
	Normalized φ $[cm^{-2} \cdot s^{-1}]$	u_r [%]	Normalized φ $[cm^{-2} \cdot s^{-1}]$	u_r [%]	Normalized φ $[cm^{-2} \cdot s^{-1}]$	u_r [%]
5.7	4.384E-10	8.2	4.433E-10	8.3	4.231E-10	8.1
5.8	4.213E-10	8.0	4.200E-10	7.7	4.045E-10	7.6
5.9	4.042E-10	7.8	3.971E-10	7.5	3.859E-10	7.5
6.0	3.878E-10	7.8	3.737E-10	7.6	3.679E-10	7.6
6.1	3.713E-10	8.2	3.509E-10	8.0	3.500E-10	8.0
6.2	3.506E-10	8.1	3.380E-10	7.9	3.375E-10	7.9
6.3	3.305E-10	8.1	3.251E-10	8.0	3.250E-10	8.0
6.4	3.191E-10	8.4	3.112E-10	8.4	3.142E-10	8.3
6.5	3.077E-10	8.8	2.975E-10	8.8	3.034E-10	8.7
6.6	2.892E-10	9.0	2.863E-10	9.0	2.878E-10	8.9
6.7	2.713E-10	9.4	2.750E-10	9.4	2.724E-10	9.3
6.8	2.518E-10	9.1	2.614E-10	9.2	2.598E-10	9.1
6.9	2.331E-10	9.2	2.481E-10	9.4	2.473E-10	9.3
7.0	2.179E-10	9.5	2.353E-10	9.6	2.325E-10	9.5
7.1	2.032E-10	9.9	2.228E-10	9.9	2.180E-10	9.9
7.2	1.932E-10	9.3	2.097E-10	9.1	2.040E-10	9.2
7.3	1.835E-10	9.2	1.969E-10	9.0	1.906E-10	9.1
7.4	1.699E-10	9.1	1.793E-10	9.1	1.786E-10	9.0
7.5	1.571E-10	9.4	1.628E-10	9.5	1.670E-10	9.2
7.6	1.485E-10	9.7	1.571E-10	9.6	1.570E-10	9.5
7.7	1.401E-10	10.0	1.514E-10	9.8	1.472E-10	9.8
7.8	1.326E-10	9.3	1.428E-10	9.0	1.406E-10	9.1
7.9	1.252E-10	8.5	1.346E-10	8.2	1.341E-10	8.4
8.0	1.183E-10	9.2	1.273E-10	9.1	1.279E-10	9.3
8.1	1.116E-10	10.1	1.203E-10	10.0	1.218E-10	10.3
8.2	1.088E-10	9.9	1.152E-10	9.8	1.146E-10	9.9
8.3	1.060E-10	9.7	1.103E-10	9.8	1.077E-10	9.7
8.4	1.009E-10	8.8	1.076E-10	9.0	1.038E-10	8.8
8.5	9.588E-11	8.8	1.050E-10	9.3	9.993E-11	8.9
8.6	9.332E-11	9.2	1.001E-10	9.7	9.423E-11	9.2
8.7	9.071E-11	9.9	9.542E-11	10.6	8.869E-11	10.1
8.8	8.708E-11	10.8	9.243E-11	11.5	8.301E-11	10.9
8.9	8.349E-11	11.7	8.943E-11	12.5	7.754E-11	11.8
9.0	8.081E-11	10.8	8.614E-11	11.6	7.490E-11	10.9
9.1	7.815E-11	10.7	8.290E-11	11.6	7.227E-11	10.9
9.2	7.487E-11	10.1	7.946E-11	11.0	6.956E-11	10.5
9.3	7.166E-11	9.6	7.608E-11	10.7	6.689E-11	10.2
9.4	6.662E-11	8.3	7.504E-11	9.4	6.422E-11	9.1
9.5	6.182E-11	8.7	7.397E-11	9.8	6.160E-11	9.6
9.6	5.806E-11	8.6	6.923E-11	9.3	6.049E-11	9.3
9.7	5.445E-11	12.7	6.470E-11	13.0	5.936E-11	13.2
9.8	5.001E-11	12.4	6.050E-11	13.3	5.503E-11	12.7
9.9	4.584E-11	16.2	5.649E-11	17.5	5.093E-11	16.3
10.0	4.255E-11	14.9	5.261E-11	16.4	4.752E-11	15.1

Table 2.7 (cont. 2) Evaluated neutron fluxes, normalized to one source neutron per second.

Energy Group E_{up} [MeV]	Normalized neutron fluxes from three separate measurements					
	Measurement 1		Measurement 2		Measurement 3	
	Normalized φ [cm^{-2}·s^{-1}]	u_r [%]	Normalized φ [cm^{-2}·s^{-1}]	u_r [%]	Normalized φ [cm^{-2}·s^{-1}]	u_r [%]
10.1	3.943E-11	14.2	4.891E-11	15.8	4.427E-11	14.3
10.2	3.928E-11	13.5	4.701E-11	15.2	4.289E-11	13.1
10.3	3.910E-11	16.0	4.513E-11	17.7	4.152E-11	15.4
10.4	3.656E-11	17.6			3.790E-11	17.0
10.5	3.413E-11	21.1			3.453E-11	20.9
10.6	3.108E-11	21.8			3.189E-11	22.0
10.7	2.823E-11	24.4			2.940E-11	25.0
10.8	2.585E-11	27.1			2.674E-11	27.4
10.9	2.363E-11	31.5			2.426E-11	31.6
11.0	2.212E-11	28.5			2.340E-11	28.7

3.0   BENCHMARK SPECIFICATIONS

3.1.   <u>Evaluation of the Benchmark</u>

The specifications of the experiment are based on the evaluated geometry and material composition data from Sections 1 and 2.

The benchmarks are based on the experiment specifications. To support the transformation from the experiment specifications to benchmark models and results (simplifications), Section 3.1 refers to descriptions of the simplifications and to Section 3.2 figures of the benchmark model. Benchmark model overviews, including the location of the detector, i.e. the volume where the neutron flux is to be determined, are shown in Figure 27. The benchmark model of the flexo-rabbit end cap with a ^{252}Cf source is shown in Figure 28, which shows the coordinates relative to the source center. The benchmark model of the copper block, with localization of the source in the copper block, is presented in Figures 29 and 30.

3.1.1.   Description of the Benchmark Model Simplifications

The evaluated experiment specifications are simplified to obtain the benchmark specifications. The Al support of the block, Cu holders, stainless steel screws, laboratory ceilings, floor, and walls are omitted. The dural (Al alloy) components are simplified to pure Al. The stainless steel encapsulation is considered in the model as a full block (see Figure 28). The cavity on the bottom of the transport holder is omitted. The holes in spacer ring are neglected. The air is neglected, because air density is about 10 000 times lower than copper density. The influences on the neutron leakage flux of these simplifications were found to be negligible in the previous sections.

The ^{252}Cf(s.f) source is a volume source that is distributed uniformly throughout the central cavity volume, shown in white within the SS304L encapsulation shown in green in Figure 28. The actual source and its substrate are omitted from the model.

The stilbene detector materials are not included in the benchmark model because the response function is determined for the defined crystal placed in the probe. The source capsule shape is simplified; however, it does not influence the results.

The three measurements specified in Section 2 are simplified into one single benchmark. The expected result of this benchmark is the neutron leakage flux from the block, averaged over the three measurements.

In the case of copper, the XRF analysis and experimental density are used. For the Al source structural components, pure Al is used. Parameters of stainless steel cladding of Cf are based on data supplied by the producer. The felt parameters are taken from Compendium of Material Composition Data (see chapter 1.3).

The results and uncertainties of the measurements, as specified in Section 2.5, are not affected by the benchmark simplifications. The averaged results, including uncertainties, are provided in Section 3.5.

3.2. **Dimensions**

An overview of the benchmark model, including the detector, is shown in Figure 27. The boundary conditions are vacuum. The geometry of the source in flexo-rabbit ending and corresponding model is shown in Figure 28, the geometry of the block is plotted in Figure 29, 30.

The center of the cylindrical ⌀ 10 mm × 10 mm detector is 100 cm from the center of the Cf source which is placed in the center of the Cu block. The cylinder axis is on the horizontal plane through the center of the source, perpendicular to the nearest copper block surface. The cavity is positioned on the opposite side; thus neutrons are passing through at least 22.75 cm copper.

The geometrical parameters of the neutron source are listed in Table 3.1, parameters of the flexo rabbit in Table 3.2 and parameters of the whole Cu block in Table 3.3.
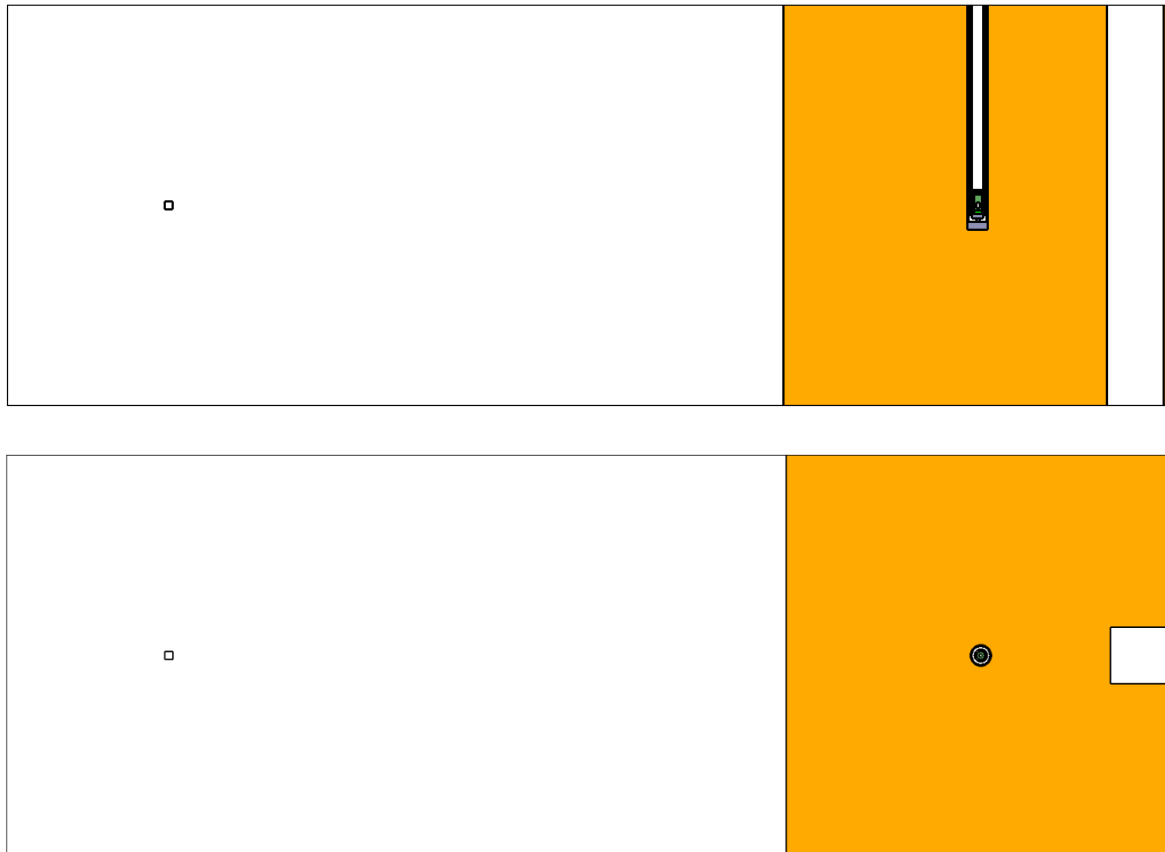
Figure 27: Benchmark model layout. Above: Vertical cut, below: horizontal cut. Dimensions in cm. (yellow =felt, light blue = Al, light green = steel 304L, red-orange = copper)
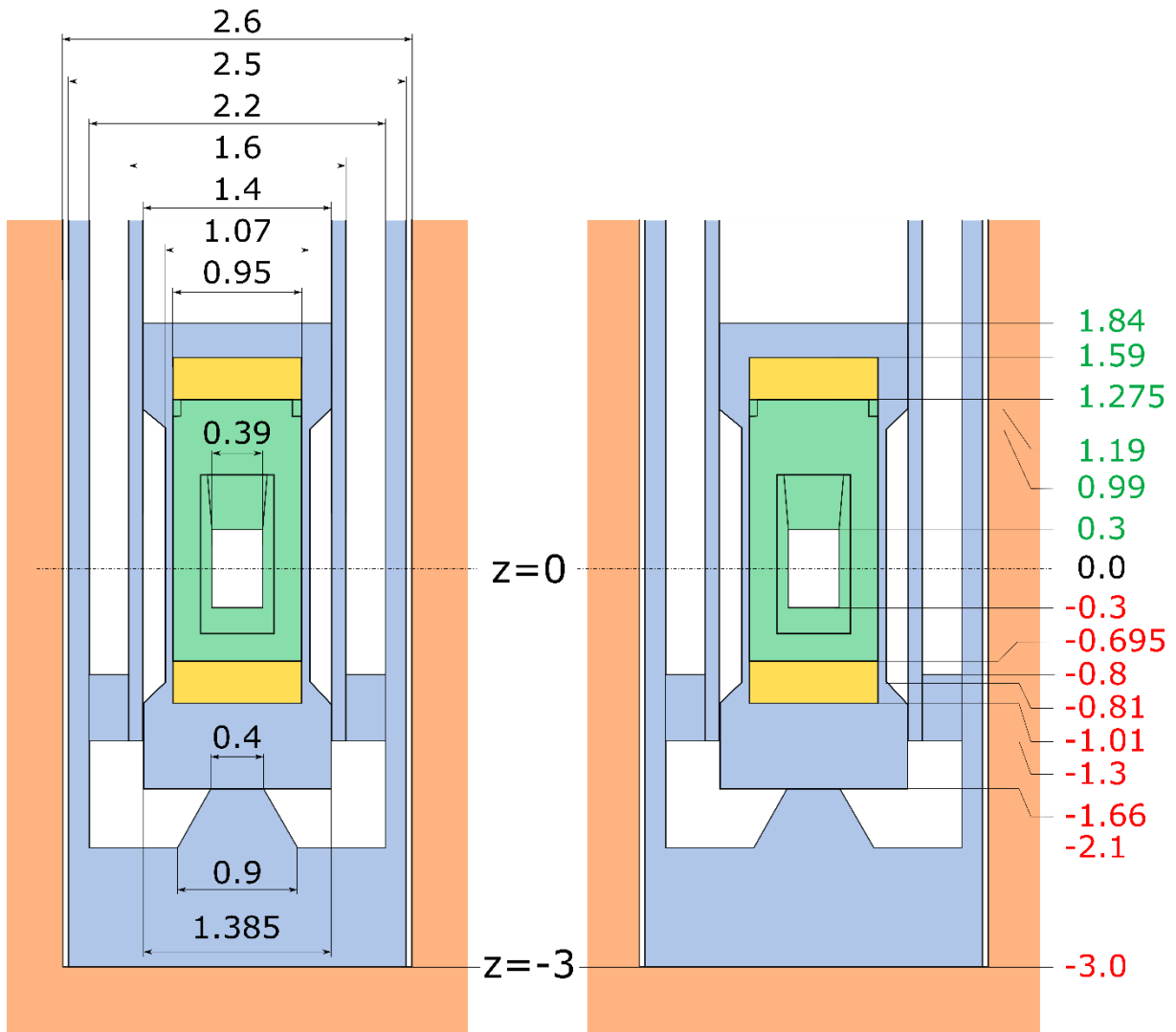
Figure 28: Detail View of Source in Flexo-Rabbit End in Copper Block. Dimensions in cm.
(yellow =felt, light blue = Al, light green = steel 304L, red-orange = copper)
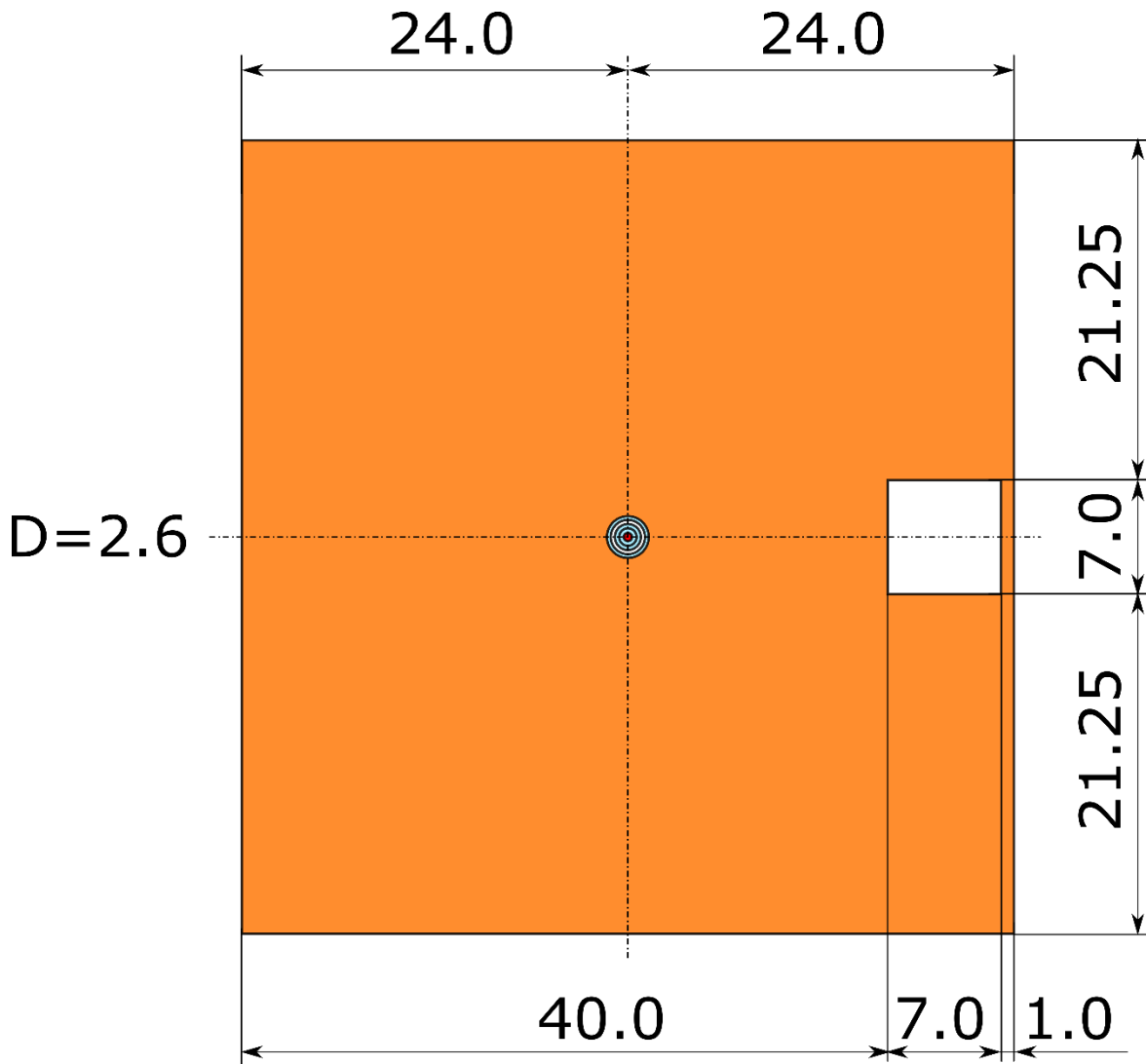
Figure 29: Benchmark Model with Cu Block. In horizontal plane. Dimensions in cm.
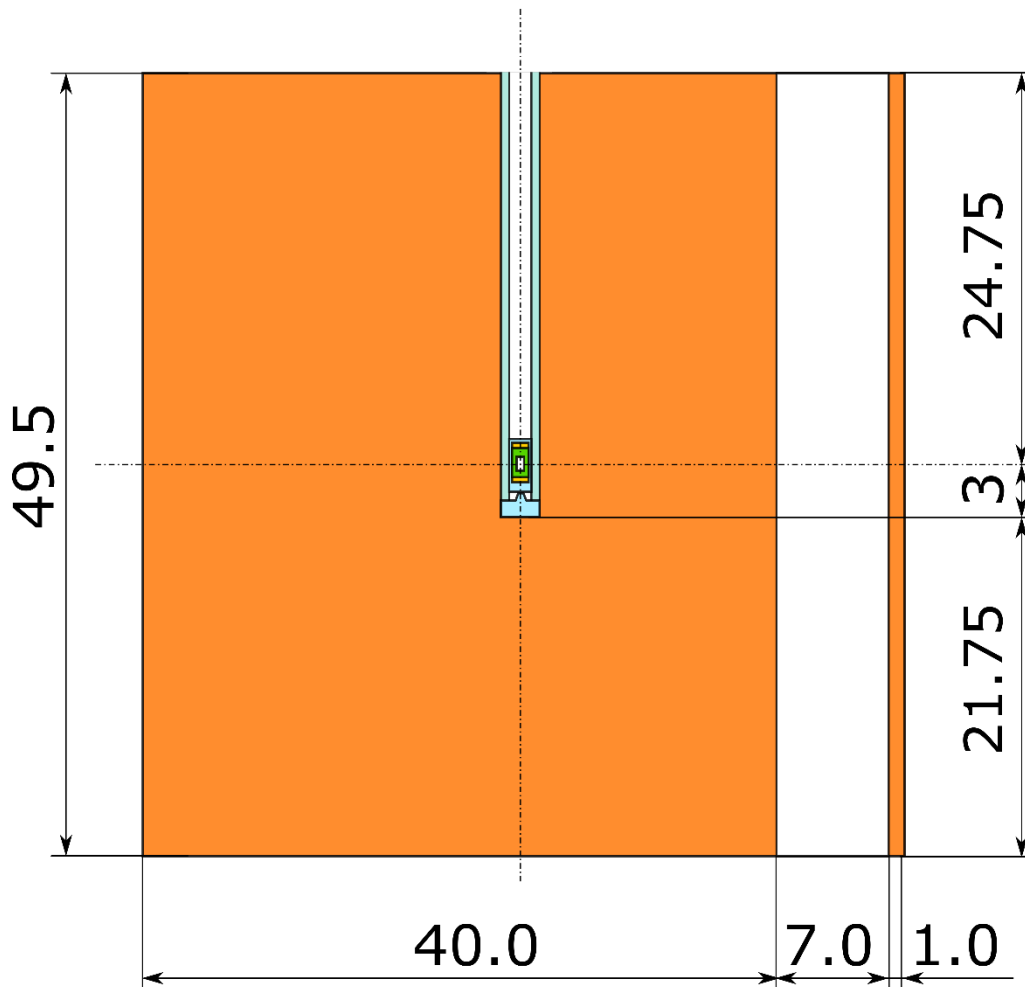
Figure 30: Benchmark Model with Cu Block. In vertical plane. Dimensions in cm.

Table 3.1. Geometry of ^{252}Cf Neutron Source in capsule and sealing.

Parameter	Dimension [cm]
Outside diameter	0.95
Outside length	1.97
Cf source outside diameter	0.39
Cf source length	0.6
Lower bottom thickness	0.395
Upper bottom thickness	0.975

Table 3.2. Geometry of flexo-rabbit end and transport Al holder.

Parameter	Dimension [cm]
Diameter of hole in Cu block	2.6
Outer diameter of flexo-rabbit	2.5
Inner diameter of flexo-rabbit	2.2
Outer diameter of transport tube	1.6
Inner diameter of transport tube	1.4
Outer diameter of Cf transport holder	1.385
Inner diameter of Cf transport holder	0.95
Length of hole for Cf and felt in transport holder	2.6
Thickness of felt layers	0.315
Thickness of upper transport holder wall	0.25
Thickness of lower transport holder wall	0.65
Length of upper/lower conical part on transport holder	0.2
Length of central part of transport holder	1.8
Length of upper part of transport holder	0.65
Length of lower part of transport holder (identical with lower transport holder wall)	0.65
Skittle below transport capsule upper diameter	0.3
Skittle below transport capsule lower diameter	0.6
Flexo rabbit bottom part thickness	0.9
Distance between flexo-rabbit and source holder (identical with height of Al skittle)	0.44
Distance between transport tube and flexo-rabbit bottom	0.8
Spacing ring outer diameter	2.2
Spacing ring inner diameter	1.6
Spacing ring height	0.5

Table 3.3. Geometry of copper block.

Parameter	Dimension [cm]
Copper block height	48
Copper block length	49.5
Copper block wideness	49.5
Hole diameter	2.6
Hole length	27.75
Cavity in block length	7
Cavity in block wideness	7
Cavity in block height	49.5
Distance of cavity to block side	21.25

3.3. Material Data

Atom densities of aluminum, stainless steel, felt and Cu are given in Tables 3.4 to 3.7.

Table 3.4. atom density Aluminum atom density (density 2.7 g/cm^3).

Atom	Atom density [(b·cm)$^{-1}$]	Mass fraction
^{27}Al	6.00003E-02	1.00000E+00

Table 3.5. Stainless Steel 304 atom density (density 8 g/cm^3).

Atom	Atom density [(b·cm)$^{-1}$]	Mass fraction
C	6.0165E-05	1.5000E-04
Si	8.5784E-04	5.0000E-03
P	3.5774E-05	2.3000E-04
S	2.2537E-05	1.5000E-04
Cr	1.7606E-02	1.9000E-01
Mn	8.7692E-04	1.0000E-02
Fe	5.9913E-02	6.9446E-01
Ni	8.2147E-03	1.0001E-01

Table 3.6. Felt atom density (density 0.185 g/cm^3).

Atom	Atom density [(b·cm)$^{-1}$]]	Mass fraction
^{1}H	4.8860E-03	4.4200E-02
C	4.0311E-03	4.3460E-01
^{14}N	1.4042E-03	1.7650E-01
^{16}O	2.4009E-03	3.4470E-01

Table 3.7. Copper block atom density (density 8.8635). g/cm^3.

Nuclide	Atom density [(b·cm)$^{-1}$]	Mass fraction
Cu	8.3900E-02	9.9900E-01
Cl	6.4700E-05	4.3000E-04
Ni	1.0084E-05	1.1088E-04
Ca	1.8500E-05	1.3800E-04
K	3.1000E-05	2.3180E-04
Ag	1.6800E-06	3.3900E-05
Fe	6.7268E-06	7.0324E-05

3.4. Source Strength

The neutron leakage fluxes in the benchmark are normalized to one source neutron per second. The input ^{252}Cf(s.f) spontaneous fission neutron spectrum is not specified[a].

---

[a] One source from IAEA project is available at www-nds.iaea.org/IRDFFtest/irdff_sp_Cf252_ln.dat,. Transformed into a histogram, this spectrum is listed in Table A1.

3.5. Experimental and Benchmark-Model Fundamental Physics Parameters

The benchmark neutron flux, normalized to one source neutron per second, together with one associated relative standard uncertainty are listed in Table 3.8.

Table 3.8 Evaluated normalized neutron leakage flux and its relative standard uncertainty.

Energy Group E_{up} [MeV]	Φ [cm^{-2} s^{-1}]	u_r [%]
1.1	5.48282E-08	12.9
1.2	4.66325E-08	8.5
1.3	4.00395E-08	8.7
1.4	3.09300E-08	6.4
1.5	2.37358E-08	6.6
1.6	1.85435E-08	6.2
1.7	1.43622E-08	7.5
1.8	1.21837E-08	6.8
1.9	1.02378E-08	6.2
2.0	8.85043E-09	5.6
2.1	7.59145E-09	5.1
2.2	6.69804E-09	4.5
2.3	5.86301E-09	4.2
2.4	5.16311E-09	4.1
2.5	4.51244E-09	4.0
2.6	4.00483E-09	4.1
2.7	3.53112E-09	4.3
2.8	3.17194E-09	4.1
2.9	2.83220E-09	4.1
3.0	2.58575E-09	4.1
3.1	2.34840E-09	4.1
3.2	2.12258E-09	4.1
3.3	1.90817E-09	4.1
3.4	1.73267E-09	3.9
3.5	1.56553E-09	4.0
3.6	1.44190E-09	3.9
3.7	1.32238E-09	3.9
3.8	1.23259E-09	3.8
3.9	1.14462E-09	4.0
4.0	1.07743E-09	4.1
4.1	1.01109E-09	4.3
4.2	9.48998E-10	4.3
4.3	8.88053E-10	4.3
4.4	8.40086E-10	4.2
4.5	7.92484E-10	4.2
4.6	7.51078E-10	4.2
4.7	7.09975E-10	4.2
4.8	6.71987E-10	4.1
4.9	6.34318E-10	4.0
5.0	6.07827E-10	4.1
5.1	5.81217E-10	4.6
5.2	5.54221E-10	4.6
5.3	5.27401E-10	4.7
5.4	5.02215E-10	4.8
5.5	4.77192E-10	4.9
5.6	4.56006E-10	4.7

Table 3.8 (cont. 1) Evaluated normalized neutron leakage flux and its relative standard uncertainty.

Energy Group E_{up} [MeV]	Φ [cm^{-2} s^{-1}]	u_r [%]
5.7	4.34921E-10	4.9
5.8	4.15260E-10	4.6
5.9	3.95737E-10	4.5
6.0	3.76454E-10	4.6
6.1	3.57368E-10	4.9
6.2	3.42030E-10	4.7
6.3	3.26868E-10	4.7
6.4	3.14851E-10	4.9
6.5	3.02865E-10	5.1
6.6	2.87759E-10	5.2
6.7	2.72906E-10	5.4
6.8	2.57674E-10	5.4
6.9	2.42828E-10	5.6
7.0	2.28557E-10	5.8
7.1	2.14676E-10	6.1
7.2	2.02320E-10	5.7
7.3	1.90325E-10	5.5
7.4	1.75931E-10	5.4
7.5	1.62287E-10	5.6
7.6	1.54156E-10	5.7
7.7	1.46227E-10	6.0
7.8	1.38664E-10	5.6
7.9	1.31301E-10	5.2
8.0	1.24495E-10	5.7
8.1	1.17877E-10	6.3
8.2	1.12888E-10	5.9
8.3	1.07983E-10	5.7
8.4	1.04107E-10	5.4
8.5	1.00253E-10	5.6
8.6	9.58973E-11	5.7
8.7	9.16077E-11	6.2
8.8	8.75056E-11	6.9
8.9	8.34893E-11	7.7
9.0	8.06182E-11	7.2
9.1	7.77722E-11	7.2
9.2	7.46319E-11	6.9
9.3	7.15404E-11	6.6
9.4	6.86260E-11	6.5
9.5	6.57939E-11	7.5
9.6	6.25918E-11	6.9
9.7	5.95007E-11	8.6
9.8	5.51777E-11	8.7
9.9	5.10860E-11	10.9
10.0	4.75640E-11	10.3
10.1	4.42048E-11	10.0
10.2	4.30590E-11	9.2
10.3	4.19158E-11	10.1
10.4	3.72322E-11	12.3
10.5	3.43335E-11	14.9

Table 3.8 (cont. 2) Evaluated normalized neutron leakage flux and its relative standard uncertainty.

Energy Group E_{up}[MeV]	Φ [cm^{-2} s^{-1}]	u_r [%]
10.6	3.14852E-11	15.5
10.7	2.88151E-11	17.5
10.8	2.62945E-11	19.3
10.9	2.39466E-11	22.3
11.0	2.27585E-11	20.3

4.0   RESULTS OF SAMPLE CALCULATIONS

4.1.   MCNP calculations with several nuclear data libraries

The benchmark was calculated using the MCNP6.2 code with nuclear library ENDF /B-VII.1. The fluxes were calculated using the Next-Event Estimator, (neutron flux tally F5 in MCNP code - flux at a point, i. e. point detector) with steps of 100 keV. The calculation model was otherwise identical to the benchmark model described in Section 3.

The calculated neutron leakage fluxes using default ENDF/B-VII.1 library are listed in Table 4.1. An additional set of MCNP6.2 calculations was realized using ENDF/B-VIII.1, JEFF-3.3 and JENDL-4 and INDEN collaboration libraries. The results are listed in Table 4.2.

In the tables in section 4, the energy E_{up} is the upper limit of the group.

The neutron flux results are shown in Figure 31. A graphical comparison of calculation (C) and experiment (E), in the form of a C/E-1 parameter, is shown in Figure 32. The comparison for new IAEA evaluation of copper cross sections is plotted in Figure 33.

Table 4.1 Calculated, normalized to one source neutron per second,
neutron leakage flux from Cu block in ENDF/B/VII.1 data library.

Energy Group	ENDF/B-VIII	
E_{up} [MeV]	Φ [cm$^{-2}\cdot$s^{-1}]	u_r
1.1	7.07E-08	1.00E-04
1.2	6.67E-08	1.00E-04
1.3	5.02E-08	1.00E-04
1.4	3.98E-08	1.00E-04
1.5	3.10E-08	1.00E-04
1.6	2.39E-08	1.00E-04
1.7	2.01E-08	1.00E-04
1.8	1.58E-08	1.00E-04
1.9	1.39E-08	2.00E-04
2.0	1.10E-08	2.00E-04
2.1	9.82E-09	2.00E-04
2.2	8.69E-09	2.00E-04
2.3	7.65E-09	2.00E-04
2.4	6.76E-09	3.00E-04
2.5	5.84E-09	3.00E-04
2.6	5.22E-09	3.00E-04
2.7	4.80E-09	3.00E-04
2.8	4.31E-09	3.00E-04
2.9	3.84E-09	4.00E-04
3.0	3.35E-09	4.00E-04
3.1	3.01E-09	5.00E-04
3.2	2.76E-09	5.00E-04
3.3	2.54E-09	5.00E-04
3.4	2.34E-09	6.00E-04
3.5	2.18E-09	6.00E-04
3.6	1.99E-09	6.00E-04
3.7	1.82E-09	7.00E-04
3.8	1.65E-09	7.00E-04
3.9	1.52E-09	8.00E-04
4.0	1.39E-09	8.00E-04
4.1	1.27E-09	8.00E-04
4.2	1.18E-09	9.00E-04
4.3	1.09E-09	9.00E-04
4.4	1.02E-09	1.00E-03
4.5	9.56E-10	1.00E-03
4.6	8.95E-10	1.10E-03
4.7	8.39E-10	1.10E-03
4.8	7.88E-10	1.20E-03
4.9	7.41E-10	1.20E-03
5.0	6.95E-10	1.30E-03
5.1	6.56E-10	1.30E-03
5.2	6.23E-10	1.40E-03
5.3	5.90E-10	1.40E-03
5.4	5.59E-10	1.50E-03
5.5	5.33E-10	1.50E-03
5.6	5.04E-10	1.60E-03

Table 4.1 (cont. 1) Calculated, normalized to one source neutron per second, neutron leakage flux from Cu block in ENDF/B/VII.1 data library.

Energy Group	ENDF/B-VIII	
E_{up} [MeV]	Φ [$cm^{-2} \cdot s^{-1}$]	u_r
5.7	4.80E-10	1.70E-03
5.8	4.54E-10	1.70E-03
5.9	4.31E-10	1.80E-03
6.0	4.10E-10	1.80E-03
6.1	3.89E-10	1.90E-03
6.2	3.70E-10	2.00E-03
6.3	3.51E-10	2.00E-03
6.4	3.32E-10	2.10E-03
6.5	3.17E-10	2.20E-03
6.6	3.01E-10	2.20E-03
6.7	2.86E-10	2.30E-03
6.8	2.73E-10	2.40E-03
6.9	2.59E-10	2.50E-03
7.0	2.45E-10	2.50E-03
7.1	2.33E-10	2.60E-03
7.2	2.21E-10	2.70E-03
7.3	2.08E-10	2.80E-03
7.4	1.97E-10	2.90E-03
7.5	1.86E-10	3.00E-03
7.6	1.76E-10	3.10E-03
7.7	1.67E-10	3.20E-03
7.8	1.58E-10	3.30E-03
7.9	1.48E-10	3.40E-03
8.0	1.40E-10	3.50E-03
8.1	1.33E-10	3.60E-03
8.2	1.25E-10	3.70E-03
8.3	1.19E-10	3.80E-03
8.4	1.13E-10	4.00E-03
8.5	1.05E-10	4.10E-03
8.6	9.94E-11	4.20E-03
8.7	9.32E-11	4.40E-03
8.8	8.83E-11	4.50E-03
8.9	8.27E-11	4.70E-03
9.0	7.86E-11	4.80E-03
9.1	7.32E-11	5.00E-03
9.2	6.92E-11	5.20E-03
9.3	6.50E-11	5.30E-03
9.4	6.11E-11	5.50E-03
9.5	5.74E-11	5.70E-03
9.6	5.39E-11	5.90E-03
9.7	5.06E-11	6.20E-03
9.8	4.80E-11	6.30E-03
9.9	4.49E-11	6.50E-03
10.0	4.24E-11	6.80E-03
10.1	4.01E-11	6.90E-03
10.2	3.78E-11	7.20E-03

Table 4.1 (cont. 2) Calculated, normalized to one source neutron per second, neutron leakage flux from Cu block in ENDF/B/VII.1 data library.

Energy Group E_{up} [MeV]	ENDF/B-VIII	
	Φ [cm^{-2}·s^{-1}]	u_r
10.3	3.61E-11	7.40E-03
10.4	3.42E-11	7.50E-03
10.5	3.22E-11	7.90E-03
10.6	2.99E-11	8.10E-03
10.7	2.86E-11	8.30E-03
10.8	2.69E-11	8.70E-03
10.9	2.49E-11	8.90E-03
11.0	2.40E-11	9.30E-03

Table 4.2 Sample calculation results of neutron leakage flux,
normalized to one source neutron per second, using various nuclear data libraries.

Energy Group E_{up} [MeV]	ENDF/B-VIII Φ [cm$^{-2}\cdot$s^{-1}]	u_r	JEFF-3.3 Φ [cm$^{-2}\cdot$s^{-1}]	u_r	JENDL-4 Φ [cm$^{-2}\cdot$s^{-1}]	u_r	INDEN Φ [cm$^{-2}\cdot$s^{-1}]	u_r
1.1	5.33E-08	1.0E-04	6.13E-08	1.0E-04	6.48E-08	1.0E-04	5.34E-08	1E-04
1.2	4.93E-08	1.0E-04	5.84E-08	1.0E-04	5.35E-08	1.0E-04	4.94E-08	1E-04
1.3	3.68E-08	1.0E-04	4.36E-08	1.0E-04	4.15E-08	1.0E-04	3.68E-08	1E-04
1.4	2.94E-08	1.0E-04	3.64E-08	1.0E-04	3.30E-08	1.0E-04	2.95E-08	1E-04
1.5	2.38E-08	1.0E-04	2.96E-08	1.0E-04	2.58E-08	1.0E-04	2.38E-08	1E-04
1.6	1.85E-08	1.0E-04	2.33E-08	1.0E-04	2.07E-08	1.0E-04	1.85E-08	1E-04
1.7	1.58E-08	1.0E-04	1.98E-08	1.0E-04	1.73E-08	1.0E-04	1.58E-08	1E-04
1.8	1.28E-08	2.0E-04	1.61E-08	1.0E-04	1.46E-08	2.0E-04	1.28E-08	2E-04
1.9	1.13E-08	2.0E-04	1.44E-08	2.0E-04	1.25E-08	2.0E-04	1.14E-08	2E-04
2.0	9.11E-09	2.0E-04	1.16E-08	2.0E-04	1.08E-08	2.0E-04	9.13E-09	2E-04
2.1	8.15E-09	2.0E-04	1.03E-08	2.0E-04	9.35E-09	2.0E-04	8.16E-09	2E-04
2.2	7.17E-09	2.0E-04	9.17E-09	2.0E-04	8.12E-09	2.0E-04	7.18E-09	2E-04
2.3	6.25E-09	3.0E-04	8.03E-09	2.0E-04	7.12E-09	2.0E-04	6.26E-09	3E-04
2.4	5.55E-09	3.0E-04	7.31E-09	2.0E-04	6.30E-09	3.0E-04	5.56E-09	3E-04
2.5	4.87E-09	3.0E-04	6.50E-09	3.0E-04	5.55E-09	3.0E-04	4.88E-09	3E-04
2.6	4.28E-09	3.0E-04	5.87E-09	3.0E-04	4.89E-09	3.0E-04	4.28E-09	3E-04
2.7	3.81E-09	4.0E-04	5.18E-09	3.0E-04	4.38E-09	3.0E-04	3.82E-09	4E-04
2.8	3.40E-09	4.0E-04	4.62E-09	3.0E-04	3.92E-09	4.0E-04	3.40E-09	4E-04
2.9	3.01E-09	4.0E-04	4.16E-09	4.0E-04	3.53E-09	4.0E-04	3.02E-09	4E-04
3.0	2.70E-09	5.0E-04	3.77E-09	4.0E-04	3.18E-09	4.0E-04	2.70E-09	5E-04
3.1	2.42E-09	5.0E-04	3.44E-09	4.0E-04	2.88E-09	5.0E-04	2.43E-09	5E-04
3.2	2.18E-09	5.0E-04	3.16E-09	4.0E-04	2.61E-09	5.0E-04	2.18E-09	5E-04
3.3	1.96E-09	6.0E-04	2.91E-09	5.0E-04	2.38E-09	5.0E-04	1.97E-09	6E-04
3.4	1.79E-09	6.0E-04	2.69E-09	5.0E-04	2.16E-09	6.0E-04	1.80E-09	6E-04
3.5	1.64E-09	6.0E-04	2.49E-09	5.0E-04	1.98E-09	6.0E-04	1.65E-09	6E-04
3.6	1.51E-09	7.0E-04	2.30E-09	6.0E-04	1.80E-09	7.0E-04	1.51E-09	7E-04
3.7	1.39E-09	7.0E-04	2.13E-09	6.0E-04	1.64E-09	7.0E-04	1.39E-09	7E-04
3.8	1.27E-09	8.0E-04	1.98E-09	6.0E-04	1.49E-09	7.0E-04	1.28E-09	8E-04
3.9	1.18E-09	8.0E-04	1.85E-09	7.0E-04	1.37E-09	8.0E-04	1.18E-09	8E-04
4.0	1.09E-09	9.0E-04	1.72E-09	7.0E-04	1.26E-09	8.0E-04	1.10E-09	9E-04
4.1	1.01E-09	9.0E-04	1.60E-09	7.0E-04	1.16E-09	9.0E-04	1.02E-09	9E-04
4.2	9.38E-10	1.0E-03	1.50E-09	8.0E-04	1.08E-09	9.0E-04	9.42E-10	1E-03
4.3	8.69E-10	1.0E-03	1.41E-09	8.0E-04	1.01E-09	1.0E-03	8.74E-10	1E-03
4.4	8.13E-10	1.1E-03	1.32E-09	8.0E-04	9.41E-10	1.0E-03	8.14E-10	1E-03
4.5	7.63E-10	1.1E-03	1.25E-09	9.0E-04	8.81E-10	1.1E-03	7.60E-10	1E-03
4.6	7.17E-10	1.2E-03	1.18E-09	9.0E-04	8.24E-10	1.1E-03	7.12E-10	1E-03
4.7	6.73E-10	1.2E-03	1.11E-09	1.0E-03	7.69E-10	1.2E-03	6.68E-10	1E-03
4.8	6.34E-10	1.3E-03	1.05E-09	1.0E-03	7.18E-10	1.2E-03	6.29E-10	1E-03
4.9	5.98E-10	1.3E-03	9.92E-10	1.1E-03	6.73E-10	1.3E-03	5.92E-10	1E-03
5.0	5.64E-10	1.4E-03	9.36E-10	1.1E-03	6.31E-10	1.3E-03	5.58E-10	1E-03
5.1	5.32E-10	1.5E-03	8.87E-10	1.1E-03	5.96E-10	1.4E-03	5.24E-10	2E-03
5.2	5.04E-10	1.5E-03	8.43E-10	1.2E-03	5.64E-10	1.4E-03	4.94E-10	2E-03
5.3	4.75E-10	1.6E-03	8.01E-10	1.2E-03	5.36E-10	1.5E-03	4.64E-10	2E-03
5.4	4.47E-10	1.6E-03	7.59E-10	1.3E-03	5.11E-10	1.6E-03	4.38E-10	2E-03
5.5	4.26E-10	1.7E-03	7.24E-10	1.3E-03	4.89E-10	1.6E-03	4.22E-10	2E-03

Table 4.2 (cont. 1) Sample calculation results of neutron leakage flux,
normalized to one source neutron per second, using various nuclear data libraries.

Energy Group E_{up} [MeV]	ENDF/B-VIII Φ [$cm^{-2} \cdot s^{-1}$]	u_r	JEFF-3.3 Φ [$cm^{-2} \cdot s^{-1}$]	u_r	JENDL-4 Φ [$cm^{-2} \cdot s^{-1}$]	u_r	INDEN Φ [$cm^{-2} \cdot s^{-1}$]	u_r
5.6	4.03E-10	1.8E-03	6.88E-10	1.4E-03	4.66E-10	1.7E-03	4.05E-10	2E-03
5.7	3.84E-10	1.8E-03	6.54E-10	1.4E-03	4.45E-10	1.7E-03	3.90E-10	2E-03
5.8	3.64E-10	1.9E-03	6.21E-10	1.5E-03	4.24E-10	1.8E-03	3.73E-10	2E-03
5.9	3.47E-10	2.0E-03	5.90E-10	1.5E-03	4.05E-10	1.8E-03	3.59E-10	2E-03
6.0	3.32E-10	2.0E-03	5.62E-10	1.6E-03	3.86E-10	1.9E-03	3.44E-10	2E-03
6.1	3.15E-10	2.1E-03	5.37E-10	1.6E-03	3.68E-10	2.0E-03	3.30E-10	2E-03
6.2	2.99E-10	2.2E-03	5.10E-10	1.7E-03	3.51E-10	2.0E-03	3.19E-10	2E-03
6.3	2.82E-10	2.3E-03	4.85E-10	1.7E-03	3.35E-10	2.1E-03	3.05E-10	2E-03
6.4	2.67E-10	2.3E-03	4.59E-10	1.8E-03	3.19E-10	2.1E-03	2.95E-10	2E-03
6.5	2.54E-10	2.4E-03	4.37E-10	1.9E-03	3.06E-10	2.2E-03	2.83E-10	2E-03
6.6	2.43E-10	2.5E-03	4.16E-10	1.9E-03	2.91E-10	2.3E-03	2.71E-10	2E-03
6.7	2.31E-10	2.6E-03	3.94E-10	2.0E-03	2.78E-10	2.4E-03	2.60E-10	3E-03
6.8	2.18E-10	2.6E-03	3.75E-10	2.1E-03	2.65E-10	2.4E-03	2.48E-10	3E-03
6.9	2.07E-10	2.7E-03	3.55E-10	2.1E-03	2.51E-10	2.5E-03	2.37E-10	3E-03
7.0	1.98E-10	2.8E-03	3.37E-10	2.2E-03	2.39E-10	2.6E-03	2.28E-10	3E-03
7.1	1.88E-10	2.9E-03	3.19E-10	2.3E-03	2.28E-10	2.7E-03	2.17E-10	3E-03
7.2	1.77E-10	3.0E-03	3.03E-10	2.3E-03	2.18E-10	2.7E-03	2.08E-10	3E-03
7.3	1.68E-10	3.1E-03	2.88E-10	2.4E-03	2.05E-10	2.8E-03	1.98E-10	3E-03
7.4	1.59E-10	3.2E-03	2.72E-10	2.5E-03	1.96E-10	2.9E-03	1.89E-10	3E-03
7.5	1.51E-10	3.3E-03	2.56E-10	2.6E-03	1.86E-10	3.0E-03	1.81E-10	3E-03
7.6	1.42E-10	3.4E-03	2.43E-10	2.7E-03	1.77E-10	3.1E-03	1.73E-10	3E-03
7.7	1.36E-10	3.5E-03	2.31E-10	2.8E-03	1.70E-10	3.2E-03	1.66E-10	3E-03
7.8	1.28E-10	3.6E-03	2.18E-10	2.8E-03	1.61E-10	3.3E-03	1.59E-10	3E-03
7.9	1.21E-10	3.8E-03	2.06E-10	2.9E-03	1.52E-10	3.4E-03	1.51E-10	4E-03
8.0	1.15E-10	3.9E-03	1.93E-10	3.0E-03	1.45E-10	3.5E-03	1.45E-10	4E-03
8.1	1.09E-10	4.0E-03	1.84E-10	3.1E-03	1.37E-10	3.6E-03	1.38E-10	4E-03
8.2	1.03E-10	4.1E-03	1.73E-10	3.2E-03	1.30E-10	3.7E-03	1.31E-10	4E-03
8.3	9.70E-11	4.3E-03	1.63E-10	3.4E-03	1.23E-10	3.8E-03	1.25E-10	4E-03
8.4	9.22E-11	4.4E-03	1.54E-10	3.5E-03	1.18E-10	4.0E-03	1.20E-10	4E-03
8.5	8.56E-11	4.6E-03	1.46E-10	3.6E-03	1.10E-10	4.1E-03	1.14E-10	4E-03
8.6	8.16E-11	4.7E-03	1.37E-10	3.7E-03	1.05E-10	4.2E-03	1.08E-10	4E-03
8.7	7.69E-11	4.9E-03	1.29E-10	3.8E-03	9.92E-11	4.4E-03	1.02E-10	4E-03
8.8	7.32E-11	5.0E-03	1.23E-10	3.9E-03	9.48E-11	4.5E-03	9.73E-11	5E-03
8.9	6.90E-11	5.2E-03	1.16E-10	4.1E-03	8.96E-11	4.7E-03	9.20E-11	5E-03
9.0	6.55E-11	5.4E-03	1.09E-10	4.2E-03	8.50E-11	4.8E-03	8.74E-11	5E-03
9.1	6.18E-11	5.5E-03	1.03E-10	4.3E-03	7.95E-11	5.0E-03	8.19E-11	5E-03
9.2	5.81E-11	5.7E-03	9.78E-11	4.5E-03	7.55E-11	5.1E-03	7.72E-11	5E-03
9.3	5.49E-11	5.9E-03	9.28E-11	4.6E-03	7.16E-11	5.3E-03	7.29E-11	5E-03
9.4	5.17E-11	6.1E-03	8.77E-11	4.7E-03	6.75E-11	5.5E-03	6.86E-11	6E-03
9.5	4.87E-11	6.2E-03	8.38E-11	4.9E-03	6.41E-11	5.6E-03	6.50E-11	6E-03
9.6	4.54E-11	6.6E-03	7.95E-11	5.0E-03	6.02E-11	5.8E-03	6.07E-11	6E-03
9.7	4.30E-11	6.8E-03	7.59E-11	5.2E-03	5.73E-11	6.0E-03	5.66E-11	6E-03
9.8	4.09E-11	7.0E-03	7.26E-11	5.3E-03	5.39E-11	6.2E-03	5.34E-11	6E-03
9.9	3.84E-11	7.2E-03	6.87E-11	5.4E-03	5.13E-11	6.4E-03	4.98E-11	7E-03
10.0	3.64E-11	7.6E-03	6.52E-11	5.6E-03	4.84E-11	6.6E-03	4.63E-11	7E-03

Table 4.2 (cont. 2) Sample calculation results of neutron leakage flux,
normalized to one source neutron per second, using various nuclear data libraries.

| Energy Group E_{up} [MeV]	ENDF/B-VIII		JEFF-3.3		JENDL-4		INDEN	
	Φ [cm^{-2}·s^{-1}]	u_r	Φ [cm^{-2}·s^{-1}]	u_r	Φ [cm^{-2}·s^{-1}]	u_r	Φ [cm^{-2}·s^{-1}]	u_r
10.1	3.39E-11	7.7E-03	6.16E-11	5.8E-03	4.55E-11	6.8E-03	4.38E-11	7E-03
10.2	3.15E-11	8.0E-03	5.85E-11	5.9E-03	4.28E-11	7.1E-03	4.08E-11	7E-03
10.3	3.01E-11	8.3E-03	5.54E-11	6.1E-03	4.07E-11	7.3E-03	3.86E-11	8E-03
10.4	2.81E-11	8.5E-03	5.22E-11	6.3E-03	3.83E-11	7.5E-03	3.63E-11	8E-03
10.5	2.64E-11	8.8E-03	5.01E-11	6.6E-03	3.59E-11	7.8E-03	3.41E-11	8E-03
10.6	2.50E-11	9.2E-03	4.67E-11	6.7E-03	3.36E-11	8.0E-03	3.16E-11	8E-03
10.7	2.36E-11	9.4E-03	4.49E-11	7.0E-03	3.20E-11	8.3E-03	3.01E-11	9E-03
10.8	2.26E-11	9.9E-03	4.23E-11	7.2E-03	3.03E-11	8.7E-03	2.77E-11	9E-03
10.9	2.09E-11	1.0E-02	3.96E-11	7.4E-03	2.84E-11	8.9E-03	2.54E-11	9E-03
11.0	2.00E-11	1.0E-02	3.73E-11	7.6E-03	2.71E-11	9.2E-03	2.46E-11	1E-02
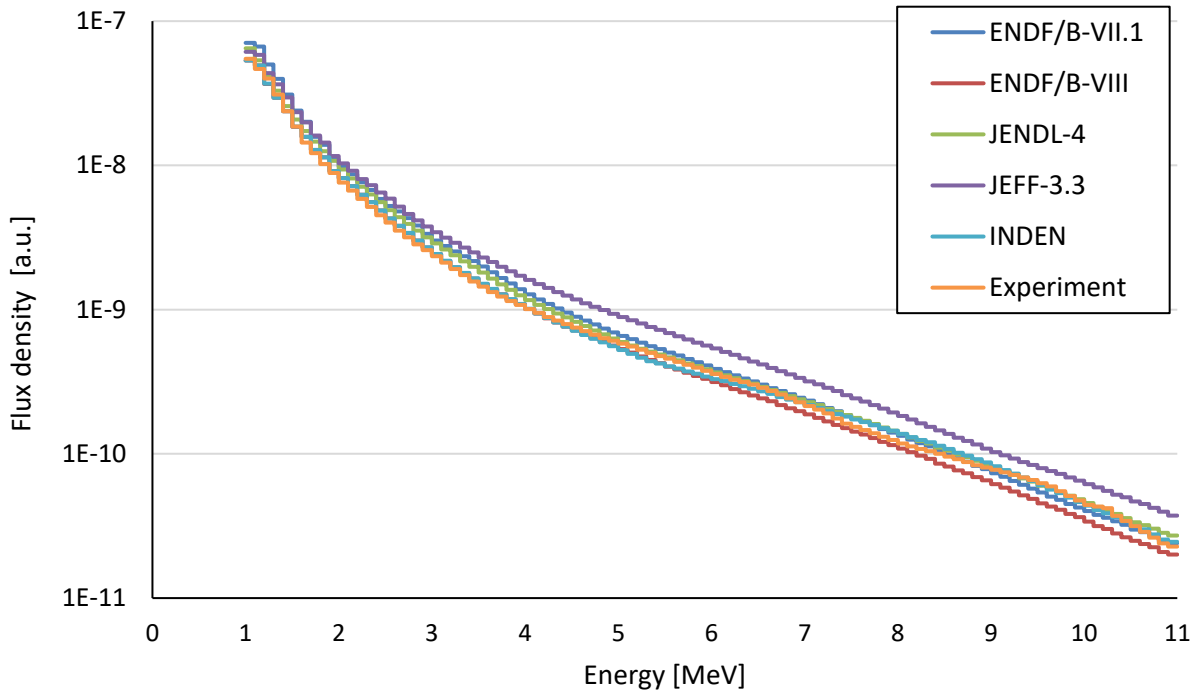
Figure 31. Comparison of measured neutron Leakage Flux from Copper Block
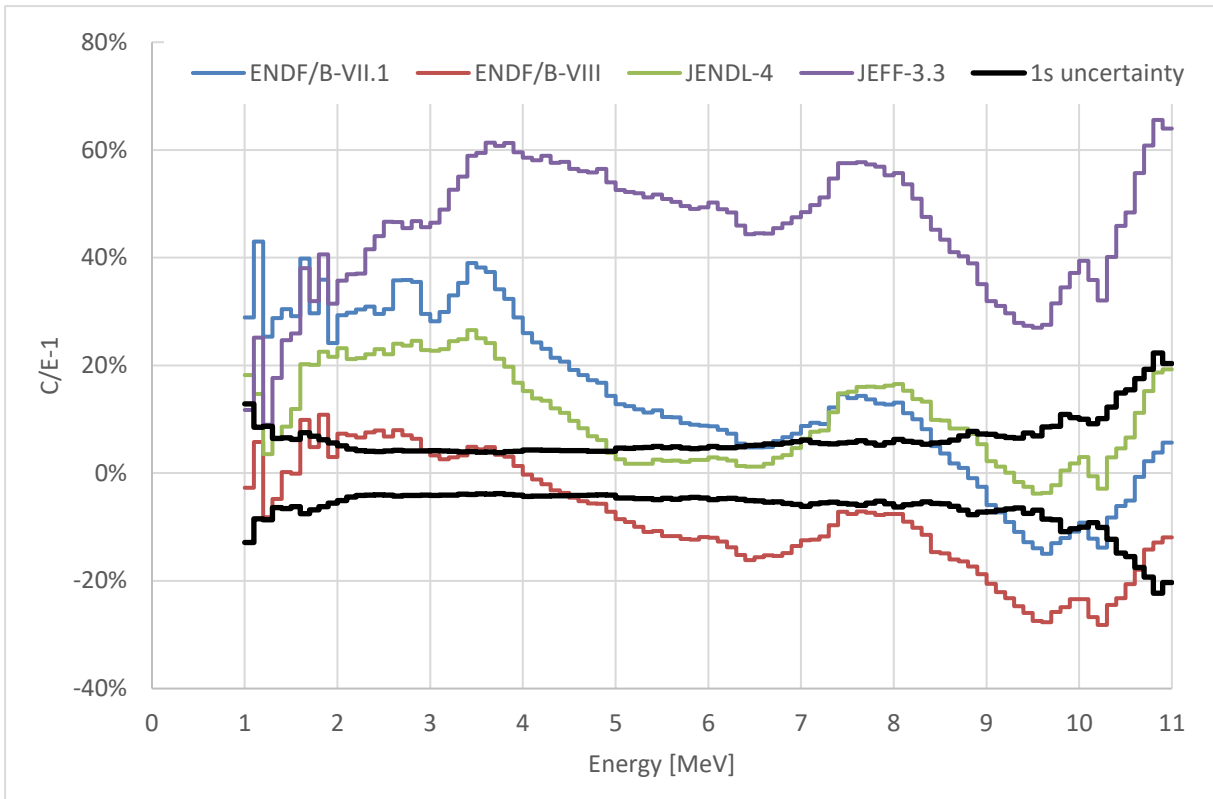with sample calculation using various nuclear data libraries

Figure 32. C/E-1 Comparison of Neutron Leakage Flux from Copper Block
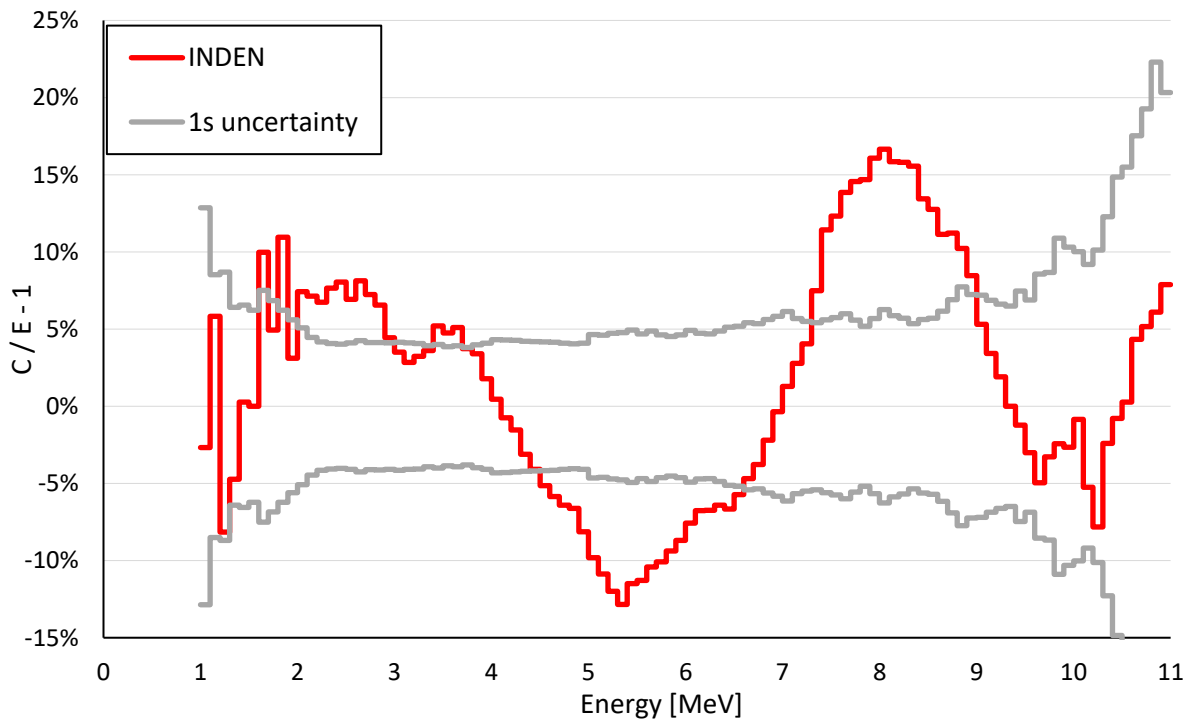with calculation in various nuclear data libraries

Figure 33. C/E-1 Comparison of Neutron Leakage Flux from Copper Block
with calculation using new INDEN evaluation

4.2. SCALE calculations

The sample calculation was realized also using SCALE simulation with ENDF /B-VII.1. nuclear data library and latest IRDFF-II 725 group fission spectrum of ^{252}Cf(s.f.) as source. The fluxes calculated by SCALE are in second column of Table 4.3 The upper energy (in eV) of each bin is in column A and the relative error is in column D. The calculation model was otherwise identical to the benchmark model described in Section 3. The C/E-1 plot is in Figure 34.

Table 4.3. SCALE 6.2.4 – Calculation with ENDF/B-VII.1, IRDFF-II MG Cf-252 Fission Spectrum

Upper energy (ev)	flux	abs err	rel err	C/E	C/E 2*abs err
1.00E+06					
1.10E+06	6.16E-08	1.44E-10	0.00234	1.12E+00	2.90E-01
1.20E+06	6.26E-08	1.51E-10	0.00241	1.34E+00	2.28E-01
1.30E+06	4.74E-08	1.28E-10	0.00269	1.18E+00	2.06E-01
1.40E+06	3.83E-08	1.12E-10	0.00293	1.24E+00	1.59E-01
1.50E+06	3.02E-08	6.26E-11	0.00207	1.27E+00	1.68E-01
1.60E+06	2.33E-08	4.81E-11	0.00206	1.26E+00	1.56E-01
1.70E+06	1.96E-08	4.38E-11	0.00224	1.36E+00	2.04E-01
1.80E+06	1.55E-08	3.79E-11	0.00244	1.28E+00	1.74E-01
1.90E+06	1.36E-08	3.48E-11	0.00257	1.33E+00	1.65E-01
2.00E+06	1.07E-08	3.06E-11	0.00286	1.21E+00	1.36E-01
2.10E+06	9.56E-09	2.94E-11	0.00307	1.26E+00	1.29E-01
2.20E+06	8.44E-09	2.81E-11	0.00332	1.26E+00	1.14E-01
2.30E+06	7.44E-09	2.66E-11	0.00358	1.27E+00	1.07E-01
2.40E+06	6.56E-09	2.55E-11	0.00389	1.27E+00	1.05E-01
2.50E+06	5.64E-09	2.38E-11	0.00421	1.25E+00	1.01E-01
2.60E+06	5.02E-09	2.28E-11	0.00454	1.25E+00	1.04E-01
2.70E+06	4.64E-09	2.27E-11	0.0049	1.31E+00	1.14E-01
2.80E+06	4.14E-09	2.19E-11	0.00528	1.31E+00	1.08E-01
2.90E+06	3.70E-09	2.12E-11	0.00573	1.31E+00	1.08E-01
3.00E+06	3.26E-09	2.03E-11	0.00622	1.26E+00	1.05E-01
3.10E+06	2.88E-09	1.43E-11	0.00498	1.23E+00	1.01E-01
3.20E+06	2.67E-09	1.40E-11	0.00525	1.26E+00	1.04E-01
3.30E+06	2.45E-09	1.36E-11	0.00555	1.29E+00	1.06E-01
3.40E+06	2.26E-09	1.34E-11	0.00592	1.30E+00	1.03E-01
3.50E+06	2.09E-09	1.31E-11	0.00627	1.33E+00	1.08E-01
3.60E+06	1.89E-09	1.25E-11	0.00662	1.31E+00	1.04E-01
3.70E+06	1.74E-09	1.22E-11	0.00698	1.32E+00	1.05E-01
3.80E+06	1.60E-09	1.18E-11	0.00737	1.30E+00	1.00E-01
3.90E+06	1.44E-09	1.12E-11	0.00776	1.26E+00	1.03E-01
4.00E+06	1.31E-09	1.07E-11	0.00819	1.21E+00	1.01E-01
4.10E+06	1.22E-09	1.05E-11	0.0086	1.21E+00	1.06E-01
4.20E+06	1.16E-09	1.05E-11	0.00909	1.22E+00	1.07E-01
4.30E+06	1.04E-09	9.98E-12	0.00955	1.18E+00	1.04E-01
4.40E+06	9.81E-10	9.74E-12	0.00993	1.17E+00	1.01E-01
4.50E+06	9.41E-10	9.76E-12	0.01037	1.19E+00	1.03E-01

4.60E+06	8.62E-10	9.21E-12	0.01069	1.15E+00	9.95E-02
4.70E+06	8.18E-10	9.17E-12	0.0112	1.15E+00	1.00E-01
4.80E+06	7.65E-10	8.92E-12	0.01166	1.14E+00	9.70E-02
4.90E+06	7.20E-10	8.83E-12	0.01227	1.13E+00	9.49E-02
5.00E+06	6.77E-10	8.51E-12	0.01256	1.11E+00	9.55E-02
5.10E+06	6.25E-10	8.25E-12	0.0132	1.08E+00	1.03E-01
5.20E+06	5.91E-10	8.08E-12	0.01366	1.07E+00	1.02E-01
5.30E+06	5.60E-10	7.93E-12	0.01417	1.06E+00	1.04E-01
5.40E+06	5.32E-10	7.83E-12	0.01471	1.06E+00	1.06E-01
5.50E+06	5.09E-10	7.80E-12	0.01531	1.07E+00	1.10E-01
5.60E+06	4.86E-10	7.50E-12	0.01544	1.06E+00	1.05E-01
5.70E+06	4.62E-10	7.54E-12	0.01631	1.06E+00	1.10E-01
5.80E+06	4.41E-10	7.50E-12	0.01699	1.06E+00	1.04E-01
5.90E+06	4.24E-10	7.40E-12	0.01745	1.07E+00	1.03E-01
6.00E+06	3.91E-10	7.00E-12	0.01789	1.04E+00	1.03E-01
6.10E+06	3.92E-10	7.15E-12	0.01826	1.10E+00	1.15E-01
6.20E+06	3.67E-10	7.13E-12	0.01942	1.07E+00	1.09E-01
6.30E+06	3.38E-10	6.75E-12	0.01997	1.03E+00	1.06E-01
6.40E+06	3.27E-10	6.01E-12	0.01836	1.04E+00	1.09E-01
6.50E+06	3.09E-10	4.65E-12	0.01505	1.02E+00	1.08E-01
6.60E+06	2.97E-10	4.61E-12	0.01555	1.03E+00	1.12E-01
6.70E+06	2.77E-10	4.46E-12	0.01607	1.02E+00	1.15E-01
6.80E+06	2.62E-10	4.32E-12	0.01652	1.02E+00	1.15E-01
6.90E+06	2.39E-10	4.04E-12	0.01692	9.83E-01	1.15E-01
7.00E+06	2.29E-10	4.07E-12	0.01781	1.00E+00	1.21E-01
7.10E+06	2.17E-10	4.01E-12	0.01847	1.01E+00	1.29E-01
7.20E+06	2.13E-10	4.04E-12	0.01894	1.05E+00	1.27E-01
7.30E+06	2.05E-10	4.08E-12	0.0199	1.08E+00	1.26E-01
7.40E+06	1.91E-10	3.86E-12	0.02023	1.08E+00	1.25E-01
7.50E+06	1.78E-10	3.80E-12	0.02131	1.10E+00	1.32E-01
7.60E+06	1.68E-10	3.66E-12	0.02183	1.09E+00	1.33E-01
7.70E+06	1.58E-10	3.53E-12	0.0223	1.08E+00	1.38E-01
7.80E+06	1.50E-10	3.47E-12	0.02305	1.08E+00	1.31E-01
7.90E+06	1.38E-10	3.29E-12	0.02389	1.05E+00	1.20E-01
8.00E+06	1.29E-10	3.10E-12	0.02411	1.03E+00	1.28E-01
8.10E+06	1.31E-10	3.26E-12	0.0249	1.11E+00	1.50E-01
8.20E+06	1.21E-10	3.08E-12	0.02537	1.07E+00	1.38E-01
8.30E+06	1.19E-10	3.23E-12	0.02714	1.10E+00	1.39E-01
8.40E+06	1.08E-10	2.99E-12	0.02763	1.04E+00	1.26E-01
8.50E+06	1.04E-10	3.02E-12	0.02905	1.04E+00	1.31E-01
8.60E+06	9.64E-11	2.85E-12	0.02955	1.01E+00	1.29E-01
8.70E+06	8.63E-11	2.75E-12	0.03188	9.42E-01	1.31E-01
8.80E+06	8.33E-11	2.68E-12	0.03217	9.52E-01	1.45E-01
8.90E+06	7.71E-11	2.64E-12	0.03421	9.23E-01	1.56E-01
9.00E+06	7.11E-11	2.42E-12	0.03399	8.81E-01	1.40E-01
9.10E+06	6.89E-11	2.41E-12	0.03494	8.87E-01	1.42E-01

| 9.20E+06	6.81E-11	2.50E-12	0.0367	9.12E-01	1.43E-01
9.30E+06	5.97E-11	2.40E-12	0.04013	8.35E-01	1.29E-01
9.40E+06	5.99E-11	2.45E-12	0.04091	8.72E-01	1.34E-01
9.50E+06	5.51E-11	2.29E-12	0.04159	8.38E-01	1.44E-01
9.60E+06	5.35E-11	2.31E-12	0.04317	8.54E-01	1.39E-01
9.70E+06	5.23E-11	2.30E-12	0.04396	8.78E-01	1.70E-01
9.80E+06	4.65E-11	2.06E-12	0.04435	8.43E-01	1.65E-01
9.90E+06	4.51E-11	2.18E-12	0.04839	8.83E-01	2.11E-01
1.00E+07	4.17E-11	1.99E-12	0.04782	8.77E-01	1.99E-01
1.01E+07	3.95E-11	1.93E-12	0.04876	8.94E-01	1.99E-01
1.02E+07	3.85E-11	1.96E-12	0.0508	8.95E-01	1.88E-01
1.03E+07	3.45E-11	1.91E-12	0.05524	8.24E-01	1.90E-01
1.04E+07	3.42E-11	1.84E-12	0.05385	9.18E-01	2.47E-01
1.05E+07	3.36E-11	1.89E-12	0.05605	9.80E-01	3.12E-01
1.06E+07	3.04E-11	1.82E-12	0.05982	9.65E-01	3.21E-01
1.07E+07	2.86E-11	1.74E-12	0.06084	9.92E-01	3.68E-01
1.08E+07	2.55E-11	1.56E-12	0.06107	9.69E-01	3.92E-01
1.09E+07	2.60E-11	1.87E-12	0.07189	1.09E+00	5.09E-01
1.10E+07	2.20E-11	1.49E-12	0.06806	9.65E-01	4.13E-01
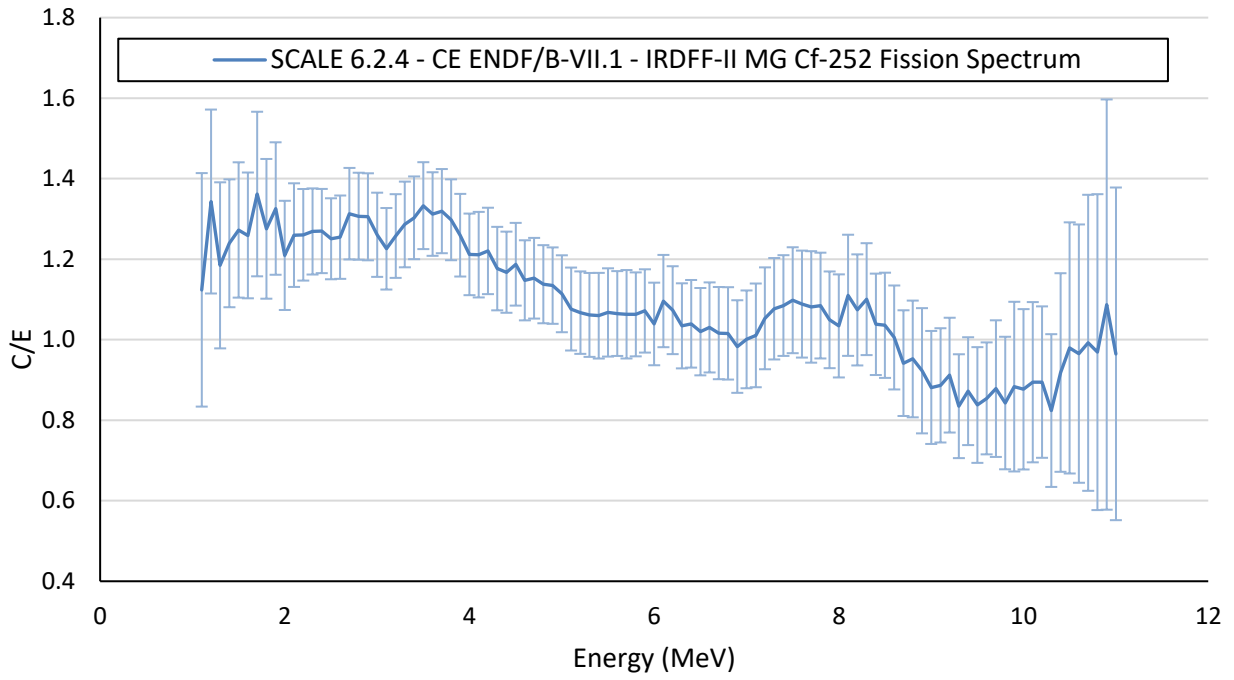
Figure 34. Comparison Between SCALE 6.2.4, with Continuous Energy ENDF/B-VII.1 Cross Sections and the IRDFF-II MG Cf-252 Fission Spectrum, and the Experimental Measurement by means of C/E

5.0   REFERENCES

1. M. Schulc, M. Košťál, E Novák, V. Rypar, Measuring neutron leakage spectra using spherical benchmarks with ²⁵²Cf source in its centers, Nuclear Inst. and Methods in Physics Research, A 914 (2019) 53–56.

2. M. Schulc, M. Košťal, E.Novak, R. Kubin, J. Šimon, Application of ²⁵²Cf neutron source for precise nuclear data experiments, Applied Radiation and Isotopes 151 (2019) 187–195.

3.   Fast neutron spectra measurement in a copper using a ²⁵²Cf standard neutron source, (2022) Radiation Physics and Chemistry, 192, art. no. 109871

4. Schulc, M., Košťál, M., Novák, E., Šimon, J., Copper neutron transport libraries validation by means of a ²⁵²Cf standard neutron source, (2021) Nuclear Engineering and Technology, 53 (10), pp. 3151-3157

APPENDIX A. COMPUTER CODES, CROSS SECTIONS, AND INPUT LISTINGS

A.1.   MCNP6.2

A.1.1 Name(s) of Code System(s) Used

Monte Carlo n-Particle, version 6.2 (MCNP6)

A.1.2 Bibliographic References for the Codes Used

T. Goorley, et al., "Initial MCNP6 Release Overview", Nuclear Technology, **180**, pp 298-315 (Dec 2012).
D.B. Pelowitz (Ed.), MCNP6™ User's Manual, Los Alamos National Laboratory Report, LA-CP-13–00634 (2013)

A.1.3 Origin of Cross-section Data

The Evaluated Neutron Data File library, ENDF/B-VII.1.

A.1.4 Spectral Calculations and Data Reduction Methods Used

No variance reduction was used.

A.1.5 Number of Energy Groups or if Continuous-Energy Cross Sections are used in the Different Phases of the Calculation

100 energy groups in (0, 10 MeV) interval.

A.1.6 Component Calculations

Type of cell calculation – block of copper
Geometry – slab
Theory used – not applicable
Method used – Monte Carlo
Calculation characteristics – histories 2.5e10 energy groups in steps of 100 keV

A.1.7   Other Assumptions and Characteristics

The input ^{252}Cf(sf) neutron spectrum was taken from the IAEA project on validation of the IRDFF webpage at https://www-nds.iaea.org/IRDFF/spectra/irdff_sp_Cf252_ln.g725. In Table A1, the spectra are transformed into groups from [1/eV] units presented in IRDFF-II.

Table A1. Tabulated ^{252}Cf(s.f) neutron spectrum

Energy Group E_{up} [MeV]	Group flux [a.u.]	Energy Group E_{up} [MeV]	Group flux [a.u.]	Energy Group Eup [MeV]	Group flux [a.u.]	Energy Group Eup [MeV]	Group flux [a.u.]
1.00E-11	0	8.80E-08	7.542E-13	7.60E-04	6.992E-07	4.60E+00	5.756E-03
1.05E-11	1.029E-18	9.20E-08	7.715E-13	8.00E-04	7.179E-07	4.70E+00	5.409E-03
1.10E-11	1.054E-18	9.60E-08	7.884E-13	8.40E-04	7.360E-07	4.80E+00	5.082E-03
1.15E-11	1.078E-18	1.00E-07	8.050E-13	8.80E-04	7.538E-07	4.90E+00	4.773E-03
1.20E-11	1.102E-18	1.05E-07	1.029E-12	9.20E-04	7.711E-07	5.00E+00	4.483E-03
1.28E-11	1.696E-18	1.10E-07	1.054E-12	9.60E-04	7.880E-07	5.10E+00	4.209E-03
1.35E-11	1.747E-18	1.15E-07	1.078E-12	1.00E-03	8.046E-07	5.20E+00	3.952E-03
1.43E-11	1.796E-18	1.20E-07	1.102E-12	1.05E-03	1.029E-06	5.30E+00	3.709E-03
1.50E-11	1.844E-18	1.27E-07	1.696E-12	1.10E-03	1.053E-06	5.40E+00	3.480E-03
1.60E-11	2.531E-18	1.35E-07	1.747E-12	1.15E-03	1.077E-06	5.50E+00	3.266E-03
1.70E-11	2.611E-18	1.42E-07	1.796E-12	1.20E-03	1.101E-06	5.60E+00	3.064E-03
1.80E-11	2.689E-18	1.50E-07	1.844E-12	1.28E-03	1.695E-06	5.70E+00	2.873E-03
1.90E-11	2.765E-18	1.60E-07	2.531E-12	1.35E-03	1.745E-06	5.80E+00	2.695E-03
2.00E-11	2.839E-18	1.70E-07	2.611E-12	1.43E-03	1.794E-06	5.90E+00	2.527E-03
2.10E-11	2.911E-18	1.80E-07	2.689E-12	1.50E-03	1.842E-06	6.00E+00	2.369E-03
2.20E-11	2.981E-18	1.90E-07	2.765E-12	1.60E-03	2.528E-06	6.10E+00	2.220E-03
2.30E-11	3.049E-18	2.00E-07	2.839E-12	1.70E-03	2.608E-06	6.20E+00	2.081E-03
2.40E-11	3.116E-18	2.10E-07	2.911E-12	1.80E-03	2.686E-06	6.30E+00	1.950E-03
2.55E-11	4.797E-18	2.20E-07	2.981E-12	1.90E-03	2.762E-06	6.40E+00	1.827E-03
2.70E-11	4.940E-18	2.30E-07	3.049E-12	2.00E-03	2.835E-06	6.50E+00	1.711E-03
2.80E-11	3.371E-18	2.40E-07	3.116E-12	2.10E-03	2.906E-06	6.60E+00	1.602E-03
3.00E-11	6.924E-18	2.55E-07	4.797E-12	2.20E-03	2.976E-06	6.70E+00	1.500E-03
3.20E-11	7.158E-18	2.70E-07	4.940E-12	2.30E-03	3.045E-06	6.80E+00	1.404E-03
3.40E-11	7.386E-18	2.80E-07	3.371E-12	2.40E-03	3.111E-06	6.90E+00	1.315E-03
3.60E-11	7.606E-18	3.00E-07	6.924E-12	2.55E-03	4.789E-06	7.00E+00	1.231E-03
3.80E-11	7.821E-18	3.20E-07	7.158E-12	2.70E-03	4.931E-06	7.10E+00	1.152E-03
4.00E-11	8.029E-18	3.40E-07	7.386E-12	2.80E-03	3.365E-06	7.20E+00	1.078E-03
4.25E-11	1.032E-17	3.60E-07	7.606E-12	3.00E-03	6.910E-06	7.30E+00	1.009E-03
4.50E-11	1.063E-17	3.80E-07	7.821E-12	3.20E-03	7.143E-06	7.40E+00	9.438E-04
4.75E-11	1.093E-17	4.00E-07	8.029E-12	3.40E-03	7.369E-06	7.50E+00	8.831E-04
5.00E-11	1.122E-17	4.25E-07	1.032E-11	3.60E-03	7.588E-06	7.60E+00	8.262E-04
5.25E-11	1.151E-17	4.50E-07	1.063E-11	3.80E-03	7.800E-06	7.70E+00	7.730E-04
5.50E-11	1.178E-17	4.75E-07	1.093E-11	4.00E-03	8.007E-06	7.80E+00	7.231E-04
5.75E-11	1.205E-17	5.00E-07	1.122E-11	4.25E-03	1.029E-05	7.90E+00	6.764E-04
6.00E-11	1.232E-17	5.25E-07	1.151E-11	4.50E-03	1.060E-05	8.00E+00	6.328E-04
6.30E-11	1.513E-17	5.50E-07	1.178E-11	4.75E-03	1.089E-05	8.10E+00	5.920E-04
6.60E-11	1.549E-17	5.75E-07	1.205E-11	5.00E-03	1.118E-05	8.20E+00	5.539E-04
6.90E-11	1.585E-17	6.00E-07	1.232E-11	5.25E-03	1.146E-05	8.30E+00	5.182E-04
7.20E-11	1.619E-17	6.30E-07	1.513E-11	5.50E-03	1.174E-05	8.40E+00	4.848E-04
7.60E-11	2.212E-17	6.60E-07	1.549E-11	5.75E-03	1.201E-05	8.50E+00	4.535E-04
8.00E-11	2.271E-17	6.90E-07	1.585E-11	6.00E-03	1.227E-05	8.60E+00	4.242E-04
8.40E-11	2.329E-17	7.20E-07	1.619E-11	6.30E-03	1.506E-05	8.70E+00	3.969E-04
8.80E-11	2.385E-17	7.60E-07	2.212E-11	6.60E-03	1.542E-05	8.80E+00	3.713E-04
9.20E-11	2.440E-17	8.00E-07	2.271E-11	6.90E-03	1.577E-05	8.90E+00	3.474E-04
9.60E-11	2.494E-17	8.40E-07	2.329E-11	7.20E-03	1.611E-05	9.00E+00	3.250E-04
1.00E-10	2.546E-17	8.80E-07	2.385E-11	7.60E-03	2.201E-05	9.10E+00	3.040E-04

Table A1.(cont. 1) Tabulated ^{252}Cf(s.f) neutron spectrum

Energy Group E_{up} [MeV]	Group flux [a.u.]	Energy Group E_{up} [MeV]	Group flux [a.u.]	Energy Group E_{up} [MeV]	Group flux [a.u.]	Energy Group E_{up} [MeV]	Group flux [a.u.]
1.05E-10	3.255E-17	9.20E-07	2.440E-11	8.00E-03	2.259E-05	9.20E+00	2.844E-04
1.10E-10	3.333E-17	9.60E-07	2.494E-11	8.40E-03	2.315E-05	9.30E+00	2.661E-04
1.15E-10	3.410E-17	1.00E-06	2.546E-11	8.80E-03	2.371E-05	9.40E+00	2.489E-04
1.20E-10	3.485E-17	1.05E-06	3.255E-11	9.20E-03	2.424E-05	9.50E+00	2.329E-04
1.28E-10	5.364E-17	1.10E-06	3.333E-11	9.60E-03	2.477E-05	9.60E+00	2.178E-04
1.35E-10	5.525E-17	1.15E-06	3.410E-11	1.00E-02	2.529E-05	9.70E+00	2.037E-04
1.43E-10	5.680E-17	1.20E-06	3.485E-11	1.05E-02	3.231E-05	9.80E+00	1.906E-04
1.50E-10	5.832E-17	1.27E-06	5.364E-11	1.10E-02	3.308E-05	9.90E+00	1.782E-04
1.60E-10	8.005E-17	1.35E-06	5.525E-11	1.15E-02	3.383E-05	1.00E+01	1.666E-04
1.70E-10	8.259E-17	1.42E-06	5.680E-11	1.20E-02	3.456E-05	1.01E+01	1.558E-04
1.80E-10	8.506E-17	1.50E-06	5.832E-11	1.28E-02	5.318E-05	1.02E+01	1.457E-04
1.90E-10	8.745E-17	1.60E-06	8.005E-11	1.35E-02	5.474E-05	1.03E+01	1.362E-04
2.00E-10	8.978E-17	1.70E-06	8.259E-11	1.43E-02	5.625E-05	1.04E+01	1.274E-04
2.10E-10	9.206E-17	1.80E-06	8.506E-11	1.50E-02	5.772E-05	1.05E+01	1.191E-04
2.20E-10	9.428E-17	1.90E-06	8.745E-11	1.60E-02	7.918E-05	1.06E+01	1.113E-04
2.30E-10	9.645E-17	2.00E-06	8.978E-11	1.70E-02	8.164E-05	1.07E+01	1.041E-04
2.40E-10	9.857E-17	2.10E-06	9.206E-11	1.80E-02	8.402E-05	1.08E+01	9.739E-05
2.55E-10	1.517E-16	2.20E-06	9.428E-11	1.90E-02	8.632E-05	1.09E+01	9.105E-05
2.70E-10	1.563E-16	2.30E-06	9.644E-11	2.00E-02	8.856E-05	1.10E+01	8.514E-05
2.80E-10	1.066E-16	2.40E-06	9.857E-11	2.10E-02	9.074E-05	1.11E+01	7.961E-05
3.00E-10	2.190E-16	2.55E-06	1.517E-10	2.20E-02	9.286E-05	1.12E+01	7.444E-05
3.20E-10	2.264E-16	2.70E-06	1.563E-10	2.30E-02	9.493E-05	1.13E+01	6.960E-05
3.40E-10	2.336E-16	2.80E-06	1.066E-10	2.40E-02	9.695E-05	1.14E+01	6.508E-05
3.60E-10	2.406E-16	3.00E-06	2.190E-10	2.55E-02	1.491E-04	1.15E+01	6.085E-05
3.80E-10	2.474E-16	3.20E-06	2.264E-10	2.70E-02	1.534E-04	1.16E+01	5.690E-05
4.00E-10	2.540E-16	3.40E-06	2.336E-10	2.80E-02	1.046E-04	1.17E+01	5.319E-05
4.25E-10	3.265E-16	3.60E-06	2.406E-10	3.00E-02	2.145E-04	1.18E+01	4.973E-05
4.50E-10	3.363E-16	3.80E-06	2.474E-10	3.20E-02	2.215E-04	1.19E+01	4.649E-05
4.75E-10	3.457E-16	4.00E-06	2.540E-10	3.40E-02	2.282E-04	1.20E+01	4.346E-05
5.00E-10	3.550E-16	4.25E-06	3.265E-10	3.60E-02	2.348E-04	1.21E+01	4.063E-05
5.25E-10	3.639E-16	4.50E-06	3.363E-10	3.80E-02	2.411E-04	1.22E+01	3.797E-05
5.50E-10	3.727E-16	4.75E-06	3.457E-10	4.00E-02	2.472E-04	1.23E+01	3.549E-05
5.75E-10	3.813E-16	5.00E-06	3.550E-10	4.25E-02	3.172E-04	1.24E+01	3.317E-05
6.00E-10	3.896E-16	5.25E-06	3.640E-10	4.50E-02	3.261E-04	1.25E+01	3.100E-05
6.30E-10	4.784E-16	5.50E-06	3.727E-10	4.75E-02	3.348E-04	1.26E+01	2.897E-05
6.60E-10	4.899E-16	5.75E-06	3.813E-10	5.00E-02	3.431E-04	1.27E+01	2.708E-05
6.90E-10	5.012E-16	6.00E-06	3.897E-10	5.25E-02	3.513E-04	1.28E+01	2.530E-05
7.20E-10	5.122E-16	6.30E-06	4.784E-10	5.50E-02	3.591E-04	1.29E+01	2.364E-05
7.60E-10	6.996E-16	6.60E-06	4.899E-10	5.75E-02	3.668E-04	1.30E+01	2.208E-05
8.00E-10	7.183E-16	6.90E-06	5.012E-10	6.00E-02	3.742E-04	1.31E+01	2.063E-05
8.40E-10	7.364E-16	7.20E-06	5.122E-10	6.30E-02	4.586E-04	1.32E+01	1.927E-05
8.80E-10	7.542E-16	7.60E-06	6.996E-10	6.60E-02	4.688E-04	1.33E+01	1.800E-05
9.20E-10	7.715E-16	8.00E-06	7.183E-10	6.90E-02	4.786E-04	1.34E+01	1.682E-05
9.60E-10	7.884E-16	8.40E-06	7.364E-10	7.20E-02	4.882E-04	1.35E+01	1.570E-05
1.00E-09	8.050E-16	8.80E-06	7.542E-10	7.60E-02	6.652E-04	1.36E+01	1.466E-05
1.05E-09	1.029E-15	9.20E-06	7.715E-10	8.00E-02	6.811E-04	1.37E+01	1.369E-05

Table A1.(cont. 2) Tabulated ^{252}Cf(s.f) neutron spectrum[f]

Energy Group E$_{up}$ [MeV]	Group flux [a.u.]	Energy Group E$_{up}$ [MeV]	Group flux [a.u.]	Energy Group E$_{up}$ [MeV]	Group flux [a.u.]	Energy Group E$_{up}$ [MeV]	Group flux [a.u.]
1.10E-09	1.054E-15	9.60E-06	7.884E-10	8.40E-02	6.964E-04	1.38E+01	1.279E-05
1.15E-09	1.078E-15	1.00E-05	8.050E-10	8.80E-02	7.113E-04	1.39E+01	1.194E-05
1.20E-09	1.102E-15	1.05E-05	1.029E-09	9.20E-02	7.257E-04	1.40E+01	1.116E-05
1.28E-09	1.696E-15	1.10E-05	1.054E-09	9.60E-02	7.397E-04	1.41E+01	1.042E-05
1.35E-09	1.747E-15	1.15E-05	1.078E-09	1.00E-01	7.533E-04	1.42E+01	9.731E-06
1.43E-09	1.796E-15	1.20E-05	1.102E-09	1.05E-01	9.602E-04	1.43E+01	9.084E-06
1.50E-09	1.844E-15	1.28E-05	1.696E-09	1.10E-01	9.800E-04	1.44E+01	8.483E-06
1.60E-09	2.531E-15	1.35E-05	1.747E-09	1.15E-01	9.992E-04	1.45E+01	7.921E-06
1.70E-09	2.611E-15	1.43E-05	1.796E-09	1.20E-01	1.018E-03	1.46E+01	7.396E-06
1.80E-09	2.689E-15	1.50E-05	1.844E-09	1.28E-01	1.560E-03	1.47E+01	6.906E-06
1.90E-09	2.765E-15	1.60E-05	2.531E-09	1.35E-01	1.598E-03	1.48E+01	6.448E-06
2.00E-09	2.839E-15	1.70E-05	2.611E-09	1.43E-01	1.635E-03	1.49E+01	6.021E-06
2.10E-09	2.911E-15	1.80E-05	2.689E-09	1.50E-01	1.670E-03	1.50E+01	5.622E-06
2.20E-09	2.981E-15	1.90E-05	2.765E-09	1.60E-01	2.279E-03	1.51E+01	5.249E-06
2.30E-09	3.049E-15	2.00E-05	2.839E-09	1.70E-01	2.336E-03	1.52E+01	4.901E-06
2.40E-09	3.116E-15	2.10E-05	2.911E-09	1.80E-01	2.389E-03	1.53E+01	4.575E-06
2.55E-09	4.797E-15	2.20E-05	2.981E-09	1.90E-01	2.440E-03	1.54E+01	4.272E-06
2.70E-09	4.940E-15	2.30E-05	3.049E-09	2.00E-01	2.489E-03	1.55E+01	3.989E-06
2.80E-09	3.371E-15	2.40E-05	3.116E-09	2.10E-01	2.535E-03	1.56E+01	3.724E-06
3.00E-09	6.924E-15	2.55E-05	4.797E-09	2.20E-01	2.578E-03	1.57E+01	3.477E-06
3.20E-09	7.158E-15	2.70E-05	4.940E-09	2.30E-01	2.620E-03	1.58E+01	3.246E-06
3.40E-09	7.386E-15	2.80E-05	3.371E-09	2.40E-01	2.660E-03	1.59E+01	3.030E-06
3.60E-09	7.606E-15	3.00E-05	6.924E-09	2.55E-01	4.060E-03	1.60E+01	2.829E-06
3.80E-09	7.821E-15	3.20E-05	7.158E-09	2.70E-01	4.139E-03	1.61E+01	2.641E-06
4.00E-09	8.029E-15	3.40E-05	7.386E-09	2.80E-01	2.801E-03	1.62E+01	2.466E-06
4.25E-09	1.032E-14	3.60E-05	7.606E-09	3.00E-01	5.695E-03	1.63E+01	2.302E-06
4.50E-09	1.063E-14	3.80E-05	7.821E-09	3.20E-01	5.810E-03	1.64E+01	2.149E-06
4.75E-09	1.093E-14	4.00E-05	8.029E-09	3.40E-01	5.915E-03	1.65E+01	2.006E-06
5.00E-09	1.122E-14	4.25E-05	1.032E-08	3.60E-01	6.010E-03	1.66E+01	1.872E-06
5.25E-09	1.151E-14	4.50E-05	1.063E-08	3.80E-01	6.098E-03	1.67E+01	1.748E-06
5.50E-09	1.178E-14	4.75E-05	1.093E-08	4.00E-01	6.177E-03	1.68E+01	1.631E-06
5.75E-09	1.205E-14	5.00E-05	1.122E-08	4.25E-01	7.822E-03	1.69E+01	1.523E-06
6.00E-09	1.232E-14	5.25E-05	1.151E-08	4.50E-01	7.922E-03	1.70E+01	1.421E-06
6.30E-09	1.513E-14	5.50E-05	1.178E-08	4.75E-01	8.010E-03	1.71E+01	1.327E-06
6.60E-09	1.549E-14	5.75E-05	1.205E-08	5.00E-01	8.086E-03	1.72E+01	1.238E-06
6.90E-09	1.585E-14	6.00E-05	1.232E-08	5.25E-01	8.152E-03	1.73E+01	1.156E-06
7.20E-09	1.619E-14	6.30E-05	1.512E-08	5.50E-01	8.211E-03	1.74E+01	1.079E-06
7.60E-09	2.212E-14	6.60E-05	1.549E-08	5.75E-01	8.261E-03	1.75E+01	1.007E-06
8.00E-09	2.271E-14	6.90E-05	1.585E-08	6.00E-01	8.304E-03	1.76E+01	9.396E-07
8.40E-09	2.329E-14	7.20E-05	1.619E-08	6.30E-01	1.001E-02	1.77E+01	8.769E-07
8.80E-09	2.385E-14	7.60E-05	2.212E-08	6.60E-01	1.005E-02	1.78E+01	8.183E-07
9.20E-09	2.440E-14	8.00E-05	2.271E-08	6.90E-01	1.007E-02	1.79E+01	7.636E-07
9.60E-09	2.494E-14	8.40E-05	2.329E-08	7.20E-01	1.009E-02	1.80E+01	7.126E-07
1.00E-08	2.546E-14	8.80E-05	2.385E-08	7.60E-01	1.346E-02	1.81E+01	6.649E-07
1.05E-08	3.255E-14	9.20E-05	2.440E-08	8.00E-01	1.346E-02	1.82E+01	6.204E-07
1.10E-08	3.333E-14	9.60E-05	2.493E-08	8.40E-01	1.344E-02	1.83E+01	5.788E-07

Table A1.(cont. 3) Tabulated ^{252}Cf(s.f) neutron spectrum

Energy Group E$_{up}$ [MeV]	Group flux [a.u.]	Energy Group E$_{up}$ [MeV]	Group flux [a.u.]	Energy Group E$_{up}$ [MeV]	Group flux [a.u.]	Energy Group E$_{up}$ [MeV]	Group flux [a.u.]
1.15E-08	3.410E-14	1.00E-04	2.546E-08	8.80E-01	1.340E-02	1.84E+01	5.400E-07
1.20E-08	3.485E-14	1.05E-04	3.254E-08	9.20E-01	1.334E-02	1.85E+01	5.038E-07
1.28E-08	5.364E-14	1.10E-04	3.333E-08	9.60E-01	1.328E-02	1.86E+01	4.700E-07
1.35E-08	5.525E-14	1.15E-04	3.409E-08	1.00E+00	1.320E-02	1.87E+01	4.385E-07
1.43E-08	5.680E-14	1.20E-04	3.484E-08	1.10E+00	3.259E-02	1.88E+01	4.091E-07
1.50E-08	5.832E-14	1.28E-04	5.364E-08	1.20E+00	3.190E-02	1.89E+01	3.816E-07
1.60E-08	8.005E-14	1.35E-04	5.524E-08	1.30E+00	3.109E-02	1.90E+01	3.560E-07
1.70E-08	8.259E-14	1.43E-04	5.679E-08	1.40E+00	3.019E-02	1.91E+01	3.320E-07
1.80E-08	8.505E-14	1.50E-04	5.831E-08	1.50E+00	2.924E-02	1.92E+01	3.097E-07
1.90E-08	8.745E-14	1.60E-04	8.004E-08	1.60E+00	2.823E-02	1.93E+01	2.889E-07
2.00E-08	8.978E-14	1.70E-04	8.258E-08	1.70E+00	2.719E-02	1.94E+01	2.695E-07
2.10E-08	9.206E-14	1.80E-04	8.504E-08	1.80E+00	2.614E-02	1.95E+01	2.514E-07
2.20E-08	9.428E-14	1.90E-04	8.744E-08	1.90E+00	2.509E-02	1.96E+01	2.344E-07
2.30E-08	9.645E-14	2.00E-04	8.977E-08	2.00E+00	2.404E-02	1.97E+01	2.187E-07
2.40E-08	9.857E-14	2.10E-04	9.205E-08	2.10E+00	2.300E-02	1.98E+01	2.040E-07
2.55E-08	1.517E-13	2.20E-04	9.426E-08	2.20E+00	2.197E-02	1.99E+01	1.902E-07
2.70E-08	1.563E-13	2.30E-04	9.643E-08	2.30E+00	2.096E-02	2.00E+01	1.774E-07
2.80E-08	1.066E-13	2.40E-04	9.855E-08	2.40E+00	1.998E-02	2.05E+01	7.241E-07
3.00E-08	2.190E-13	2.55E-04	1.517E-07	2.50E+00	1.903E-02	2.10E+01	5.123E-07
3.20E-08	2.264E-13	2.70E-04	1.562E-07	2.60E+00	1.810E-02	2.15E+01	3.624E-07
3.40E-08	2.336E-13	2.80E-04	1.066E-07	2.70E+00	1.721E-02	2.20E+01	2.562E-07
3.60E-08	2.406E-13	3.00E-04	2.189E-07	2.80E+00	1.634E-02	2.25E+01	1.811E-07
3.80E-08	2.474E-13	3.20E-04	2.263E-07	2.90E+00	1.550E-02	2.30E+01	1.280E-07
4.00E-08	2.540E-13	3.40E-04	2.335E-07	3.00E+00	1.470E-02	2.35E+01	9.041E-08
4.25E-08	3.265E-13	3.60E-04	2.405E-07	3.10E+00	1.393E-02	2.40E+01	6.385E-08
4.50E-08	3.362E-13	3.80E-04	2.473E-07	3.20E+00	1.318E-02	2.45E+01	4.508E-08
4.75E-08	3.457E-13	4.00E-04	2.539E-07	3.30E+00	1.247E-02	2.50E+01	3.182E-08
5.00E-08	3.550E-13	4.25E-04	3.263E-07	3.40E+00	1.179E-02	2.55E+01	2.246E-08
5.25E-08	3.639E-13	4.50E-04	3.361E-07	3.50E+00	1.114E-02	2.60E+01	1.585E-08
5.50E-08	3.727E-13	4.75E-04	3.455E-07	3.60E+00	1.051E-02	2.65E+01	1.118E-08
5.75E-08	3.813E-13	5.00E-04	3.547E-07	3.70E+00	9.922E-03	2.70E+01	7.882E-09
6.00E-08	3.896E-13	5.25E-04	3.637E-07	3.80E+00	9.357E-03	2.75E+01	5.558E-09
6.30E-08	4.784E-13	5.50E-04	3.725E-07	3.90E+00	8.819E-03	2.80E+01	3.918E-09
6.60E-08	4.899E-13	5.75E-04	3.810E-07	4.00E+00	8.307E-03	2.85E+01	2.761E-09
6.90E-08	5.012E-13	6.00E-04	3.894E-07	4.10E+00	7.822E-03	2.90E+01	1.945E-09
7.20E-08	5.122E-13	6.30E-04	4.781E-07	4.20E+00	7.362E-03	2.95E+01	1.371E-09
7.60E-08	6.996E-13	6.60E-04	4.896E-07	4.30E+00	6.926E-03	3.00E+01	9.654E-10
8.00E-08	7.183E-13	6.90E-04	5.009E-07	4.40E+00	6.514E-03		
8.40E-08	7.364E-13	7.20E-04	5.119E-07	4.50E+00	6.124E-03		

Typical Input Listings

A.1. MCNP6.2

```
c Cu cube
c
c 3s unc.  + -
c density + - 8.8899 / 8.8371
c width + - 1.5 cm side
c height + - 1.5 cm up
c thickness  + - 6 mm both sides
c detector distance 1.5 mm  -100.15 0 0 1  /  -99.85 0 0 1
c detector misalignment 1.5 mm -100 0 0.15 1  /  -100 0 -0.15 1
c Cu isotopes min 29063.80c 0.690174 29065.80c 0.308386
c        max 29063.80c 0.696118 29065.80c 0.302442
c
c Sensitivities
c holder  (add )
c gaps  +2mm ro 8.8267
c no Al
c no steel
c Al bottom  (add )
c Screws    (add )
c impurities (only Cu)
c
c Room effect
c Full geometry with walls (add )
c Transmission by cones    (add )
c Transmission by cones in presence of walls (add )
c
c
c isotopic composition
c JENDL-4     29063.89c 0.690504 29065.89c 0.308056
c JEFF-3.3    29063.08c 0.690504 29065.08c 0.308056
c ENDF/B-VIII 29063.31c 0.690504 29065.31c 0.308056
c INDEN       29063.34c 0.690504 29065.34c 0.308056
c
c
c cell card
1 0  6 -7 -20 imp:n=1 $ source
2 1 -8  5 -9 -21 (-6:7:20) imp:n=1 $ steel cladding
3 2 -0.185 4 -5 -21 imp:n=1 $
4 2 -0.185 9 -10 -21 imp:n=1 $
5 4 -2.7  3 -11 -30 (-4:10:21) (-4:8:-22:30) imp:n=1 $ Al transport holder
6 0 3 -11 23 -30 imp:n=1
10 4 -2.7 1 -2 -26 imp:n=1 $ bottom
11 4 -2.7 12 -14 23 -24 imp:n=1 $ inner tube
12 4 -2.7 12 -13 24 -25 imp:n=1 $ spacer
13 4 -2.7 2 -14 25 -26 imp:n=1 $ outer tube
c
14 0 2 -3 100 -30 imp:n=1
15 0 2 -12 30 -25 imp:n=1
16 0 13 -14 24 -25 imp:n=1 $ air spacer
17 0 11 -14 -23 imp:n=1 $ air cenral tube
18 0 30 -23 12 -11 imp:n=1 $ air Cf - tube
19 0 1 -14 26 -27 imp:n=1 $ air tube to Cu
```

20 0 (4 -8 22 -30 102 101) imp:n=1 $ air
c
c Cu
30 5 -8.8635 (40 -14 41 -42 43 -44) (27:-1) (-45:46:-47:48) imp:n=1 $ Cu block
31 0 45 -46 47 -48 40 -14 imp:n=1 $ cavity Cu block
c
c air around
50 0 -99 (-40:14:-41:42:-43:44) imp:n=1
c
60 4 -2.7 -100 2 -30 -3 imp:n=1 $ skittle
61 4 -2.7 -101 4 22 -30 imp:n=1 $ lower conical part
62 4 -2.7 -102 -8 22 -30 imp:n=1 $ upper conical part
c
70 0 99 imp:n=0

c surfaces
1 pz -3
2 pz -2.1
3 pz -1.66
4 pz -1.01
5 pz -0.695
6 pz -0.3
7 pz 0.3
8 pz 1.19
9 pz 1.275
10 pz 1.59
11 pz 1.84
12 pz -1.3
13 pz -0.8
14 pz 24.75
c
20 cz 0.195
21 cz 0.475
22 cz 0.535
23 cz 0.7
24 cz 0.8
25 cz 1.1
26 cz 1.25
27 cz 1.3
30 cz 0.6925
c
40 pz -24.75
41 py -24.75
42 py 24.75
43 px -24
44 px 24
45 px 16
46 px 23
47 py -3.5
48 py 3.5
c
99 so 300
c
100 kz -1.3114 0.3333 -1
101 kz -0.130635 0.62015636 -1
102 kz 0.310635 0.62015636 1

```
C OTHERS
mode n p
c zdroj Mannhart Cf spectra IAEA
sdef par=1 pos=0 0 -0.3 axs=0 0 1 rad=d1 ext=d2 erg=d3
c
si1  0 0.195
sp1  -21 1
si2  0 0.6
sp2  -21 0
c
c https://nds.iaea.org/IRDFF/spectra/irdff_sp_Cf252_ln.g725
c  Elow
# si3 sp3
 1.00E-11 0.0000E+00
 1.05E-11 1.0291E-18
 1.10E-11 1.0539E-18
 1.15E-11 1.0782E-18
 1.20E-11 1.1019E-18
 1.28E-11 1.6961E-18
 1.35E-11 1.7468E-18
 1.43E-11 1.7960E-18
 1.50E-11 1.8439E-18
 1.60E-11 2.5309E-18
 1.70E-11 2.6113E-18
 1.80E-11 2.6892E-18
 1.90E-11 2.7650E-18
 2.00E-11 2.8387E-18
 2.10E-11 2.9106E-18
 2.20E-11 2.9808E-18
 2.30E-11 3.0493E-18
 2.40E-11 3.1164E-18
 2.55E-11 4.7971E-18
 2.70E-11 4.9404E-18
 2.80E-11 3.3712E-18
 3.00E-11 6.9236E-18
 3.20E-11 7.1584E-18
 3.40E-11 7.3858E-18
 3.60E-11 7.6064E-18
 3.80E-11 7.8208E-18
 4.00E-11 8.0294E-18
 4.25E-11 1.0322E-17
 4.50E-11 1.0631E-17
 4.75E-11 1.0930E-17
 5.00E-11 1.1222E-17
 5.25E-11 1.1506E-17
 5.50E-11 1.1783E-17
 5.75E-11 1.2054E-17
 6.00E-11 1.2320E-17
 6.30E-11 1.5125E-17
 6.60E-11 1.5490E-17
 6.90E-11 1.5846E-17
 7.20E-11 1.6195E-17
 7.60E-11 2.2123E-17
 8.00E-11 2.2713E-17
 8.40E-11 2.3288E-17
 8.80E-11 2.3850E-17
 9.20E-11 2.4399E-17
```

9.60E-11 2.4935E-17
1.00E-10 2.5461E-17
1.05E-10 3.2549E-17
1.10E-10 3.3333E-17
1.15E-10 3.4099E-17
1.20E-10 3.4849E-17
1.28E-10 5.3645E-17
1.35E-10 5.5246E-17
1.43E-10 5.6803E-17
1.50E-10 5.8318E-17
1.60E-10 8.0047E-17
1.70E-10 8.2589E-17
1.80E-10 8.5055E-17
1.90E-10 8.7451E-17
2.00E-10 8.9783E-17
2.10E-10 9.2057E-17
2.20E-10 9.4277E-17
2.30E-10 9.6445E-17
2.40E-10 9.8566E-17
2.55E-10 1.5173E-16
2.70E-10 1.5626E-16
2.80E-10 1.0663E-16
3.00E-10 2.1898E-16
3.20E-10 2.2642E-16
3.40E-10 2.3362E-16
3.60E-10 2.4060E-16
3.80E-10 2.4738E-16
4.00E-10 2.5398E-16
4.25E-10 3.2650E-16
4.50E-10 3.3625E-16
4.75E-10 3.4573E-16
5.00E-10 3.5498E-16
5.25E-10 3.6395E-16
5.50E-10 3.7273E-16
5.75E-10 3.8128E-16
6.00E-10 3.8965E-16
6.30E-10 4.7841E-16
6.60E-10 4.8993E-16
6.90E-10 5.0118E-16
7.20E-10 5.1219E-16
7.60E-10 6.9964E-16
8.00E-10 7.1828E-16
8.40E-10 7.3644E-16
8.80E-10 7.5416E-16
9.20E-10 7.7148E-16
9.60E-10 7.8844E-16
1.00E-09 8.0500E-16
1.05E-09 1.0291E-15
1.10E-09 1.0539E-15
1.15E-09 1.0782E-15
1.20E-09 1.1019E-15
1.28E-09 1.6961E-15
1.35E-09 1.7468E-15
1.43E-09 1.7960E-15
1.50E-09 1.8439E-15
1.60E-09 2.5309E-15
1.70E-09 2.6113E-15

1.80E-09 2.6892E-15
1.90E-09 2.7650E-15
2.00E-09 2.8387E-15
2.10E-09 2.9106E-15
2.20E-09 2.9808E-15
2.30E-09 3.0493E-15
2.40E-09 3.1164E-15
2.55E-09 4.7972E-15
2.70E-09 4.9404E-15
2.80E-09 3.3712E-15
3.00E-09 6.9236E-15
3.20E-09 7.1584E-15
3.40E-09 7.3858E-15
3.60E-09 7.6064E-15
3.80E-09 7.8208E-15
4.00E-09 8.0294E-15
4.25E-09 1.0322E-14
4.50E-09 1.0631E-14
4.75E-09 1.0930E-14
5.00E-09 1.1222E-14
5.25E-09 1.1506E-14
5.50E-09 1.1783E-14
5.75E-09 1.2054E-14
6.00E-09 1.2320E-14
6.30E-09 1.5125E-14
6.60E-09 1.5490E-14
6.90E-09 1.5846E-14
7.20E-09 1.6195E-14
7.60E-09 2.2123E-14
8.00E-09 2.2713E-14
8.40E-09 2.3288E-14
8.80E-09 2.3850E-14
9.20E-09 2.4399E-14
9.60E-09 2.4935E-14
1.00E-08 2.5461E-14
1.05E-08 3.2549E-14
1.10E-08 3.3333E-14
1.15E-08 3.4099E-14
1.20E-08 3.4849E-14
1.28E-08 5.3644E-14
1.35E-08 5.5246E-14
1.43E-08 5.6803E-14
1.50E-08 5.8318E-14
1.60E-08 8.0047E-14
1.70E-08 8.2589E-14
1.80E-08 8.5055E-14
1.90E-08 8.7451E-14
2.00E-08 8.9783E-14
2.10E-08 9.2057E-14
2.20E-08 9.4277E-14
2.30E-08 9.6445E-14
2.40E-08 9.8566E-14
2.55E-08 1.5173E-13
2.70E-08 1.5626E-13
2.80E-08 1.0663E-13
3.00E-08 2.1898E-13
3.20E-08 2.2642E-13

3.40E-08 2.3362E-13
3.60E-08 2.4060E-13
3.80E-08 2.4738E-13
4.00E-08 2.5398E-13
4.25E-08 3.2650E-13
4.50E-08 3.3625E-13
4.75E-08 3.4572E-13
5.00E-08 3.5498E-13
5.25E-08 3.6395E-13
5.50E-08 3.7273E-13
5.75E-08 3.8128E-13
6.00E-08 3.8965E-13
6.30E-08 4.7841E-13
6.60E-08 4.8993E-13
6.90E-08 5.0118E-13
7.20E-08 5.1219E-13
7.60E-08 6.9964E-13
8.00E-08 7.1828E-13
8.40E-08 7.3644E-13
8.80E-08 7.5416E-13
9.20E-08 7.7148E-13
9.60E-08 7.8844E-13
1.00E-07 8.0500E-13
1.05E-07 1.0291E-12
1.10E-07 1.0539E-12
1.15E-07 1.0782E-12
1.20E-07 1.1019E-12
1.27E-07 1.6961E-12
1.35E-07 1.7468E-12
1.42E-07 1.7960E-12
1.50E-07 1.8439E-12
1.60E-07 2.5309E-12
1.70E-07 2.6113E-12
1.80E-07 2.6892E-12
1.90E-07 2.7650E-12
2.00E-07 2.8387E-12
2.10E-07 2.9106E-12
2.20E-07 2.9808E-12
2.30E-07 3.0493E-12
2.40E-07 3.1164E-12
2.55E-07 4.7972E-12
2.70E-07 4.9404E-12
2.80E-07 3.3712E-12
3.00E-07 6.9236E-12
3.20E-07 7.1584E-12
3.40E-07 7.3858E-12
3.60E-07 7.6064E-12
3.80E-07 7.8208E-12
4.00E-07 8.0294E-12
4.25E-07 1.0322E-11
4.50E-07 1.0631E-11
4.75E-07 1.0930E-11
5.00E-07 1.1222E-11
5.25E-07 1.1506E-11
5.50E-07 1.1783E-11
5.75E-07 1.2054E-11
6.00E-07 1.2320E-11

6.30E-07 1.5125E-11
6.60E-07 1.5490E-11
6.90E-07 1.5846E-11
7.20E-07 1.6195E-11
7.60E-07 2.2123E-11
8.00E-07 2.2713E-11
8.40E-07 2.3288E-11
8.80E-07 2.3850E-11
9.20E-07 2.4399E-11
9.60E-07 2.4935E-11
1.00E-06 2.5461E-11
1.05E-06 3.2549E-11
1.10E-06 3.3333E-11
1.15E-06 3.4099E-11
1.20E-06 3.4849E-11
1.27E-06 5.3644E-11
1.35E-06 5.5246E-11
1.42E-06 5.6803E-11
1.50E-06 5.8318E-11
1.60E-06 8.0047E-11
1.70E-06 8.2589E-11
1.80E-06 8.5055E-11
1.90E-06 8.7451E-11
2.00E-06 8.9783E-11
2.10E-06 9.2057E-11
2.20E-06 9.4277E-11
2.30E-06 9.6445E-11
2.40E-06 9.8566E-11
2.55E-06 1.5173E-10
2.70E-06 1.5626E-10
2.80E-06 1.0663E-10
3.00E-06 2.1899E-10
3.20E-06 2.2642E-10
3.40E-06 2.3361E-10
3.60E-06 2.4059E-10
3.80E-06 2.4737E-10
4.00E-06 2.5398E-10
4.25E-06 3.2650E-10
4.50E-06 3.3626E-10
4.75E-06 3.4574E-10
5.00E-06 3.5497E-10
5.25E-06 3.6395E-10
5.50E-06 3.7272E-10
5.75E-06 3.8128E-10
6.00E-06 3.8966E-10
6.30E-06 4.7840E-10
6.60E-06 4.8992E-10
6.90E-06 5.0117E-10
7.20E-06 5.1218E-10
7.60E-06 6.9963E-10
8.00E-06 7.1828E-10
8.40E-06 7.3645E-10
8.80E-06 7.5418E-10
9.20E-06 7.7150E-10
9.60E-06 7.8844E-10
1.00E-05 8.0502E-10
1.05E-05 1.0291E-09

1.10E-05 1.0539E-09
1.15E-05 1.0781E-09
1.20E-05 1.1018E-09
1.28E-05 1.6961E-09
1.35E-05 1.7467E-09
1.43E-05 1.7960E-09
1.50E-05 1.8439E-09
1.60E-05 2.5309E-09
1.70E-05 2.6113E-09
1.80E-05 2.6892E-09
1.90E-05 2.7650E-09
2.00E-05 2.8388E-09
2.10E-05 2.9106E-09
2.20E-05 2.9808E-09
2.30E-05 3.0493E-09
2.40E-05 3.1164E-09
2.55E-05 4.7972E-09
2.70E-05 4.9404E-09
2.80E-05 3.3712E-09
3.00E-05 6.9236E-09
3.20E-05 7.1585E-09
3.40E-05 7.3859E-09
3.60E-05 7.6064E-09
3.80E-05 7.8208E-09
4.00E-05 8.0294E-09
4.25E-05 1.0322E-08
4.50E-05 1.0630E-08
4.75E-05 1.0930E-08
5.00E-05 1.1222E-08
5.25E-05 1.1506E-08
5.50E-05 1.1783E-08
5.75E-05 1.2054E-08
6.00E-05 1.2319E-08
6.30E-05 1.5125E-08
6.60E-05 1.5489E-08
6.90E-05 1.5846E-08
7.20E-05 1.6194E-08
7.60E-05 2.2121E-08
8.00E-05 2.2711E-08
8.40E-05 2.3286E-08
8.80E-05 2.3847E-08
9.20E-05 2.4396E-08
9.60E-05 2.4932E-08
1.00E-04 2.5457E-08
1.05E-04 3.2543E-08
1.10E-04 3.3328E-08
1.15E-04 3.4094E-08
1.20E-04 3.4844E-08
1.28E-04 5.3636E-08
1.35E-04 5.5238E-08
1.43E-04 5.6795E-08
1.50E-04 5.8310E-08
1.60E-04 8.0037E-08
1.70E-04 8.2579E-08
1.80E-04 8.5045E-08
1.90E-04 8.7441E-08
2.00E-04 8.9773E-08

2.10E-04 9.2046E-08
2.20E-04 9.4264E-08
2.30E-04 9.6430E-08
2.40E-04 9.8548E-08
2.55E-04 1.5170E-07
2.70E-04 1.5622E-07
2.80E-04 1.0660E-07
3.00E-04 2.1893E-07
3.20E-04 2.2635E-07
3.40E-04 2.3353E-07
3.60E-04 2.4049E-07
3.80E-04 2.4727E-07
4.00E-04 2.5385E-07
4.25E-04 3.2633E-07
4.50E-04 3.3606E-07
4.75E-04 3.4552E-07
5.00E-04 3.5473E-07
5.25E-04 3.6370E-07
5.50E-04 3.7246E-07
5.75E-04 3.8103E-07
6.00E-04 3.8940E-07
6.30E-04 4.7809E-07
6.60E-04 4.8961E-07
6.90E-04 5.0086E-07
7.20E-04 5.1187E-07
7.60E-04 6.9922E-07
8.00E-04 7.1786E-07
8.40E-04 7.3603E-07
8.80E-04 7.5376E-07
9.20E-04 7.7108E-07
9.60E-04 7.8803E-07
1.00E-03 8.0462E-07
1.05E-03 1.0286E-06
1.10E-03 1.0533E-06
1.15E-03 1.0775E-06
1.20E-03 1.1011E-06
1.28E-03 1.6949E-06
1.35E-03 1.7454E-06
1.43E-03 1.7944E-06
1.50E-03 1.8422E-06
1.60E-03 2.5284E-06
1.70E-03 2.6085E-06
1.80E-03 2.6861E-06
1.90E-03 2.7615E-06
2.00E-03 2.8349E-06
2.10E-03 2.9065E-06
2.20E-03 2.9763E-06
2.30E-03 3.0446E-06
2.40E-03 3.1113E-06
2.55E-03 4.7889E-06
2.70E-03 4.9314E-06
2.80E-03 3.3647E-06
3.00E-03 6.9096E-06
3.20E-03 7.1429E-06
3.40E-03 7.3688E-06
3.60E-03 7.5878E-06
3.80E-03 7.8005E-06

4.00E-03 8.0074E-06
4.25E-03 1.0292E-05
4.50E-03 1.0598E-05
4.75E-03 1.0895E-05
5.00E-03 1.1183E-05
5.25E-03 1.1464E-05
5.50E-03 1.1739E-05
5.75E-03 1.2007E-05
6.00E-03 1.2269E-05
6.30E-03 1.5060E-05
6.60E-03 1.5420E-05
6.90E-03 1.5771E-05
7.20E-03 1.6115E-05
7.60E-03 2.2008E-05
8.00E-03 2.2589E-05
8.40E-03 2.3155E-05
8.80E-03 2.3706E-05
9.20E-03 2.4245E-05
9.60E-03 2.4771E-05
1.00E-02 2.5286E-05
1.05E-02 3.2315E-05
1.10E-02 3.3082E-05
1.15E-02 3.3831E-05
1.20E-02 3.4562E-05
1.28E-02 5.3180E-05
1.35E-02 5.4739E-05
1.43E-02 5.6251E-05
1.50E-02 5.7721E-05
1.60E-02 7.9180E-05
1.70E-02 8.1637E-05
1.80E-02 8.4015E-05
1.90E-02 8.6322E-05
2.00E-02 8.8562E-05
2.10E-02 9.0740E-05
2.20E-02 9.2861E-05
2.30E-02 9.4929E-05
2.40E-02 9.6948E-05
2.55E-02 1.4910E-04
2.70E-02 1.5338E-04
2.80E-02 1.0456E-04
3.00E-02 2.1449E-04
3.20E-02 2.2147E-04
3.40E-02 2.2824E-04
3.60E-02 2.3478E-04
3.80E-02 2.4107E-04
4.00E-02 2.4716E-04
4.25E-02 3.1724E-04
4.50E-02 3.2615E-04
4.75E-02 3.3477E-04
5.00E-02 3.4314E-04
5.25E-02 3.5126E-04
5.50E-02 3.5914E-04
5.75E-02 3.6679E-04
6.00E-02 3.7424E-04
6.30E-02 4.5864E-04
6.60E-02 4.6877E-04
6.90E-02 4.7860E-04

7.20E-02 4.8815E-04
7.60E-02 6.6522E-04
8.00E-02 6.8109E-04
8.40E-02 6.9642E-04
8.80E-02 7.1126E-04
9.20E-02 7.2572E-04
9.60E-02 7.3973E-04
1.00E-01 7.5333E-04
1.05E-01 9.6015E-04
1.10E-01 9.7999E-04
1.15E-01 9.9915E-04
1.20E-01 1.0177E-03
1.28E-01 1.5600E-03
1.35E-01 1.5985E-03
1.43E-01 1.6352E-03
1.50E-01 1.6703E-03
1.60E-01 2.2792E-03
1.70E-01 2.3358E-03
1.80E-01 2.3894E-03
1.90E-01 2.4403E-03
2.00E-01 2.4886E-03
2.10E-01 2.5346E-03
2.20E-01 2.5784E-03
2.30E-01 2.6200E-03
2.40E-01 2.6598E-03
2.55E-01 4.0601E-03
2.70E-01 4.1395E-03
2.80E-01 2.8011E-03
3.00E-01 5.6949E-03
3.20E-01 5.8097E-03
3.40E-01 5.9146E-03
3.60E-01 6.0103E-03
3.80E-01 6.0976E-03
4.00E-01 6.1771E-03
4.25E-01 7.8222E-03
4.50E-01 7.9222E-03
4.75E-01 8.0100E-03
5.00E-01 8.0856E-03
5.25E-01 8.1524E-03
5.50E-01 8.2112E-03
5.75E-01 8.2614E-03
6.00E-01 8.3038E-03
6.30E-01 1.0010E-02
6.60E-01 1.0047E-02
6.90E-01 1.0074E-02
7.20E-01 1.0091E-02
7.60E-01 1.3465E-02
8.00E-01 1.3459E-02
8.40E-01 1.3436E-02
8.80E-01 1.3396E-02
9.20E-01 1.3343E-02
9.60E-01 1.3277E-02
1.00E+00 1.3199E-02
1.10E+00 3.2589E-02
1.20E+00 3.1901E-02
1.30E+00 3.1094E-02
1.40E+00 3.0195E-02

1.50E+00 2.9241E-02
1.60E+00 2.8234E-02
1.70E+00 2.7191E-02
1.80E+00 2.6138E-02
1.90E+00 2.5085E-02
2.00E+00 2.4039E-02
2.10E+00 2.2998E-02
2.20E+00 2.1968E-02
2.30E+00 2.0961E-02
2.40E+00 1.9981E-02
2.50E+00 1.9027E-02
2.60E+00 1.8101E-02
2.70E+00 1.7206E-02
2.80E+00 1.6340E-02
2.90E+00 1.5504E-02
3.00E+00 1.4700E-02
3.10E+00 1.3927E-02
3.20E+00 1.3184E-02
3.30E+00 1.2474E-02
3.40E+00 1.1792E-02
3.50E+00 1.1137E-02
3.60E+00 1.0514E-02
3.70E+00 9.9220E-03
3.80E+00 9.3572E-03
3.90E+00 8.8188E-03
4.00E+00 8.3074E-03
4.10E+00 7.8219E-03
4.20E+00 7.3618E-03
4.30E+00 6.9259E-03
4.40E+00 6.5138E-03
4.50E+00 6.1244E-03
4.60E+00 5.7565E-03
4.70E+00 5.4091E-03
4.80E+00 5.0817E-03
4.90E+00 4.7732E-03
5.00E+00 4.4828E-03
5.10E+00 4.2094E-03
5.20E+00 3.9516E-03
5.30E+00 3.7087E-03
5.40E+00 3.4804E-03
5.50E+00 3.2660E-03
5.60E+00 3.0638E-03
5.70E+00 2.8734E-03
5.80E+00 2.6945E-03
5.90E+00 2.5266E-03
6.00E+00 2.3687E-03
6.10E+00 2.2202E-03
6.20E+00 2.0807E-03
6.30E+00 1.9498E-03
6.40E+00 1.8265E-03
6.50E+00 1.7106E-03
6.60E+00 1.6018E-03
6.70E+00 1.4998E-03
6.80E+00 1.4043E-03
6.90E+00 1.3149E-03
7.00E+00 1.2308E-03
7.10E+00 1.1518E-03

7.20E+00 1.0779E-03
7.30E+00 1.0087E-03
7.40E+00 9.4380E-04
7.50E+00 8.8307E-04
7.60E+00 8.2621E-04
7.70E+00 7.7298E-04
7.80E+00 7.2313E-04
7.90E+00 6.7644E-04
8.00E+00 6.3281E-04
8.10E+00 5.9202E-04
8.20E+00 5.5387E-04
8.30E+00 5.1818E-04
8.40E+00 4.8476E-04
8.50E+00 4.5347E-04
8.60E+00 4.2422E-04
8.70E+00 3.9688E-04
8.80E+00 3.7133E-04
8.90E+00 3.4744E-04
9.00E+00 3.2504E-04
9.10E+00 3.0404E-04
9.20E+00 2.8442E-04
9.30E+00 2.6608E-04
9.40E+00 2.4892E-04
9.50E+00 2.3288E-04
9.60E+00 2.1784E-04
9.70E+00 2.0374E-04
9.80E+00 1.9055E-04
9.90E+00 1.7821E-04
1.00E+01 1.6663E-04
1.01E+01 1.5579E-04
1.02E+01 1.4566E-04
1.03E+01 1.3622E-04
1.04E+01 1.2737E-04
1.05E+01 1.1907E-04
1.06E+01 1.1134E-04
1.07E+01 1.0414E-04
1.08E+01 9.7389E-05
1.09E+01 9.1051E-05
1.10E+01 8.5135E-05
1.11E+01 7.9612E-05
1.12E+01 7.4442E-05
1.13E+01 6.9604E-05
1.14E+01 6.5081E-05
1.15E+01 6.0852E-05
1.16E+01 5.6895E-05
1.17E+01 5.3191E-05
1.18E+01 4.9728E-05
1.19E+01 4.6489E-05
1.20E+01 4.3459E-05
1.21E+01 4.0625E-05
1.22E+01 3.7972E-05
1.23E+01 3.5488E-05
1.24E+01 3.3166E-05
1.25E+01 3.0997E-05
1.26E+01 2.8970E-05
1.27E+01 2.7076E-05
1.28E+01 2.5300E-05

1.29E+01 2.3635E-05
1.30E+01 2.2082E-05
1.31E+01 2.0633E-05
1.32E+01 1.9273E-05
1.33E+01 1.8001E-05
1.34E+01 1.6816E-05
1.35E+01 1.5704E-05
1.36E+01 1.4663E-05
1.37E+01 1.3693E-05
1.38E+01 1.2788E-05
1.39E+01 1.1944E-05
1.40E+01 1.1156E-05
1.41E+01 1.0421E-05
1.42E+01 9.7307E-06
1.43E+01 9.0843E-06
1.44E+01 8.4825E-06
1.45E+01 7.9205E-06
1.46E+01 7.3957E-06
1.47E+01 6.9057E-06
1.48E+01 6.4482E-06
1.49E+01 6.0208E-06
1.50E+01 5.6217E-06
1.51E+01 5.2488E-06
1.52E+01 4.9006E-06
1.53E+01 4.5754E-06
1.54E+01 4.2718E-06
1.55E+01 3.9885E-06
1.56E+01 3.7239E-06
1.57E+01 3.4768E-06
1.58E+01 3.2460E-06
1.59E+01 3.0304E-06
1.60E+01 2.8291E-06
1.61E+01 2.6412E-06
1.62E+01 2.4656E-06
1.63E+01 2.3017E-06
1.64E+01 2.1486E-06
1.65E+01 2.0056E-06
1.66E+01 1.8721E-06
1.67E+01 1.7475E-06
1.68E+01 1.6312E-06
1.69E+01 1.5227E-06
1.70E+01 1.4213E-06
1.71E+01 1.3267E-06
1.72E+01 1.2383E-06
1.73E+01 1.1558E-06
1.74E+01 1.0788E-06
1.75E+01 1.0068E-06
1.76E+01 9.3961E-07
1.77E+01 8.7686E-07
1.78E+01 8.1829E-07
1.79E+01 7.6361E-07
1.80E+01 7.1258E-07
1.81E+01 6.6494E-07
1.82E+01 6.2043E-07
1.83E+01 5.7884E-07
1.84E+01 5.4003E-07
1.85E+01 5.0381E-07

```
1.86E+01 4.7002E-07
1.87E+01 4.3848E-07
1.88E+01 4.0905E-07
1.89E+01 3.8158E-07
1.90E+01 3.5595E-07
1.91E+01 3.3203E-07
1.92E+01 3.0972E-07
1.93E+01 2.8890E-07
1.94E+01 2.6947E-07
1.95E+01 2.5135E-07
1.96E+01 2.3444E-07
1.97E+01 2.1867E-07
1.98E+01 2.0395E-07
1.99E+01 1.9022E-07
2.00E+01 1.7741E-07
2.05E+01 7.2410E-07
2.10E+01 5.1230E-07
2.15E+01 3.6236E-07
2.20E+01 2.5621E-07
2.25E+01 1.8110E-07
2.30E+01 1.2798E-07
2.35E+01 9.0405E-08
2.40E+01 6.3850E-08
2.45E+01 4.5082E-08
2.50E+01 3.1823E-08
2.55E+01 2.2458E-08
2.60E+01 1.5845E-08
2.65E+01 1.1177E-08
2.70E+01 7.8820E-09
2.75E+01 5.5575E-09
2.80E+01 3.9175E-09
2.85E+01 2.7610E-09
2.90E+01 1.9455E-09
2.95E+01 1.3706E-09
3.00E+01 9.6535E-10
c
C 304L STEEL rho = 8.0 g/cc
m1 6000.80c -0.000150
   14028.80c -0.0046115
   14029.80c -0.0002335
   14030.80c -0.000155
   15031.80c -0.000230
   16032.80c -0.00014253
   16034.80c -0.00000747
   24050.80c -0.0082555
   24052.80c -0.1591991
   24053.80c -0.0180519
   24054.80c -0.0044935
   25055.80c -0.010000
   26054.80c -0.0402798
   26056.80c -0.636957
   26057.80c -0.015278
   26058.80c -0.0019452
   28058.80c -0.068077
   28060.80c -0.026233
   28061.80c -0.00114
   28062.80c -0.00456
```

C FELT rho = 0.185 g/cc PDF material list
m2   1001.80c -0.0442
     6000.80c -0.4346
     7014.80c -0.1765
     8016.80c -0.3447
C
C Hlinik rho = 2.7 g/cc
m4 13027.80c 1
C
C COPPER CUBE
m5 29063.80c 0.690504 29065.80c 0.308056 17037.80c 0.000186571 17035.80c
   0.000583429 28064.80c 1.1112E-06 28061.80c 0.000001368 28060.80c
   3.14796E-05 28058.80c 8.16924E-05 28062.80c 4.3608E-06 20040.80c
   0.00022 19039.80c 0.000214521 19041.80c 0.00015479 47107.80c 1.03678E-05
   47109.80c 9.6322E-06 26056.80c 0.000073376 26054.80c 0.00000464
   26057.80c 0.00000176 26058.80c 0.000000224
c Pure Copper
m11 29063.80c 0.6915 29065.80c 0.3085
C TALLY JEMNE
f5:n -100 0 0 1
E5 0.1 108i 11
c
prdmp 2.5e9 2.5e9 1
cut:n j 0.98
print
nps 2.5e10

A.2. SCALE .6.2.3

=mavric
alarm-cf-cu-shield-003 scale 6.2.4 ce endf/b-vii.1
v7.1-28n19g

read comp
' aluminum for source and tube
 al-27 1 0 6.0300e-2 end

' stainless steel 304L for source
  C   2 0 6.0165E-5 end
  Si-28 2 0 7.9410E-4 end
  Si-29 2 0 3.8822E-5 end
  Si-30 2 0 2.4913E-5 end
  P-31 2 0 3.5774E-5 end
  S-32 2 0 2.1477E-5 end
  S-34 2 0 1.0595E-6 end
  Cr-50 2 0 7.9630E-4 end
  Cr-52 2 0 1.4766E-2 end
  Cr-53 2 0 1.6427E-3 end
  Cr-54 2 0 4.0134E-4 end
  Mn-55 2 0 8.7692E-4 end
  Fe-54 2 0 3.5976E-3 end
  Fe-56 2 0 5.4861E-2 end
  Fe-57 2 0 1.2928E-3 end
  Fe-58 2 0 1.6176E-4 end
  Ni-58 2 0 5.6610E-3 end
  Ni-60 2 0 2.1088E-3 end
  Ni-61 2 0 9.0136E-5 end
  Ni-62 2 0 3.5474E-4 end

' felt for source
  H-1 3 0 4.8860E-3 end
  C   3 0 4.0311E-3 end
  N-14 3 0 1.4042E-3 end
  O-16 3 0 2.4009E-3 end

' copper for shielding block
  Cu-63 4 0 5.8000E-2 end
  Cu-65 4 0 2.5900E-2 end
  Cl-37 4 0 1.5700E-5 end
  Cl-35 4 0 4.9000E-5 end
  Ni-64 4 0 9.3400E-8 end
  Ni-61 4 0 1.1500E-7 end
  Ni-60 4 0 2.6500E-6 end
  Ni-58 4 0 6.8600E-6 end
  Ni-62 4 0 3.6600E-7 end
  Ca-40 4 0 1.8500E-5 end
  K-39   4 0 1.8000E-5 end
  K-41   4 0 1.3000E-5 end
  Ag-107 4 0 8.7100E-7 end
  Ag-109 4 0 8.0900E-7 end
  Fe-56 4 0 6.1700E-6 end
  Fe-54 4 0 3.9000E-7 end
  Fe-57 4 0 1.4800E-7 end
  Fe-58 4 0 1.8800E-8 end

end comp

read geometry
 unit 1
  com="source capsule"
  zcylinder 1 0.195 0.3 -0.3
  zcylinder 2 0.475 1.275 -0.695
  zcylinder 3 0.475 1.59 -1.01
  zcylinder 4 0.535 1.84 -1.66
  cone 5 0.535 -0.81 0.7 -1.01
  zcylinder 6 0.7 1.19 -1.01
  cone 7 0.7 1.19 0.535 0.99
  zcylinder 8 0.7 1.84 -1.66

  media 0 1 1
  media 2 1 2 -1
  media 3 1 3 -2
  media 1 1 4 -3
  media 1 1 5 -4
  media 0 1 6 -7 -5 -4
  media 1 1 7 -4
  media 1 1 8 -6 -4
 boundary 8

 unit 2
  com="aluminum source tube"
  cone 1 0.15 -1.66 0.3 -2.1
  zcylinder 2 1.1 -1.3 -2.1
  zcylinder 3 0.7 24.75 -1.3
  zcylinder 4 0.8 24.75 -1.3
  zcylinder 5 1.1 -0.8 -1.3
  zcylinder 6 1.1 24.75 -0.8
  zcylinder 7 1.25 24.75 -3
  zcylinder 8 1.3 24.75 -3

  media 1 1 1
  media 0 1 2 -1
  media 0 1 3
  media 1 1 4 -3
  media 1 1 5 -4
  media 0 1 6 -4
  media 1 1 7 -6 -5 -2
  media 0 1 8 -7

  hole 1
 boundary 8

 global unit 3
  com="global unit: block of Cu and detector location"
  cuboid 1 24.0 -24.0 24.75 -24.75 24.75 -24.75
  cuboid 2 -16 -23 3.5 -3.5 24.75 -24.75
  cuboid 3 105 -24 24.75 -24.75 24.75 -24.75

  media 4 1 1 -2
  media 0 1 2
  media 0 1 3 -1

```
    hole 2
  boundary 3
end geometry

read definitions
  location 1
    title="location for point detector"
    position 100 0 0
  end location

  response 1
    title="flat distribtuion from 1 to 11 MeV"
    neutron
    bounds 1.0e6 11.0e6 end
    values 1.0 1.0 end
  end response

  gridGeometry 1
    title="mesh for denovo / weight windows"
    xLinear 10 -24 24
    xlinear 8 24 105
    xPlanes -23 -16 -1.3 -1.1 -0.8 -0.7 -0.535 -0.195 0.195 0.535 0.7 0.8 1.1 1.3 end

    ylinear 10 -24.75 24.75
    yPlanes -3.5 -1.3 -1.1 -0.8 -0.7 -0.535 -0.195 0.195 0.535 0.7 0.8 1.1 1.3 3.5 end

    zlinear 10 -24.75 24.75
    zPlanes -3 -2.1 -1.66 -1.3 -1.01 -0.695 -0.3 0.3 1.275 1.59 1.84 end
  end gridGeometry

  distribution 252
    title="Cf-252 energy spectrum - CE ENDF / IRDFF-II - https://www-
nds.iaea.org/IRDFF/spectra/irdff_sp_Cf252_ln.g725 - convert units from n/eV to n and normalize"
    abscissa 9.50000E-06 1.00000E-05 1.05000E-05 1.10000E-05 1.15000E-05 1.20000E-05
1.27500E-05 1.35000E-05 1.42500E-05 1.50000E-05 1.60000E-05 1.70000E-05
        1.80000E-05 1.90000E-05 2.00000E-05 2.10000E-05 2.20000E-05 2.30000E-05 2.40000E-05
2.55000E-05 2.70000E-05 2.80000E-05 3.00000E-05 3.20000E-05
        3.40000E-05 3.60000E-05 3.80000E-05 4.00000E-05 4.25000E-05 4.50000E-05 4.75000E-05
5.00000E-05 5.25000E-05 5.50000E-05 5.75000E-05 6.00000E-05
        6.30000E-05 6.60000E-05 6.90000E-05 7.20000E-05 7.60000E-05 8.00000E-05 8.40000E-05
8.80000E-05 9.20000E-05 9.60000E-05 1.00000E-04 1.05000E-04
        1.10000E-04 1.15000E-04 1.20000E-04 1.27500E-04 1.35000E-04 1.42500E-04 1.50000E-04
1.60000E-04 1.70000E-04 1.80000E-04 1.90000E-04 2.00000E-04
        2.10000E-04 2.20000E-04 2.30000E-04 2.40000E-04 2.55000E-04 2.70000E-04 2.80000E-04
3.00000E-04 3.20000E-04 3.40000E-04 3.60000E-04 3.80000E-04
        4.00000E-04 4.25000E-04 4.50000E-04 4.75000E-04 5.00000E-04 5.25000E-04 5.50000E-04
5.75000E-04 6.00000E-04 6.30000E-04 6.60000E-04 6.90000E-04
        7.20000E-04 7.60000E-04 8.00000E-04 8.40000E-04 8.80000E-04 9.20000E-04 9.60000E-04
1.00000E-03 1.05000E-03 1.10000E-03 1.15000E-03 1.20000E-03
        1.27500E-03 1.35000E-03 1.42500E-03 1.50000E-03 1.60000E-03 1.70000E-03 1.80000E-03
1.90000E-03 2.00000E-03 2.10000E-03 2.20000E-03 2.30000E-03
        2.40000E-03 2.55000E-03 2.70000E-03 2.80000E-03 3.00000E-03 3.20000E-03 3.40000E-03
3.60000E-03 3.80000E-03 4.00000E-03 4.25000E-03 4.50000E-03
        4.75000E-03 5.00000E-03 5.25000E-03 5.50000E-03 5.75000E-03 6.00000E-03 6.30000E-03
6.60000E-03 6.90000E-03 7.20000E-03 7.60000E-03 8.00000E-03
        8.40000E-03 8.80000E-03 9.20000E-03 9.60000E-03 1.00000E-02 1.05000E-02 1.10000E-02
1.15000E-02 1.20000E-02 1.27500E-02 1.35000E-02 1.42500E-02
```

1.50000E-02 1.60000E-02 1.70000E-02 1.80000E-02 1.90000E-02 2.00000E-02 2.10000E-02 2.20000E-02 2.30000E-02 2.40000E-02 2.55000E-02 2.70000E-02

2.80000E-02 3.00000E-02 3.20000E-02 3.40000E-02 3.60000E-02 3.80000E-02 4.00000E-02 4.25000E-02 4.50000E-02 4.75000E-02 5.00000E-02 5.25000E-02

5.50000E-02 5.75000E-02 6.00000E-02 6.30000E-02 6.60000E-02 6.90000E-02 7.20000E-02 7.60000E-02 8.00000E-02 8.40000E-02 8.80000E-02 9.20000E-02

9.60000E-02 1.00000E-01 1.05000E-01 1.10000E-01 1.15000E-01 1.20000E-01 1.27500E-01 1.35000E-01 1.42500E-01 1.50000E-01 1.60000E-01 1.70000E-01

1.80000E-01 1.90000E-01 2.00000E-01 2.10000E-01 2.20000E-01 2.30000E-01 2.40000E-01 2.55000E-01 2.70000E-01 2.80000E-01 3.00000E-01 3.20000E-01

3.40000E-01 3.60000E-01 3.80000E-01 4.00000E-01 4.25000E-01 4.50000E-01 4.75000E-01 5.00000E-01 5.25000E-01 5.50000E-01 5.75000E-01 6.00000E-01

6.30000E-01 6.60000E-01 6.90000E-01 7.20000E-01 7.60000E-01 8.00000E-01 8.40000E-01 8.80000E-01 9.20000E-01 9.60000E-01 1.00000E+00 1.05000E+00

1.10000E+00 1.15000E+00 1.20000E+00 1.27500E+00 1.35000E+00 1.42500E+00 1.50000E+00 1.60000E+00 1.70000E+00 1.80000E+00 1.90000E+00 2.00000E+00

2.10000E+00 2.20000E+00 2.30000E+00 2.40000E+00 2.55000E+00 2.70000E+00 2.80000E+00 3.00000E+00 3.20000E+00 3.40000E+00 3.60000E+00 3.80000E+00

4.00000E+00 4.25000E+00 4.50000E+00 4.75000E+00 5.00000E+00 5.25000E+00 5.50000E+00 5.75000E+00 6.00000E+00 6.30000E+00 6.60000E+00 6.90000E+00

7.20000E+00 7.60000E+00 8.00000E+00 8.40000E+00 8.80000E+00 9.20000E+00 9.60000E+00 1.00000E+01 1.05000E+01 1.10000E+01 1.15000E+01 1.20000E+01

1.27500E+01 1.35000E+01 1.42500E+01 1.50000E+01 1.60000E+01 1.70000E+01 1.80000E+01 1.90000E+01 2.00000E+01 2.10000E+01 2.20000E+01 2.30000E+01

2.40000E+01 2.55000E+01 2.70000E+01 2.80000E+01 3.00000E+01 3.20000E+01 3.40000E+01 3.60000E+01 3.80000E+01 4.00000E+01 4.25000E+01 4.50000E+01

4.75000E+01 5.00000E+01 5.25000E+01 5.50000E+01 5.75000E+01 6.00000E+01 6.30000E+01 6.60000E+01 6.90000E+01 7.20000E+01 7.60000E+01 8.00000E+01

8.40000E+01 8.80000E+01 9.20000E+01 9.60000E+01 1.00000E+02 1.05000E+02 1.10000E+02 1.15000E+02 1.20000E+02 1.27500E+02 1.35000E+02 1.42500E+02

1.50000E+02 1.60000E+02 1.70000E+02 1.80000E+02 1.90000E+02 2.00000E+02 2.10000E+02 2.20000E+02 2.30000E+02 2.40000E+02 2.55000E+02 2.70000E+02

2.80000E+02 3.00000E+02 3.20000E+02 3.40000E+02 3.60000E+02 3.80000E+02 4.00000E+02 4.25000E+02 4.50000E+02 4.75000E+02 5.00000E+02 5.25000E+02

5.50000E+02 5.75000E+02 6.00000E+02 6.30000E+02 6.60000E+02 6.90000E+02 7.20000E+02 7.60000E+02 8.00000E+02 8.40000E+02 8.80000E+02 9.20000E+02

9.60000E+02 1.00000E+03 1.05000E+03 1.10000E+03 1.15000E+03 1.20000E+03 1.27500E+03 1.35000E+03 1.42500E+03 1.50000E+03 1.60000E+03 1.70000E+03

1.80000E+03 1.90000E+03 2.00000E+03 2.10000E+03 2.20000E+03 2.30000E+03 2.40000E+03 2.55000E+03 2.70000E+03 2.80000E+03 3.00000E+03 3.20000E+03

3.40000E+03 3.60000E+03 3.80000E+03 4.00000E+03 4.25000E+03 4.50000E+03 4.75000E+03 5.00000E+03 5.25000E+03 5.50000E+03 5.75000E+03 6.00000E+03

6.30000E+03 6.60000E+03 6.90000E+03 7.20000E+03 7.60000E+03 8.00000E+03 8.40000E+03 8.80000E+03 9.20000E+03 9.60000E+03 1.00000E+04 1.05000E+04

1.10000E+04 1.15000E+04 1.20000E+04 1.27500E+04 1.35000E+04 1.42500E+04 1.50000E+04 1.60000E+04 1.70000E+04 1.80000E+04 1.90000E+04 2.00000E+04

2.10000E+04 2.20000E+04 2.30000E+04 2.40000E+04 2.55000E+04 2.70000E+04 2.80000E+04 3.00000E+04 3.20000E+04 3.40000E+04 3.60000E+04 3.80000E+04

4.00000E+04 4.25000E+04 4.50000E+04 4.75000E+04 5.00000E+04 5.25000E+04 5.50000E+04 5.75000E+04 6.00000E+04 6.30000E+04 6.60000E+04 6.90000E+04

7.20000E+04 7.60000E+04 8.00000E+04 8.40000E+04 8.80000E+04 9.20000E+04 9.60000E+04 1.00000E+05 1.05000E+05 1.10000E+05 1.15000E+05 1.20000E+05

1.27500E+05 1.35000E+05 1.42500E+05 1.50000E+05 1.60000E+05 1.70000E+05 1.80000E+05 1.90000E+05 2.00000E+05 2.10000E+05 2.20000E+05 2.30000E+05

2.40000E+05 2.55000E+05 2.70000E+05 2.80000E+05 3.00000E+05 3.20000E+05 3.40000E+05 3.60000E+05 3.80000E+05 4.00000E+05 4.25000E+05 4.50000E+05

       4.75000E+05 5.00000E+05 5.25000E+05 5.50000E+05 5.75000E+05 6.00000E+05
6.30000E+05 6.60000E+05 6.90000E+05 7.20000E+05 7.60000E+05 8.00000E+05
       8.40000E+05 8.80000E+05 9.20000E+05 9.60000E+05 1.00000E+06 1.10000E+06
1.20000E+06 1.30000E+06 1.40000E+06 1.50000E+06 1.60000E+06 1.70000E+06
       1.80000E+06 1.90000E+06 2.00000E+06 2.10000E+06 2.20000E+06 2.30000E+06
2.40000E+06 2.50000E+06 2.60000E+06 2.70000E+06 2.80000E+06 2.90000E+06
       3.00000E+06 3.10000E+06 3.20000E+06 3.30000E+06 3.40000E+06 3.50000E+06
3.60000E+06 3.70000E+06 3.80000E+06 3.90000E+06 4.00000E+06 4.10000E+06
       4.20000E+06 4.30000E+06 4.40000E+06 4.50000E+06 4.60000E+06 4.70000E+06
4.80000E+06 4.90000E+06 5.00000E+06 5.10000E+06 5.20000E+06 5.30000E+06
       5.40000E+06 5.50000E+06 5.60000E+06 5.70000E+06 5.80000E+06 5.90000E+06
6.00000E+06 6.10000E+06 6.20000E+06 6.30000E+06 6.40000E+06 6.50000E+06
       6.60000E+06 6.70000E+06 6.80000E+06 6.90000E+06 7.00000E+06 7.10000E+06
7.20000E+06 7.30000E+06 7.40000E+06 7.50000E+06 7.60000E+06 7.70000E+06
       7.80000E+06 7.90000E+06 8.00000E+06 8.10000E+06 8.20000E+06 8.30000E+06
8.40000E+06 8.50000E+06 8.60000E+06 8.70000E+06 8.80000E+06 8.90000E+06
       9.00000E+06 9.10000E+06 9.20000E+06 9.30000E+06 9.40000E+06 9.50000E+06
9.60000E+06 9.70000E+06 9.80000E+06 9.90000E+06 1.00000E+07 1.01000E+07
       1.02000E+07 1.03000E+07 1.04000E+07 1.05000E+07 1.06000E+07 1.07000E+07
1.08000E+07 1.09000E+07 1.10000E+07 1.11000E+07 1.12000E+07 1.13000E+07
       1.14000E+07 1.15000E+07 1.16000E+07 1.17000E+07 1.18000E+07 1.19000E+07
1.20000E+07 1.21000E+07 1.22000E+07 1.23000E+07 1.24000E+07 1.25000E+07
       1.26000E+07 1.27000E+07 1.28000E+07 1.29000E+07 1.30000E+07 1.31000E+07
1.32000E+07 1.33000E+07 1.34000E+07 1.35000E+07 1.36000E+07 1.37000E+07
       1.38000E+07 1.39000E+07 1.40000E+07 1.41000E+07 1.42000E+07 1.43000E+07
1.44000E+07 1.45000E+07 1.46000E+07 1.47000E+07 1.48000E+07 1.49000E+07
       1.50000E+07 1.51000E+07 1.52000E+07 1.53000E+07 1.54000E+07 1.55000E+07
1.56000E+07 1.57000E+07 1.58000E+07 1.59000E+07 1.60000E+07 1.61000E+07
       1.62000E+07 1.63000E+07 1.64000E+07 1.65000E+07 1.66000E+07 1.67000E+07
1.68000E+07 1.69000E+07 1.70000E+07 1.71000E+07 1.72000E+07 1.73000E+07
       1.74000E+07 1.75000E+07 1.76000E+07 1.77000E+07 1.78000E+07 1.79000E+07
1.80000E+07 1.81000E+07 1.82000E+07 1.83000E+07 1.84000E+07 1.85000E+07
       1.86000E+07 1.87000E+07 1.88000E+07 1.89000E+07 1.90000E+07 1.91000E+07
1.92000E+07 1.93000E+07 1.94000E+07 1.95000E+07 1.96000E+07 1.97000E+07
       1.98000E+07 1.99000E+07 2.00000E+07 2.05000E+07 2.10000E+07 2.15000E+07
2.20000E+07 2.25000E+07 2.30000E+07 2.35000E+07 2.40000E+07 2.45000E+07
       2.50000E+07 2.55000E+07 2.60000E+07 2.65000E+07 2.70000E+07 2.75000E+07
2.80000E+07 2.85000E+07 2.90000E+07 2.95000E+07 end
   truePDF 1.02910E-18 1.05390E-18 1.07815E-18 1.10185E-18 1.13075E-18 1.74675E-18
1.79595E-18 1.84388E-18 1.89818E-18 2.61130E-18 2.68920E-18 2.76500E-18
       2.83870E-18 2.91060E-18 2.98080E-18 3.04930E-18 3.11640E-18 3.19810E-18 4.94040E-18
5.05680E-18 3.46180E-18 7.15840E-18 7.38580E-18 7.60640E-18
       7.82080E-18 8.02940E-18 8.25780E-18 1.06305E-17 1.09300E-17 1.12218E-17 1.15060E-17
1.17833E-17 1.20543E-17 1.23195E-17 1.26045E-17 1.54902E-17
       1.58463E-17 1.61949E-17 1.65921E-17 2.27132E-17 2.32884E-17 2.38500E-17 2.43988E-17
2.49352E-17 2.54608E-17 2.60388E-17 3.33330E-17 3.40990E-17
       3.48485E-17 3.57630E-17 5.52458E-17 5.68027E-17 5.83177E-17 6.00352E-17 8.25890E-17
8.50550E-17 8.74510E-17 8.97830E-17 9.20570E-17 9.42770E-17
       9.64450E-17 9.85660E-17 1.01150E-16 1.56255E-16 1.59945E-16 1.09490E-16 2.26420E-16
2.33620E-16 2.40600E-16 2.47380E-16 2.53980E-16 2.61200E-16
       3.36250E-16 3.45725E-16 3.54975E-16 3.63950E-16 3.72725E-16 3.81275E-16 3.89650E-16
3.98675E-16 4.89930E-16 5.01180E-16 5.12190E-16 5.24730E-16
       7.18280E-16 7.36440E-16 7.54160E-16 7.71480E-16 7.88440E-16 8.05000E-16 8.23280E-16
1.05390E-15 1.07815E-15 1.10185E-15 1.13075E-15 1.74675E-15
       1.79595E-15 1.84388E-15 1.89818E-15 2.61130E-15 2.68920E-15 2.76500E-15 2.83870E-15
2.91060E-15 2.98080E-15 3.04930E-15 3.11640E-15 3.19810E-15

4.94040E-15 5.05680E-15 3.46180E-15 7.15840E-15 7.38580E-15 7.60640E-15 7.82080E-15 8.02940E-15 8.25780E-15 1.06305E-14 1.09300E-14 1.12218E-14

1.15060E-14 1.17833E-14 1.20543E-14 1.23195E-14 1.26045E-14 1.54902E-14 1.58463E-14 1.61949E-14 1.65921E-14 2.27132E-14 2.32884E-14 2.38500E-14

2.43988E-14 2.49352E-14 2.54608E-14 2.60388E-14 3.33330E-14 3.40990E-14 3.48485E-14 3.57630E-14 5.52457E-14 5.68028E-14 5.83178E-14 6.00352E-14

8.25890E-14 8.50550E-14 8.74510E-14 8.97830E-14 9.20570E-14 9.42770E-14 9.64450E-14 9.85660E-14 1.01150E-13 1.56255E-13 1.59945E-13 1.09490E-13

2.26420E-13 2.33620E-13 2.40600E-13 2.47380E-13 2.53980E-13 2.61200E-13 3.36250E-13 3.45725E-13 3.54975E-13 3.63950E-13 3.72725E-13 3.81275E-13

3.89650E-13 3.98675E-13 4.89930E-13 5.01180E-13 5.12190E-13 5.24730E-13 7.18280E-13 7.36440E-13 7.54160E-13 7.71480E-13 7.88440E-13 8.05000E-13

8.23280E-13 1.05390E-12 1.07815E-12 1.10185E-12 1.13075E-12 1.74675E-12 1.79595E-12 1.84387E-12 1.89818E-12 2.61130E-12 2.68920E-12 2.76500E-12

2.83870E-12 2.91060E-12 2.98080E-12 3.04930E-12 3.11640E-12 3.19810E-12 4.94040E-12 5.05680E-12 3.46180E-12 7.15840E-12 7.38580E-12 7.60640E-12

7.82080E-12 8.02940E-12 8.25780E-12 1.06305E-11 1.09300E-11 1.12218E-11 1.15060E-11 1.17833E-11 1.20543E-11 1.23195E-11 1.26045E-11 1.54902E-11

1.58463E-11 1.61949E-11 1.65921E-11 2.27132E-11 2.32884E-11 2.38500E-11 2.43988E-11 2.49352E-11 2.54608E-11 2.60388E-11 3.33330E-11 3.40990E-11

3.48485E-11 3.57630E-11 5.52458E-11 5.68028E-11 5.83178E-11 6.00353E-11 8.25890E-11 8.50550E-11 8.74510E-11 8.97830E-11 9.20570E-11 9.42770E-11

9.64450E-11 9.85660E-11 1.01152E-10 1.56260E-10 1.59942E-10 1.09494E-10 2.26418E-10 2.33612E-10 2.40592E-10 2.47374E-10 2.53976E-10 2.61200E-10

3.36255E-10 3.45738E-10 3.54965E-10 3.63953E-10 3.72718E-10 3.81283E-10 3.89658E-10 3.98665E-10 4.89918E-10 5.01174E-10 5.12181E-10 5.24724E-10

7.18276E-10 7.36448E-10 7.54180E-10 7.71496E-10 7.88436E-10 8.05020E-10 8.23276E-10 1.05390E-09 1.07813E-09 1.10183E-09 1.13073E-09 1.74674E-09

1.79596E-09 1.84385E-09 1.89818E-09 2.61127E-09 2.68924E-09 2.76500E-09 2.83875E-09 2.91064E-09 2.98080E-09 3.04934E-09 3.11638E-09 3.19813E-09

4.94045E-09 5.05682E-09 3.46182E-09 7.15848E-09 7.38586E-09 7.60644E-09 7.82080E-09 8.02944E-09 8.25776E-09 1.06305E-08 1.09301E-08 1.12217E-08

1.15059E-08 1.17832E-08 1.20541E-08 1.23191E-08 1.26040E-08 1.54894E-08 1.58456E-08 1.61939E-08 1.65908E-08 2.27111E-08 2.32862E-08 2.38475E-08

2.43957E-08 2.49320E-08 2.54570E-08 2.60347E-08 3.33278E-08 3.40941E-08 3.48436E-08 3.57576E-08 5.52381E-08 5.67947E-08 5.83096E-08 6.00277E-08

8.25788E-08 8.50446E-08 8.74408E-08 8.97734E-08 9.20463E-08 9.42636E-08 9.64298E-08 9.85483E-08 1.01132E-07 1.56224E-07 1.59902E-07 1.09463E-07

2.26346E-07 2.33528E-07 2.40494E-07 2.47266E-07 2.53854E-07 2.61064E-07 3.36063E-07 3.45523E-07 3.54728E-07 3.63700E-07 3.72465E-07 3.81028E-07

3.89403E-07 3.98405E-07 4.89606E-07 5.00862E-07 5.11869E-07 5.24412E-07 7.17860E-07 7.36032E-07 7.53764E-07 7.71084E-07 7.88032E-07 8.04616E-07

8.22852E-07 1.05331E-06 1.07748E-06 1.10112E-06 1.12993E-06 1.74539E-06 1.79444E-06 1.84218E-06 1.89631E-06 2.60846E-06 2.68610E-06 2.76152E-06

2.83492E-06 2.90648E-06 2.97633E-06 3.04456E-06 3.11127E-06 3.19260E-06 4.93139E-06 5.04710E-06 3.45479E-06 7.14292E-06 7.36876E-06 7.58776E-06

7.80048E-06 8.00744E-06 8.23382E-06 1.05978E-05 1.08945E-05 1.11832E-05 1.14644E-05 1.17388E-05 1.20067E-05 1.22686E-05 1.25500E-05 1.54199E-05

1.57713E-05 1.61148E-05 1.65059E-05 2.25888E-05 2.31547E-05 2.37064E-05 2.42450E-05 2.47713E-05 2.52861E-05 2.58520E-05 3.30822E-05 3.38309E-05

3.45623E-05 3.54532E-05 5.47388E-05 5.62512E-05 5.77211E-05 5.93849E-05 8.16369E-05 8.40153E-05 8.63216E-05 8.85616E-05 9.07400E-05 9.28614E-05

9.49294E-05 9.69476E-05 9.94020E-05 1.53380E-04 1.56840E-04 1.07245E-04 2.21468E-04 2.28242E-04 2.34784E-04 2.41072E-04 2.47160E-04 2.53790E-04

3.26145E-04 3.34773E-04 3.43140E-04 3.51255E-04 3.59135E-04 3.66790E-04 3.74238E-04 3.82200E-04 4.68771E-04 4.78605E-04 4.88151E-04 4.98915E-04

    6.81088E-04 6.96416E-04 7.11264E-04 7.25716E-04 7.39728E-04 7.53328E-04 7.68120E-04
9.79990E-04 9.99150E-04 1.01768E-03 1.03998E-03 1.59845E-03
    1.63520E-03 1.67033E-03 1.70939E-03 2.33579E-03 2.38943E-03 2.44032E-03 2.48864E-03
2.53461E-03 2.57836E-03 2.62004E-03 2.65976E-03 2.70674E-03
    4.13948E-03 4.20161E-03 2.84746E-03 5.80972E-03 5.91462E-03 6.01034E-03 6.09764E-03
6.17712E-03 6.25776E-03 7.92218E-03 8.01000E-03 8.08563E-03
    8.15238E-03 8.21118E-03 8.26143E-03 8.30378E-03 8.34130E-03 1.00471E-02 1.00739E-02
1.00908E-02 1.00987E-02 1.34591E-02 1.34356E-02 1.33962E-02
    1.33428E-02 1.32765E-02 1.31985E-02 1.30354E-02 3.19009E-02 3.10938E-02 3.01946E-02
2.92407E-02 2.82343E-02 2.71912E-02 2.61384E-02 2.50852E-02
    2.40392E-02 2.29981E-02 2.19680E-02 2.09613E-02 1.99809E-02 1.90267E-02 1.81007E-02
1.72064E-02 1.63404E-02 1.55035E-02 1.47004E-02 1.39271E-02
    1.31839E-02 1.24740E-02 1.17917E-02 1.11368E-02 1.05139E-02 9.92197E-03 9.35717E-03
8.81876E-03 8.30735E-03 7.82195E-03 7.36181E-03 6.92590E-03
    6.51379E-03 6.12438E-03 5.75648E-03 5.40906E-03 5.08167E-03 4.77324E-03 4.48280E-03
4.20937E-03 3.95159E-03 3.70866E-03 3.48039E-03 3.26595E-03
    3.06383E-03 2.87338E-03 2.69452E-03 2.52657E-03 2.36865E-03 2.22019E-03 2.08074E-03
1.94979E-03 1.82653E-03 1.71057E-03 1.60182E-03 1.49985E-03
    1.40433E-03 1.31486E-03 1.23079E-03 1.15182E-03 1.07787E-03 1.00865E-03 9.43804E-04
8.83074E-04 8.26214E-04 7.72982E-04 7.23128E-04 6.76444E-04
    6.32808E-04 5.92022E-04 5.53869E-04 5.18181E-04 4.84763E-04 4.53474E-04 4.24225E-04
3.96885E-04 3.71326E-04 3.47435E-04 3.25038E-04 3.04045E-04
    2.84421E-04 2.66078E-04 2.48922E-04 2.32878E-04 2.17838E-04 2.03743E-04 1.90552E-04
1.78206E-04 1.66634E-04 1.55787E-04 1.45665E-04 1.36219E-04
    1.27365E-04 1.19068E-04 1.11341E-04 1.04143E-04 9.73890E-05 9.10510E-05 8.51350E-05
7.96120E-05 7.44420E-05 6.96040E-05 6.50810E-05 6.08520E-05
    5.68950E-05 5.31910E-05 4.97280E-05 4.64890E-05 4.34590E-05 4.06250E-05 3.79720E-05
3.54880E-05 3.31660E-05 3.09970E-05 2.89700E-05 2.70760E-05
    2.53000E-05 2.36350E-05 2.20820E-05 2.06330E-05 1.92730E-05 1.80010E-05 1.68160E-05
1.57040E-05 1.46630E-05 1.36930E-05 1.27880E-05 1.19440E-05
    1.11560E-05 1.04210E-05 9.73070E-06 9.08430E-06 8.48250E-06 7.92050E-06 7.39570E-06
6.90570E-06 6.44820E-06 6.02080E-06 5.62170E-06 5.24880E-06
    4.90060E-06 4.57540E-06 4.27180E-06 3.98850E-06 3.72390E-06 3.47680E-06 3.24600E-06
3.03040E-06 2.82910E-06 2.64120E-06 2.46560E-06 2.30170E-06
    2.14860E-06 2.00560E-06 1.87210E-06 1.74750E-06 1.63120E-06 1.52270E-06 1.42130E-06
1.32670E-06 1.23830E-06 1.15580E-06 1.07880E-06 1.00680E-06
    9.39610E-07 8.76860E-07 8.18290E-07 7.63610E-07 7.12580E-07 6.64940E-07 6.20430E-07
5.78840E-07 5.40030E-07 5.03810E-07 4.70020E-07 4.38480E-07
    4.09050E-07 3.81580E-07 3.55950E-07 3.32030E-07 3.09720E-07 2.88900E-07 2.69470E-07
2.51350E-07 2.34440E-07 2.18670E-07 2.03950E-07 1.90220E-07
    1.77410E-07 1.44820E-07 5.12300E-07 3.62355E-07 2.56210E-07 1.81100E-07 1.27975E-07
9.04050E-08 6.38500E-08 4.50815E-08 3.18225E-08 2.24575E-08
    1.58450E-08 1.11765E-08 7.88200E-09 5.55750E-09 3.91750E-09 2.76095E-09 1.94545E-09
1.37055E-09 9.65350E-10 end
  end distribution

  energyBounds 1
    title="energy bins for neutron flux tally"
    linear 100 1e6 11e6
  end energyBounds
end definitions

read sources
  src 252
    title="Cf-252 in holder/cylinder, but only above 1.0 MeV"
    neutron
    strength=1.0

```
    zcylinder 0.195 0.3 -0.3
    eDistributionID=252
  end src
end sources

read tallies
  pointDetector 1
    title="neutron flux point detector tally, 100 cm from source, 100 keV bins"
    locationID=1
    neutron
    responseID=1
    energyBoundsID=1
  end pointDetector
end tallies

read parameters
  perBatch=1000000 batches=20
  neutron noPhoton
  fissionMult=0 secondaryMult=0
  nMinEnergy=0.98e6
  nMaxEnergy=30.0e6
  ceLibrary="ce_v7.1_endf.xml"
end parameters

read importanceMap
  gridGeometryID=1

  adjointSource 1
    locationID=1
    responseID=1
  end adjointSource

  macromaterial
    mmPointTest
  end macromaterial

  subCells=7
  fluxWeighting
  firstCollision
  windowRatio=3.0
  quadType=2
  legendre=5
  tportCorrection=1
  polarsPerOct=6
  azimuthsPerOct=6
  diagnostics=1
  output=1
  tolerance=1.0e-4
end importanceMap

end data
end
```

APPENDIX B. STILBENE DETECTOR DATA EVALUATION

Neutron spectrometry systems with stilbene detector have been developed, tested and used in many laboratories around the world. In RCR and collaborating institutions [a][b], neutron spectrometry in mixed gamma and neutron fields with energies above 0.5 MeV has been studied and developed. Digital systems with stilbene have been used for the measurement in mixed gamma and neutron fields. This spectrometer uses the instrumental separation of neutron and photon impulses according to their energy, with their separation using a two-parameter measuring system.

A so-called *deconvolution* or *unfolding* problem applies to the intention of determining the total neutron flux in a volume, when it contains no nuclides, from the measured recoil proton flux obtained from reactions of the neutrons with nuclides inserted in that volume.

Using mathematics, it can be formulated as follows: Let $g(x)$ and $A(x,y)$ be continuous functions. A function $f(y)$ is to be found such that

$$g(x) = \int_{(I)} A(x,y) f(y) dy \qquad (B.1)$$

The above equation models the process of a continuous energy measurement. It is a Fredholm integral equation of the first kind where:

- $A(x,y)$ is the *convolution kernel*, a characteristic of the measuring device, often called the *response function*,
- $g(x)$ is the experimental data,
- $f(y)$ is the result to be found, and
- (I) is the energy range.

When applied to spectrometry, the following issues arise:

- In general, there is no analytic solution to the equation (B.1).
- The response function $A(x,y)$ of the measuring device has to be determined. It can be done by combination of stochastic (or deterministic) computation with an experiment. The uncertainties associated with function A are usually very hard to find.

The neutron and proton fluxes are obtained from sources that do not emit continuous energy particles. The individual particles react with nuclides that they encounter in physics processes that are not in continuous energy form. The mathematic Eq. (B.1) is not a real representation of the relationship between the neutron and proton fluxes.

A discrete form of Eq (B.1) represents the real observations:

$$\boldsymbol{g} = \boldsymbol{A}\,\boldsymbol{f} \qquad (B.2)$$

where $\boldsymbol{g} = (g_1,...,g_m)^T$, $\boldsymbol{A}$ is an $m \times n$ matrix, and $\boldsymbol{f} = (f_1,...,f_m)^T$ (^{T} means transposition). We examine the case $m=n$, since it is relevant for stilbene and NE-213 detectors etc. In this case, $m \approx 10^3$.

The interpretation of $\boldsymbol{f}$, $\boldsymbol{g}$, and $\boldsymbol{A}$ is the following:

- g_m is the measured proton (resp. electron) response, i.e. experimental data in proton energy group m. (Neutrons are detected by means of protons and photons by means of electrons.)

---

[a] Z. Matěj, J. Cvachovec, F. Cvachovec, and V. Přenosil, Digitized Two-Parameter Spectrometer for Neutron-Gamma Mixed Field, Advances in Military Technology, Vol. 1, No. 2, 2007.
[b] B. Jánský, Z. Turzík, E. Novák, M. Karáč, F. Cvachovec, Neutron and gamma spektrometry in mixed neutron and gamma fields, UJV 11947-R,D, 2003 (in Czech).

- A_{mn} is the detector response matrix element for proton energy group m and neutron energy group n. It is determined by a Monte Carlo method and measurement of mono-energetic sources of neutrons and photons.
- f_n is the resulting neutron (resp. gamma) flux to be found for neutron energy group n.
- The unit of f_n is [$m^{-2}s^{-1}$].

The linear system Eq. (B.2) cannot be solved by usual procedures since the matrix A is usually ill-conditioned. The determinant of our matrix response function for a cylindrical detector ⌀ 20 mm × 20 mm is $|A| = 3 \cdot 10^{-133}$. The resulting neutron (resp. gamma) spectrum has to satisfy a few conditions originating from its physical properties; above all, non-negativity is required: $f_i \geq 0$, $1 \leq i \leq n$.

The neutron flux and uncertainties are evaluated using maximum likelihood estimation[a]. The maximum likelihood estimation is a standard statistical tool for point estimations. For the maximizing of the likelihood function, a general iterative algorithm called *Expectation Maximization*, originally developed for image reconstruction in astronomy, medicine etc., is used.

The code NEU-7 evaluates data measured by cylindrical stilbene detector sized ⌀ 10 mm × 10 mm, in the energy range 0.1-15 MeV.

Model Description

The measuring device provides proton recoil values in finite channels, representing energy bins. These are adapted to the purpose of the user to obtain (usually equidistant) energy intervals (groups).

Experiments show that if the energetic intervals are narrow enough then the number of particles with energy falling into an interval has a Poisson distribution. Therefore, it is natural to model the proton (and neutron) flux with a random vector with Poisson distributed components. We can further assume that the components are mutually independent.

Stilbene response function

The response function A_{mn} is possible to obtain by measurement, but this procedure requires a series of mono-energy neutron sources, which are not easily available. Mostly the response function is calculated with a stochastic Monte Carlo method. The calculations are verified by available neutron fields, either mono energy or standard leakage spectra from D_2O, H_2O or stainless steel spheres with neutron source in their center.

The calculation includes neutron elastic scattering on hydrogen, neutron elastic scattering on carbon, neutron non-elastic scattering on carbon, $^{12}_6C(n, 3\alpha + n')$, proton leakage from detector, multiple interactions, neutrons impacting parallel to the axis of the cylindrical detector. Used nuclear data are from available libraries.

The calculated response function g_m was offset by a Gaussian function whose half-width was selected in accordance with the energy resolution function $\eta(E)$ obtained from the measurement of gamma lines, reactions (d, D) and (d, T).

The neutron response matrices for the respective detectors were computed by a Monte Carlo method (code NEU-7). For several neutron energies (1.2 MeV, 2.5 MeV, 5 MeV, 14.6 MeV, and 19.8 MeV) they were experimentally verified in PTB Braunschweig. The calculation includes the possibility of neutrons impacting at any angle to the axis of the detector, the selection of the detector size, and the influence of the anisotropy of the light yield of stilbene crystal.

---

[a] J. Cvachovec, F. Cvachovec, Maximum Likelihood Estimation of a Neutron Spectrum and Associated Uncertainties, Advances in Military Technology, Vol.1, No. 2 January 2007, pp. 5 – 28

Verification of stilbene response function

The measured neutron flux is obtained from observation of the time-integrated flux during a specific period. The flux is obtained directly through division by this period, measured in units of seconds.

The most reliable confirmation of the accuracy of the response function is the comparison of the calculated flux with experiments performed on mono-energetic neutron sources. The measurements were carried out with neutron energies 1.2 MeV, 2.5 MeV, 5 MeV, 14.6 MeV, and 19.0 MeV at PTB Braunschweig, where also the function of light yield from literature[a] was tested and specified. The detector response was measured for dimensions of stilbene crystal 10 mm × 10 mm, 20 mm × 20 mm, and 45 mm × 45 mm and under neutron impact angles relative to the axis of the detector 0º, 30º, 60º, 90º.

Within the experiment the following goals were watched:

- Comparing the response to the mono-energetic source with the calculation, the credibility of the modeling algorithm can be concluded. Within reasonable limits, it can be interpolated and extrapolated into energy areas where there is no possibility of experimental verification on a mono-energetic source.
- Obtain data used for correction function of the light yield.
- To obtain data for light yield anisotropy.
- Refinement of function of energy resolution.

The sources of mono-energy neutrons in PTB are very precisely monitored, which creates the possibility to control the detection efficiency calculated based on the response function

$$\varepsilon(E_n, E_{threshold}) = \int_{E_{treshold}}^{E_{max}} K(E_p, E_n)dE_p$$

Verification and response function tests of stilbene spectrometer have been carried out using neutron flux measurements around ^{252}Cf neutron source and a neutron flux in an LVR-15 reactor vertical beam (RCR) after Si filter as well as measurement of AmBe leakage flux.

Agreement between experimental and calculated neutron fluxes in the interval 1 MeV to 12 MeV is satisfactory with (C/E-1) less than 4 %.

Propagation of uncertainties

The uncertainties of the computed neutron flux should, above all, include uncertainties from the measured proton response and uncertainty caused by energy calibration.

Uncertainties originating from the measured proton response

- Uncertainties resulting from the stochastic nature of the measurement.
- Uncertainties resulting from operation of the measuring device.
- In case of sources with variable emission, the uncertainties resulting from output monitoring have to be included.

Uncertainties caused by energy calibration

- Possible uncertainties inserted by unfolding. (It does not have to be deterministic.)
- Uncertainties of the response matrix originating from the data and computational model used.
- Uncertainties of the prior information about the neutron spectrum (in few-channel spectrometry, it is not the case of stilbene spectrometry).

---

[a] V. I. Kuchtevic,V.I., O. A. Trykov,, L. A. Trykov,.: ODNOKRYSTALLNYJ SCINTILLJACIONNYJ SPEKTROMETR, Moskva, Atomizdat,1973.

In general, uncertainties can be evaluated in two ways:

1. Standard usage of the error propagation law. This procedure requires an unambiguous, analytically expressed, and roughly linear relation between the proton and neutron fluxes. The advantages include low computational complexity and possibility to evaluate the contributions of each source of uncertainty. The main disadvantage consists in limited applicability for iterative unfolding methods. If the relationship between the proton and neutron fluxes does not satisfy one of the above conditions, it is sometimes possible to simulate it with an appropriate function satisfying all of them.
2. Monte Carlo method. In this case, we generate random modifications of input data such that the modifications represent possible variations of the input data in the range of their uncertainties.

For each generated sample the corresponding result is computed. The final uncertainties (variance, confidence intervals etc.) are estimated using all of these results.

This procedure enables the evaluation of type A uncertainties regardless of the unfolding method used; when the number of generated samples is sufficiently high, the computed uncertainties are very truthful. However, the computing complexity is often high and there is no possibility to evaluate the contributions of each source of uncertainty.

Validation of methodology in well-defined fields

Validation in VR-1 reactor

The set of measurements was realized in the Czech Technical University in Prague zero power reactor VR-1 radial channel beam[a] (see Figure B.1). A satisfactory agreement was reached (Figure B.2). As $^{235}U(n_{th}, fiss)$ is a secondary neutron standard, and it was independently validated that the flux in VR-1 between 6 MeV and 11 MeV is indistinguishable from ^{235}U PFNS[bc], this can be understood as validation in the region 6 MeV to 11 MeV.

In the next experiment, the stability of the measurements was demonstrated. The flux in the same geometrical position was measured again after 18 months. The results show that the difference between both measurements is in most cases below the related uncertainty (Figure B.3).
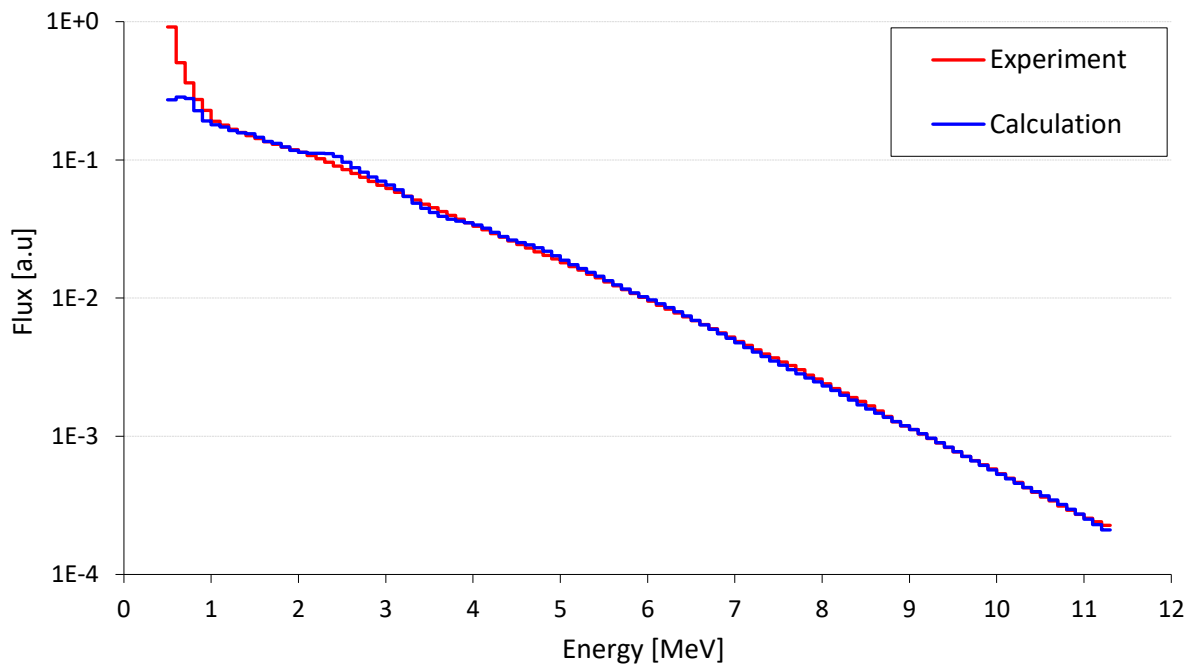
Figure B.1 Comparison of calculated and measured neutron fluxes in radial channel of VR-1 reactor.

[a]M. Košťál, E. Losa, Z. Matěj et al., Characterization of mixed N/G beam of the VR-1 reactor, Annals of Nuclear Energy, 122, (2018), pp. 69–78

[b] M. Kostal, Z. Matej, E. Losa, On similarity of various reactor spectra and 235U prompt fission neutron spectrum, Appl. Rad. and Isot., Vol. 135 (2018), pp. 83–91

[c] M. Košťál, E. Losa, M. Schulc et al., Validation of IRDFF-II library in VR-1 reactor field using thin targets, Annals of Nuclear Energy, 158, (2021), p. 108268
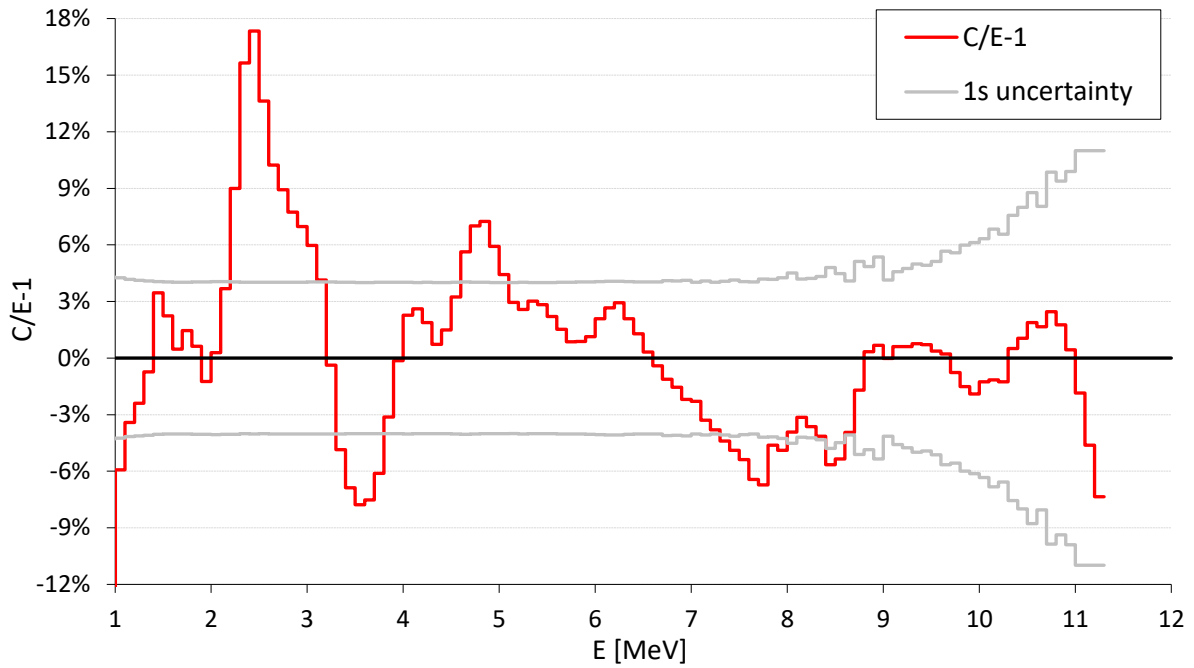
Figure B.2 C/E-1 of calculated and measured neutron fluxes in radial channel of VR-1 reactor.
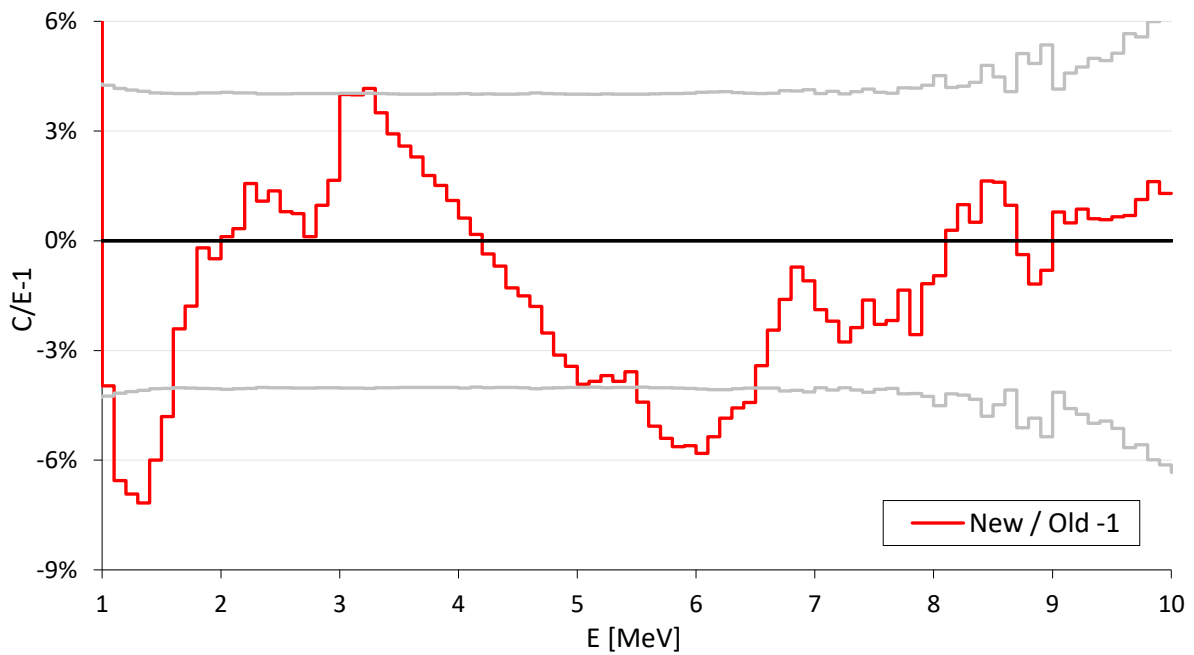
Figure B.3 Stability of measurement – neutron fluxes in same geometrical arrangement measured in 2017 and 2018.

The above presented agreement between results of independent measurements of the neutron flux in the same VR-1 radial channel (see Figure B.3) demonstrates repeatability of the measurements. The verification of evaluation using indirect calibration and deconvolution is realized in the peak flux (see Figure B4).

Validation in Si filtered spectra

The only neutron standard is defined as ^{252}Cf(s.f.), while the secondary standard is ^{235}U(n$_{th}$,fiss). Both of them are fission spectra which used in validation cannot reveal specific problems in the deconvolution matrix of the detection system. This is general issue which may stay hidden in smooth fission spectra based neutron fields.

For validation of the methodology, a measurement in the neutron field formed by the transmission of fission neutrons through a 1 m thick Si block in the radial channel in LVR-15 reactor was carried out. The results are listed in Figure B4. The results show a high level of agreement between the experimental data and simulation, thus proving the accuracy of the used deconvolution matrix.
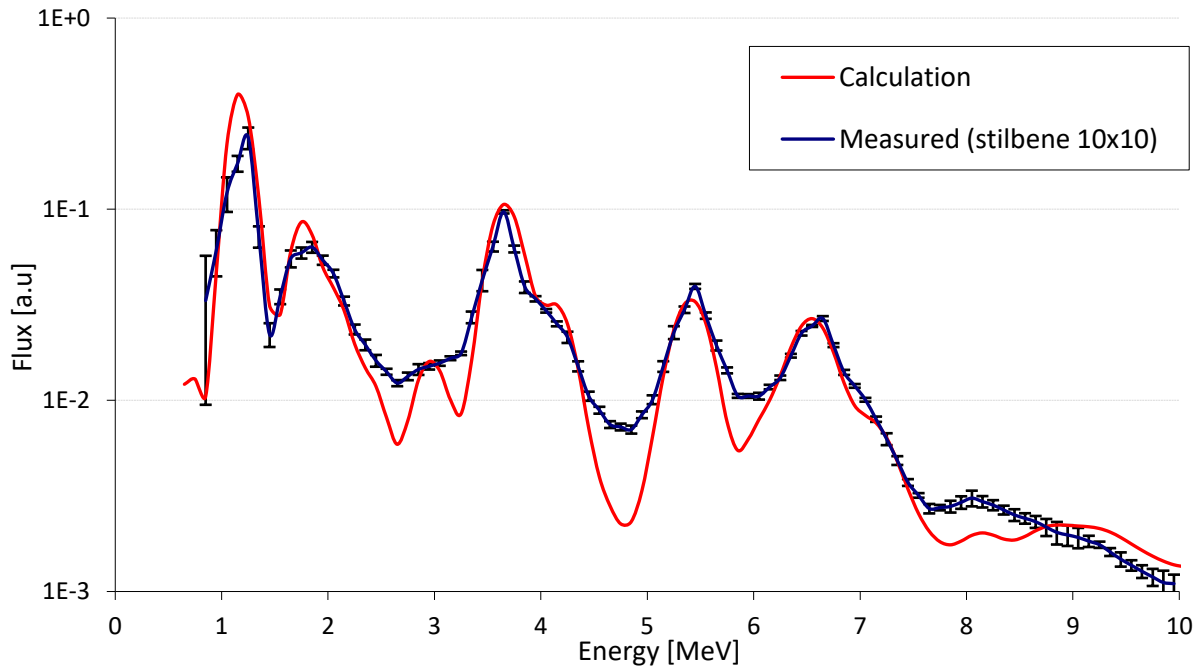
Figure B.4 Comparison of calculated and measured Si filtered fluxes.

Validation in AmBe spectrum

The validation using AmBe, a radioisotope neutron source[a], has been carried out to cover another known neutron field. The AmBe neutron spectrum is not standard because the energy distribution of neutrons formed in the nuclear reaction on Be, namely ^{9}Be+^{4}He -> ^{12}C* + n, is driven by the energy of the interacting alpha particle. The alpha particles have very low penetrating properties and can be strongly attenuated even by air. Thus, the energy distribution of leaking neutrons highly depends on the distance between the place of the creation of the alpha and the Be atom – which is highly affected by the grain size of both Be and AmO$_2$ and its porosity. However, the reached agreement with tabulated data allows to conclude that the methodology gives reliable results.

---

[a] M. Kostal, M. Schulc, E. Novak, T. Czakoj, Z. Matej, F. Cvachovec, F. Mravec, B. Jansky and L. Leal, Validation of heavy water cross section using AmBe neutron source, EPJ Web Conf., 239 (2020) 18008
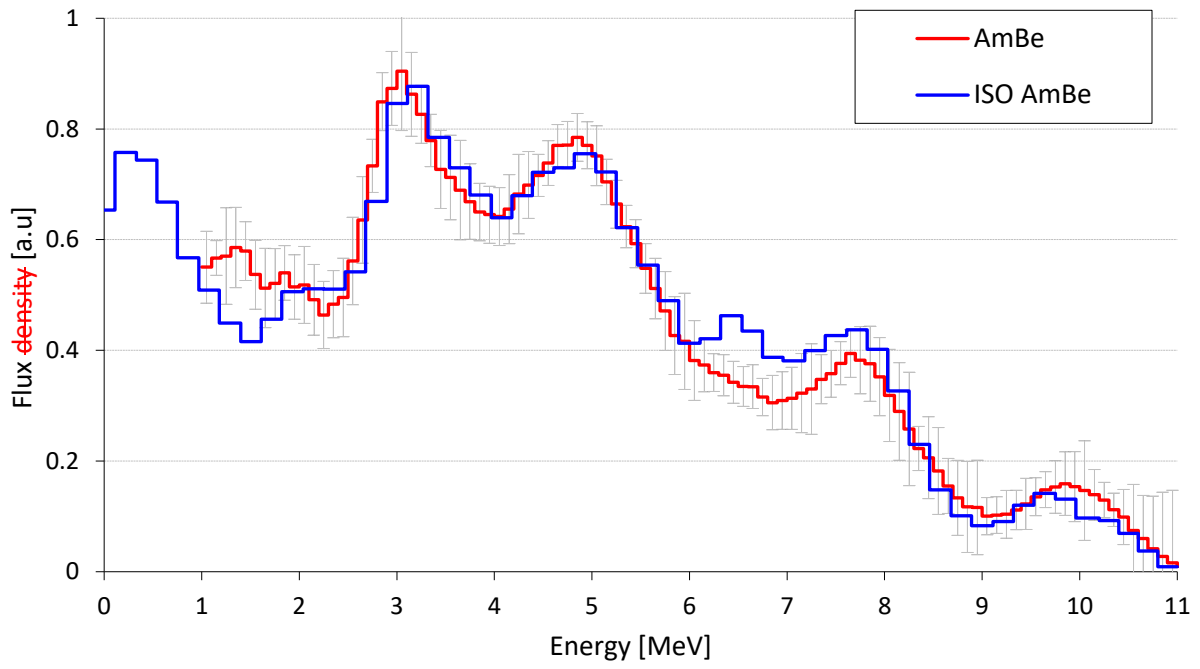
Figure B.5: Measured spectrum compared with tabulated values

APPENDIX C. ILLUSTRATION PHOTOS

Figure C.1 Detail of the block hanging on the crane.

Figure C.2 Details block on the support table
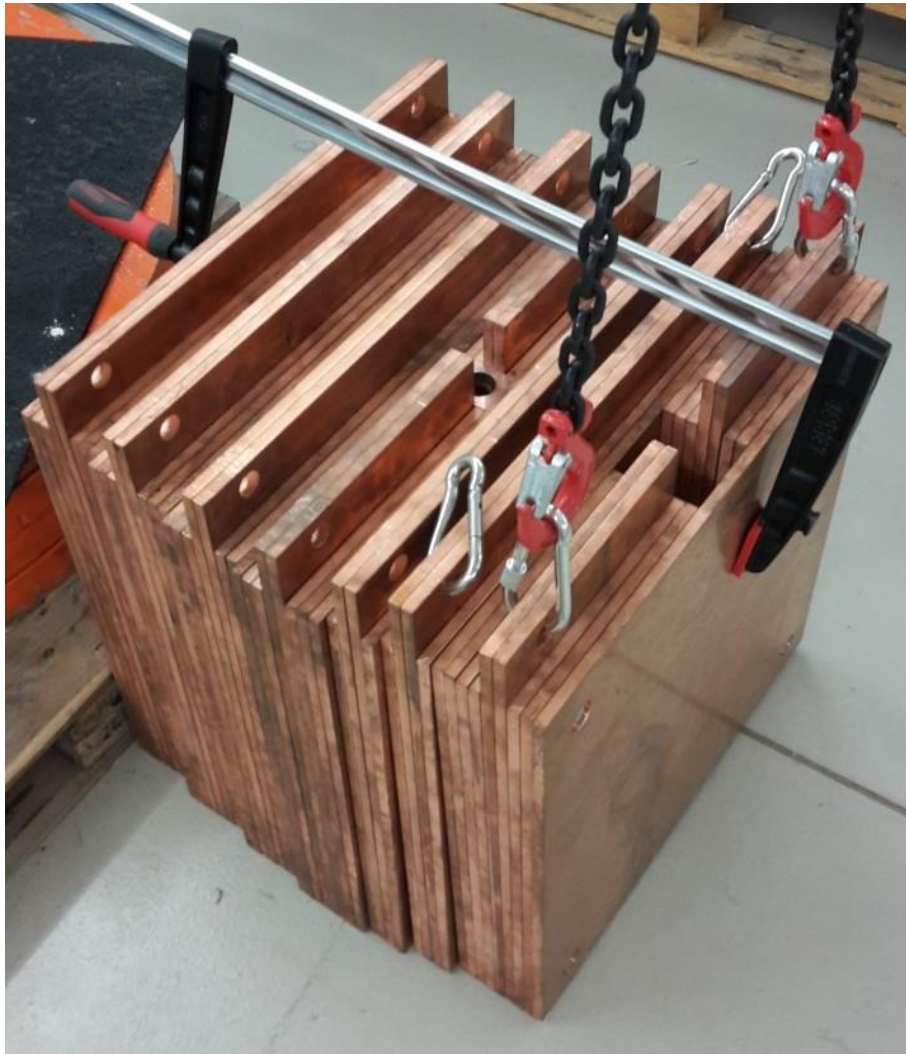
Figure C.3 Detail of the Cu block on the floor.
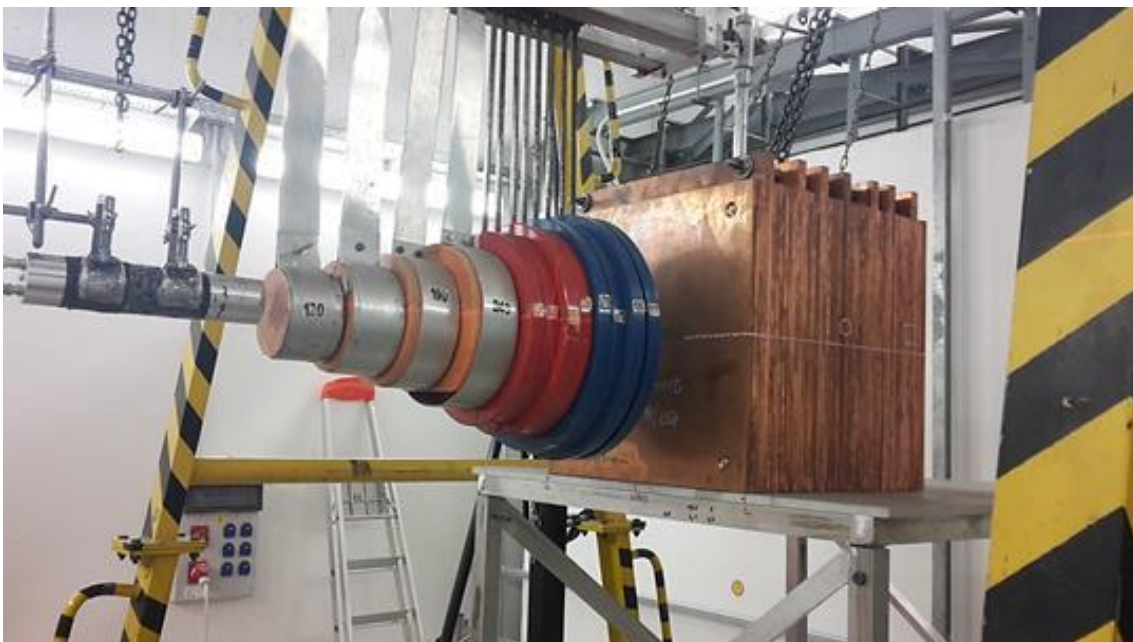
Figure C.4 Photo of Shielding Cone in front of copper block benchmark assembly.

Figure C.5 Photo of NGA-01 analyzer

Figure C.6 Photo Multiplier Tube (Burle 8575) for Stilbene Crystal ø10 mm × 10 mm and ø45 mm × 45 mm.

APPENDIX D. ^{252}CF FRONTIER TECHNOLOGY CORPORATION INFORMATION

Information taken from www.frontier-cf252.com/neutron-sources/.

REVISIONS

SYM.	DESCRIPTION	DATE	APPROVAL

DE | MFG | QA

ITEM NO	REQ'D	PART NO	DESCRIPTION
01	1	SEE BELOW	CONTAINER
02	1	SEE BELOW	PLUG

.235
P.FIT WITH .234 DIA.
.0005
.0008
.141 DIA.
.090
.050
.180
.002 MAX. CHAM.
.325 DIA.
.235
.231 DIA.
5°
.775
.695
.050
.370
.371
NOTE 3

NOTES:
1. Break all corners .010-.020 unless otherwise specified.
2. TIG weld, minimum 0.050 weld penetration.
3. Electroetch, engrave, or imprint identification marking no more than .005 deep on surface indicated.

FRONTIER TECHNOLOGY CORPORATION
Xenia, Ohio, U.S.A.

Standard Neutron Source
Model 100 SNS Capsule

SCALE 2X   WT. CALC / ACT.

DWG. NO. A10100-PA04   REV 0

CODE IDENT NO

SHEET   OF

DIMENSIONS ARE IN X INCHES [] MILLIMETERS
UNLESS OTHERWISE SPECIFIED
TOLERANCES   FRACTIONS
DECIMALS
.XX   ±.005   ANGLES
.XXX BASIC   30'
ALL SURFACES

MATERIAL 304L S.S. PER ASTM A276 OR A479

APPROVAL		
QA		
MFG		
DE		
DRAWN		
SIGNATURE		DATE

APPENDIX E. SENSITIVITY CALCULATIONS

The MCNP6.2 code with the nuclear library ENDF /B-VII.1 was used for the sensitivity estimations. The fluxes were calculated using the Next-Event Estimator, (neutron flux tally F5 in MCNP code - flux at a point, i. e. a point detector) with steps of 100 keV.

The reference model for calculation of the neutron flux perturbation values is identical to the benchmark model described in Section 3.

The reference model was used as a basis for detailed sensitivity analysis, uncertainty estimation, background calculations, and transmission through the cone. The cone was simulated accurately, with known dimensions and tabulated density. The room effect was calculated using well-known dimensions (from lab technical drawings) and tabulated composition of concrete.

The chemical analysis sensitivities are not covered here since they are discussed in Section 2.

The calculated neutron leakage reference flux is listed in Table 4.1.

The following calculated neutron leakage fluxes are used in uncertainty evaluation in chapter 2.1.1:

- Room-return results are listed in Table E.1.
- Copper density results are listed in Table E.2.a.
- Dimension results (copper thickness and width) are listed in Table E.2.b.
- Copper height results and copper isotopic composition are listed in Table E.2.c.
- Source distance and misalignment results are listed in Table E.2.d.
- Block support component results are listed in Tables E.3.a.
- Block and source composition results are listed in Table E.3.b.

Time periods of total and background neutron flux calculations were one day and several weeks, respectively. E_{up} in the tables means the upper energy of the group.

Table E.1 Calculated, normalized neutron leakage flux Φ_{ng}. Surrounding components.

Energy Group E_{up} [MeV]	Calculated, normalized neutron leakage flux Φ_{ng} for various case					
	Full geometry with walls		Transmission by cone		Full geometry withs walls and cone	
	Φ_{ng} [cm^{-2}·s^{-1}]	u_r	Φ_{ng} [cm^{-2}·s^{-1}]	u_r	Φ_{ng} [cm^{-2}·s^{-1}]	u_r
1.1	7.25E-08	1.00E-04	4.76E-11	1.67E-02	1.68E-09	7.00E-04
1.2	6.85E-08	1.00E-04	4.66E-11	1.64E-02	1.65E-09	6.00E-04
1.3	5.16E-08	1.00E-04	3.16E-11	1.64E-02	1.34E-09	6.00E-04
1.4	4.09E-08	1.00E-04	2.46E-11	2.22E-02	9.38E-10	7.00E-04
1.5	3.21E-08	1.00E-04	1.89E-11	2.02E-02	1.02E-09	6.00E-04
1.6	2.45E-08	1.00E-04	1.48E-11	1.84E-02	5.22E-10	9.00E-04
1.7	2.05E-08	1.00E-04	1.22E-11	2.75E-02	4.16E-10	1.10E-03
1.8	1.62E-08	1.00E-04	1.02E-11	2.97E-02	3.97E-10	1.20E-03
1.9	1.41E-08	2.00E-04	8.09E-12	2.99E-02	2.17E-10	1.80E-03
2.0	1.12E-08	2.00E-04	6.40E-12	2.36E-02	1.85E-10	1.80E-03
2.1	1.00E-08	2.00E-04	5.71E-12	3.24E-02	2.03E-10	1.50E-03
2.2	8.91E-09	2.00E-04	5.95E-12	4.36E-02	1.97E-10	1.50E-03
2.3	7.85E-09	2.00E-04	5.20E-12	3.81E-02	1.87E-10	1.50E-03
2.4	6.98E-09	2.00E-04	4.31E-12	2.29E-02	1.98E-10	1.60E-03
2.5	6.05E-09	3.00E-04	3.87E-12	5.01E-02	1.86E-10	1.50E-03
2.6	5.42E-09	3.00E-04	3.25E-12	5.28E-02	1.81E-10	1.20E-03
2.7	4.99E-09	3.00E-04	2.82E-12	2.44E-02	1.73E-10	7.00E-04
2.8	4.46E-09	3.00E-04	2.50E-12	4.60E-02	1.33E-10	1.20E-03
2.9	3.93E-09	4.00E-04	2.05E-12	7.53E-02	8.75E-11	1.80E-03
3.0	3.43E-09	4.00E-04	1.60E-12	7.08E-02	7.39E-11	1.80E-03
3.1	3.07E-09	4.00E-04	1.86E-12	4.29E-02	5.13E-11	2.80E-03
3.2	2.81E-09	5.00E-04	1.48E-12	6.03E-02	4.58E-11	3.10E-03
3.3	2.59E-09	5.00E-04	1.18E-12	7.41E-02	4.42E-11	2.20E-03
3.4	2.39E-09	5.00E-04	1.43E-12	1.32E-01	3.93E-11	3.70E-03
3.5	2.20E-09	6.00E-04	8.86E-13	1.13E-01	2.61E-11	4.50E-03
3.6	2.02E-09	6.00E-04	7.65E-13	3.70E-02	2.40E-11	3.20E-03
3.7	1.84E-09	7.00E-04	7.95E-13	7.72E-02	2.02E-11	6.50E-03
3.8	1.67E-09	7.00E-04	7.90E-13	1.10E-01	1.91E-11	4.70E-03
3.9	1.54E-09	7.00E-04	7.27E-13	4.88E-02	1.88E-11	5.80E-03
4.0	1.41E-09	8.00E-04	8.37E-13	9.56E-02	2.17E-11	4.60E-03
4.1	1.30E-09	8.00E-04	9.27E-13	8.96E-02	2.33E-11	5.70E-03
4.2	1.20E-09	9.00E-04	8.20E-13	8.33E-02	2.15E-11	1.70E-03
4.3	1.11E-09	9.00E-04	8.00E-13	1.44E-01	1.68E-11	7.20E-03
4.4	1.03E-09	1.00E-03	6.51E-13	1.27E-01	1.40E-11	4.90E-03
4.5	9.69E-10	1.00E-03	6.25E-13	3.02E-02	1.18E-11	7.80E-03
4.6	9.05E-10	1.10E-03	8.86E-13	1.37E-01	9.65E-12	7.00E-03
4.7	8.53E-10	1.10E-03	7.61E-13	1.24E-01	1.25E-11	6.10E-03
4.8	7.97E-10	1.20E-03	6.67E-13	4.07E-02	8.92E-12	1.02E-02
4.9	7.48E-10	1.20E-03	7.09E-13	7.07E-02	7.07E-12	1.19E-02
5.0	7.04E-10	1.30E-03	6.74E-13	6.40E-02	8.44E-12	6.80E-03
5.1	6.64E-10	1.30E-03	6.97E-13	7.07E-02	7.73E-12	8.10E-03
5.2	6.29E-10	1.40E-03	5.66E-13	3.46E-02	5.94E-12	6.60E-03
5.3	5.97E-10	1.40E-03	7.24E-13	7.39E-02	6.61E-12	3.60E-03
5.4	5.64E-10	1.50E-03	6.44E-13	1.54E-01	6.02E-12	1.66E-02
5.5	5.39E-10	1.50E-03	6.44E-13	7.82E-02	5.92E-12	1.12E-02

Table E.1 (cont. 1) Calculated, normalized neutron leakage flux Φ_{ng}. Surrounding components.

Energy Group E_{up} [MeV]	Calculated, normalized neutron leakage flux Φ_{ng} for various case					
	Full geometry with walls		Transmission by cone		Full geometry withs walls and cone	
	Φ_{ng} [cm$^{-2}\cdot$s^{-1}]	u_r	Φ_{ng} [cm$^{-2}\cdot$s^{-1}]	u_r	Φ_{ng} [cm$^{-2}\cdot$s^{-1}]	u_r
5.6	5.08E-10	1.60E-03	5.90E-13	6.28E-02	4.84E-12	1.71E-02
5.7	4.84E-10	1.60E-03	4.87E-13	4.96E-02	3.89E-12	5.40E-03
5.8	4.58E-10	1.70E-03	6.13E-13	1.14E-01	3.72E-12	1.82E-02
5.9	4.34E-10	1.80E-03	5.94E-13	1.48E-01	3.32E-12	1.20E-02
6.0	4.12E-10	1.80E-03	6.75E-13	1.54E-01	2.55E-12	6.00E-03
6.1	3.91E-10	1.90E-03	5.14E-13	5.39E-02	2.56E-12	1.32E-02
6.2	3.72E-10	1.90E-03	4.83E-13	8.29E-02	2.69E-12	1.84E-02
6.3	3.53E-10	2.00E-03	3.60E-13	5.32E-02	2.32E-12	3.08E-02
6.4	3.34E-10	2.10E-03	3.58E-13	5.80E-02	2.51E-12	5.86E-02
6.5	3.19E-10	2.20E-03	4.78E-13	6.08E-02	2.53E-12	2.80E-02
6.6	3.03E-10	2.20E-03	5.22E-13	1.03E-01	2.51E-12	4.06E-02
6.7	2.88E-10	2.30E-03	4.53E-13	5.11E-02	2.20E-12	3.45E-02
6.8	2.75E-10	2.40E-03	4.90E-13	6.39E-02	1.95E-12	1.23E-02
6.9	2.60E-10	2.40E-03	5.27E-13	1.21E-01	1.84E-12	3.05E-02
7.0	2.46E-10	2.50E-03	4.53E-13	4.84E-02	1.52E-12	4.33E-02
7.1	2.34E-10	2.60E-03	4.52E-13	5.76E-02	1.17E-12	1.45E-02
7.2	2.22E-10	2.70E-03	3.94E-13	4.43E-02	1.17E-12	4.30E-02
7.3	2.08E-10	2.80E-03	4.21E-13	8.99E-02	1.05E-12	3.57E-02
7.4	1.98E-10	2.90E-03	2.97E-13	1.20E-01	9.41E-13	6.40E-02
7.5	1.87E-10	3.00E-03	2.30E-13	6.96E-02	9.51E-13	6.66E-02
7.6	1.76E-10	3.00E-03	2.08E-13	4.72E-02	8.84E-13	6.67E-02
7.7	1.68E-10	3.20E-03	3.32E-13	2.23E-01	8.63E-13	1.07E-01
7.8	1.58E-10	3.20E-03	2.02E-13	1.91E-01	6.86E-13	2.66E-02
7.9	1.49E-10	3.30E-03	2.22E-13	2.06E-01	6.64E-13	2.67E-02
8.0	1.41E-10	3.50E-03	2.02E-13	1.08E-01	7.02E-13	4.27E-02
8.1	1.34E-10	3.60E-03	1.63E-13	6.31E-02	7.50E-13	1.19E-01
8.2	1.26E-10	3.70E-03	1.51E-13	5.89E-02	7.23E-13	1.25E-01
8.3	1.19E-10	3.80E-03	2.18E-13	1.40E-01	6.58E-13	4.97E-02
8.4	1.13E-10	3.90E-03	1.88E-13	6.09E-02	5.95E-13	2.50E-02
8.5	1.06E-10	4.10E-03	2.24E-13	7.82E-02	6.97E-13	6.56E-02
8.6	1.00E-10	4.20E-03	1.87E-13	4.86E-02	6.80E-13	1.72E-02
8.7	9.37E-11	4.30E-03	1.96E-13	1.06E-01	5.95E-13	1.77E-02
8.8	8.88E-11	4.50E-03	2.02E-13	9.04E-02	5.12E-13	2.37E-02
8.9	8.31E-11	4.60E-03	1.94E-13	1.41E-01	4.79E-13	5.37E-02
9.0	7.88E-11	4.80E-03	1.59E-13	7.63E-02	4.08E-13	3.14E-02
9.1	7.34E-11	5.00E-03	1.64E-13	7.63E-02	3.36E-13	2.39E-02
9.2	6.95E-11	5.20E-03	1.93E-13	2.77E-01	4.46E-13	1.93E-01
9.3	6.52E-11	5.30E-03	1.26E-13	7.45E-02	2.67E-13	2.88E-02
9.4	6.13E-11	5.50E-03	1.11E-13	7.05E-02	2.60E-13	4.38E-02
9.5	5.75E-11	5.70E-03	1.09E-13	7.87E-02	3.72E-13	2.05E-01
9.6	5.39E-11	5.90E-03	9.93E-14	6.67E-02	2.53E-13	1.93E-01
9.7	5.06E-11	6.20E-03	1.15E-13	1.56E-01	1.94E-13	5.67E-02
9.8	4.82E-11	6.30E-03	1.01E-13	1.09E-01	1.87E-13	7.44E-02
9.9	4.50E-11	6.50E-03	1.33E-13	2.29E-01	1.65E-13	6.08E-02
10.0	4.25E-11	6.80E-03	9.75E-14	8.98E-02	1.60E-13	4.37E-02

Table E.1 (cont.2) Calculated, normalized neutron leakage flux Φ_{ng}. Surrounding components.

Energy Group E_{up} [MeV]	Calculated, normalized neutron leakage flux Φ_{ng} for various case					
	Full geometry with walls		Transmission by cone		Full geometry withs walls and cone	
	Φ_{ng} [cm^{-2}·s^{-1}]	u_r	Φ_{ng} [cm^{-2}·s^{-1}]	u_r	Φ_{ng} [cm^{-2}·s^{-1}]	u_r
10.1	4.02E-11	6.90E-03	1.35E-13	2.76E-01	1.60E-13	5.63E-02
10.2	3.79E-11	7.20E-03	1.07E-13	1.44E-01	1.39E-13	4.98E-02
10.3	3.62E-11	7.40E-03	9.58E-14	1.50E-01	1.49E-13	8.10E-02
10.4	3.42E-11	7.50E-03	7.17E-14	8.76E-02	1.36E-13	8.03E-02
10.5	3.23E-11	7.90E-03	1.51E-13	3.05E-01	1.30E-13	7.08E-02
10.6	2.99E-11	8.10E-03	7.69E-14	1.15E-01	1.14E-13	1.19E-01
10.7	2.86E-11	8.30E-03	9.45E-14	1.92E-01	1.13E-13	1.34E-01
10.8	2.69E-11	8.70E-03	8.85E-14	1.86E-01	1.24E-13	1.29E-01
10.9	2.49E-11	8.90E-03	6.61E-14	8.99E-02	1.07E-13	1.90E-01
11.0	2.41E-11	9.30E-03	5.24E-14	1.38E-01	9.56E-14	2.13E-01

Table E.2.a Perturbation of copper density with three standard uncertainties.

Energy Group E_{up} [MeV]	Calculated, normalized neutron leakage flux Φ_{ng} perturbed by three standard uncertainties			
	Decreased Cu density		Increased Cu density	
	Φ_{ng} [cm$^{-2}\cdot$s^{-1}]	u_r	Φ_{ng} [cm$^{-2}\cdot$s^{-1}]	u_r
1.1	7.13E-08	1.00E-04	7.01E-08	1.00E-04
1.2	6.73E-08	1.00E-04	6.61E-08	1.00E-04
1.3	5.07E-08	1.00E-04	4.97E-08	1.00E-04
1.4	4.02E-08	1.00E-04	3.94E-08	1.00E-04
1.5	3.13E-08	1.00E-04	3.06E-08	1.00E-04
1.6	2.42E-08	1.00E-04	2.37E-08	1.00E-04
1.7	2.03E-08	1.00E-04	1.99E-08	1.00E-04
1.8	1.60E-08	1.00E-04	1.56E-08	1.00E-04
1.9	1.41E-08	2.00E-04	1.38E-08	2.00E-04
2.0	1.11E-08	2.00E-04	1.09E-08	2.00E-04
2.1	9.93E-09	2.00E-04	9.70E-09	2.00E-04
2.2	8.80E-09	2.00E-04	8.59E-09	2.00E-04
2.3	7.74E-09	2.00E-04	7.56E-09	2.00E-04
2.4	6.84E-09	2.00E-04	6.68E-09	3.00E-04
2.5	5.92E-09	3.00E-04	5.77E-09	3.00E-04
2.6	5.29E-09	3.00E-04	5.16E-09	3.00E-04
2.7	4.86E-09	3.00E-04	4.74E-09	3.00E-04
2.8	4.36E-09	3.00E-04	4.26E-09	4.00E-04
2.9	3.88E-09	4.00E-04	3.79E-09	4.00E-04
3.0	3.39E-09	4.00E-04	3.31E-09	4.00E-04
3.1	3.05E-09	4.00E-04	2.97E-09	5.00E-04
3.2	2.79E-09	5.00E-04	2.72E-09	5.00E-04
3.3	2.57E-09	5.00E-04	2.51E-09	5.00E-04
3.4	2.38E-09	5.00E-04	2.32E-09	6.00E-04
3.5	2.20E-09	6.00E-04	2.15E-09	6.00E-04
3.6	2.02E-09	6.00E-04	1.97E-09	6.00E-04
3.7	1.84E-09	7.00E-04	1.79E-09	7.00E-04
3.8	1.68E-09	7.00E-04	1.63E-09	7.00E-04
3.9	1.54E-09	7.00E-04	1.50E-09	8.00E-04
4.0	1.41E-09	8.00E-04	1.37E-09	8.00E-04
4.1	1.29E-09	8.00E-04	1.26E-09	9.00E-04
4.2	1.20E-09	9.00E-04	1.16E-09	9.00E-04
4.3	1.11E-09	9.00E-04	1.08E-09	9.00E-04
4.4	1.03E-09	1.00E-03	1.01E-09	1.00E-03
4.5	9.69E-10	1.00E-03	9.44E-10	1.00E-03
4.6	9.07E-10	1.10E-03	8.83E-10	1.10E-03
4.7	8.50E-10	1.10E-03	8.28E-10	1.10E-03
4.8	7.99E-10	1.20E-03	7.78E-10	1.20E-03
4.9	7.51E-10	1.20E-03	7.31E-10	1.20E-03
5.0	7.04E-10	1.30E-03	6.86E-10	1.30E-03
5.1	6.64E-10	1.30E-03	6.47E-10	1.30E-03
5.2	6.31E-10	1.40E-03	6.15E-10	1.40E-03
5.3	5.98E-10	1.40E-03	5.82E-10	1.40E-03
5.4	5.66E-10	1.50E-03	5.51E-10	1.50E-03
5.5	5.40E-10	1.50E-03	5.26E-10	1.60E-03

Table E.2.a (cont. 1) Perturbation of copper density with three standard uncertainties.

Energy Group E_{up} [MeV]	Calculated, normalized neutron leakage flux Φ_{ng} perturbed by three standard uncertainties			
	Decreased Cu density		Increased Cu density	
	Φ_{ng} [cm$^{-2} \cdot$s^{-1}]	u_r	Φ_{ng} [cm$^{-2} \cdot$s^{-1}]	u_r
5.6	5.10E-10	1.60E-03	4.97E-10	1.60E-03
5.7	4.86E-10	1.60E-03	4.74E-10	1.70E-03
5.8	4.60E-10	1.70E-03	4.48E-10	1.70E-03
5.9	4.37E-10	1.80E-03	4.26E-10	1.80E-03
6.0	4.15E-10	1.80E-03	4.04E-10	1.80E-03
6.1	3.93E-10	1.90E-03	3.84E-10	1.90E-03
6.2	3.74E-10	1.90E-03	3.65E-10	2.00E-03
6.3	3.55E-10	2.00E-03	3.46E-10	2.00E-03
6.4	3.36E-10	2.10E-03	3.28E-10	2.10E-03
6.5	3.21E-10	2.20E-03	3.13E-10	2.20E-03
6.6	3.06E-10	2.20E-03	2.98E-10	2.20E-03
6.7	2.90E-10	2.30E-03	2.82E-10	2.30E-03
6.8	2.77E-10	2.40E-03	2.70E-10	2.40E-03
6.9	2.62E-10	2.40E-03	2.56E-10	2.50E-03
7.0	2.48E-10	2.50E-03	2.42E-10	2.50E-03
7.1	2.36E-10	2.60E-03	2.31E-10	2.60E-03
7.2	2.24E-10	2.70E-03	2.18E-10	2.70E-03
7.3	2.10E-10	2.70E-03	2.05E-10	2.80E-03
7.4	2.00E-10	2.90E-03	1.95E-10	2.90E-03
7.5	1.88E-10	2.90E-03	1.84E-10	3.00E-03
7.6	1.78E-10	3.00E-03	1.74E-10	3.10E-03
7.7	1.69E-10	3.20E-03	1.65E-10	3.20E-03
7.8	1.59E-10	3.20E-03	1.56E-10	3.30E-03
7.9	1.50E-10	3.30E-03	1.47E-10	3.40E-03
8.0	1.42E-10	3.40E-03	1.39E-10	3.50E-03
8.1	1.35E-10	3.60E-03	1.32E-10	3.60E-03
8.2	1.27E-10	3.70E-03	1.24E-10	3.70E-03
8.3	1.20E-10	3.80E-03	1.17E-10	3.80E-03
8.4	1.14E-10	3.90E-03	1.11E-10	4.00E-03
8.5	1.07E-10	4.10E-03	1.04E-10	4.10E-03
8.6	1.01E-10	4.20E-03	9.83E-11	4.20E-03
8.7	9.44E-11	4.30E-03	9.22E-11	4.40E-03
8.8	8.93E-11	4.50E-03	8.74E-11	4.60E-03
8.9	8.36E-11	4.60E-03	8.18E-11	4.70E-03
9.0	7.95E-11	4.80E-03	7.77E-11	4.90E-03
9.1	7.40E-11	5.00E-03	7.24E-11	5.00E-03
9.2	7.02E-11	5.10E-03	6.85E-11	5.20E-03
9.3	6.57E-11	5.30E-03	6.43E-11	5.40E-03
9.4	6.18E-11	5.50E-03	6.05E-11	5.60E-03
9.5	5.81E-11	5.70E-03	5.68E-11	5.70E-03
9.6	5.45E-11	5.90E-03	5.32E-11	5.90E-03
9.7	5.12E-11	6.10E-03	5.00E-11	6.20E-03
9.8	4.85E-11	6.30E-03	4.75E-11	6.40E-03
9.9	4.56E-11	6.50E-03	4.45E-11	6.60E-03
10.0	4.29E-11	6.70E-03	4.19E-11	6.80E-03

Table E.2.a (cont. 2) Perturbation of copper density with three standard uncertainties.

Energy Group E_{up} [MeV]	Calculated, normalized neutron leakage flux Φ_{ng} perturbed by three standard uncertainties			
	Decreased Cu density		Increased Cu density	
	Φ_{ng} [cm$^{-2}\cdot$s^{-1}]	u_r	Φ_{ng} [cm$^{-2}\cdot$s^{-1}]	u_r
10.1	4.06E-11	6.90E-03	3.98E-11	7.00E-03
10.2	3.82E-11	7.10E-03	3.74E-11	7.20E-03
10.3	3.65E-11	7.40E-03	3.57E-11	7.50E-03
10.4	3.45E-11	7.50E-03	3.38E-11	7.60E-03
10.5	3.26E-11	7.80E-03	3.18E-11	7.90E-03
10.6	3.02E-11	8.00E-03	2.96E-11	8.10E-03
10.7	2.89E-11	8.30E-03	2.83E-11	8.40E-03
10.8	2.72E-11	8.70E-03	2.66E-11	8.80E-03
10.9	2.51E-11	8.90E-03	2.46E-11	9.00E-03
11.0	2.42E-11	9.20E-03	2.38E-11	9.30E-03

Table E.2.b Perturbation of block dimensions with three standard uncertainties.

Energy Group E_{up} [MeV]	Calculated, normalized neutron leakage flux Φ_{ng} perturbed by three standard uncertainties							
	Decreased thickness		Increased thickness		Decreased width		Increased width	
	Φ_{ng} [cm^{-2}·s^{-1}]	u_r	Φ_{ng} [cm^{-2}·s^{-1}]	u_r	Φ_{ng} [cm^{-2}·s^{-1}]	u_r	Φ_{ng} [cm^{-2}·s^{-1}]	u_r
1.1	7.36E-08	1.0E-4	6.79E-08	1.0E-4	7.02E-08	1.0E-4	7.11E-08	1.0E-4
1.2	6.94E-08	1.0E-4	6.41E-08	1.0E-4	6.63E-08	1.0E-4	6.70E-08	1.0E-4
1.3	5.23E-08	1.0E-4	4.81E-08	1.0E-4	4.99E-08	1.0E-4	5.04E-08	1.0E-4
1.4	4.16E-08	1.0E-4	3.82E-08	1.0E-4	3.97E-08	1.0E-4	4.00E-08	1.0E-4
1.5	3.24E-08	1.0E-4	2.96E-08	1.0E-4	3.09E-08	1.0E-4	3.11E-08	1.0E-4
1.6	2.51E-08	1.0E-4	2.29E-08	1.0E-4	2.39E-08	1.0E-4	2.40E-08	1.0E-4
1.7	2.10E-08	1.0E-4	1.92E-08	1.0E-4	2.00E-08	1.0E-4	2.01E-08	1.0E-4
1.8	1.66E-08	1.0E-4	1.51E-08	2.0E-4	1.58E-08	1.0E-4	1.58E-08	1.0E-4
1.9	1.46E-08	2.0E-4	1.33E-08	2.0E-4	1.39E-08	2.0E-4	1.39E-08	2.0E-4
2.0	1.16E-08	2.0E-4	1.05E-08	2.0E-4	1.10E-08	2.0E-4	1.10E-08	2.0E-4
2.1	1.03E-08	2.0E-4	9.34E-09	2.0E-4	9.80E-09	2.0E-4	9.84E-09	2.0E-4
2.2	9.15E-09	2.0E-4	8.26E-09	2.0E-4	8.68E-09	2.0E-4	8.71E-09	2.0E-4
2.3	8.05E-09	2.0E-4	7.26E-09	2.0E-4	7.63E-09	2.0E-4	7.66E-09	2.0E-4
2.4	7.12E-09	2.0E-4	6.42E-09	3.0E-4	6.75E-09	3.0E-4	6.77E-09	3.0E-4
2.5	6.16E-09	3.0E-4	5.55E-09	3.0E-4	5.84E-09	3.0E-4	5.85E-09	3.0E-4
2.6	5.51E-09	3.0E-4	4.95E-09	3.0E-4	5.21E-09	3.0E-4	5.23E-09	3.0E-4
2.7	5.06E-09	3.0E-4	4.55E-09	3.0E-4	4.79E-09	3.0E-4	4.80E-09	3.0E-4
2.8	4.55E-09	3.0E-4	4.09E-09	4.0E-4	4.30E-09	4.0E-4	4.31E-09	3.0E-4
2.9	4.05E-09	4.0E-4	3.63E-09	4.0E-4	3.83E-09	4.0E-4	3.84E-09	4.0E-4
3.0	3.54E-09	4.0E-4	3.17E-09	4.0E-4	3.35E-09	4.0E-4	3.35E-09	4.0E-4
3.1	3.18E-09	4.0E-4	2.85E-09	5.0E-4	3.01E-09	5.0E-4	3.01E-09	4.0E-4
3.2	2.91E-09	5.0E-4	2.61E-09	5.0E-4	2.75E-09	5.0E-4	2.76E-09	5.0E-4
3.3	2.68E-09	5.0E-4	2.40E-09	5.0E-4	2.53E-09	5.0E-4	2.54E-09	5.0E-4
3.4	2.48E-09	5.0E-4	2.22E-09	6.0E-4	2.34E-09	6.0E-4	2.35E-09	6.0E-4
3.5	2.30E-09	6.0E-4	2.06E-09	6.0E-4	2.17E-09	6.0E-4	2.18E-09	6.0E-4
3.6	2.11E-09	6.0E-4	1.88E-09	6.0E-4	1.99E-09	6.0E-4	1.99E-09	6.0E-4
3.7	1.92E-09	6.0E-4	1.72E-09	7.0E-4	1.81E-09	7.0E-4	1.82E-09	7.0E-4
3.8	1.75E-09	7.0E-4	1.56E-09	7.0E-4	1.65E-09	7.0E-4	1.65E-09	7.0E-4
3.9	1.60E-09	7.0E-4	1.43E-09	8.0E-4	1.51E-09	8.0E-4	1.52E-09	8.0E-4
4.0	1.47E-09	8.0E-4	1.31E-09	8.0E-4	1.39E-09	8.0E-4	1.39E-09	8.0E-4
4.1	1.35E-09	8.0E-4	1.20E-09	9.0E-4	1.27E-09	8.0E-4	1.27E-09	8.0E-4
4.2	1.25E-09	9.0E-4	1.11E-09	9.0E-4	1.18E-09	9.0E-4	1.18E-09	9.0E-4
4.3	1.16E-09	9.0E-4	1.03E-09	1.0E-3	1.09E-09	9.0E-4	1.09E-09	9.0E-4
4.4	1.08E-09	1.0E-3	9.63E-10	1.0E-3	1.02E-09	1.0E-3	1.02E-09	1.0E-3
4.5	1.01E-09	1.0E-3	9.03E-10	1.1E-3	9.55E-10	1.0E-3	9.57E-10	1.0E-3
4.6	9.48E-10	1.0E-3	8.45E-10	1.1E-3	8.94E-10	1.1E-3	8.96E-10	1.1E-3
4.7	8.89E-10	1.1E-3	7.92E-10	1.2E-3	8.39E-10	1.1E-3	8.40E-10	1.1E-3
4.8	8.35E-10	1.1E-3	7.44E-10	1.2E-3	7.87E-10	1.2E-3	7.89E-10	1.2E-3
4.9	7.84E-10	1.2E-3	6.99E-10	1.3E-3	7.40E-10	1.2E-3	7.41E-10	1.2E-3
5.0	7.36E-10	1.2E-3	6.56E-10	1.3E-3	6.94E-10	1.3E-3	6.96E-10	1.3E-3
5.1	6.94E-10	1.3E-3	6.20E-10	1.4E-3	6.55E-10	1.3E-3	6.56E-10	1.3E-3
5.2	6.59E-10	1.3E-3	5.88E-10	1.4E-3	6.23E-10	1.4E-3	6.24E-10	1.4E-3
5.3	6.24E-10	1.4E-3	5.57E-10	1.5E-3	5.89E-10	1.4E-3	5.90E-10	1.4E-3
5.4	5.91E-10	1.4E-3	5.28E-10	1.5E-3	5.58E-10	1.5E-3	5.59E-10	1.5E-3
5.5	5.64E-10	1.5E-3	5.04E-10	1.6E-3	5.32E-10	1.5E-3	5.33E-10	1.5E-3

Table E.2.b (cont. 1) Perturbation of block dimensions with three standard uncertainties.

Energy Group E_{up} [MeV]	Calculated, normalized neutron leakage flux Φ_{ng} perturbed by three standard uncertainties							
	Decreased thickness		Increased thickness		Decreased width		Increased width	
	Φ_{ng} [cm$^{-2}\cdot$s^{-1}]	u_r	Φ_{ng} [cm$^{-2}\cdot$s^{-1}]	u_r	Φ_{ng} [cm$^{-2}\cdot$s^{-1}]	u_r	Φ_{ng} [cm$^{-2}\cdot$s^{-1}]	u_r
5.6	5.33E-10	1.5E-3	4.76E-10	1.6E-3	5.03E-10	1.6E-3	5.04E-10	1.6E-3
5.7	5.07E-10	1.6E-3	4.53E-10	1.7E-3	4.79E-10	1.7E-3	4.80E-10	1.7E-3
5.8	4.79E-10	1.7E-3	4.29E-10	1.8E-3	4.53E-10	1.7E-3	4.54E-10	1.7E-3
5.9	4.55E-10	1.7E-3	4.08E-10	1.8E-3	4.31E-10	1.8E-3	4.31E-10	1.8E-3
6.0	4.33E-10	1.8E-3	3.87E-10	1.9E-3	4.09E-10	1.8E-3	4.10E-10	1.8E-3
6.1	4.11E-10	1.8E-3	3.68E-10	1.9E-3	3.88E-10	1.9E-3	3.89E-10	1.9E-3
6.2	3.91E-10	1.9E-3	3.50E-10	2.0E-3	3.69E-10	2.0E-3	3.70E-10	2.0E-3
6.3	3.70E-10	2.0E-3	3.32E-10	2.1E-3	3.50E-10	2.0E-3	3.51E-10	2.0E-3
6.4	3.51E-10	2.0E-3	3.14E-10	2.2E-3	3.32E-10	2.1E-3	3.32E-10	2.1E-3
6.5	3.35E-10	2.1E-3	3.01E-10	2.2E-3	3.17E-10	2.2E-3	3.17E-10	2.2E-3
6.6	3.18E-10	2.2E-3	2.85E-10	2.3E-3	3.01E-10	2.2E-3	3.02E-10	2.2E-3
6.7	3.02E-10	2.2E-3	2.71E-10	2.4E-3	2.86E-10	2.3E-3	2.86E-10	2.3E-3
6.8	2.88E-10	2.3E-3	2.59E-10	2.5E-3	2.73E-10	2.4E-3	2.73E-10	2.4E-3
6.9	2.73E-10	2.4E-3	2.45E-10	2.5E-3	2.59E-10	2.5E-3	2.59E-10	2.5E-3
7.0	2.59E-10	2.4E-3	2.33E-10	2.6E-3	2.45E-10	2.5E-3	2.45E-10	2.5E-3
7.1	2.46E-10	2.5E-3	2.21E-10	2.7E-3	2.33E-10	2.6E-3	2.34E-10	2.6E-3
7.2	2.33E-10	2.6E-3	2.10E-10	2.8E-3	2.21E-10	2.7E-3	2.21E-10	2.7E-3
7.3	2.19E-10	2.7E-3	1.97E-10	2.8E-3	2.07E-10	2.8E-3	2.08E-10	2.8E-3
7.4	2.08E-10	2.8E-3	1.87E-10	3.0E-3	1.97E-10	2.9E-3	1.98E-10	2.9E-3
7.5	1.96E-10	2.9E-3	1.76E-10	3.1E-3	1.86E-10	3.0E-3	1.86E-10	3.0E-3
7.6	1.85E-10	3.0E-3	1.67E-10	3.1E-3	1.75E-10	3.1E-3	1.76E-10	3.0E-3
7.7	1.76E-10	3.1E-3	1.59E-10	3.3E-3	1.67E-10	3.2E-3	1.67E-10	3.2E-3
7.8	1.66E-10	3.2E-3	1.50E-10	3.4E-3	1.58E-10	3.3E-3	1.58E-10	3.3E-3
7.9	1.56E-10	3.3E-3	1.41E-10	3.5E-3	1.48E-10	3.4E-3	1.48E-10	3.4E-3
8.0	1.48E-10	3.4E-3	1.33E-10	3.6E-3	1.40E-10	3.5E-3	1.40E-10	3.5E-3
8.1	1.40E-10	3.5E-3	1.27E-10	3.7E-3	1.33E-10	3.6E-3	1.33E-10	3.6E-3
8.2	1.32E-10	3.6E-3	1.20E-10	3.8E-3	1.25E-10	3.7E-3	1.26E-10	3.7E-3
8.3	1.25E-10	3.7E-3	1.13E-10	3.9E-3	1.19E-10	3.8E-3	1.19E-10	3.8E-3
8.4	1.18E-10	3.8E-3	1.07E-10	4.1E-3	1.13E-10	4.0E-3	1.13E-10	4.0E-3
8.5	1.11E-10	4.0E-3	1.00E-10	4.2E-3	1.05E-10	4.1E-3	1.05E-10	4.1E-3
8.6	1.05E-10	4.1E-3	9.43E-11	4.3E-3	9.94E-11	4.2E-3	9.94E-11	4.2E-3
8.7	9.82E-11	4.3E-3	8.85E-11	4.5E-3	9.32E-11	4.4E-3	9.33E-11	4.4E-3
8.8	9.26E-11	4.4E-3	8.41E-11	4.7E-3	8.83E-11	4.5E-3	8.84E-11	4.5E-3
8.9	8.69E-11	4.5E-3	7.89E-11	4.8E-3	8.27E-11	4.7E-3	8.27E-11	4.7E-3
9.0	8.25E-11	4.7E-3	7.48E-11	5.0E-3	7.85E-11	4.8E-3	7.86E-11	4.8E-3
9.1	7.70E-11	4.9E-3	6.96E-11	5.1E-3	7.31E-11	5.0E-3	7.32E-11	5.0E-3
9.2	7.27E-11	5.0E-3	6.59E-11	5.3E-3	6.92E-11	5.2E-3	6.92E-11	5.2E-3
9.3	6.84E-11	5.2E-3	6.18E-11	5.5E-3	6.50E-11	5.3E-3	6.51E-11	5.3E-3
9.4	6.42E-11	5.4E-3	5.83E-11	5.7E-3	6.11E-11	5.5E-3	6.12E-11	5.5E-3
9.5	6.03E-11	5.5E-3	5.47E-11	5.9E-3	5.73E-11	5.7E-3	5.74E-11	5.7E-3
9.6	5.67E-11	5.8E-3	5.12E-11	6.1E-3	5.38E-11	5.9E-3	5.39E-11	5.9E-3
9.7	5.31E-11	6.0E-3	4.82E-11	6.3E-3	5.06E-11	6.2E-3	5.06E-11	6.2E-3
9.8	5.05E-11	6.2E-3	4.57E-11	6.5E-3	4.80E-11	6.3E-3	4.80E-11	6.3E-3
9.9	4.73E-11	6.4E-3	4.29E-11	6.7E-3	4.49E-11	6.5E-3	4.49E-11	6.5E-3
10.0	4.46E-11	6.6E-3	4.04E-11	6.9E-3	4.24E-11	6.8E-3	4.24E-11	6.8E-3

Table E.2.b (cont. 2) Perturbation of block dimensions with three standard uncertainties.

Energy Group E_{up} [MeV]	Calculated, normalized neutron leakage flux Φ_{ng} perturbed by three standard uncertainties							
	Decreased thickness		Increased thickness		Decreased width		Increased width	
	Φ_{ng} [cm$^{-2}\cdot$s^{-1}]	u_r	Φ_{ng} [cm$^{-2}\cdot$s^{-1}]	u_r	Φ_{ng} [cm$^{-2}\cdot$s^{-1}]	u_r	Φ_{ng} [cm$^{-2}\cdot$s^{-1}]	u_r
10.1	4.22E-11	6.8E-3	3.83E-11	7.1E-3	4.01E-11	6.9E-3	4.02E-11	6.9E-3
10.2	3.96E-11	6.9E-3	3.62E-11	7.4E-3	3.78E-11	7.2E-3	3.78E-11	7.2E-3
10.3	3.79E-11	7.2E-3	3.43E-11	7.6E-3	3.61E-11	7.4E-3	3.61E-11	7.4E-3
10.4	3.59E-11	7.3E-3	3.26E-11	7.8E-3	3.41E-11	7.5E-3	3.42E-11	7.5E-3
10.5	3.38E-11	7.7E-3	3.07E-11	8.1E-3	3.22E-11	7.9E-3	3.22E-11	7.9E-3
10.6	3.14E-11	7.9E-3	2.85E-11	8.3E-3	2.99E-11	8.1E-3	2.99E-11	8.1E-3
10.7	3.00E-11	8.1E-3	2.73E-11	8.6E-3	2.86E-11	8.3E-3	2.86E-11	8.3E-3
10.8	2.82E-11	8.5E-3	2.57E-11	9.0E-3	2.69E-11	8.7E-3	2.69E-11	8.7E-3
10.9	2.61E-11	8.7E-3	2.38E-11	9.2E-3	2.48E-11	8.9E-3	2.49E-11	8.9E-3
11.0	2.51E-11	8.9E-3	2.29E-11	9.5E-3	2.40E-11	9.3E-3	2.41E-11	9.3E-3

Table E.2.c Perturbation of block height and isotope composition with three standard uncertainties.

Energy Group E_{up} [MeV]	Calculated, normalized neutron leakage flux Φ_{ng} perturbed by three standard uncertainties							
	Decreased height		Increased height		Chessy composition		Atacama composition	
	Φ_{ng} [cm^{-2}·s^{-1}]	u_r	Φ_{ng} [cm^{-2}·s^{-1}]	u_r	Φ_{ng} [cm^{-2}·s^{-1}]	u_r	Φ_{ng} [cm^{-2}·s^{-1}]	u_r
1.1	7.02E-08	1.0E-04	7.11E-08	1.0E-04	7.07E-08	1.0E-4	7.05E-08	1.0E-4
1.2	6.63E-08	1.0E-04	6.70E-08	1.0E-04	6.67E-08	1.0E-4	6.65E-08	1.0E-4
1.3	4.99E-08	1.0E-04	5.04E-08	1.0E-04	5.02E-08	1.0E-4	5.01E-08	1.0E-4
1.4	3.96E-08	1.0E-04	4.00E-08	1.0E-04	3.98E-08	1.0E-4	3.97E-08	1.0E-4
1.5	3.08E-08	1.0E-04	3.11E-08	1.0E-04	3.10E-08	1.0E-4	3.09E-08	1.0E-4
1.6	2.39E-08	1.0E-04	2.40E-08	1.0E-04	2.39E-08	1.0E-4	2.39E-08	1.0E-4
1.7	2.00E-08	1.0E-04	2.01E-08	1.0E-04	2.01E-08	1.0E-4	2.00E-08	1.0E-4
1.8	1.57E-08	1.0E-04	1.58E-08	1.0E-04	1.58E-08	1.0E-4	1.58E-08	1.0E-4
1.9	1.39E-08	2.0E-04	1.39E-08	2.0E-04	1.39E-08	2.0E-4	1.39E-08	2.0E-4
2.0	1.10E-08	2.0E-04	1.10E-08	2.0E-04	1.10E-08	2.0E-4	1.10E-08	2.0E-4
2.1	9.79E-09	2.0E-04	9.84E-09	2.0E-04	9.82E-09	2.0E-4	9.80E-09	2.0E-4
2.2	8.67E-09	2.0E-04	8.71E-09	2.0E-04	8.69E-09	2.0E-4	8.68E-09	2.0E-4
2.3	7.63E-09	2.0E-04	7.66E-09	2.0E-04	7.65E-09	2.0E-4	7.63E-09	2.0E-4
2.4	6.74E-09	3.0E-04	6.77E-09	3.0E-04	6.76E-09	3.0E-4	6.75E-09	3.0E-4
2.5	5.83E-09	3.0E-04	5.85E-09	3.0E-04	5.85E-09	3.0E-4	5.84E-09	3.0E-4
2.6	5.21E-09	3.0E-04	5.23E-09	3.0E-04	5.22E-09	3.0E-4	5.22E-09	3.0E-4
2.7	4.79E-09	3.0E-04	4.80E-09	3.0E-04	4.80E-09	3.0E-4	4.79E-09	3.0E-4
2.8	4.30E-09	4.0E-04	4.32E-09	3.0E-04	4.31E-09	3.0E-4	4.31E-09	3.0E-4
2.9	3.83E-09	4.0E-04	3.84E-09	4.0E-04	3.84E-09	4.0E-4	3.83E-09	4.0E-4
3.0	3.34E-09	4.0E-04	3.35E-09	4.0E-04	3.35E-09	4.0E-4	3.35E-09	4.0E-4
3.1	3.01E-09	5.0E-04	3.01E-09	4.0E-04	3.01E-09	5.0E-4	3.01E-09	5.0E-4
3.2	2.75E-09	5.0E-04	2.76E-09	5.0E-04	2.76E-09	5.0E-4	2.75E-09	5.0E-4
3.3	2.53E-09	5.0E-04	2.54E-09	5.0E-04	2.54E-09	5.0E-4	2.54E-09	5.0E-4
3.4	2.34E-09	6.0E-04	2.35E-09	6.0E-04	2.35E-09	6.0E-4	2.34E-09	6.0E-4
3.5	2.17E-09	6.0E-04	2.18E-09	6.0E-04	2.18E-09	6.0E-4	2.17E-09	6.0E-4
3.6	1.99E-09	6.0E-04	1.99E-09	6.0E-04	1.99E-09	6.0E-4	1.99E-09	6.0E-4
3.7	1.81E-09	7.0E-04	1.82E-09	7.0E-04	1.82E-09	7.0E-4	1.82E-09	7.0E-4
3.8	1.65E-09	7.0E-04	1.65E-09	7.0E-04	1.65E-09	7.0E-4	1.65E-09	7.0E-4
3.9	1.51E-09	8.0E-04	1.52E-09	8.0E-04	1.52E-09	8.0E-4	1.51E-09	8.0E-4
4.0	1.39E-09	8.0E-04	1.39E-09	8.0E-04	1.39E-09	8.0E-4	1.39E-09	8.0E-4
4.1	1.27E-09	8.0E-04	1.28E-09	8.0E-04	1.27E-09	8.0E-4	1.27E-09	8.0E-4
4.2	1.18E-09	9.0E-04	1.18E-09	9.0E-04	1.18E-09	9.0E-4	1.18E-09	9.0E-4
4.3	1.09E-09	9.0E-04	1.09E-09	9.0E-04	1.09E-09	9.0E-4	1.09E-09	9.0E-4
4.4	1.02E-09	1.0E-03	1.02E-09	1.0E-03	1.02E-09	1.0E-3	1.02E-09	1.0E-3
4.5	9.55E-10	1.0E-03	9.57E-10	1.0E-03	9.56E-10	1.0E-3	9.56E-10	1.0E-3
4.6	8.94E-10	1.1E-03	8.96E-10	1.1E-03	8.95E-10	1.1E-3	8.95E-10	1.1E-3
4.7	8.39E-10	1.1E-03	8.40E-10	1.1E-03	8.39E-10	1.1E-3	8.39E-10	1.1E-3
4.8	7.87E-10	1.2E-03	7.89E-10	1.2E-03	7.88E-10	1.2E-3	7.88E-10	1.2E-3
4.9	7.40E-10	1.2E-03	7.41E-10	1.2E-03	7.41E-10	1.2E-3	7.41E-10	1.2E-3
5.0	6.94E-10	1.3E-03	6.96E-10	1.3E-03	6.95E-10	1.3E-3	6.95E-10	1.3E-3
5.1	6.55E-10	1.3E-03	6.56E-10	1.3E-03	6.56E-10	1.3E-3	6.55E-10	1.3E-3
5.2	6.22E-10	1.4E-03	6.24E-10	1.4E-03	6.23E-10	1.4E-3	6.23E-10	1.4E-3
5.3	5.89E-10	1.4E-03	5.90E-10	1.4E-03	5.90E-10	1.4E-3	5.90E-10	1.4E-3

Table E.2.c (cont. 1) Perturbation of block height and isotope composition with three standard uncertainties.

Energy Group E_{up} [MeV]	Calculated, normalized neutron leakage flux Φ_{ng} perturbed by three standard uncertainties							
	Decreased height		Increased height		Chessy composition		Atacama composition	
	Φ_{ng} [cm^{-2}·s^{-1}]	u_r	Φ_{ng} [cm^{-2}·s^{-1}]	u_r	Φ_{ng} [cm^{-2}·s^{-1}]	u_r	Φ_{ng} [cm^{-2}·s^{-1}]	u_r
5.4	5.58E-10	1.50E-03	5.59E-10	1.50E-03	5.59E-10	1.5E-3	5.59E-10	1.5E-3
5.5	5.32E-10	1.5E-03	5.33E-10	1.5E-03	5.33E-10	1.5E-3	5.33E-10	1.5E-3
5.6	5.03E-10	1.6E-03	5.04E-10	1.6E-03	5.04E-10	1.6E-3	5.03E-10	1.6E-3
5.7	4.79E-10	1.7E-03	4.80E-10	1.7E-03	4.80E-10	1.7E-3	4.80E-10	1.7E-3
5.8	4.53E-10	1.7E-03	4.54E-10	1.7E-03	4.54E-10	1.7E-3	4.54E-10	1.7E-3
5.9	4.31E-10	1.8E-03	4.32E-10	1.8E-03	4.31E-10	1.8E-3	4.31E-10	1.8E-3
6.0	4.09E-10	1.8E-03	4.10E-10	1.8E-03	4.10E-10	1.8E-3	4.10E-10	1.8E-3
6.1	3.88E-10	1.9E-03	3.89E-10	1.9E-03	3.89E-10	1.9E-3	3.88E-10	1.9E-3
6.2	3.69E-10	2.0E-03	3.70E-10	2.0E-03	3.70E-10	2.0E-3	3.70E-10	2.0E-3
6.3	3.50E-10	2.0E-03	3.51E-10	2.0E-03	3.51E-10	2.0E-3	3.51E-10	2.0E-3
6.4	3.32E-10	2.1E-03	3.32E-10	2.1E-03	3.32E-10	2.1E-3	3.32E-10	2.1E-3
6.5	3.17E-10	2.2E-03	3.17E-10	2.2E-03	3.17E-10	2.2E-3	3.17E-10	2.2E-3
6.6	3.01E-10	2.2E-03	3.02E-10	2.2E-03	3.02E-10	2.2E-3	3.01E-10	2.2E-3
6.7	2.86E-10	2.3E-03	2.86E-10	2.3E-03	2.86E-10	2.3E-3	2.86E-10	2.3E-3
6.8	2.73E-10	2.4E-03	2.73E-10	2.4E-03	2.73E-10	2.4E-3	2.73E-10	2.4E-3
6.9	2.59E-10	2.5E-03	2.59E-10	2.5E-03	2.59E-10	2.5E-3	2.59E-10	2.5E-3
7.0	2.45E-10	2.5E-03	2.46E-10	2.5E-03	2.45E-10	2.5E-3	2.45E-10	2.5E-3
7.1	2.33E-10	2.6E-03	2.34E-10	2.6E-03	2.33E-10	2.6E-3	2.33E-10	2.6E-3
7.2	2.21E-10	2.7E-03	2.21E-10	2.7E-03	2.21E-10	2.7E-3	2.21E-10	2.7E-3
7.3	2.07E-10	2.8E-03	2.08E-10	2.8E-03	2.08E-10	2.8E-3	2.07E-10	2.8E-3
7.4	1.97E-10	2.9E-03	1.98E-10	2.9E-03	1.97E-10	2.9E-3	1.97E-10	2.9E-3
7.5	1.86E-10	3.0E-03	1.86E-10	3.0E-03	1.86E-10	3.0E-3	1.86E-10	3.0E-3
7.6	1.75E-10	3.1E-03	1.76E-10	3.0E-03	1.76E-10	3.1E-3	1.75E-10	3.0E-3
7.7	1.67E-10	3.2E-03	1.67E-10	3.2E-03	1.67E-10	3.2E-3	1.67E-10	3.2E-3
7.8	1.57E-10	3.3E-03	1.58E-10	3.3E-03	1.58E-10	3.3E-3	1.58E-10	3.3E-3
7.9	1.48E-10	3.4E-03	1.48E-10	3.4E-03	1.48E-10	3.4E-3	1.48E-10	3.4E-3
8.0	1.40E-10	3.5E-03	1.40E-10	3.5E-03	1.40E-10	3.5E-3	1.40E-10	3.5E-3
8.1	1.33E-10	3.6E-03	1.33E-10	3.6E-03	1.33E-10	3.6E-3	1.33E-10	3.6E-3
8.2	1.25E-10	3.7E-03	1.26E-10	3.7E-03	1.25E-10	3.7E-3	1.25E-10	3.7E-3
8.3	1.19E-10	3.8E-03	1.19E-10	3.8E-03	1.19E-10	3.8E-3	1.19E-10	3.8E-3
8.4	1.13E-10	4.0E-03	1.13E-10	4.0E-03	1.13E-10	4.0E-3	1.13E-10	4.0E-3
8.5	1.05E-10	4.1E-03	1.05E-10	4.1E-03	1.05E-10	4.1E-3	1.05E-10	4.1E-3
8.6	9.93E-11	4.2E-03	9.95E-11	4.2E-03	9.94E-11	4.2E-3	9.93E-11	4.2E-3
8.7	9.32E-11	4.4E-03	9.33E-11	4.4E-03	9.32E-11	4.4E-3	9.33E-11	4.4E-3
8.8	8.83E-11	4.5E-03	8.84E-11	4.5E-03	8.83E-11	4.5E-3	8.83E-11	4.5E-3
8.9	8.26E-11	4.7E-03	8.27E-11	4.7E-03	8.27E-11	4.7E-3	8.27E-11	4.7E-3
9.0	7.85E-11	4.8E-03	7.86E-11	4.8E-03	7.86E-11	4.8E-3	7.86E-11	4.8E-3
9.1	7.31E-11	5.0E-03	7.32E-11	5.0E-03	7.32E-11	5.0E-3	7.31E-11	5.0E-3
9.2	6.92E-11	5.2E-03	6.92E-11	5.2E-03	6.92E-11	5.2E-3	6.92E-11	5.2E-3
9.3	6.50E-11	5.3E-03	6.51E-11	5.3E-03	6.51E-11	5.3E-3	6.51E-11	5.3E-3
9.4	6.11E-11	5.5E-03	6.12E-11	5.5E-03	6.11E-11	5.5E-3	6.11E-11	5.5E-3
9.5	5.73E-11	5.7E-03	5.74E-11	5.7E-03	5.74E-11	5.7E-3	5.73E-11	5.7E-3
9.6	5.38E-11	5.9E-03	5.39E-11	5.9E-03	5.39E-11	5.9E-3	5.38E-11	5.9E-3

Table E.2.c (cont. 2) Perturbation of block height and isotope composition with three standard uncertainties.

Energy Group E_{up} [MeV]	Calculated, normalized neutron leakage flux Φ_{ng} perturbed by three standard uncertainties							
	Decreased height		Increased height		Chessy composition		Atacama composition	
	Φ_{ng} [cm$^{-2}\cdot$s^{-1}]	u_r	Φ_{ng} [cm$^{-2}\cdot$s^{-1}]	u_r	Φ_{ng} [cm$^{-2}\cdot$s^{-1}]	u_r	Φ_{ng} [cm$^{-2}\cdot$s^{-1}]	u_r
9.7	5.06E-11	6.2E-03	5.06E-11	6.2E-03	5.06E-11	6.2E-3	5.05E-11	6.2E-3
9.8	4.80E-11	6.3E-03	4.80E-11	6.3E-03	4.80E-11	6.3E-3	4.80E-11	6.3E-3
9.9	4.49E-11	6.5E-03	4.49E-11	6.5E-03	4.49E-11	6.5E-3	4.49E-11	6.5E-3
10.0	4.24E-11	6.8E-03	4.24E-11	6.8E-03	4.24E-11	6.8E-3	4.24E-11	6.8E-3
10.1	4.01E-11	6.9E-03	4.02E-11	6.9E-03	4.01E-11	6.9E-3	4.01E-11	6.9E-3
10.2	3.78E-11	7.2E-03	3.78E-11	7.2E-03	3.78E-11	7.2E-3	3.78E-11	7.2E-3
10.3	3.61E-11	7.4E-03	3.61E-11	7.4E-03	3.61E-11	7.4E-3	3.61E-11	7.4E-3
10.4	3.41E-11	7.5E-03	3.42E-11	7.5E-03	3.42E-11	7.5E-3	3.41E-11	7.5E-3
10.5	3.22E-11	7.9E-03	3.22E-11	7.9E-03	3.22E-11	7.9E-3	3.22E-11	7.9E-3
10.6	2.99E-11	8.1E-03	2.99E-11	8.1E-03	2.99E-11	8.1E-3	2.98E-11	8.1E-3
10.7	2.86E-11	8.3E-03	2.86E-11	8.3E-03	2.86E-11	8.3E-3	2.86E-11	8.3E-3
10.8	2.69E-11	8.7E-03	2.69E-11	8.7E-03	2.69E-11	8.7E-3	2.69E-11	8.7E-3
10.9	2.48E-11	8.9E-03	2.49E-11	8.9E-03	2.49E-11	8.9E-3	2.49E-11	8.9E-3
11.0	2.40E-11	9.3E-03	2.41E-11	9.3E-03	2.40E-11	9.3E-3	2.40E-11	9.3E-3

Table E.2.d Perturbation of block height and isotope composition with three standard uncertainties.

Energy Group E_{up} [MeV]	Calculated, normalized neutron leakage flux Φ_{ng} perturbed by three standard uncertainties							
	Decreased distance		Increased distance		Misalignment below		Misalignment over	
	Φ_{ng} [cm$^{-2}\cdot$s^{-1}]	u_r	Φ_{ng} [cm$^{-2}\cdot$s^{-1}]	u_r	Φ_{ng} [cm$^{-2}\cdot$s^{-1}]	u_r	Φ_{ng} [cm$^{-2}\cdot$s^{-1}]	u_r
1.1	7.04E-08	1.0E-04	7.09E-08	1.00E-04	7.07E-08	1.00E-04	7.07E-08	1.00E-04
1.2	6.65E-08	1.0E-04	6.69E-08	1.00E-04	6.67E-08	1.00E-04	6.67E-08	1.00E-04
1.3	5.00E-08	1.0E-04	5.04E-08	1.00E-04	5.02E-08	1.00E-04	5.02E-08	1.00E-04
1.4	3.97E-08	1.0E-04	4.00E-08	1.00E-04	3.98E-08	1.00E-04	3.98E-08	1.00E-04
1.5	3.09E-08	1.0E-04	3.11E-08	1.00E-04	3.10E-08	1.00E-04	3.10E-08	1.00E-04
1.6	2.39E-08	1.0E-04	2.40E-08	1.00E-04	2.39E-08	1.00E-04	2.39E-08	1.00E-04
1.7	2.00E-08	1.0E-04	2.01E-08	1.00E-04	2.01E-08	1.00E-04	2.01E-08	1.00E-04
1.8	1.57E-08	1.0E-04	1.59E-08	1.00E-04	1.58E-08	1.00E-04	1.58E-08	1.00E-04
1.9	1.39E-08	2.0E-04	1.40E-08	2.00E-04	1.39E-08	2.00E-04	1.39E-08	2.00E-04
2.0	1.10E-08	2.0E-04	1.10E-08	2.00E-04	1.10E-08	2.00E-04	1.10E-08	2.00E-04
2.1	9.79E-09	2.0E-04	9.85E-09	2.00E-04	9.82E-09	2.00E-04	9.82E-09	2.00E-04
2.2	8.67E-09	2.0E-04	8.72E-09	2.00E-04	8.69E-09	2.00E-04	8.69E-09	2.00E-04
2.3	7.62E-09	2.0E-04	7.67E-09	2.00E-04	7.65E-09	2.00E-04	7.65E-09	2.00E-04
2.4	6.74E-09	3.0E-04	6.78E-09	3.00E-04	6.76E-09	3.00E-04	6.76E-09	3.00E-04
2.5	5.83E-09	3.0E-04	5.86E-09	3.00E-04	5.84E-09	3.00E-04	5.84E-09	3.00E-04
2.6	5.21E-09	3.0E-04	5.24E-09	3.00E-04	5.22E-09	3.00E-04	5.22E-09	3.00E-04
2.7	4.78E-09	3.0E-04	4.81E-09	3.00E-04	4.80E-09	3.00E-04	4.80E-09	3.00E-04
2.8	4.30E-09	3.0E-04	4.32E-09	3.00E-04	4.31E-09	3.00E-04	4.31E-09	3.00E-04
2.9	3.82E-09	4.0E-04	3.85E-09	4.00E-04	3.84E-09	4.00E-04	3.84E-09	4.00E-04
3.0	3.34E-09	4.0E-04	3.36E-09	4.00E-04	3.35E-09	4.00E-04	3.35E-09	4.00E-04
3.1	3.00E-09	5.0E-04	3.02E-09	5.00E-04	3.01E-09	5.00E-04	3.01E-09	5.00E-04
3.2	2.75E-09	5.0E-04	2.77E-09	5.00E-04	2.76E-09	5.00E-04	2.76E-09	5.00E-04
3.3	2.53E-09	5.0E-04	2.55E-09	5.00E-04	2.54E-09	5.00E-04	2.54E-09	5.00E-04
3.4	2.34E-09	6.0E-04	2.35E-09	6.00E-04	2.34E-09	6.00E-04	2.34E-09	6.00E-04
3.5	2.17E-09	6.0E-04	2.18E-09	6.00E-04	2.18E-09	6.00E-04	2.18E-09	6.00E-04
3.6	1.99E-09	6.0E-04	2.00E-09	6.00E-04	1.99E-09	6.00E-04	1.99E-09	6.00E-04
3.7	1.81E-09	7.0E-04	1.82E-09	7.00E-04	1.82E-09	7.00E-04	1.82E-09	7.00E-04
3.8	1.65E-09	7.0E-04	1.66E-09	7.00E-04	1.65E-09	7.00E-04	1.65E-09	7.00E-04
3.9	1.51E-09	8.0E-04	1.52E-09	8.00E-04	1.51E-09	8.00E-04	1.52E-09	8.00E-04
4.0	1.38E-09	8.0E-04	1.39E-09	8.00E-04	1.39E-09	8.00E-04	1.39E-09	8.00E-04
4.1	1.27E-09	8.0E-04	1.28E-09	8.00E-04	1.27E-09	8.00E-04	1.27E-09	8.00E-04
4.2	1.18E-09	9.0E-04	1.18E-09	9.00E-04	1.18E-09	9.00E-04	1.18E-09	9.00E-04
4.3	1.09E-09	9.0E-04	1.10E-09	9.00E-04	1.09E-09	9.00E-04	1.09E-09	9.00E-04
4.4	1.02E-09	1.0E-03	1.02E-09	1.00E-03	1.02E-09	1.00E-03	1.02E-09	1.00E-03
4.5	9.53E-10	1.0E-03	9.59E-10	1.00E-03	9.56E-10	1.00E-03	9.56E-10	1.00E-03
4.6	8.92E-10	1.1E-03	8.98E-10	1.10E-03	8.95E-10	1.10E-03	8.95E-10	1.10E-03
4.7	8.37E-10	1.1E-03	8.42E-10	1.10E-03	8.39E-10	1.10E-03	8.39E-10	1.10E-03
4.8	7.85E-10	1.2E-03	7.90E-10	1.20E-03	7.88E-10	1.20E-03	7.88E-10	1.20E-03
4.9	7.38E-10	1.2E-03	7.43E-10	1.20E-03	7.41E-10	1.20E-03	7.40E-10	1.20E-03
5.0	6.93E-10	1.3E-03	6.97E-10	1.30E-03	6.95E-10	1.30E-03	6.95E-10	1.30E-03
5.1	6.54E-10	1.3E-03	6.58E-10	1.30E-03	6.56E-10	1.30E-03	6.56E-10	1.30E-03
5.2	6.21E-10	1.4E-03	6.25E-10	1.40E-03	6.23E-10	1.40E-03	6.23E-10	1.40E-03
5.3	5.88E-10	1.4E-03	5.92E-10	1.40E-03	5.90E-10	1.40E-03	5.90E-10	1.40E-03
5.4	5.57E-10	1.5E-03	5.61E-10	1.50E-03	5.59E-10	1.50E-03	5.59E-10	1.50E-03
5.5	5.31E-10	1.5E-03	5.35E-10	1.50E-03	5.33E-10	1.50E-03	5.33E-10	1.50E-03

Table E.2.d (cont 1) Perturbation of block height and isotope composition with three standard uncertainties.

Energy Group E_{up} [MeV]	Calculated, normalized neutron leakage flux Φ_{ng} perturbed by three standard uncertainties							
	Decreased distance		Increased distance		Misalignment below		Misalignment over	
	Φ_{ng} [cm$^{-2}\cdot$s^{-1}]	u_r	Φ_{ng} [cm$^{-2}\cdot$s^{-1}]	u_r	Φ_{ng} [cm$^{-2}\cdot$s^{-1}]	u_r	Φ_{ng} [cm$^{-2}\cdot$s^{-1}]	u_r
5.6	5.02E-10	1.6E-03	5.05E-10	1.60E-03	5.04E-10	1.60E-03	5.04E-10	1.60E-03
5.7	4.78E-10	1.7E-03	4.81E-10	1.70E-03	4.80E-10	1.70E-03	4.80E-10	1.70E-03
5.8	4.52E-10	1.7E-03	4.55E-10	1.70E-03	4.54E-10	1.70E-03	4.54E-10	1.70E-03
5.9	4.30E-10	1.8E-03	4.33E-10	1.80E-03	4.31E-10	1.80E-03	4.31E-10	1.80E-03
6.0	4.08E-10	1.8E-03	4.11E-10	1.80E-03	4.10E-10	1.80E-03	4.10E-10	1.80E-03
6.1	3.87E-10	1.9E-03	3.90E-10	1.90E-03	3.89E-10	1.90E-03	3.88E-10	1.90E-03
6.2	3.68E-10	2.0E-03	3.71E-10	2.00E-03	3.70E-10	2.00E-03	3.70E-10	2.00E-03
6.3	3.50E-10	2.0E-03	3.52E-10	2.00E-03	3.51E-10	2.00E-03	3.51E-10	2.00E-03
6.4	3.31E-10	2.1E-03	3.33E-10	2.10E-03	3.32E-10	2.10E-03	3.32E-10	2.10E-03
6.5	3.16E-10	2.2E-03	3.18E-10	2.20E-03	3.17E-10	2.20E-03	3.17E-10	2.20E-03
6.6	3.01E-10	2.2E-03	3.02E-10	2.20E-03	3.02E-10	2.20E-03	3.02E-10	2.20E-03
6.7	2.85E-10	2.3E-03	2.87E-10	2.30E-03	2.86E-10	2.30E-03	2.86E-10	2.30E-03
6.8	2.72E-10	2.4E-03	2.74E-10	2.40E-03	2.73E-10	2.40E-03	2.73E-10	2.40E-03
6.9	2.58E-10	2.5E-03	2.60E-10	2.50E-03	2.59E-10	2.50E-03	2.59E-10	2.50E-03
7.0	2.45E-10	2.5E-03	2.46E-10	2.50E-03	2.45E-10	2.50E-03	2.45E-10	2.50E-03
7.1	2.33E-10	2.6E-03	2.34E-10	2.60E-03	2.33E-10	2.60E-03	2.33E-10	2.60E-03
7.2	2.21E-10	2.7E-03	2.22E-10	2.70E-03	2.21E-10	2.70E-03	2.21E-10	2.70E-03
7.3	2.07E-10	2.8E-03	2.08E-10	2.80E-03	2.08E-10	2.80E-03	2.08E-10	2.80E-03
7.4	1.97E-10	2.9E-03	1.98E-10	2.90E-03	1.97E-10	2.90E-03	1.97E-10	2.90E-03
7.5	1.85E-10	3.0E-03	1.87E-10	3.00E-03	1.86E-10	3.00E-03	1.86E-10	3.00E-03
7.6	1.75E-10	3.0E-03	1.76E-10	3.10E-03	1.76E-10	3.10E-03	1.76E-10	3.10E-03
7.7	1.67E-10	3.2E-03	1.68E-10	3.20E-03	1.67E-10	3.20E-03	1.67E-10	3.20E-03
7.8	1.57E-10	3.3E-03	1.58E-10	3.30E-03	1.58E-10	3.30E-03	1.58E-10	3.30E-03
7.9	1.48E-10	3.4E-03	1.49E-10	3.40E-03	1.48E-10	3.40E-03	1.48E-10	3.40E-03
8.0	1.40E-10	3.5E-03	1.41E-10	3.50E-03	1.40E-10	3.50E-03	1.40E-10	3.50E-03
8.1	1.33E-10	3.6E-03	1.34E-10	3.60E-03	1.33E-10	3.60E-03	1.33E-10	3.60E-03
8.2	1.25E-10	3.7E-03	1.26E-10	3.70E-03	1.26E-10	3.70E-03	1.25E-10	3.70E-03
8.3	1.18E-10	3.8E-03	1.19E-10	3.80E-03	1.19E-10	3.80E-03	1.19E-10	3.80E-03
8.4	1.12E-10	4.0E-03	1.13E-10	4.00E-03	1.13E-10	4.00E-03	1.13E-10	4.00E-03
8.5	1.05E-10	4.1E-03	1.06E-10	4.10E-03	1.05E-10	4.10E-03	1.05E-10	4.10E-03
8.6	9.91E-11	4.2E-03	9.97E-11	4.20E-03	9.94E-11	4.20E-03	9.94E-11	4.20E-03
8.7	9.30E-11	4.4E-03	9.35E-11	4.40E-03	9.32E-11	4.40E-03	9.32E-11	4.40E-03
8.8	8.80E-11	4.5E-03	8.86E-11	4.50E-03	8.84E-11	4.50E-03	8.83E-11	4.50E-03
8.9	8.24E-11	4.7E-03	8.30E-11	4.70E-03	8.27E-11	4.70E-03	8.27E-11	4.70E-03
9.0	7.83E-11	4.8E-03	7.88E-11	4.80E-03	7.85E-11	4.80E-03	7.86E-11	4.80E-03
9.1	7.30E-11	5.0E-03	7.34E-11	5.00E-03	7.32E-11	5.00E-03	7.31E-11	5.00E-03
9.2	6.90E-11	5.2E-03	6.94E-11	5.20E-03	6.92E-11	5.20E-03	6.92E-11	5.20E-03
9.3	6.48E-11	5.3E-03	6.52E-11	5.30E-03	6.50E-11	5.30E-03	6.50E-11	5.30E-03
9.4	6.09E-11	5.5E-03	6.13E-11	5.50E-03	6.11E-11	5.50E-03	6.12E-11	5.50E-03
9.5	5.72E-11	5.7E-03	5.76E-11	5.70E-03	5.74E-11	5.70E-03	5.74E-11	5.70E-03
9.6	5.37E-11	5.9E-03	5.40E-11	5.90E-03	5.39E-11	5.90E-03	5.38E-11	5.90E-03
9.7	5.04E-11	6.2E-03	5.07E-11	6.20E-03	5.06E-11	6.20E-03	5.06E-11	6.20E-03
9.8	4.79E-11	6.3E-03	4.82E-11	6.30E-03	4.80E-11	6.30E-03	4.81E-11	6.30E-03
9.9	4.48E-11	6.5E-03	4.51E-11	6.50E-03	4.49E-11	6.50E-03	4.49E-11	6.50E-03
10.0	4.23E-11	6.8E-03	4.25E-11	6.80E-03	4.24E-11	6.80E-03	4.24E-11	6.80E-03

Table E.2.d (cont 2) Perturbation of block height and isotope composition with three standard uncertainties.

Energy Group E_{up} [MeV]	Calculated, normalized neutron leakage flux Φ_{ng} perturbed by three standard uncertainties							
	Decreased distance		Increased distance		Misalignment below		Misalignment over	
	Φ_{ng} [cm$^{-2}\cdot$s^{-1}]	u_r	Φ_{ng} [cm$^{-2}\cdot$s^{-1}]	u_r	Φ_{ng} [cm$^{-2}\cdot$s^{-1}]	u_r	Φ_{ng} [cm$^{-2}\cdot$s^{-1}]	u_r
10.1	4.00E-11	6.9E-03	4.03E-11	6.90E-03	4.01E-11	6.90E-03	4.01E-11	6.90E-03
10.2	3.77E-11	7.2E-03	3.80E-11	7.20E-03	3.78E-11	7.20E-03	3.78E-11	7.20E-03
10.3	3.60E-11	7.4E-03	3.62E-11	7.40E-03	3.61E-11	7.40E-03	3.61E-11	7.40E-03
10.4	3.41E-11	7.5E-03	3.43E-11	7.50E-03	3.42E-11	7.50E-03	3.42E-11	7.50E-03
10.5	3.21E-11	7.9E-03	3.23E-11	7.90E-03	3.22E-11	7.90E-03	3.22E-11	7.90E-03
10.6	2.98E-11	8.1E-03	3.00E-11	8.10E-03	2.99E-11	8.10E-03	2.99E-11	8.10E-03
10.7	2.85E-11	8.3E-03	2.87E-11	8.30E-03	2.86E-11	8.30E-03	2.86E-11	8.30E-03
10.8	2.68E-11	8.7E-03	2.70E-11	8.70E-03	2.69E-11	8.70E-03	2.69E-11	8.70E-03
10.9	2.48E-11	8.9E-03	2.49E-11	8.90E-03	2.49E-11	8.90E-03	2.49E-11	8.90E-03
11.0	2.40E-11	9.3E-03	2.41E-11	9.30E-03	2.41E-11	9.30E-03	2.40E-11	9.30E-03

Table E.3.a Calculated, normalized neutron leakage flux Φ_{ng}. Block support components.

Energy Group E_{up} [MeV]	Calculated, normalized neutron leakage flux Φ_{ng} perturbed by three standard uncertainties							
	Effect of Al table		Holder of blocks		Screws		Gaps between	
	Φ_{ng} [cm^{-2}·s^{-1}]	u_r	Φ_{ng} [cm^{-2}·s^{-1}]	u_r	Φ_{ng} [cm^{-2}·s^{-1}]	u_r	Φ_{ng} [cm^{-2}·s^{-1}]	u_r
1.1	7.08E-08	1.0E-4	7.10E-08	1.0E-4	7.07E-08	1.00E-04	7.06E-08	1.0E-4
1.2	6.68E-08	1.0E-4	6.69E-08	1.0E-4	6.67E-08	1.00E-04	6.66E-08	1.0E-4
1.3	5.02E-08	1.0E-4	5.03E-08	1.0E-4	5.02E-08	1.00E-04	5.02E-08	1.0E-4
1.4	3.99E-08	1.0E-4	3.99E-08	1.0E-4	3.98E-08	1.00E-04	3.98E-08	1.0E-4
1.5	3.10E-08	1.0E-4	3.10E-08	1.0E-4	3.10E-08	1.00E-04	3.09E-08	1.0E-4
1.6	2.40E-08	1.0E-4	2.40E-08	1.0E-4	2.39E-08	1.00E-04	2.39E-08	1.0E-4
1.7	2.01E-08	1.0E-4	2.01E-08	1.0E-4	2.01E-08	1.00E-04	2.01E-08	1.0E-4
1.8	1.58E-08	1.0E-4	1.58E-08	1.0E-4	1.58E-08	1.00E-04	1.58E-08	1.0E-4
1.9	1.39E-08	2.0E-4	1.39E-08	2.0E-4	1.39E-08	2.00E-04	1.39E-08	2.0E-4
2	1.10E-08	2.0E-4	1.10E-08	2.0E-4	1.10E-08	2.00E-04	1.10E-08	2.0E-4
2.1	9.83E-09	2.0E-4	9.83E-09	2.0E-4	9.82E-09	2.00E-04	9.81E-09	2.0E-4
2.2	8.70E-09	2.0E-4	8.71E-09	2.0E-4	8.69E-09	2.00E-04	8.69E-09	2.0E-4
2.3	7.65E-09	2.0E-4	7.66E-09	2.0E-4	7.65E-09	2.00E-04	7.64E-09	2.0E-4
2.4	6.76E-09	3.0E-4	6.77E-09	3.0E-4	6.76E-09	3.00E-04	6.76E-09	3.0E-4
2.5	5.85E-09	3.0E-4	5.85E-09	3.0E-4	5.84E-09	3.00E-04	5.84E-09	3.0E-4
2.6	5.23E-09	3.0E-4	5.23E-09	3.0E-4	5.22E-09	3.00E-04	5.22E-09	3.0E-4
2.7	4.80E-09	3.0E-4	4.80E-09	3.0E-4	4.80E-09	3.00E-04	4.79E-09	3.0E-4
2.8	4.31E-09	3.0E-4	4.31E-09	3.0E-4	4.31E-09	3.00E-04	4.31E-09	4.0E-4
2.9	3.84E-09	4.0E-4	3.84E-09	4.0E-4	3.84E-09	4.00E-04	3.83E-09	4.0E-4
3	3.35E-09	4.0E-4	3.35E-09	4.0E-4	3.35E-09	4.00E-04	3.35E-09	4.0E-4
3.1	3.01E-09	5.0E-4	3.01E-09	4.0E-4	3.01E-09	5.00E-04	3.01E-09	5.0E-4
3.2	2.76E-09	5.0E-4	2.76E-09	5.0E-4	2.76E-09	5.00E-04	2.76E-09	5.0E-4
3.3	2.54E-09	5.0E-4	2.54E-09	5.0E-4	2.54E-09	5.00E-04	2.54E-09	5.0E-4
3.4	2.35E-09	6.0E-4	2.35E-09	6.0E-4	2.34E-09	6.00E-04	2.34E-09	6.0E-4
3.5	2.18E-09	6.0E-4	2.18E-09	6.0E-4	2.18E-09	6.00E-04	2.17E-09	6.0E-4
3.6	1.99E-09	6.0E-4	1.99E-09	6.0E-4	1.99E-09	6.00E-04	1.99E-09	6.0E-4
3.7	1.82E-09	7.0E-4	1.82E-09	7.0E-4	1.82E-09	7.00E-04	1.82E-09	7.0E-4
3.8	1.65E-09	7.0E-4	1.65E-09	7.0E-4	1.65E-09	7.00E-04	1.65E-09	7.0E-4
3.9	1.52E-09	8.0E-4	1.52E-09	8.0E-4	1.52E-09	8.00E-04	1.51E-09	8.0E-4
4	1.39E-09	8.0E-4	1.39E-09	8.0E-4	1.39E-09	8.00E-04	1.39E-09	8.0E-4
4.1	1.27E-09	8.0E-4	1.27E-09	8.0E-4	1.27E-09	8.00E-04	1.27E-09	8.0E-4
4.2	1.18E-09	9.0E-4	1.18E-09	9.0E-4	1.18E-09	9.00E-04	1.18E-09	9.0E-4
4.3	1.09E-09	9.0E-4	1.09E-09	9.0E-4	1.09E-09	9.00E-04	1.09E-09	9.0E-4
4.4	1.02E-09	1.0E-3	1.02E-09	1.0E-3	1.02E-09	1.00E-03	1.02E-09	1.0E-3
4.5	9.57E-10	1.0E-3	9.57E-10	1.0E-3	9.56E-10	1.00E-03	9.56E-10	1.0E-3
4.6	8.95E-10	1.1E-3	8.96E-10	1.1E-3	8.95E-10	1.10E-03	8.95E-10	1.1E-3
4.7	8.40E-10	1.1E-3	8.40E-10	1.1E-3	8.39E-10	1.10E-03	8.39E-10	1.1E-3
4.8	7.88E-10	1.2E-3	7.89E-10	1.2E-3	7.88E-10	1.20E-03	7.87E-10	1.2E-3
4.9	7.41E-10	1.2E-3	7.41E-10	1.2E-3	7.41E-10	1.20E-03	7.40E-10	1.2E-3
5	6.95E-10	1.3E-3	6.96E-10	1.3E-3	6.95E-10	1.30E-03	6.95E-10	1.3E-3
5.1	6.56E-10	1.3E-3	6.56E-10	1.3E-3	6.56E-10	1.30E-03	6.55E-10	1.3E-3
5.2	6.23E-10	1.4E-3	6.24E-10	1.4E-3	6.23E-10	1.40E-03	6.23E-10	1.4E-3

Table E.3.a Calculated, normalized neutron leakage flux Φ_{ng}. Block support components.

Energy Group Eup [MeV]	Calculated, normalized neutron leakage flux Φ_{ng} perturbed by three standard uncertainties							
	Effect of Al table		Holder of blocks		Effect of Al table		Gaps between	
	Φ_{ng} [cm^{-2}·s^{-1}]	u_r	Φ_{ng} [cm^{-2}·s^{-1}]	u_r	Φ_{ng} [cm^{-2}·s^{-1}]	u_r	Φ_{ng} [cm^{-2}·s^{-1}]	u_r
5.3	5.90E-10	1.4E-3	5.90E-10	1.4E-3	5.90E-10	1.40E-03	5.90E-10	1.4E-3
5.4	5.59E-10	1.5E-3	5.59E-10	1.5E-3	5.59E-10	1.50E-03	5.58E-10	1.5E-3
5.5	5.33E-10	1.5E-3	5.33E-10	1.5E-3	5.33E-10	1.50E-03	5.32E-10	1.5E-3
5.6	5.04E-10	1.6E-3	5.04E-10	1.6E-3	5.04E-10	1.60E-03	5.03E-10	1.6E-3
5.7	4.80E-10	1.7E-3	4.80E-10	1.7E-3	4.80E-10	1.70E-03	4.80E-10	1.7E-3
5.8	4.54E-10	1.7E-3	4.54E-10	1.7E-3	4.54E-10	1.70E-03	4.54E-10	1.7E-3
5.9	4.31E-10	1.8E-3	4.31E-10	1.8E-3	4.31E-10	1.80E-03	4.31E-10	1.8E-3
6	4.10E-10	1.8E-3	4.10E-10	1.8E-3	4.10E-10	1.80E-03	4.09E-10	1.8E-3
6.1	3.89E-10	1.9E-3	3.89E-10	1.9E-3	3.89E-10	1.90E-03	3.88E-10	1.9E-3
6.2	3.70E-10	2.0E-3	3.70E-10	2.0E-3	3.70E-10	2.00E-03	3.69E-10	2.0E-3
6.3	3.51E-10	2.0E-3	3.51E-10	2.0E-3	3.51E-10	2.00E-03	3.51E-10	2.0E-3
6.4	3.32E-10	2.1E-3	3.32E-10	2.1E-3	3.32E-10	2.10E-03	3.32E-10	2.1E-3
6.5	3.17E-10	2.2E-3	3.17E-10	2.2E-3	3.17E-10	2.20E-03	3.17E-10	2.2E-3
6.6	3.02E-10	2.2E-3	3.02E-10	2.2E-3	3.01E-10	2.20E-03	3.01E-10	2.2E-3
6.7	2.86E-10	2.3E-3	2.86E-10	2.3E-3	2.86E-10	2.30E-03	2.86E-10	2.3E-3
6.8	2.73E-10	2.4E-3	2.73E-10	2.4E-3	2.73E-10	2.40E-03	2.73E-10	2.4E-3
6.9	2.59E-10	2.5E-3	2.59E-10	2.5E-3	2.59E-10	2.50E-03	2.59E-10	2.5E-3
7	2.45E-10	2.5E-3	2.45E-10	2.5E-3	2.45E-10	2.50E-03	2.45E-10	2.5E-3
7.1	2.34E-10	2.6E-3	2.34E-10	2.6E-3	2.33E-10	2.60E-03	2.33E-10	2.6E-3
7.2	2.21E-10	2.7E-3	2.21E-10	2.7E-3	2.21E-10	2.70E-03	2.21E-10	2.7E-3
7.3	2.08E-10	2.8E-3	2.08E-10	2.8E-3	2.08E-10	2.80E-03	2.08E-10	2.8E-3
7.4	1.97E-10	2.9E-3	1.98E-10	2.9E-3	1.97E-10	2.90E-03	1.97E-10	2.9E-3
7.5	1.86E-10	3.0E-3	1.86E-10	3.0E-3	1.86E-10	3.00E-03	1.86E-10	3.0E-3
7.6	1.76E-10	3.1E-3	1.76E-10	3.0E-3	1.76E-10	3.10E-03	1.76E-10	3.1E-3
7.7	1.67E-10	3.2E-3	1.67E-10	3.2E-3	1.67E-10	3.20E-03	1.67E-10	3.2E-3
7.8	1.58E-10	3.3E-3	1.58E-10	3.3E-3	1.58E-10	3.30E-03	1.58E-10	3.3E-3
7.9	1.48E-10	3.4E-3	1.48E-10	3.4E-3	1.48E-10	3.40E-03	1.48E-10	3.4E-3
8	1.40E-10	3.5E-3	1.40E-10	3.5E-3	1.40E-10	3.50E-03	1.40E-10	3.5E-3
8.1	1.33E-10	3.6E-3	1.33E-10	3.6E-3	1.33E-10	3.60E-03	1.33E-10	3.6E-3
8.2	1.25E-10	3.7E-3	1.26E-10	3.7E-3	1.25E-10	3.70E-03	1.25E-10	3.7E-3
8.3	1.19E-10	3.8E-3	1.19E-10	3.8E-3	1.19E-10	3.80E-03	1.19E-10	3.8E-3
8.4	1.13E-10	4.0E-3	1.13E-10	4.0E-3	1.13E-10	4.00E-03	1.13E-10	4.0E-3
8.5	1.05E-10	4.1E-3	1.05E-10	4.1E-3	1.05E-10	4.10E-03	1.05E-10	4.1E-3
8.6	9.94E-11	4.2E-3	9.94E-11	4.2E-3	9.94E-11	4.20E-03	9.93E-11	4.2E-3
8.7	9.32E-11	4.4E-3	9.33E-11	4.4E-3	9.32E-11	4.40E-03	9.32E-11	4.4E-3
8.8	8.83E-11	4.5E-3	8.84E-11	4.5E-3	8.83E-11	4.50E-03	8.83E-11	4.5E-3
8.9	8.27E-11	4.7E-3	8.27E-11	4.7E-3	8.27E-11	4.70E-03	8.26E-11	4.7E-3
9	7.86E-11	4.8E-3	7.86E-11	4.8E-3	7.85E-11	4.80E-03	7.85E-11	4.9E-3
9.1	7.32E-11	5.0E-3	7.32E-11	5.0E-3	7.32E-11	5.00E-03	7.31E-11	5.0E-3
9.2	6.92E-11	5.2E-3	6.92E-11	5.2E-3	6.92E-11	5.20E-03	6.92E-11	5.2E-3
9.3	6.50E-11	5.3E-3	6.51E-11	5.3E-3	6.50E-11	5.30E-03	6.50E-11	5.3E-3

Table E.3.a Calculated, normalized neutron leakage flux Φ_{ng}. Block support components.

Energy Group Eup [MeV]	Calculated, normalized neutron leakage flux Φ_{ng} perturbed by three standard uncertainties							
	Effect of Al table		Holder of blocks		Effect of Al table		Gaps between	
	Φ_{ng} [cm$^{-2}\cdot$s^{-1}]	u_r	Φ_{ng} [cm$^{-2}\cdot$s^{-1}]	u_r	Φ_{ng} [cm$^{-2}\cdot$s^{-1}]	u_r	Φ_{ng} [cm$^{-2}\cdot$s^{-1}]	u_r
9.4	6.11E-11	5.5E-3	6.12E-11	5.5E-3	6.11E-11	5.50E-03	6.11E-11	5.5E-3
9.5	5.74E-11	5.7E-3	5.74E-11	5.7E-3	5.74E-11	5.70E-03	5.73E-11	5.7E-3
9.6	5.39E-11	5.9E-3	5.39E-11	5.9E-3	5.39E-11	5.90E-03	5.38E-11	5.9E-3
9.7	5.06E-11	6.2E-3	5.06E-11	6.2E-3	5.06E-11	6.20E-03	5.05E-11	6.2E-3
9.8	4.80E-11	6.3E-3	4.80E-11	6.3E-3	4.80E-11	6.30E-03	4.80E-11	6.3E-3
9.9	4.49E-11	6.5E-3	4.49E-11	6.5E-3	4.49E-11	6.50E-03	4.49E-11	6.5E-3
10	4.24E-11	6.8E-3	4.24E-11	6.8E-3	4.24E-11	6.80E-03	4.24E-11	6.8E-3
10.1	4.01E-11	6.9E-3	4.02E-11	6.9E-3	4.01E-11	6.90E-03	4.01E-11	6.9E-3
10.2	3.78E-11	7.2E-3	3.78E-11	7.2E-3	3.78E-11	7.20E-03	3.78E-11	7.2E-3
10.3	3.61E-11	7.4E-3	3.61E-11	7.4E-3	3.61E-11	7.40E-03	3.61E-11	7.4E-3
10.4	3.42E-11	7.5E-3	3.42E-11	7.5E-3	3.42E-11	7.50E-03	3.41E-11	7.5E-3
10.5	3.22E-11	7.9E-3	3.22E-11	7.9E-3	3.22E-11	7.90E-03	3.22E-11	7.9E-3
10.6	2.99E-11	8.1E-3	2.99E-11	8.1E-3	2.99E-11	8.10E-03	2.99E-11	8.1E-3
10.7	2.86E-11	8.3E-3	2.86E-11	8.3E-3	2.86E-11	8.30E-03	2.86E-11	8.3E-3
10.8	2.69E-11	8.7E-3	2.69E-11	8.7E-3	2.69E-11	8.70E-03	2.69E-11	8.7E-3
10.9	2.49E-11	8.9E-3	2.49E-11	8.9E-3	2.49E-11	8.90E-03	2.49E-11	8.9E-3
11	2.40E-11	9.3E-3	2.41E-11	9.3E-3	2.40E-11	9.30E-03	2.40E-11	9.3E-3

Table E.3.b Calculated, normalized neutron leakage flux Φ_{ng}. Block and source compositions.

| Energy Group Eup [MeV] | Calculated, normalized neutron leakage flux Φ_{ng} perturbed by three standard uncertainties | | | | | | | |
| | Cu contamination | | No source structural Al | | No source structural steel 304L | | Absence of cavity | |
	Φ_{ng} [cm$^{-2}\cdot$s^{-1}]	u_r	Φ_{ng} [cm$^{-2}\cdot$s^{-1}]	u_r	Φ_{ng} [cm$^{-2}\cdot$s^{-1}]	u_r	Φ_{ng} [cm$^{-2}\cdot$s^{-1}]	u_r
1.1	7.07E-08	1.00E-04	7.10E-08	1.0E-4	7.11E-08	1.0E-4	7.07E-08	1.00E-04
1.2	6.67E-08	1.00E-04	6.71E-08	1.0E-4	6.71E-08	1.0E-4	6.67E-08	1.00E-04
1.3	5.02E-08	1.00E-04	5.04E-08	1.0E-4	5.07E-08	1.0E-4	5.02E-08	1.00E-04
1.4	3.98E-08	1.00E-04	4.00E-08	1.0E-4	4.02E-08	1.0E-4	3.98E-08	1.00E-04
1.5	3.10E-08	1.00E-04	3.11E-08	1.0E-4	3.13E-08	1.0E-4	3.10E-08	1.00E-04
1.6	2.40E-08	1.00E-04	2.41E-08	1.0E-4	2.43E-08	1.0E-4	2.39E-08	1.00E-04
1.7	2.01E-08	1.00E-04	2.02E-08	1.0E-4	2.03E-08	1.0E-4	2.01E-08	1.00E-04
1.8	1.58E-08	1.00E-04	1.59E-08	1.0E-4	1.60E-08	1.0E-4	1.58E-08	1.00E-04
1.9	1.39E-08	2.00E-04	1.40E-08	2.0E-4	1.42E-08	2.0E-4	1.39E-08	2.00E-04
2	1.10E-08	2.00E-04	1.11E-08	2.0E-4	1.12E-08	2.0E-4	1.10E-08	2.00E-04
2.1	9.82E-09	2.00E-04	9.90E-09	2.0E-4	9.99E-09	2.0E-4	9.82E-09	2.00E-04
2.2	8.70E-09	2.00E-04	8.76E-09	2.0E-4	8.85E-09	2.0E-4	8.69E-09	2.00E-04
2.3	7.65E-09	2.00E-04	7.70E-09	2.0E-4	7.79E-09	2.0E-4	7.65E-09	2.00E-04
2.4	6.76E-09	3.00E-04	6.78E-09	3.0E-4	6.88E-09	2.0E-4	6.76E-09	3.00E-04
2.5	5.85E-09	3.00E-04	5.87E-09	3.0E-4	5.97E-09	3.0E-4	5.85E-09	3.00E-04
2.6	5.23E-09	3.00E-04	5.29E-09	3.0E-4	5.34E-09	3.0E-4	5.22E-09	3.00E-04
2.7	4.80E-09	3.00E-04	4.84E-09	3.0E-4	4.91E-09	3.0E-4	4.80E-09	3.00E-04
2.8	4.31E-09	3.00E-04	4.36E-09	3.0E-4	4.41E-09	3.0E-4	4.31E-09	3.00E-04
2.9	3.84E-09	4.00E-04	3.88E-09	4.0E-4	3.94E-09	4.0E-4	3.84E-09	4.00E-04
3	3.35E-09	4.00E-04	3.39E-09	4.0E-4	3.44E-09	4.0E-4	3.35E-09	4.00E-04
3.1	3.01E-09	5.00E-04	3.05E-09	4.0E-4	3.10E-09	4.0E-4	3.01E-09	5.00E-04
3.2	2.76E-09	5.00E-04	2.79E-09	5.0E-4	2.84E-09	5.0E-4	2.76E-09	5.00E-04
3.3	2.54E-09	5.00E-04	2.57E-09	5.0E-4	2.61E-09	5.0E-4	2.54E-09	5.00E-04
3.4	2.35E-09	6.00E-04	2.38E-09	5.0E-4	2.42E-09	5.0E-4	2.34E-09	6.00E-04
3.5	2.18E-09	6.00E-04	2.20E-09	6.0E-4	2.25E-09	6.0E-4	2.18E-09	6.00E-04
3.6	1.99E-09	6.00E-04	2.03E-09	6.0E-4	2.06E-09	6.0E-4	1.99E-09	6.00E-04
3.7	1.82E-09	7.00E-04	1.84E-09	7.0E-4	1.88E-09	7.0E-4	1.82E-09	7.00E-04
3.8	1.66E-09	7.00E-04	1.68E-09	7.0E-4	1.71E-09	7.0E-4	1.65E-09	7.00E-04
3.9	1.52E-09	8.00E-04	1.54E-09	7.0E-4	1.57E-09	7.0E-4	1.52E-09	8.00E-04
4	1.39E-09	8.00E-04	1.41E-09	8.0E-4	1.44E-09	8.0E-4	1.39E-09	8.00E-04
4.1	1.28E-09	8.00E-04	1.29E-09	8.0E-4	1.32E-09	8.0E-4	1.27E-09	8.00E-04
4.2	1.18E-09	9.00E-04	1.20E-09	9.0E-4	1.23E-09	9.0E-4	1.18E-09	9.00E-04
4.3	1.09E-09	9.00E-04	1.11E-09	9.0E-4	1.14E-09	9.0E-4	1.09E-09	9.00E-04
4.4	1.02E-09	1.00E-03	1.04E-09	1.0E-3	1.06E-09	1.0E-3	1.02E-09	1.00E-03
4.5	9.58E-10	1.00E-03	9.74E-10	1.0E-3	9.96E-10	1.0E-3	9.56E-10	1.00E-03
4.6	8.96E-10	1.10E-03	9.09E-10	1.1E-3	9.32E-10	1.1E-3	8.95E-10	1.10E-03
4.7	8.40E-10	1.10E-03	8.55E-10	1.1E-3	8.73E-10	1.1E-3	8.39E-10	1.10E-03
4.8	7.89E-10	1.20E-03	8.02E-10	1.2E-3	8.18E-10	1.2E-3	7.88E-10	1.20E-03
4.9	7.41E-10	1.20E-03	7.53E-10	1.2E-3	7.71E-10	1.2E-3	7.41E-10	1.20E-03
5	6.96E-10	1.30E-03	7.11E-10	1.3E-3	7.26E-10	1.3E-3	6.95E-10	1.30E-03
5.1	6.57E-10	1.30E-03	6.70E-10	1.3E-3	6.84E-10	1.3E-3	6.56E-10	1.30E-03

Table E.3.b (cont 1) Calculated, normalized neutron leakage flux Φ_{ng}. Block and source compositions.

Energy Group Eup [MeV]	Calculated, normalized neutron leakage flux Φng perturbed by three standard uncertainties							
	Cu contamination		No source structural Al		No source structural steel 304L		Absence of cavity	
	Φ_{ng} [cm$^{-2}\cdot$s^{-1}]	u_r	Φ_{ng} [cm$^{-2}\cdot$s^{-1}]	u_r	Φ_{ng} [cm$^{-2}\cdot$s^{-1}]	u_r	Φ_{ng} [cm$^{-2}\cdot$s^{-1}]	u_r
5.2	6.24E-10	1.40E-03	6.35E-10	1.4E-3	6.50E-10	1.4E-3	6.23E-10	1.40E-03
5.3	5.91E-10	1.40E-03	6.01E-10	1.4E-3	6.15E-10	1.4E-3	5.90E-10	1.40E-03
5.4	5.60E-10	1.50E-03	5.72E-10	1.5E-3	5.83E-10	1.5E-3	5.59E-10	1.50E-03
5.5	5.34E-10	1.50E-03	5.43E-10	1.5E-3	5.56E-10	1.5E-3	5.33E-10	1.50E-03
5.6	5.04E-10	1.60E-03	5.15E-10	1.6E-3	5.26E-10	1.6E-3	5.04E-10	1.60E-03
5.7	4.80E-10	1.70E-03	4.88E-10	1.6E-3	4.99E-10	1.6E-3	4.80E-10	1.70E-03
5.8	4.54E-10	1.70E-03	4.64E-10	1.7E-3	4.73E-10	1.7E-3	4.54E-10	1.70E-03
5.9	4.32E-10	1.80E-03	4.39E-10	1.8E-3	4.49E-10	1.7E-3	4.31E-10	1.80E-03
6	4.10E-10	1.80E-03	4.18E-10	1.8E-3	4.26E-10	1.8E-3	4.10E-10	1.80E-03
6.1	3.89E-10	1.90E-03	3.98E-10	1.9E-3	4.06E-10	1.9E-3	3.89E-10	1.90E-03
6.2	3.70E-10	2.00E-03	3.79E-10	1.9E-3	3.86E-10	1.9E-3	3.70E-10	2.00E-03
6.3	3.51E-10	2.00E-03	3.57E-10	2.0E-3	3.64E-10	2.0E-3	3.51E-10	2.00E-03
6.4	3.33E-10	2.10E-03	3.40E-10	2.1E-3	3.47E-10	2.0E-3	3.32E-10	2.10E-03
6.5	3.18E-10	2.20E-03	3.23E-10	2.1E-3	3.30E-10	2.1E-3	3.17E-10	2.20E-03
6.6	3.02E-10	2.20E-03	3.08E-10	2.2E-3	3.14E-10	2.2E-3	3.01E-10	2.20E-03
6.7	2.86E-10	2.30E-03	2.92E-10	2.3E-3	2.98E-10	2.3E-3	2.86E-10	2.30E-03
6.8	2.73E-10	2.40E-03	2.79E-10	2.4E-3	2.83E-10	2.3E-3	2.73E-10	2.40E-03
6.9	2.59E-10	2.50E-03	2.66E-10	2.4E-3	2.70E-10	2.4E-3	2.59E-10	2.50E-03
7	2.45E-10	2.50E-03	2.52E-10	2.5E-3	2.56E-10	2.5E-3	2.45E-10	2.50E-03
7.1	2.34E-10	2.60E-03	2.39E-10	2.6E-3	2.45E-10	2.6E-3	2.33E-10	2.60E-03
7.2	2.21E-10	2.70E-03	2.26E-10	2.7E-3	2.30E-10	2.6E-3	2.21E-10	2.70E-03
7.3	2.08E-10	2.80E-03	2.14E-10	2.8E-3	2.19E-10	2.7E-3	2.08E-10	2.80E-03
7.4	1.98E-10	2.90E-03	2.02E-10	2.8E-3	2.06E-10	2.8E-3	1.97E-10	2.90E-03
7.5	1.86E-10	3.00E-03	1.91E-10	2.9E-3	1.95E-10	2.9E-3	1.86E-10	3.00E-03
7.6	1.76E-10	3.10E-03	1.81E-10	3.0E-3	1.84E-10	3.0E-3	1.76E-10	3.10E-03
7.7	1.67E-10	3.20E-03	1.71E-10	3.1E-3	1.74E-10	3.1E-3	1.67E-10	3.20E-03
7.8	1.58E-10	3.30E-03	1.61E-10	3.2E-3	1.64E-10	3.2E-3	1.58E-10	3.30E-03
7.9	1.48E-10	3.40E-03	1.52E-10	3.3E-3	1.56E-10	3.3E-3	1.48E-10	3.40E-03
8	1.41E-10	3.50E-03	1.44E-10	3.4E-3	1.46E-10	3.4E-3	1.40E-10	3.50E-03
8.1	1.33E-10	3.60E-03	1.37E-10	3.5E-3	1.39E-10	3.5E-3	1.33E-10	3.60E-03
8.2	1.26E-10	3.70E-03	1.29E-10	3.7E-3	1.32E-10	3.6E-3	1.25E-10	3.70E-03
8.3	1.19E-10	3.80E-03	1.23E-10	3.8E-3	1.25E-10	3.7E-3	1.19E-10	3.80E-03
8.4	1.13E-10	4.00E-03	1.15E-10	3.9E-3	1.18E-10	3.9E-3	1.13E-10	4.00E-03
8.5	1.05E-10	4.10E-03	1.08E-10	4.1E-3	1.11E-10	4.0E-3	1.05E-10	4.10E-03
8.6	9.94E-11	4.20E-03	1.02E-10	4.2E-3	1.04E-10	4.2E-3	9.94E-11	4.20E-03
8.7	9.33E-11	4.40E-03	9.56E-11	4.3E-3	9.78E-11	4.3E-3	9.32E-11	4.40E-03
8.8	8.85E-11	4.50E-03	8.90E-11	4.5E-3	9.15E-11	4.4E-3	8.83E-11	4.50E-03
8.9	8.29E-11	4.70E-03	8.48E-11	4.6E-3	8.64E-11	4.6E-3	8.27E-11	4.70E-03
9	7.87E-11	4.80E-03	8.02E-11	4.8E-3	8.08E-11	4.8E-3	7.86E-11	4.80E-03
9.1	7.32E-11	5.00E-03	7.52E-11	4.9E-3	7.67E-11	4.9E-3	7.32E-11	5.00E-03

Table E.3.b (cont 2) Calculated, normalized neutron leakage flux Φ_{ng}. Block and source compositions.

Energy Group Eup [MeV]	Cu contamination		No source structural Al		No source structural steel 304L		Absence of cavity	
	Φ_{ng} [cm$^{-2}\cdot$s^{-1}]	u_r	Φ_{ng} [cm$^{-2}\cdot$s^{-1}]	u_r	Φ_{ng} [cm$^{-2}\cdot$s^{-1}]	u_r	Φ_{ng} [cm$^{-2}\cdot$s^{-1}]	u_r
9.3	6.51E-11	5.30E-03	6.64E-11	5.3E-3	6.78E-11	5.3E-3	6.50E-11	5.30E-03
9.4	6.12E-11	5.50E-03	6.22E-11	5.5E-3	6.35E-11	5.4E-3	6.11E-11	5.50E-03
9.5	5.74E-11	5.70E-03	5.85E-11	5.6E-3	6.00E-11	5.6E-3	5.74E-11	5.70E-03
9.6	5.39E-11	5.90E-03	5.55E-11	5.8E-3	5.61E-11	5.8E-3	5.39E-11	5.90E-03
9.7	5.06E-11	6.20E-03	5.24E-11	6.1E-3	5.31E-11	6.0E-3	5.06E-11	6.20E-03
9.8	4.80E-11	6.30E-03	4.83E-11	6.2E-3	4.97E-11	6.2E-3	4.80E-11	6.30E-03
9.9	4.50E-11	6.50E-03	4.54E-11	6.4E-3	4.70E-11	6.4E-3	4.49E-11	6.50E-03
10	4.25E-11	6.80E-03	4.39E-11	6.7E-3	4.41E-11	6.6E-3	4.24E-11	6.80E-03
10.1	4.02E-11	6.90E-03	4.11E-11	6.9E-3	4.20E-11	6.8E-3	4.01E-11	6.90E-03
10.2	3.79E-11	7.20E-03	3.86E-11	7.1E-3	3.90E-11	7.0E-3	3.78E-11	7.20E-03
10.3	3.62E-11	7.40E-03	3.69E-11	7.3E-3	3.75E-11	7.3E-3	3.61E-11	7.40E-03
10.4	3.42E-11	7.50E-03	3.49E-11	7.5E-3	3.56E-11	7.4E-3	3.42E-11	7.50E-03
10.5	3.23E-11	7.90E-03	3.29E-11	7.8E-3	3.38E-11	7.6E-3	3.22E-11	7.90E-03
10.6	2.99E-11	8.10E-03	3.12E-11	8.0E-3	3.13E-11	8.0E-3	2.99E-11	8.10E-03
10.7	2.87E-11	8.30E-03	2.89E-11	8.2E-3	2.95E-11	8.2E-3	2.86E-11	8.30E-03
10.8	2.69E-11	8.70E-03	2.74E-11	8.5E-3	2.82E-11	8.5E-3	2.69E-11	8.70E-03
10.9	2.49E-11	8.90E-03	2.52E-11	8.7E-3	2.61E-11	8.8E-3	2.49E-11	8.90E-03
11	2.41E-11	9.30E-03	2.41E-11	9.2E-3	2.47E-11	9.1E-3	2.40E-11	9.30E-03

APPENDIX F. XRF ANALYSIS

SAMPLE ANALYSIS REPORT   THERMO FISHER SCIENTIFIC
ARL QUANT'X EDXRF ANALYZER   UNIQUANT(TM) STANDARDLESS METHOD
_____

C:\UQed\USER\RhKetA\Job\JOB.151   2021-06-11
21-EWE-Cu00-002_1_ocistene

Quant'X, Rh-X-ray, Ketec, CAL in Air
C:\UQed\USER\RhKetA\Appl\MetalAir.kap 2019-05-17
Calculated as : Elements   Matrix (Shape & ImpFc) : 13|Cu Zn
X-ray path   =   Air   Film type   = 2 Spec 4
Case number   = 0 All known
Eff.Diam.   = 5.60 mm   Eff.Area   = 24.62 mm2
KnownConc   = 0   %
Rest   = 0   %   Viewed Mass   = 1985.163 mg
Dil/Sample   = 0   Sample Height = 9.00 mm

        El   m/m%   StdErr
        --   -------- -------
        Cu   99.87   0.04
        Cl   0.083   0.011
        Ni   0.0138 0.0056
        Ca   0.0120 0.0025
        K   0.0089 0.0023

        Fe   0.0080 0.0026
        Ag   0.0031 0.0004

KnownConc= 0   REST= 0   D/S= 0
Sum Conc's before normalisation to 100% :   88.7 %

           ****

SAMPLE ANALYSIS REPORT   THERMO FISHER SCIENTIFIC
ARL QUANT'X EDXRF ANALYZER   UNIQUANT(TM) STANDARDLESS METHOD
_____

C:\UQed\USER\RhKetA\Job\JOB.149   2021-06-11
21-EWE-Cu00-002_2_dlouhe

Quant'X, Rh-X-ray, Ketec, CAL in Air
C:\UQed\USER\RhKetA\Appl\MetalAir.kap 2019-05-17
Calculated as : Elements   Matrix (Shape & ImpFc) : 13|Cu Zn
X-ray path   =   Air   Film type   = 2 Spec 4
Case number   = 0 All known
Eff.Diam.   = 5.60 mm   Eff.Area   = 24.62 mm2
KnownConc   = 0   %
Rest   = 0   %   Viewed Mass   = 1985.163 mg
Dil/Sample   = 0   Sample Height = 9.00 mm

        El   m/m%   StdErr
        --   -------- -------
        Cu   99.89   0.03

APPENDIX G. DENSITY ANALYSIS

Sample 1

PYCNOMATIC - DENSITY MEASUREMENT REPORT

Sample name: Kostla Cu 1
Comment: 9.6.2021 11:30
Operator: Robert
Analysis start: 09.06.21 10:15
Analysis end: 09.06.21 10:45
Vessel correction: 0.00000 cc
Vessel ID nr.: 0
Vessel weight: 0.00000 g
Total weight before: 8.53290 g
Sample weight before: 8.53290 g
Total weight after: 8.53290 g
Sample weight after: 8.53290 g
Weight difference: 0.00000 g

ANALYTICAL PARAMETERS

Reference: I
Reduction: Small
Reference volume: 21.46975: cc
Cell volume: 7.23968: cc
Filler volume: 0.00000 cc
Repeated analyses nr.: 3
Flow cleaning time: 0 sec
Number of cleaning cycles: 10
Sample cleaning time: 10 sec
Atm. stabilization time: 15: sec
Restriction delta pressure: 2.00000 bar
Equilibrium delta pressure: 0.00020 bar
Equilibrium delta time: 15 sec
% Standard deviation: 0.025 %
Nr. of good measurements: 3
Nr. of max. measurements: 50
High precision: Yes
Temperature set: 20.00: °C

RESULTS

Average Sample Volume: 0.96181 cc
Volume Standard Deviation: 0.00006 cc
% Standard Deviation on Volume: 0.00657 %

Average Skeletal Density: 8.87167 g/cc
Skeletal Density Deviation: 0.00058 g/cc
% Standard Deviation on Density: 0.00657 %

Average Skeletal Density after: 8.87167 g/cc

MEASUREMENT RAW DATA

Patm: Pref: Peq Temp Volume Aver.Vol Aver.Dev.
bar bar bar: °C cc cc cc
0.99844: 2.01086: 1.78170: 20.00: 0.95841: 0.95841: 0.00000
0.99847: 2.01210: 1.78273: 19.99: 0.96041: 0.95941: 0.00142
0.99849: 2.01200: 1.78269: 19.99: 0.96169: 0.96017: 0.00165

0.99854: 2.00921: 1.78054: 19.99: 0.96136: 0.96116: 0.00066
0.99856: 2.00959: 1.78077: 20.00: 0.95891: 0.96066: 0.00152
0.99864: 2.00959: 1.78084: 19.99: 0.96094: 0.96041: 0.00131
0.99861: 2.01233: 1.78295: 19.99: 0.96084: 0.96023: 0.00114
0.99857: 2.00894: 1.78034: 19.99: 0.96182: 0.96120: 0.00054
0.99858: 2.00998: 1.78115: 19.99: 0.96175: 0.96147: 0.00055
0.99860: 2.01006: 1.78122: 19.99: 0.96187: 0.96181: 0.00006

PYCNOMATIC - DENSITY MEASUREMENT REPORT

Sample name: Kostla Cu 1
Comment: 9.6.2021 11:30
Operator: Robert
Analysis start: 09.06.21 10:45
Analysis end: 09.06.21 11:07
Vessel correction: 0.00000 cc
Vessel ID nr.: 0
Vessel weight: 0.00000 g
Total weight before: 8.53290 g
Sample weight before: 8.53290 g
Total weight after: 8.53290 g
Sample weight after: 8.53290 g
Weight difference: 0.00000 g

ANALYTICAL PARAMETERS

Reference: I
Reduction: Small
Reference volume: 21.46975: cc
Cell volume: 7.23968: cc
Filler volume: 0.00000 cc
Repeated analyses nr.: 3
Flow cleaning time: 0 sec
Number of cleaning cycles: 10
Sample cleaning time: 10 sec
Atm. stabilization time: 15: sec
Restriction delta pressure: 2.00000 bar
Equilibrium delta pressure: 0.00020 bar
Equilibrium delta time: 15 sec
% Standard deviation: 0.025 %
Nr. of good measurements: 3
Nr. of max. measurements: 50
High precision: Yes
Temperature set: 20.00: °C

RESULTS

Average Sample Volume: 0.96196 cc
Volume Standard Deviation: 0.00005 cc
% Standard Deviation on Volume: 0.00571 %

Average Skeletal Density: 8.87031 g/cc
Skeletal Density Deviation: 0.00051 g/cc
% Standard Deviation on Density: 0.00571 %

Average Skeletal Density after: 8.87031 g/cc

MEASUREMENT RAW DATA

Patm: Pref: Peq Temp Volume Aver.Vol Aver.Dev.
bar bar bar: °C cc cc cc
0.99865: 2.01220: 1.78290: 19.99: 0.96256: 0.96256: 0.00000
0.99866: 2.01003: 1.78128: 19.99: 0.96423: 0.96340: 0.00118
0.99861: 2.01211: 1.78278: 20.00: 0.96088: 0.96256: 0.00167
0.99862: 2.01203: 1.78275: 19.99: 0.96199: 0.96237: 0.00171
0.99864: 2.01187: 1.78263: 19.99: 0.96190: 0.96159: 0.00061
0.99862: 2.01088: 1.78186: 19.99: 0.96200: 0.96196: 0.00005

PYCNOMATIC - DENSITY MEASUREMENT REPORT

Sample name: Kostla Cu 1
Comment: 9.6.2021 11:30
Operator: Robert
Analysis start: 09.06.21 11:07
Analysis end: 09.06.21 11:25
Vessel correction: 0.00000 cc
Vessel ID nr.: 0
Vessel weight: 0.00000 g
Total weight before: 8.53290 g
Sample weight before: 8.53290 g
Total weight after: 8.53290 g
Sample weight after: 8.53290 g
Weight difference: 0.00000 g

ANALYTICAL PARAMETERS

Reference: I
Reduction: Small
Reference volume: 21.46975: cc
Cell volume: 7.23968: cc
Filler volume: 0.00000 cc
Repeated analyses nr.: 3
Flow cleaning time: 0 sec
Number of cleaning cycles: 10
Sample cleaning time: 10 sec
Atm. stabilization time: 15: sec
Restriction delta pressure: 2.00000 bar
Equilibrium delta pressure: 0.00020 bar
Equilibrium delta time: 15 sec
% Standard deviation: 0.025 %
Nr. of good measurements: 3
Nr. of max. measurements: 50
High precision: Yes
Temperature set: 20.00: °C

RESULTS

Average Sample Volume: 0.96237 cc
Volume Standard Deviation: 0.00012 cc
% Standard Deviation on Volume: 0.01295 %

Average Skeletal Density: 8.86654 g/cc
Skeletal Density Deviation: 0.00115 g/cc
% Standard Deviation on Density: 0.01295 %

Average Skeletal Density after: 8.86654 g/cc

MEASUREMENT RAW DATA

Patm: Pref: Peq Temp Volume Aver.Vol Aver.Dev.
bar bar bar: °C cc cc cc
0.99865: 2.01258: 1.78318: 19.99: 0.96187: 0.96187: 0.00000
0.99862: 2.01013: 1.78129: 19.99: 0.96249: 0.96218: 0.00044
0.99868: 2.01221: 1.78292: 19.99: 0.96238: 0.96224: 0.00033
0.99869: 2.01154: 1.78240: 19.99: 0.96224: 0.96237: 0.00012

Sample 2

PYCNOMATIC - DENSITY MEASUREMENT REPORT

Sample name: Kostla Cu 2
Comment: 9.6.2021 14:07
Operator: Robert
Analysis start: 09.06.21 12:54
Analysis end: 09.06.21 13:18
Vessel correction: 0.00000 cc
Vessel ID nr.: 0
Vessel weight: 0.00000 g
Total weight before: 8.70810 g
Sample weight before: 8.70810 g
Total weight after: 8.70810 g
Sample weight after: 8.70810 g
Weight difference: 0.00000 g

ANALYTICAL PARAMETERS

Reference: I
Reduction: Small
Reference volume: 21.46975: cc
Cell volume: 7.23968: cc
Filler volume: 0.00000 cc
Repeated analyses nr.: 3
Flow cleaning time: 0 sec
Number of cleaning cycles: 10
Sample cleaning time: 10 sec
Atm. stabilization time: 15: sec
Restriction delta pressure: 2.00000 bar
Equilibrium delta pressure: 0.00020 bar
Equilibrium delta time: 15 sec
% Standard deviation: 0.025 %
Nr. of good measurements: 3
Nr. of max. measurements: 50
High precision: Yes
Temperature set: 20.00: °C

RESULTS

Average Sample Volume: 0.98317 cc
Volume Standard Deviation: 0.00012 cc
% Standard Deviation on Volume: 0.01193 %

Average Skeletal Density: 8.85718 g/cc
Skeletal Density Deviation: 0.00106 g/cc
% Standard Deviation on Density: 0.01192 %

Average Skeletal Density after: 8.85718 g/cc

MEASUREMENT RAW DATA

Patm: Pref: Peq Temp Volume Aver.Vol Aver.Dev.
bar bar bar: °C cc cc cc
0.99813: 2.01256: 1.78363: 19.99: 0.98258: 0.98258: 0.00000
0.99813: 2.01181: 1.78306: 19.99: 0.98292: 0.98275: 0.00025
0.99810: 2.00994: 1.78164: 19.99: 0.98391: 0.98314: 0.00069
0.99804: 2.00998: 1.78165: 19.99: 0.98372: 0.98352: 0.00052
0.99805: 2.01252: 1.78360: 19.99: 0.98330: 0.98364: 0.00031
0.99799: 2.01221: 1.78335: 19.99: 0.98314: 0.98339: 0.00030
0.99796: 2.01053: 1.78204: 19.99: 0.98307: 0.98317: 0.00012

PYCNOMATIC - DENSITY MEASUREMENT REPORT

Sample name: Kostla Cu 2
Comment: 9.6.2021 14:07
Operator: Robert
Analysis start: 09.06.21 13:18
Analysis end: 09.06.21 14:07
Vessel correction: 0.00000 cc
Vessel ID nr.: 0
Vessel weight: 0.00000 g
Total weight before: 8.70810 g
Sample weight before: 8.70810 g
Total weight after: 8.70810 g
Sample weight after: 8.70810 g
Weight difference: 0.00000 g

ANALYTICAL PARAMETERS

Reference: I
Reduction: Small
Reference volume: 21.46975: cc
Cell volume: 7.23968: cc
Filler volume: 0.00000 cc
Repeated analyses nr.: 3
Flow cleaning time: 0 sec
Number of cleaning cycles: 10
Sample cleaning time: 10 sec
Atm. stabilization time: 15: sec
Restriction delta pressure: 2.00000 bar
Equilibrium delta pressure: 0.00020 bar
Equilibrium delta time: 15 sec
% Standard deviation: 0.025 %
Nr. of good measurements: 3
Nr. of max. measurements: 50
High precision: Yes
Temperature set: 20.00: °C

RESULTS

Average Sample Volume: 0.98344 cc
Volume Standard Deviation: 0.00018 cc
% Standard Deviation on Volume: 0.01843 %

Average Skeletal Density: 8.85471 g/cc

Skeletal Density Deviation: 0.00163 g/cc
% Standard Deviation on Density: 0.01842 %

Average Skeletal Density after: 8.85471 g/cc

MEASUREMENT RAW DATA

Patm: Pref: Peq Temp Volume Aver.Vol Aver.Dev.
bar bar bar: °C cc cc cc
0.99774: 2.01229: 1.78336: 19.99: 0.98361: 0.98361: 0.00000
0.99771: 2.00880: 1.78065: 19.99: 0.98344: 0.98353: 0.00012
0.99772: 2.01237: 1.78339: 19.99: 0.98241: 0.98316: 0.00065
0.99771: 2.01200: 1.78312: 19.99: 0.98300: 0.98295: 0.00052
0.99769: 2.01262: 1.78358: 19.99: 0.98257: 0.98266: 0.00031
0.99766: 2.01304: 1.78391: 19.99: 0.98302: 0.98286: 0.00026
0.99765: 2.01342: 1.78421: 19.99: 0.98324: 0.98295: 0.00034
0.99763: 2.01023: 1.78175: 19.99: 0.98389: 0.98338: 0.00045
0.99764: 2.01173: 1.78289: 19.99: 0.98273: 0.98329: 0.00058
0.99763: 2.00923: 1.78096: 20.00: 0.98340: 0.98334: 0.00058
0.99763: 2.01066: 1.78204: 20.00: 0.98226: 0.98280: 0.00057
0.99765: 2.01113: 1.78244: 19.99: 0.98324: 0.98297: 0.00062
0.99758: 2.01279: 1.78369: 19.99: 0.98262: 0.98270: 0.00050
0.99757: 2.01118: 1.78246: 20.00: 0.98319: 0.98302: 0.00034
0.99752: 2.01255: 1.78350: 19.99: 0.98301: 0.98294: 0.00029
0.99750: 2.01060: 1.78202: 19.99: 0.98398: 0.98339: 0.00051
0.99750: 2.01045: 1.78188: 19.99: 0.98356: 0.98352: 0.00049
0.99748: 2.01192: 1.78300: 19.99: 0.98285: 0.98346: 0.00057
0.99748: 2.01179: 1.78291: 19.99: 0.98339: 0.98327: 0.00037
0.99748: 2.01184: 1.78295: 19.99: 0.98329: 0.98318: 0.00029
0.99746: 2.01159: 1.78276: 19.99: 0.98364: 0.98344: 0.00018

PYCNOMATIC - DENSITY MEASUREMENT REPORT

Sample name: Kostla Cu 2
Comment: 9.6.2021 14:07
Operator: Robert
Analysis start: 09.06.21 14:08
Analysis end: 09.06.21 14:35
Vessel correction: 0.00000 cc
Vessel ID nr.: 0
Vessel weight: 0.00000 g
Total weight before: 8.70810 g
Sample weight before: 8.70810 g
Total weight after: 8.70810 g
Sample weight after: 8.70810 g
Weight difference: 0.00000 g

ANALYTICAL PARAMETERS

Reference: I
Reduction: Small
Reference volume: 21.46975: cc
Cell volume: 7.23968: cc
Filler volume: 0.00000 cc
Repeated analyses nr.: 3
Flow cleaning time: 0 sec
Number of cleaning cycles: 10
Sample cleaning time: 10 sec

Atm. stabilization time: 15: sec
Restriction delta pressure: 2.00000 bar
Equilibrium delta pressure: 0.00020 bar
Equilibrium delta time: 15 sec
% Standard deviation: 0.025 %
Nr. of good measurements: 3
Nr. of max. measurements: 50
High precision: Yes
Temperature set: 20.00: °C

RESULTS

Average Sample Volume: 0.98276 cc
Volume Standard Deviation: 0.00019 cc
% Standard Deviation on Volume: 0.01961 %

Average Skeletal Density: 8.86087 g/cc
Skeletal Density Deviation: 0.00174 g/cc
% Standard Deviation on Density: 0.01961 %

Average Skeletal Density after: 8.86087 g/cc

MEASUREMENT RAW DATA

Patm: Pref: Peq Temp Volume Aver.Vol Aver.Dev.
bar bar bar: °C cc cc cc
0.99738: 2.01188: 1.78296: 19.99: 0.98319: 0.98319: 0.00000
0.99738: 2.00880: 1.78057: 19.99: 0.98306: 0.98312: 0.00010
0.99736: 2.00880: 1.78055: 19.99: 0.98246: 0.98290: 0.00039
0.99732: 2.01315: 1.78390: 19.99: 0.98230: 0.98261: 0.00040
0.99730: 2.01289: 1.78372: 19.99: 0.98327: 0.98268: 0.00052
0.99729: 2.01183: 1.78288: 19.99: 0.98248: 0.98268: 0.00052
0.99728: 2.01258: 1.78346: 19.99: 0.98266: 0.98280: 0.00041
0.99725: 2.01078: 1.78207: 19.99: 0.98298: 0.98271: 0.00025
0.99724: 2.01227: 1.78321: 19.99: 0.98263: 0.98276: 0.00019